A COMPARATIVE STUDY OF SHOCK ISOLATION SYSTEMS HAVING LINEAR AND NONLINEAR DAMPING

Robert Young, Eng.

A Research Thesis in
THE DEPARTMENT OF
MECHANICAL ENGINEERING

Presented in Partial Fulfillment of the Requirements for the degree of Master of Engineering at Concordia University, Montreal, Quebec, Canada

September 1979

ABSTRACT

A COMPARATIVE STUDY OF SHOCK ISOLATION SYSTEMS HAVING LINEAR AND NON-LINEAR DAMPING

Robert Young

In this thesis, a comparative study is made of various single degree-of-freedom isolator systems employing viscous, coulomb friction and combined form of viscous/coulomb damping. The coulomb dampers investigated have constant friction and adaptive friction force characteristics, whereby in the latter, the resistive force is a function of either the relative displacement or relative velocity across the isolator.

The systems are directly coupled where the ends of the damper are connected between the mass to be protected and the base where external excitations are applied, and elastically coupled where the damper is indirectly connected to the base by means of an elastic spring.

Two base excitations are used: a rounded pulse displacement consisting of a single disturbance and an oscillatory pulse displacement having a series of decaying oscillations.

It is found that the combined viscous/coulomb damped system offers the best performance, as it has low transmitted accelerations for a wide variation in the severity of the excitations while the relative displacement is maintained at levels which are generally proportional to the severity. At low severities, it behaves similar to a viscous isolator where good relative displacement control is achieved and like

coulomb isolator at high severities where the accelerations are limited by the break-out friction. Unlike the systems employing only friction damping, the combined viscous/coulomb system does not lock up and hence the mass is returned to its zero position after the base excitation has passed.

ACKNOWLEDGEMENTS

I wish to extend my thanks to Professors S. Sankar and T.S. Sankar of the Mechanical Engineering Department, Concordia Univeristy for their advice and guidance during the preparation of this thesis, and to Mr. Harold March and Mr. Bill Hertha for their assistance with the computer programming and producing of the graphs.

Most of all I would like to thank my wife Irene for her understanding and patience with me throughout these past years of study.

TABLE OF CONTENTS

		page
Abstract		i
Acknowledgements		iii
Table of Contents		iv
List of Figures		viii
List of Tables		xv
Nomenclature		xvi
Chapter 1 -	INTRODUCTION	
1.1	General Introduction	1
1.2	Recent Studies	2
1.3	Scope of Thesis	8
Chapter 2 -	EQUATIONS OF MOTION	
2.1	Viscous Damped Isolators	
2.1.1	Directly Coupled Visous Isolator (DCVI)	9
2.1.2	Elastically Coupled Viscous Isolator Type 1 (ECVI-1)	11
2.1.3	Elastically Coupled Viscous Isolator Type 2 (ECVI-2)	13
2.1.4	Comparison of ECVI Types 1 and 2	13
2.2	COULOMB FRICTION DAMPED ISOLATORS	
2.2.1	Directly Coupled Friction Isolator (DCFI)	14
2.2.2	Elastically Coupled Friction Isolator Type 1 (ECFI-1)	19
2.2.3	Elastically Coupled Friction Isolator Type 2 (ECFI-2)	21

		page
2.2.4	Comparison of ECFI-1 and ECFI-2	23
2.3	COMBINED VISCOUS/COULOMB DAMPED ISOLATOR (CVFI)	23
2.4	ADAPTIVE FRICTION DAMPING DEVICES	26
Chapter 3 -	BASE EXCITATION EQUATIONS	
3.1	General Background	30
3.2	Rounded Pulse Displacement	30
3.3	Oscillatory Pulse Displacement	32
Chapter 4	PERFORMANCE EVALUATION	
4.1	Performance Criteria of Isolators	37
4.2	Influence of Time Response on Isolator Performance	39
Chapter 5 -	RESULTS AND DISCUSSION	
5.1	METHOD OF CALCULATION	40
5.2	VISCOUS DAMPED ISOLATORS SUBJECTED TO ROUNDED PULSE DISPLACEMENTS	41
5.2.1	Performance of the Directly Coupled Viscous Isolator (DCVI)	41
5.2.2	Performance of Elastically Coupled Viscous Isolators (ECVI)Types 1 and 2	42
5.2.3	Time Response of Viscous Damped Isolators	56
5.3	COULOMB FRICTION DAMPED ISOLATORS SUBJECTED TO ROUNDED PULSE DISPLACEMENTS	68
5.3.1	Performance of the Directly Coupled Friction Isolator (DCFI)	68

		page
5.3.2	Performance of Elastically Coupled Friction Isolators (ECFI) Types 1 and 2	69
5.3.3	Performance of Adaptive Friction Isolators	81
5.3.4	Time Response of Coulomb Damped Friction Isolators	89
5.4	COMBINED VISCOUS/COULOMB DAMPED ISOLATORS SUBJECTED TO ROUNDED PULSE DISPLACEMENTS.	
5.4.1	Performance of Combined Viscous/Coulomb Damped Isolators (CVFI)	98
5.4.2	Time Response of the Combined Viscous/ Coulomb Damped Isolators (CVFI)	109
5.5	VARIOUS VISCOUS AND COULOMB DAMPED ISOLATORS SUBJECTED TO OSCILLATORY PULSE DISPLACEMENTS	118
5.5.1	Performance of Viscous Damped Isolators	118
5.5.2	Performance of Coulomb Damped Isolators	119
5.5.3	Performance of Combined Viscous/Coulomb Damped Isolators (CVFI)	121
5.5.4	Time Response of Various Isolators	131
Chapter 6	- CONCLUSIONS AND RECOMMENDATIONS	142
6.1	Performance of Viscous Damped Isolators	143
6.2	Performance of Friction Damped Isolators	144
6.3	Performance of Combined Viscous/Coulomb Damped Isolators	146
6.4	Comparison of Various Isolator Configurations	148
6.5	Recommendations for Future Work	149

		page
REFERENCES		151
APPENDICES		
A.	Friction Damped Isolator Systems having no Linear Viscous Band Characteristic.	153
B.	Fourth-Order Runge-Kutta Method of Solving Differential Equations.	157
C.	Description of the Use of the Computer Program.	159
D.	Flowchart and Listing of Computer Program.	163

LIST OF FIGURES

FIGURE		PAGE
1.	Schematic of the Directly Coupled Viscous Isolator System.	10
2.	Schematic of the Elastically Coupled Viscous Isolator System Type 1.	12
3.	Schematic of the Elastically Coupled Viscous Isolator System Type 2.	12
4.	Schematic of the Directly Coupled Coulomb Friction Isolator System.	16
5.	Ideal Coulomb Friction Characteristic.	17
6.	Coulomb Friction Characteristic with a Linear Viscous Band.	17
7.	Schematic of the Elastically Coupled Coulomb Friction Isolator System Type 1.	20
8.	Schematic of the Elastically Coupled Coulomb Friction Isolator System Type 2.	20
9.	Schematic of the Combined Viscous and Coulomb Friction Isolator System.	25
10.	Coulomb Friction Characteristic for the Displacement-Increasing Friction Damper.	28
11.	Coulomb Friction Characteristic for the Displacement-Decreasing Friction Damper.	28
12.	Coulomb Friction Characteristic for the Velocity-Increasing Friction Damper.	29

PAGE

13. Coulomb Friction Characteristic for the Velocity-Decreasing Friction Damper. 29

14. Rounded Pulse Displacement with its Corresponding Velocity and Acceleration 35

15. Oscillatory Pulse Displacement 36

ROUNDED PULSE RESPONSES

16. Performance of DCVI System for Various Damping Ratios ξ and Pulse Severities ν . 47

17. Performance of ECVI-1 System for Various Damping Ratios ξ and Pulse Severities ν. 48

18. Performance of ECVI-2 System for Various Damping Ratios ξ and Pulse Severities ν. 49

19. Performance of ECVI-1 System for Various Elastic Coupling Ratios N and Pulse Severities ν. 51

20. Performance of ECVI-2 System for Various Elastic Coupling Ratios N and Pulse Severities ν. 52

21. Performance of ECVI-1 System for Various Damping Ratios ξ and Elastic Coupling Ratios N. 54

22. Performance of ECVI-2 System for Various Damping Ratios ξ and Elastic Coupling Ratios N. 55

23. Isolator Relative Displacement Time Histories for DCVI System having 4 Values of Damping: ν=1. 59

24. Isolator Relative Displacement Time Histories for DCVI System having 4 Values of Damping: ν=5. 60

		PAGE
25.	Mass Acceleration Time Histories of DCVI System having 4 Values of Damping: ν=1.	61
26.	Mass Acceleration Time Histories of DCVI System having 4 Values of Damping: ν=5.	62
27.	Comparison of Mass Acceleration Time Histories for DCVI and ECVI Types 1 and 2 Systems.	63
28.	Comparison of Isolator Relative Displacement Time Histories for DCVI and ECVI Types 1 and 2 Systems.	64
29.	Isolator Relative Displacement Time Histories for ECVI-1 System having 4 Values of Elastic Coupling Ratio N.	65
30.	Mass Acceleration Time Histories for ECVI-1 System having 4 Values of Elastic Coupling Ratio N.	66
31.	Performance of DCFI System for Various Damping Ratios α and Pulse Severities ν.	72
32.	Performance of ECFI-1 System for Various Damping Ratios α and Pulse Severities ν.	74
33.	Performance of ECFI-2 System for Various Damping Ratios α and Pulse Severities ν.	75
34.	Performance of ECFI-1 System for Various Elastic Coupling Ratios N and Pulse Severities ν.	77
35.	Performance of ECFI-2 System for Various Elastic Coupling Ratios N and Pulse Severities ν.	78
36.	Performance of ECFI-1 System for Various Damping Ratios α and Elastic Coupling Ratios N.	79

		PAGE
37.	Performance of ECFI-2 System for Various Damping Ratios α and Elastic Coupling Ratios N.	80
38.	Comparison of Performance of DCFI System having Fixed and Adaptive Friction Devices for Various Pulse Severities ν.	84
39.	Performance of DCFI System having DIFI Device for Various Break Points and Pulse Severities.	85
40.	Performance of DCFI System having VIFI Device for Various Break Points and Pulse Severities.	86
41.	Performance of DCFI System having DDFI Device for Various Break Points and Pulse Severities.	87
42.	Performance of DCFI System having VDFI Device for Various Break Points and Pulse Severities.	88
43.	Mass Acceleration Time Histories of DCFI System having 4 Values of Damping.	91
44.	Isolator Relative Displacement Time Histories of DCFI System having 4 Values of Damping.	92
45.	Comparison of Mass Acceleration Time Histories of DCFI Systems having DIFI and Fixed Friction.	93
46.	Comparison of Mass Acceleration Time Histories of DCFI systems having DIFI and fixed friction.	94
47.	Comparison of Mass Acceleration Time Histories of DCFI Systems having VDFI and Fixed Friction.	95
48.	Comparison of Mass Acceleration Time Histories of DCFI Systems having VIFI and Fixed Friction.	96

		PAGE
49.	Comparison of Isolator Relative Displacement Time Histories of DCFI System having DDFI, DIFI, VDFI, VIFI and Fixed Friction.	97
50.	Performance of CVFI System for Various Coulomb Damping Ratios ξ and Pulse Severities: ν=0.25.	100
51.	Performance of CVFI System for Various Coulomb Damping Ratios ξ and Pulse Severities: ν=0.50.	101
52.	Performance of CVFI System for Various Viscous Damping Ratios ξ and Pulse Severities.	103
53.	Comparison of Performance of DCVI, DCFI, and CVFI Systems for Various Values of Damping.	104
54.	Comparison of Performance of CVFI System having Fixed and Adaptive Friction Devices for Various Pulse Severities.	106
55.	Performance of CVFI System having VDFI Device for Various Viscous Damping Ratios ξ and Pulse Severities.	107
56.	Performance of CVFI System having DDFI Device for Various Viscous Damping Ratios ξ and Pulse Severities.	108
57.	Isolator Relative Displacement Time Histories of CVFI System having 4 Values of Coulomb Damping.	112
58.	Isolator Relative Displacement Time Histories of CVFI System having 4 Values of Viscous Damping.	113
59.	Mass Acceleration Time Histories of CVFI System having 4 Values of Coulomb Damping.	114

		PAGE
60.	Mass Acceleration Time Histories of CVFI System having 4 Values of Viscous Damping.	115
61.	Comparison of Mass Acceleration Time Histories of DCVI, DCFI and CVFI Systems having the Same Viscous and Coulomb Damping.	116
62.	Comparison of Isolator Relative Displacement Time Histories of DCVI, DCFI and CVFI Systems having the same Viscous and Coulomb Damping.	117
	OSCILLATORY PULSE RESPONSES	
63.	Performance of DCVI System for Various Damping Ratios ξ and Pulse Severities ν.	123
64.	Performance of ECVI-1 System for Various Damping Ratios ξ and Elastic Coupling Ratios N.	124
65.	Performance of DCFI System for Various Damping Ratios α and Pulse Severities ν.	125
66.	Performance of ECFI-1 System for Various Damping Ratios α and Elastic Coupling Ratios N.	126
67.	Performance of CVFI System for Various Coulomb Damping Ratios α and Pulse Severities ν.	127
68.	Isolator Relative Displacement Time History of DCVI System.	133
69.	Isolator Relative Displacement Time History of DCFI System.	134
70.	Isolator Relative Displacement Time History of DCFI System having DDFI Device.	135

PAGE

71. Isolator Relative Displacement Time History of CVFI System. 136

72. Mass Acceleration Time History of DCVI System. 137

73. Mass Acceleration Time History of DCFI System. 138

74. Mass Acceleration Time History of DCFI System having DDFI Device. 139

75. Mass Acceleration Time History of CVFI System. 140

APPENDICES

76. Comparison of Mass Acceleration Time Histories of DCFI System with and without Linear Viscous Band Friction Characteristic: $\alpha = 0.50$. 155

77. Comparison of Mass Acceleration Time Histories of DCFI System with and without Linear Viscous Band Friction Characteristic: $\alpha = 0.25$. 156

78. Geometric Representation of the Fourth-Order Runge-Kutta Method. 158

79. Flowchart of Isolator Simulation Program. 164

LIST OF TABLES

TABLE		PAGE
	ROUNDED PULSE RESPONSES	
1.	Comparison of DCVI and ECVI Types 1 and 2 Systems having Various Damping Ratios.	50
2.	Comparison of DCVI and ECVI Types 1 and 2 Systems having Various Elastic Coupling Ratios.	53
3.	Comparison of DCVI and ECVI-1 Systems having the Same Maximum Mass Acceleration $\ddot{X}_2$.	67
4.	Comparison of DCFI and DCVI Systems having the Same Response to Low Severity Pulse.	73
5.	Comparison of DCFI and ECFI Types 1 and 2 Systems having Various Damping Ratios.	76
6.	Comparison of CVFI System with Low Coulomb Damping and Undamped DCVI System.	102
7.	Comparison of CVFI, DCVI and DCFI Systems having the Same Viscous and Coulomb Damping.	105
	OSCILLATORY PULSE RESPONSES	
8.	Comparison of RDR Response of DCFI System with Fixed and Adaptive Friction.	128
9.	Comparison of $\ddot{X}_2$ Response of DCFI System having Fixed and Adaptive Friction.	129
10.	Comparison of DCVI, DCFI and CVFI Systems having the Same Viscous and Coulomb Damping.	130
11.	Comparison of Acceleration Peaks of DCVI, DCFI with fixed α , DCFI with DDFI device and CVFI Systems.	141

NOMENCLATURE

c	=	viscous damping co-efficient
c'	=	dynamically equivalent viscous damping co-efficient of ECVI-2 system
c_{eq}	=	equivalent viscous damping co-efficient according to [2]
e	=	2.71828
F	=	coulomb friction force
F'	=	dynamically equivalent coulomb friction force of ECFI-2 system
k_1	=	elastic coupling spring stiffness
k_2	=	primary isolator spring stiffness
k_2'	=	dynamically equivalent primary isolator spring stiffness of ECVI and ECFI type 2 systems
k_{eq}	=	equivalent primary isolator spring stiffness according to [2]
M	=	mass of the body to be isolated
N	=	elastic coupling ratio $(\frac{k_2}{k_1})$
RDR	=	relative displacement ratio
S	=	Laplacian operator
t	=	time
T	=	natural period of isolator system
T_1, T_2, T_3, T_4	=	transition times of the oscillatory pulse base displacement
x_0	=	absolute displacement of the isolator base
$\dot{x}_0$	=	absolute velocity of the isolator base
$\ddot{x}_0$	=	absolute acceleration of the isolator base

x_1 = absolute displacement of the damper base (ECFI-1 and ECVI-1 systems)

X_1 = absolute displacement of isolator mid-frame (ECFI-2, ECVI-2 and CVFI systems)

$\dot{x}_1$ = absolute velocity of the damper base (ECFI-1 and ECVI-1 systems)

$\dot{X}_1$ = absolute velocity of isolator mid-frame (ECFI-2, ECVI-2 and CVFI systems)

x_2 = absolute displacement of the mass

$\dot{x}_2$ = absolute velocity of the mass

$\ddot{x}_2$ = absolute acceleration of the mass

$\dddot{x}$ = jerk of the mass

$\bar{x}$ = Laplace transform variable

$\Delta\dot{X}$ = limits of the linear viscous band of the modified coulomb friction characteristic

X_{in} = maximum displacement of the isolator base

XLAST = amplitude of oscillatory pulse displacement at $t=T_s$.

$\ddot{X}_2$ = normalized maximum acceleration transmitted to the mass

Z = independent variable controlling the coulomb friction in the adaptive friction devices

z_1, z_2 = break points of Z for constant friction levels

α = nondimensional coulomb friction

α_0 = initial coulomb friction level for adaptive friction devices

α_f = final coulomb friction level for adaptive friction devices

β = decay rate of the low frequency portion of the oscillatory pulse displacement.

ν = severity of the rounded and oscillatory pulse displacements

ψ = slope of the coulomb friction variation for adaptive friction devices.

τ = duration of the rounded pulse displacement

τ = duration of the first oscillation of the oscillatory pulse displacement

ω_n = natural frequency of the isolator system

ω_{lock} = natural frequency of the ECFI systems when the friction damper is locked up

ω_t = transition frequency according to [2]

$\omega_1, \omega_2, \omega_3$ = forcing frequencies for various portions of the oscillatory pulse displacement

The following are abbreviations for the isolator systems and damping devices used in the text:

CVFI	combined viscous/coulomb friction isolator
DCFI	directly coupled coulomb friction isolator
DCVI	directly coupled viscous isolator
DDFI	displacement-decreasing friction isolator
DIFI	displacement-increasing friction isolator
ECFI	elastically coupled coulomb friction isolator
ECFI-1	type 1 elastically coupled coulomb friction isolator
ECFI-2	type 2 elastically coupled coulomb friction isolator
ECVI	elastically coupled viscous isolator
ECVI-1	type 1 elastically coupled viscous isolator
ECVI-2	type 2 elastically coupled viscous isolator
VDFI	velocity-decreasing friction isolator
VIFI	velocity-increasing friction isolator

CHAPTER 1

INTRODUCTION

1.1 GENERAL BACKGROUND

There are many engineering systems which are subjected to external vibration or shock. A vibration is considered to be a continuous series of oscillatory disturbances which are deterministic or random in nature: an example of a deterministic vibration is an unbalanced engine on an automobile. However, if the automobile is driven on a rough, undulating roadway, it would experience random vibrations. A shock consists of a single disturbance or a short series of disturbances: the sudden impact caused when an aircraft touches down on a runway is an example of a shock.

In many cases these dynamic excitations, which if applied directly, would cause damage to the system, or prevent it from performing its function. To protect a system from these disturbances, an isolator is mounted between the system and the source of excitations. The isolator allows relative motion to occur across itself and thus suppresses the accelerations transmitted to the system. This reduction in acceleration is an essential requirement of an isolator, since the system must be capable of withstanding the inertia forces which result from the transmitted accelerations. The other major requirement of an isolator concerns the maximum relative displacement experienced across the isolator during its operation. This is important as physical limitations on the size and operating range of the isolator are often imposed. Other requirements such as weight, cost and reliability may also be important but are not considered in this thesis.

The basic elements which form an isolator system are commonly known: they consist of the system to be protected, springs which may have linear or non-linear stiffness, and energy dissipative dampers. Dampers are characterized by their force versus velocity relationships which may be linear or non-linear in form. With viscous damping, the force generated by the damper is proportional to the relative velocity across the damper. In coulomb dampers the damping force has a constant magnitude and acts in the direction to oppose motion across the damper.

1.2 RECENT STUDIES

There has been recent interest in the performance of isolator systems. That is, to know the dynamic response of an isolator system to various input excitations, and to determine how their response is affected by parameter changes within the isolator.

Ruzicka and Derby [1] have studied the influence on vibration isolation of a single degree-of-freedom system due to viscous, coulomb, quadratic, n^{th} power and hystersis damping elements which were directly and elastically coupled between the mass to be isolated and the base which was subjected to sinusoidal disturbances. A direct coupling of a damping element refers to a rigid connection of the damper ends to the mass and base. In an elastically coupled damping element, one end of the damper is indirectly connected to the base by an elastic spring. The isolator response was obtained using various exact and approximate solutions to the mathematical models. They concluded that for each type of damping element, one can obtain better

high frequency attenuation with the elastically coupled isolators, while still maintaining good control near resonance.

Snowdon [2] has studied the effects of isolators comprising non-linear hardening and softening springs in parallel with a linear viscous damper, whose base was subjected to transient disturbances. He showed that these nonlinearities can markedly affect the dynamic response of the isolator. In the case of the hardening spring, both the maximum transmitted acceleration and the maximum relative displacement were larger when compared to those with a linear spring. On the other hand the maximum values of acceleration and relative displacement were lower with a softening spring. These effects were particularly noticeable for low viscous damping. Though the softening spring isolator gave superior performance, one must also consider the ability of such an isolator to maintain acceptable levels of static deflection.

Various isolator systems having some form of non-linear damping have been proposed and analysed for transient base disturbances [3-6]. Snowdon [3] investigated the performance of a dual-phase viscous damped isolator system subject to rounded step, rounded pulse and oscillatory step displacements of the base. He describes a dual-phase damper as one having a variable damping ratio ξ which is a function of the relative velocity across the damper. At small velocities, ξ is high while at high velocities, ξ is low. For intermediate velocities there is a linear transition between the high and low values of ξ. He concluded that this type of isolator was highly effective in reducing the maximum values of absolute acceleration and displacement

as compared to a linear viscous isolator for all base disturbances except those having rise times which were greater than the natural period of the isolator system.

Cornelius [4] proposed a "dual-acting" type of isolator having a linear viscous damping force characteristic up to some saturation velocity after which the damping force became constant, and compared its performance efficiency with a conventional linear viscous isolator and an "ideal" isolator. Cornelius' "ideal" isolator would be one which would produce a constant resistive force against any base disturbance independent of the rate at which it was applied. Such an isolator would have the minimum relative displacement for a given transmitted acceleration. However, it would not return to its equilibrium position after the disturbance had passed, and would have excessive displacements under repeated shocks. From his study, he concluded that the "dual-acting" isolator gave high efficiencies, and in contrast to the "ideal" mount, it could return to its equilibrium position.

An adaptive type of isolator was proposed by Mercer and Rees [5]. It comprised a combination of viscous and coulomb dampers and return springs. The coulomb friction force was made a variable function of the relative displacement across the viscous damper: that is, the friction force was adaptive. They investigated the isolator's response to three shock acceleration pulses that were measured onboard a ship subjected to underwater explosions. The maximum amplitude of the pulses varied from 89g, to 380g, where g is the gravitational

acceleration, $9.81m/s^2$. They found that for the values of isolator parameters chosen, the isolator reduced the transmitted accelerations to 0.5g.and 1.0g., while maintaining the maximum relative displacement to 3.5 and 5.8cm.

Recently there has been a number of studies concerning optimum isolator configurations. Sevin and Pilkey have written a monograph [6] formulating the isolator design problem in terms of optimization theory. They used two methods to solve the optimization. The first was direct synthesis, where the isolator configuration was defined and the optimum values of the isolator parameters were determined in accordance with a performance criterion. In general, this criterion was selected to minimize the maximum transmitted acceleration while constraining the maximum relative displacement. This approach involved solving a constrained minimization problem by some form of numerical search technique. The second approach was a two step method of indirect synthesis. Firstly, the optimum performance of the system was determined. No isolator configuration was defined, but instead, the solution to the optimum isolator was found in terms of a force-time relationship which the isolator would have to provide, and which in general, could only be obtained by some type of active isolator. For simple problems, the optimum performance was obtained analytically by variational methods, though in the majority of cases, numerical methods such as linear or dynamic programming would have to be employed. The isolator configuration to be optimized was then defined, and the values of its parameters were chosen which gave the closest fit to the optimum

performance, without regards to the constraints. Pilkey and Sevin concluded that this two step method required less computation time, and that the isolator chosen would not violate the constraints. They have also illustrated these techniques with examples of isolators subjected to shock, random and harmonic vibrations.

Karnopp and Trikha [7] have investigated the optimization of a single degree-of-freedom isolator system subjected to both shock and random vibrations using two different performance criteria. The criteria were based on the maximum transmitted force, the maximum relative displacement and a relative weighting factor between the two quantities. They showed that an isolator which was optimized according to one criterion and one type of excitation may result in a markedly poorer performance when compared to another criterion or when subjected to a different disturbance.

Derby and Calcaterra [8] have analysed the elastically coupled linear viscous isolator to find its optimum performance when subject to acceleration impulses and to random vibrations. They concluded that an isolator with an infinitely stiff, elastic coupling (i.e. directly coupled), transmitted the minimum acceleration for a given maximum relative displacement. However, they acknowledged that some degree of elastic coupling can be desirable, such as for high frequency vibration isolation, or may be unavoidable.

Recently efforts have been made to improve isolator performance by using active control devices in conjunction with standard isolator elements. Paul and Fenoglio [9] have studied a two degree-of-freedom

model of an actively controlled automobile suspension system subjected to random guideway excitations. They proposed two configurations for the control system which consisted of conventional hydraulic components and compared their response to the performance of an optimum isolator system, which was optimized on a weighted acceleration versus relative displacement trade-off. They found that by an appropriate selection of system parameters, the two proposed active isolators did approach the optimum response.

Several investigations have been made with regards to the performance of isolators which must decelerate a mass having an initial velocity to rest. Such isolators are commonly known as shock absorbers. Bolden [10] showed that a variable orifice hydraulic shock absorber is more efficient than one having a fixed area orifice. The former, which is designed to produce a constant resistive force throughout its stroke, will bring the mass to rest in a shorter distance for the same maximum deceleration as compared to the latter which produces a velocity-squared resistive force.

Mayne [11] analysed models of fixed and variable orifice shock absorbers and included the effects of fluid compressibility, series springs and parallel return springs. He concluded that these compliances can degrade the performance of a variable orifice absorber, while, on the other hand, they can improve on that of a fixed orifice device.

Blake [12] showed that for masses which possess some internal flexibility, such as a thin walled box in which equipment is mounted, the constant resistive force profile of the variable orifice shock absorber does not produce an optimum degree of isolation. This type of

absorber highly excites secondary vibrations in the mass. Blake concluded that a resistive force having initially a versed sine and then a constant profile would be more desirable, since a great reduction in the secondary vibrations could be achieved with only a small increase in the maximum transmitted acceleration.

1.3 SCOPE OF THESIS

From a review of recent studies of isolator systems, it was found that there was a lack in the comparison of isolators subjected to transient base excitations. In the present investigation, various configurations of single degree of freedom isolator systems are modelled, which comprise a single mass that has to be protected, a base where the external excitations are applied, and an isolator. The following types of isolator configurations are investigated: "Directly Coupled" in which the damping element is in parallel with a return spring. "Elastically Coupled Type 1" in which the damping element has some elasticity in its connection to the base, and "Elastically Coupled Type 2" which consists of a directly coupled isolator having some elasticity in its base connection. The type of damping elements considered are a viscous damper, a coulomb friction damper, a combined viscous and coulomb friction damper, and an adaptive coulomb friction damper in which the resistive friction force was made a function of either the relative displacement or the relative velocity across the damper.

The isolators are subjected to rounded pulse displacements and a type of oscillatory pulse displacement [2,3]. Comparisons of isolator responses are made to form a general rationale with regards to isolator performance and the results are presented in graphical form.

CHAPTER 2

EQUATIONS OF MOTION

2.1 VISCOUS DAMPED ISOLATORS

2.1.1 DIRECTLY COUPLED VISCOUS ISOLATOR (DCVI)

Figure 1 shows a schematic diagram of a directly coupled viscous (DCVI)[1] damped isolator system: the isolator consists of a viscous damper, c, in parallel with a return spring k_2.

The equations of motion of the system is written as:

$$M\ddot{x}_2 + c(\dot{x}_2-\dot{x}_0) + k_2(x_2-x_0) = 0 \qquad (1)$$

where $\ddot{x}_2$ = the absolute acceleration of the mass

$\dot{x}_2$ = the absolute velocity of the mass

x_2 = the absolute displacement of the mass

$\dot{x}_0$ = the absolute velocity of the base

x_0 = the absolute displacement of the base

M = mass of the body

c = viscous damping coefficient

k_2 = mount spring stiffness

(Note: When a parameter is introduced for the first time, it is defined within the text.)

Defining: $\omega_n = \sqrt{\frac{k_2}{M}}$ natural frequency of the system (2)

and $\xi = \frac{c}{2M\omega_n}$ viscous damping ratio (3)

Substituting into equation (1) gives the following equation of motion:

$$\ddot{x}_2 + 2\xi\omega_n(\dot{x}_2-\dot{x}_0) + \omega_n^2(x_2-x_0) = 0 \qquad (4)$$

---

1. An abbreviated nomenclature for the description of the isolators is used in this thesis.

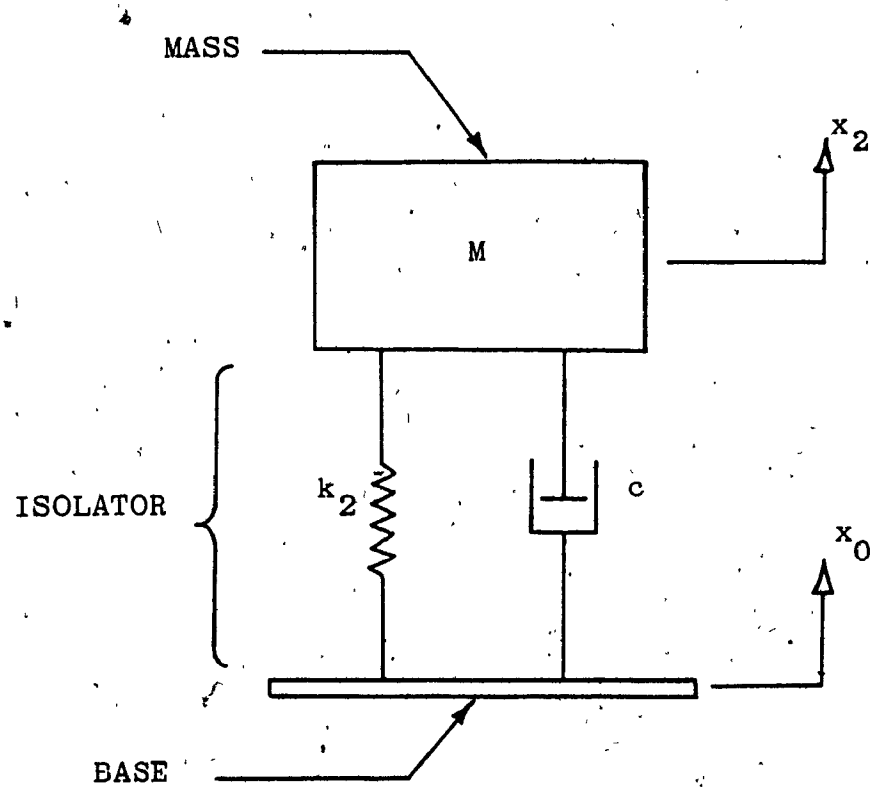

FIGURE 1: Schematic of the Directly Coupled Viscous Isolator System

2.1.2 ELASTICALLY COUPLED VISCOUS ISOLATOR TYPE 1 (ECVI-1)

Figure 2 is a schematic diagram of a type 1 elastically coupled viscous (ECVI-1) damped isolator system. The primary mount spring k_2 is directly connected between the mass and base. However, the viscous damper, c, has some elasticity in its connection to the base which is represented by the elastic coupling spring k_1. The junction between k_1 and the damper is called the base of the damper.

The equations of motion of the system are:

$$M\ddot{x}_2 + c(\dot{x}_2 - \dot{x}_1) + k_2(x_2 - x_0) = 0 \qquad (5)$$

$$c(\dot{x}_2 - \dot{x}_1) = k_1(x_1 - x_0) \qquad (6)$$

where: $\dot{x}_1$ = the absolute velocity of the base of the damper

x_1 = the absolute displacement of the base of the damper

k_1 = the elastic mount spring stiffness

Equation (5) represents the forces which are exerted on the mass. The force acting on the base of the viscous damper are given in equation (6). It can be seen from the latter equation that the damper force, $c(\dot{x}_2 - \dot{x}_1)$, is limited to that produced by the elastic mount spring k_1. Defining

$$N = \frac{k_2}{k_1}, \text{ elastic coupling ratio} \qquad (7)$$

and substituting ω_n, ξ and N as defined in equations (2), (3) and (7) results in the following equations:

$$\ddot{x}_2 + 2\xi\omega_n(\dot{x}_2 - \dot{x}_1) + \omega_n^2(x_2 - x_0) = 0 \qquad (8)$$

$$\dot{x}_2 - \dot{x}_1 = \frac{\omega_n}{2\xi N}(x_1 - x_0) \qquad (9)$$

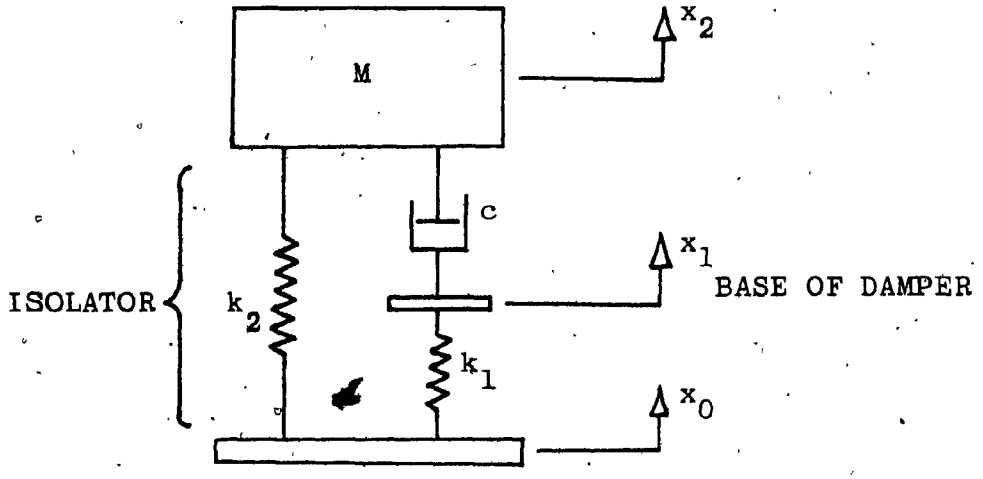

FIGURE 2: Schematic of the Elastically Coupled Viscous Isolator System Type 1.

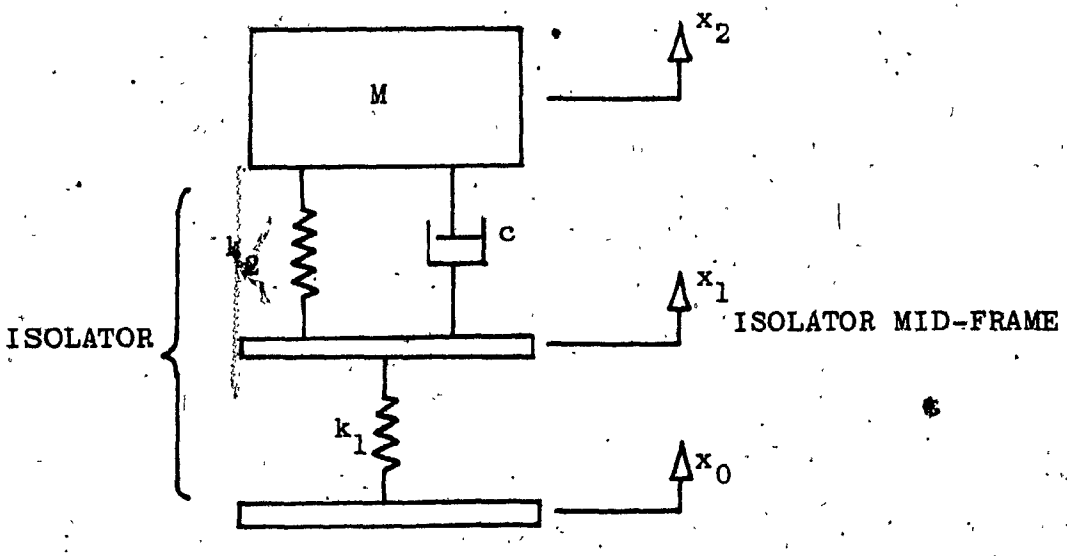

FIGURE 3: Schematic of the Elastically Coupled Viscous Isolator System Type 2.

2.1.3 ELASTICALLY COUPLED VISCOUS ISOLATOR TYPE 2 (ECVI-2)

The type 2 elastically coupled viscous damped isolator (ECVI-2) system is shown schematically in Figure 3. It is essentially a directly coupled viscous isolator which is elastically connected to the base by means of the spring k_1. The junction of k_1 to the rest of the isolator is denoted as the isolator mid-frame, and has its motion described by the variable x_1. In this investigation, the isolator mid-frame is assumed to have no mass.

The equations of motion of the system are:

$$M\ddot{x}_2 + c(\dot{x}_2-\dot{x}_1) + k_2(x_2-x_1) = 0 \tag{10}$$

$$c(\dot{x}_2-\dot{x}_1) + k_2(x_2-x_1) = k_1(x_1-x_0) \tag{11}$$

It can be seem from equation (11) that the elastic coupling spring k_1 acts to limit the force which can be transmitted to the rest of the system. Substituting ω_n, ξ and N into equations (10) and (11):

$$\ddot{x}_2 + 2\xi\omega_n(\dot{x}_2-\dot{x}_1) + \omega_n^2(x_2-x_1) = 0 \tag{12}$$

$$\dot{x}_2-\dot{x}_1 = \frac{\omega_n}{2\xi}\left[\frac{(x_1-x_0)}{N} - (x_2-x_1)\right] \tag{13}$$

2.1.4 COMPARISON OF ECVI TYPES 1 AND 2 [1]

Assuming that the system is initially at rest, the Laplace transformation of the equations of motion (5) and (6) for the ECVI-1 system are:

$$M\bar{x}_2s^2 + c(\bar{x}_2-\bar{x}_1)s + k_2(\bar{x}_2-\bar{x}_0) = 0 \tag{14}$$

$$c(\bar{x}_2-\bar{x}_1)s = k_1(\bar{x}_1-\bar{x}_0) \tag{15}$$

where S = Laplacian operator

$\bar{x}_i$ = transformed variable, $i = 0,1,2$

Algebraically combining equations (14) and (15) to eliminate the variable $\bar{x}_1$, and taking the inverse Laplace transform of the result gives the following equation of motion:

$$N\left[\frac{Mc}{k_2}\right]\dddot{x}_2 + M\ddot{x}_2 + c(1+N)(\dot{x}_2-\dot{x}_0)+k_2(x_2-x_0) = 0 \qquad (16)$$

where $\dddot{x}_2$ = rate of change of the acceleration of the mass, or "jerk"

In a similar manner, the following equation of motion for the ECVI-2 system can be derived:

$$\left(\frac{N}{1+N}\right)\left(\frac{Mc'}{k_2'}\right)\dddot{x}_2 + M\ddot{x}_2 + c'\left(\frac{1}{1+N}\right)(\dot{x}_2-\dot{x}_0)+k_2'\left(\frac{1}{1+N}\right)(x_2-x_0) = 0 \qquad (17)$$

The primed parameters are used to denote the type 2 elastically coupled system. By equating the co-efficients of like terms in the two differential equations (16) and (17), the conditions for dynamic equivalence of the ECVI type 1 and 2 systems are found to be:

$$k_2' = k_2(1+N) \qquad (18)$$

$$c' = c(1+N)^2 \qquad (19)$$

This thesis, however, considers both the types 1 and 2 isolators, to study the effects of varying the elastic coupling, directly, while keeping k_2 and c constant.

2.2 COULOMB FRICTION DAMPED ISOLATORS

2.2.1 DIRECTLY COUPLED FRICTION ISOLATOR (DCFI)

Figure 4 shows the schematic diagram of a directly coupled coulomb friction damped isolator system. The isolator in this system consists of a coulomb friction damper F, in parallel with a return spring k_2.

The coulomb damper is represented as a constant resistive force which acts to oppose motion across the damper. Its characteristic is shown in Figure 5.

The equation of motion of the system is:

$$M\ddot{x}_2 + F \operatorname{sgn}(\dot{x}_2-\dot{x}_0) + k_2(x_2-x_0) = 0 \qquad (20)$$

where F = magnitude of the coulomb friction.

and sgn = Signum function; $\operatorname{sgn}(x) = +1 \quad x>0$

$\qquad\qquad\qquad\qquad\qquad\qquad\qquad\qquad\quad -1 \quad x<0$

It can be seen from equation (20) that for low inertia forces $M\ddot{x}_2$, the coulomb friction may exceed the spring force. When this occurs the isolator "locks up" and behaves as a rigid connection between the mass and the base.

Defining: $\alpha = \frac{F}{k_2 X_{in}}$, nondimensional coulomb damping (21)

where; X_{in} = the maximum value of the isolator's base displacement

and substituting into equation (20):

$$\ddot{x}_2 + \alpha X_{in}\omega_n^2 \operatorname{sgn}(\dot{x}_2-\dot{x}_0) + \omega_n^2(x_2-x_0) = 0 \qquad (22)$$

The sharp nonlinearity in the coulomb damping force around the zero velocity point is found to introduce numerical problems in the digital simulation of the system [13]. To overcome this difficulty, a slightly modified friction characteristic can be implemented using a narrow linear viscous band of damping as shown in Figure 6.

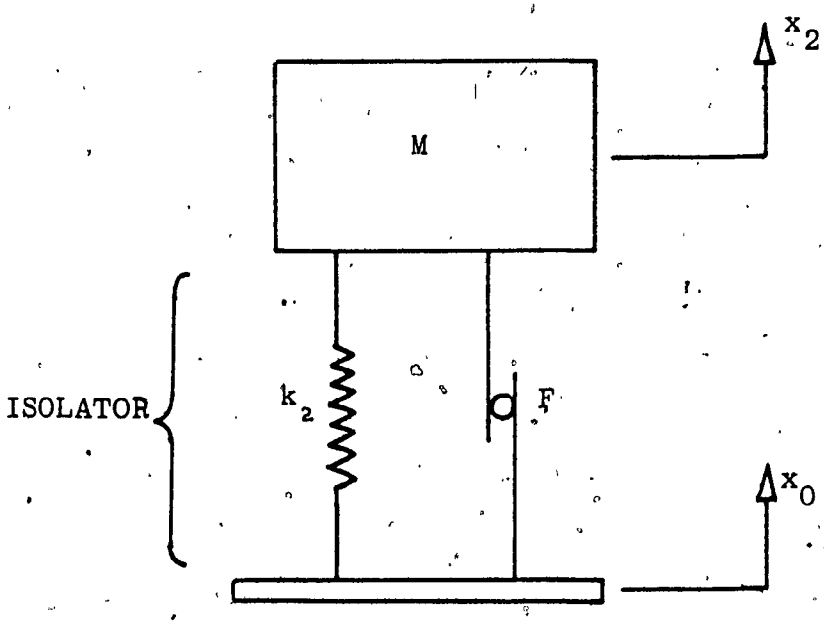

FIGURE 4: Schematic of the Directly Coupled Coulomb Friction Isolator System

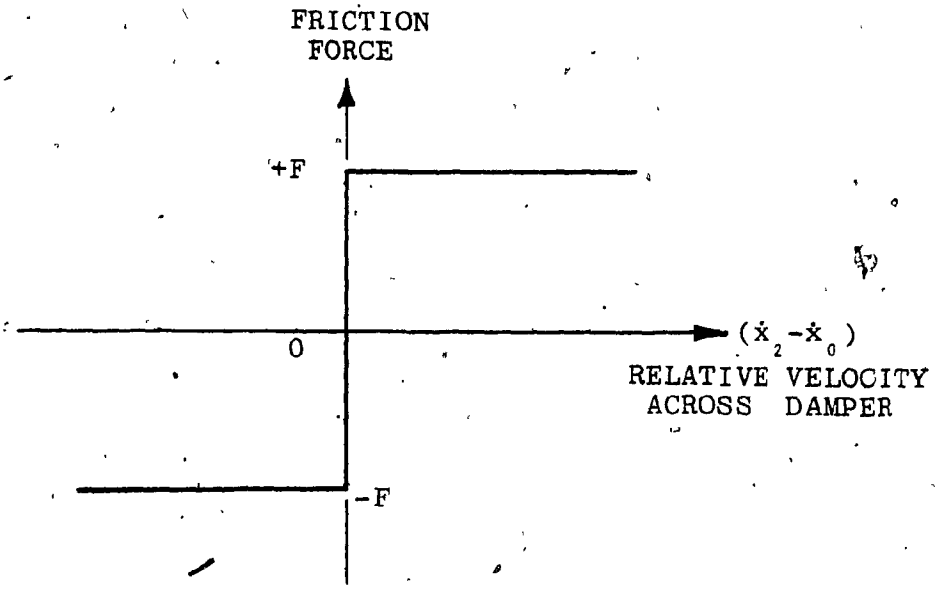

FIGURE 5: Ideal Coulomb Friction Characteristic

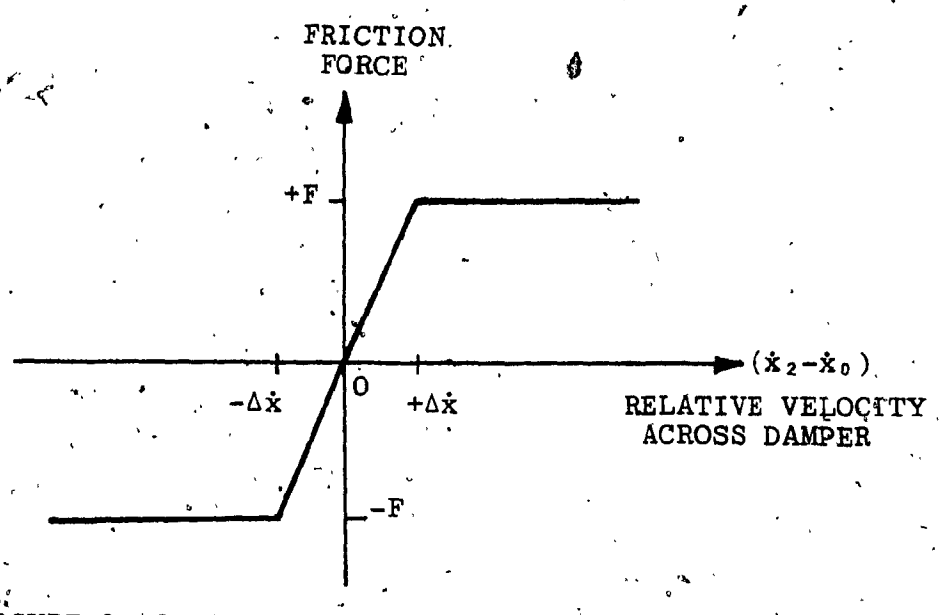

FIGURE 6: Coulomb Friction Characteristic with a Linear Viscous Band

This characteristic is useful in stabilizing the model under conditions of free oscillations, particularily for large values of α, and in simulating lock-up. As shown in Appendix A, the linear viscous band used did not influence the maximum values of acceleration or relative displacement. However, it is important that the size of the band should not be too large, as this may cause the model to behave more like a viscously damped isolator.

The equation of motion for the isolator when it is within the linear band can be expressed as:

$$\ddot{x}_2 + \frac{\alpha \chi_{in} \omega_n^2}{\Delta \dot{x}} (\dot{x}_2 - \dot{x}_0) + \omega_n^2 (x_2 - x_0) = 0 \qquad (23)$$

when $|(\dot{x}_2 - \dot{x}_0)| < \Delta \dot{x}$

where: $\pm \Delta \dot{x}$ = the limits of the linear viscous band.

Heller et al. [13] have proposed a different method to overcome the difficulties encountered in the digital simulation of coulomb damped isolator systems. They modelled the coulomb damper as a massless friction slider which was connected by means of a very stiff spring to the mass of a single degree of freedom system. The spring was used to simulate forces at the friction interface which were below the breakout level. They investigated the model under conditions of sinusoidal excitations and concluded that the model gave accurate results when compared to the exact solutions of Den Hartog [15].

In this thesis, the Coulomb friction damping for the DCFI system is modelled with a narrow linear viscous band of damping.

2.2.2 ELASTICALLY COUPLED FRICTION ISOLATOR TYPE 1 (ECFI-1)

Figure 7 shows the schematic diagram of the type-1 elastically coupled coulomb friction isolator system. Its configuration is the same as the ECVI-1 system shown in Figure 2 except that the viscous damper is replaced by the friction damper F.

Like the DCFI system, this system also exhibits a lock-up phenomenon. For no lock-up, the equations of motion of the system are:

$$M\ddot{X}_2 + F\,\mathrm{sgn}(\dot{x}_2-\dot{x}_1) + k_2(x_2-x_0) = 0 \qquad (24)$$

$$F\,\mathrm{sgn}\,(\dot{x}_2-\dot{x}_1) = k_1(x_1-x_0) \qquad (25)$$

Similar to the ECVI-1 system, there are two equations: one for the mass and another for the base of the damper. Substituting for ω_n, α and N and re-arranging:

$$\ddot{x}_2 + \alpha X_{in}\omega_n^2\,\mathrm{sgn}(\dot{x}_2-\dot{x}_1) + \omega_n^2(x_2-x_0) = 0 \qquad (26)$$

$$\dot{x}_1 = \dot{x}_0 + \alpha X_{in}N \qquad (\dot{x}_2-\dot{x}_1) > 0 \qquad (27)$$

$$\dot{x}_1 = \dot{x}_0 - \alpha X_{in}N \qquad (\dot{x}_2-\dot{x}_1) < 0 \qquad (28)$$

From equations (27) and (28) it can be seen that the base of the friction damper, x_1, has only two positions relative to the isolator base: either at $+\alpha X_{in}N$, or at $-\alpha X_{in}N$.

Differentiating equations (27) and (28):

$$\dot{x}_1 = \dot{x}_0 \qquad (29)$$

Hence as long as there is no lock-up the base of the damper follows the motion of the isolator base exactly.

Equation (25) shows that lock-up will occur when the elastic coupling spring force is less than the coulomb friction.

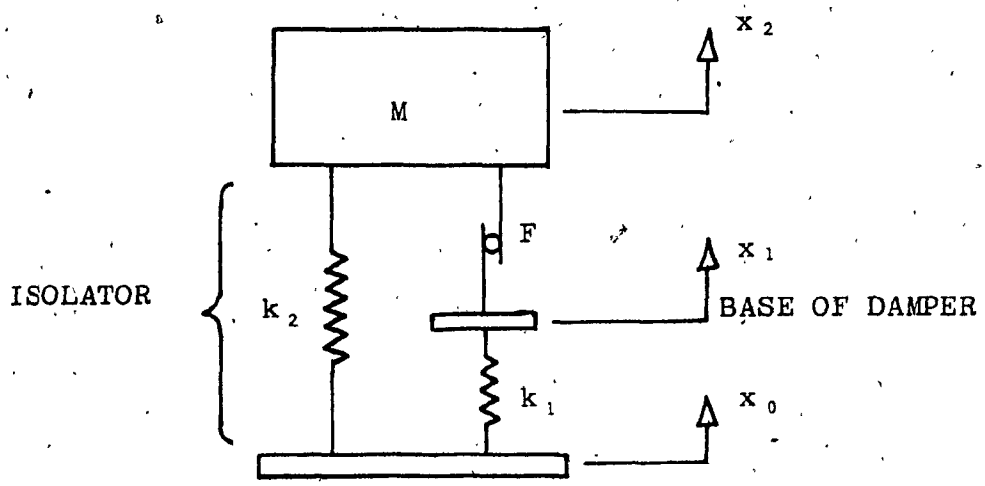

FIGURE 7: Schematic of the Elastically Coupled Coulomb Friction Isolator System Type 1

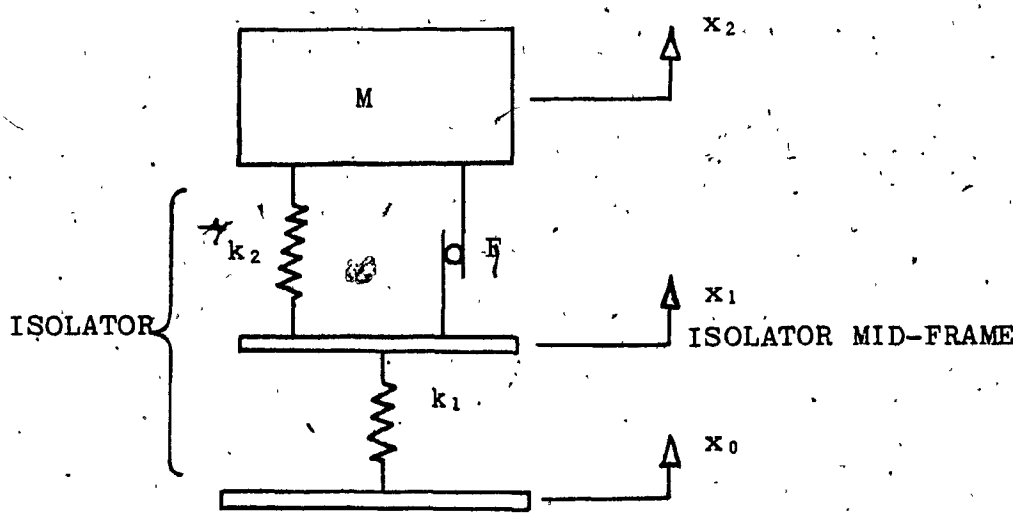

FIGURE 8: Schematic of the Elastically Coupled Coulomb Friction Isolator System Type 2.

Rewriting the equation (25) in terms of α, X_{in} and N, the lock-up condition is given as: $|x_1 - x_0| < \alpha X_{in} N$ (30)

During lock-up, the base of the damper is fixed to the mass rigidly.

Hence: $x_1 = x_2$ and $\dot{x}_1 = \dot{x}_2$ (31)(32)

The equation of motion of the mass is then:

$$M\ddot{x}_2 + k_2(x_2-x_0) + k_1(x_2-x_0) = 0$$

$$\text{or: } \ddot{x}_2 + \omega_n^2 \left(1 + \frac{1}{N}\right)(x_2-x_0) = 0 \quad (33)$$

Equation (33) shows that during lock-up the system is undamped and oscillates at the locked natural frequency, ω_{lock}, determined by the two springs:

$$\omega_{lock} = \omega_n \sqrt{1 + \frac{1}{N}} \quad (34)$$

2.2.3 ELASTICALLY COUPLED FRICTION ISOLATOR TYPE 2 (ECFI-2)

The type 2 elastically coupled coulomb friction isolator system is shown in Figure 8. It has the same configuration as the ECVI-2 system shown in Figure 3 except that the coulomb friction damper F is used as the energy dissipating device. Due to the coulomb damper, this isolator system also has a lock-up phenomenon. When the damper is not locked, the equations of motion of the system are:

$$M\ddot{x}_2 + F\,\mathrm{sgn}(\dot{x}_2-\dot{x}_1) + k_2(x_2-x_1) = 0 \quad (35)$$

$$k_2(x_2-x_1) + F = k_1(x_1-x_0) \qquad (\dot{x}_2-\dot{x}_1) > 0 \quad (36)$$

$$k_2(x_2-x_1) - F = k_1(x_1-x_0) \qquad (\dot{x}_2-\dot{x}_1) < 0 \quad (37)$$

Equation (35) represents the forces acting directly on the mass; equations (36) and (37), the forces on the isolator mid-frame. Substituting ω_n, α and N and re-arranging equations (35-37) :

$$\ddot{x}_2 + \alpha X_{in}\omega_n^2(\text{sgn}[\dot{x}_2-\dot{x}_1]) + \omega_n^2(x_2-x_1) = 0 \qquad (38)$$

$$x_1 = \frac{1}{N+1}\,[+\alpha N X_{in} + Nx_2 + x_0] \quad (\dot{x}_2-\dot{x}_1) > 0 \qquad (39)$$

$$x_1 = \frac{1}{N+1}\,[-\alpha N X_{in} + Nx_2 + x_0] \quad (\dot{x}_2-\dot{x}_1) < 0 \qquad (40)$$

Differentiating equations (39) and (40):

$$\dot{x}_1 = \frac{N\dot{x}_2 + \dot{x}_0}{(N+1)} \qquad (41)$$

Equations (39) and (40) show that there are two conditions for the lock-up of the damper, depending on the relative velocity between the mass and the isolator mid-frame. The lock-up conditions are:

$$[\tfrac{1}{N}(x_1-x_0) - (x_2-x_1)] < \alpha X_{in} \quad (\dot{x}_2-\dot{x}_1) > 0 \qquad (42)$$

$$[-\tfrac{1}{N}(x_1-x_0) + (x_2-x_1)] < \alpha X_{in} \quad (\dot{x}_2-\dot{x}_1) < 0 \qquad (43)$$

It can be seen from equations (42) and (43) that as the degree of elastic coupling is increased, that is for large values of N, the first term of the equations, $\frac{1}{N}(x_1-x_0)$, becomes small and hence is less effective in unlocking the coulomb damper.

During lock-up, the damper rigidly connects the mass to the isolator mid-frame and bypasses the primary mount spring, k_2. The equations of motion are then:

$$\ddot{x}_2 + \frac{\omega_n^2}{N}(x_1-x_0) = 0 \qquad (44)$$

$$\dot{x}_1 = \dot{x}_2 \qquad (45)$$

Equation (45) represents the locked mid-frame. Equation (44) shows the system is undamped during lock-up. The locked natural frequency is:

$$\omega_{lock} = \frac{\omega_n}{\sqrt{N}} \qquad (46)$$

2.2.4 COMPARISON OF ECFI-1 AND ECFI-2 [1]

The equations of motion for the ECFI-1 system for no lock-up were given in Sec. 2.2.2 as:

$$M\ddot{x}_2 + F\ \mathrm{sgn}\ (\dot{x}_2-\dot{x}_1) + k_2(x_2-x_0) = 0 \tag{47}$$

$$F\ \mathrm{sgn}\ (\dot{x}_2-\dot{x}_1) = k_1(x_1-x_0) \tag{48}$$

Substituting equation (48) into (47), re-arranging to solve for x_1 and differentiating gives:

$$\dot{x}_1 = \dot{x}_0 - (\frac{k_2}{k_1})(\dot{x}_2-\dot{x}_0) - M\ddot{x}_2 \tag{49}$$

Substituting (49) into (47) results in the following equation for the ECFI-1 system:

$$M\ddot{x}_2 + F\ \mathrm{sgn}\ [(1+N)(\dot{x}_2-\dot{x}_0) + N(\frac{M}{k_2})\dddot{x}_2] + k_2(x_2-x_0) = 0 \tag{50}$$

In a similar manner, $\dot{x}_1$ can be eliminated from the equations of motion of the ECFI-2 system to give:

$$M\ddot{x}_2 + (\frac{1}{1+N})F'\mathrm{sgn}[(1+N)(\dot{x}_2-\dot{x}_0) + (1+N)(N)(\frac{M}{k_2'})\dddot{x}_2]$$

$$+ k_2'(\frac{1}{1+N})(x_2-x_0) = 0 \tag{51}$$

The primed parameters denote the type 2 elastically coupled system. Comparing the co-efficients of like terms of equations (50) and (51) gives the following conditions for the dynamic equivalence between the ECFI-1 and ECFI-2 systems:

$$k_2' = k_2\ (1+N) \tag{52}$$

$$F' = F\ \ (1+N) \tag{53}$$

2.3 COMBINED VISCOUS/COULOMB DAMPED ISOLATOR (CVFI)

Figure 9 shows the schematic diagram of a combined viscous and coulomb friction (CVFI) damped isolator system. The isolator comprises a return spring k_2 and a series combination of a viscous damper c,

and a coulomb damper F. The junction between the two dampers is denoted as the isolator mid-frame and its motion is described by the variable x_1.

As in the other coulomb damped isolator systems, the CVFI system possesses a lock-up phenomenon. For no lock-up of the coulomb damper, the equations of motion are:

$$M\ddot{x}_2 + F\ \mathrm{sgn}\ (\dot{x}_2-\dot{x}_1) + k_2(x_2-x_0) = 0 \tag{54}$$

$$F\ \mathrm{sgn}\ (\dot{x}_2-\dot{x}_1) = c(\dot{x}_1-\dot{x}_0) \tag{55}$$

From these two equations, it can be seen that the transmitted force from the viscous damper to the mass is limited by the action of the coulomb friction device.

Substituting α, ξ and ω_n and re-arranging:

$$\ddot{x}_2 + \omega_n^2\ (x_2-x_0) + \alpha X_{in}\omega_n^2 \mathrm{sgn}(\dot{x}_2-\dot{x}_1) = 0 \tag{56}$$

$$\dot{x}_1 = \dot{x}_0 + \left[\frac{\alpha\omega_n X_{in}}{2\xi}\right] \mathrm{sgn}\ (\dot{x}_2-\dot{x}_1) \tag{57}$$

From equation (55) it can be seen that lock-up of the coulomb damper occurs when the viscous damper does not generate sufficient force to overcome the breakout friction. The lock-up condition is found to be:

$$|\dot{x}_1 - \dot{x}_0| < \frac{\alpha\omega_n X_{in}}{2\xi} \tag{58}$$

During lock-up the isolator mid-frame becomes rigidly attached to the mass, and the isolator behaves like a DCVI system. The equations of motion are:

$$\ddot{x}_2 + 2\xi\omega_n(\dot{x}_1-\dot{x}_0) + \omega_n^2\ (x_2-x_0) = 0 \tag{59}$$

$$\dot{x}_1 = \dot{x}_2 \tag{60}$$

(This thesis does not consider the combined isolator having the viscous and coulomb dampers in parallel, as this system could lock-up the mass to the base and might not return the mass to its zero position).

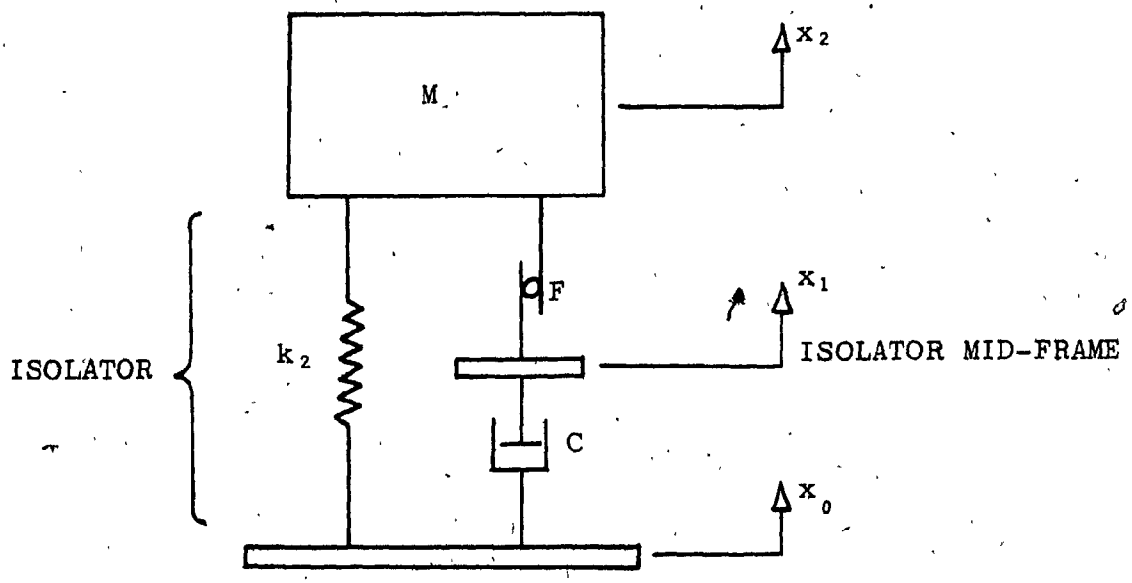

FIGURE 9: Schematic of the Combined Viscous and Coulomb Friction Isolator System

2.4 ADAPTIVE FRICTION DAMPING DEVICES

In a study of a combined viscous and friction damped isolator system [5], an adaptive friction device was proposed whereby the friction force was increased as a function of the relative displacement across the viscous stage of the isolator. This was achieved by pumping hydraulic fluid from the viscous damper to a brake device which would exert an additional friction force on the coulomb damper.

To see if any benefits in isolator performance could be derived from adaptive coulomb damping, a piecewise linear variation of the nondimensional coulomb friction α was investigated in this thesis. The variation was made a function of either the relative displacement or the relative velocity between the mass and the isolator base. Four types of adaptive friction dampers were investigated and were designated as 'displacement- increasing' friction (DIFI), 'displacement-decreasing' friction (DDFI), 'velocity-increasing' friction (VIFI),and 'velocity-decreasing' friction (VDFI). Their characteristics are shown in Figures 10 through 13.

The DIFI damper has a similar characteristic as the device proposed in ref. [5], though a different displacement parameter was used to regulate the friction force. The VDFI damper could be considered as an approximation to real life friction behaviour where there is a high static friction followed by a lower dynamic friction. The other two adaptive friction dampers might possibly be achieved from a semi-active system employing hydraulic components: however, no models for these devices are proposed in this thesis.

The equations for the adaptive friction are given below:

$$\alpha = \alpha_0 \qquad z \leq z_1 \tag{61}$$

$$\alpha = \alpha_0 + \alpha_f \psi z \qquad z_1 < z < z_2 \tag{62}$$

$$\alpha = \alpha_f \qquad z \geq z_2 \tag{63}$$

where α_0 = initial coulomb damping

α_f = final coulomb damping

z = $(x_2 - x_0)$ for displacement variable friction

z = $(\dot{x}_2 - \dot{x}_0)$ for velocity variable friction

z_1, z_2 = break points of z for constant friction

$\psi = \frac{(\alpha_f - \alpha_0)}{(z_2 - z_1)}$ slope of friction variation

Examining the equations for the friction isolators, it can be seen that both the equations of motion for the systems and the locking conditions are affected by the variable friction parameter α.

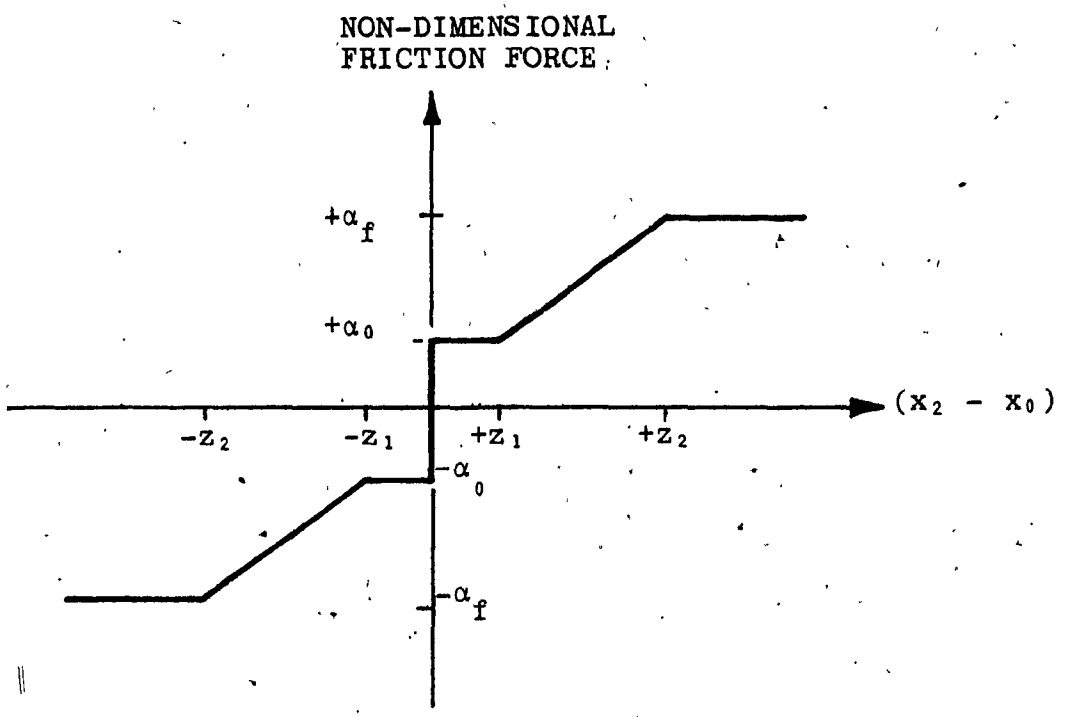

FIGURE 10: Coulomb Friction Characteristic for the Displacement-Increasing Friction Damper.

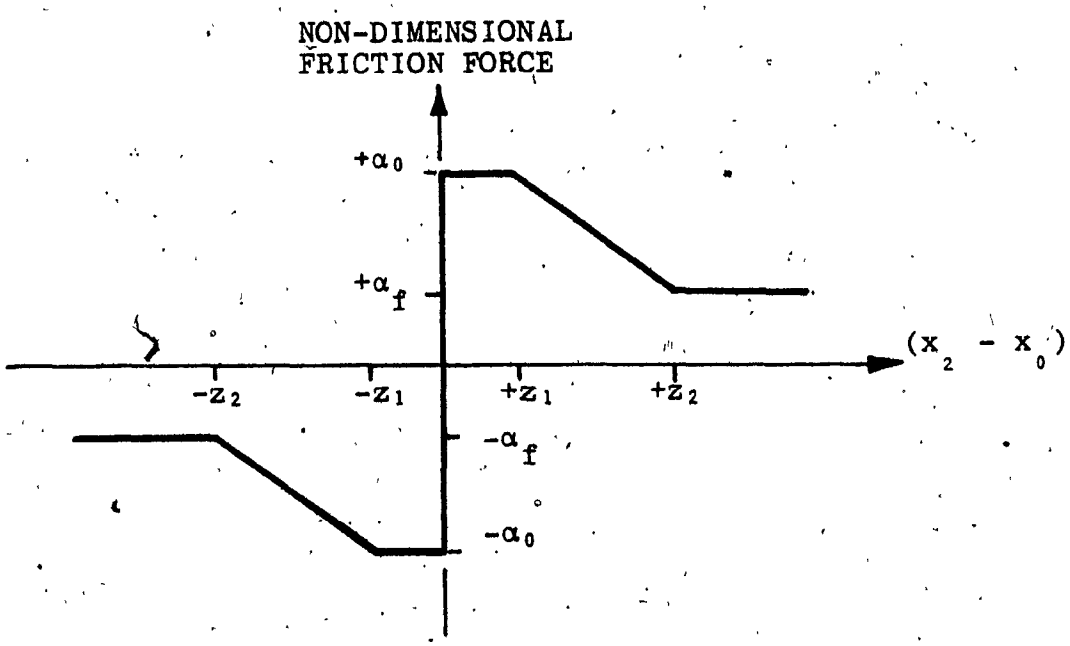

FIGURE 11: Coulomb Friction Characteristic for the Displacement-Decreasing Friction Damper.

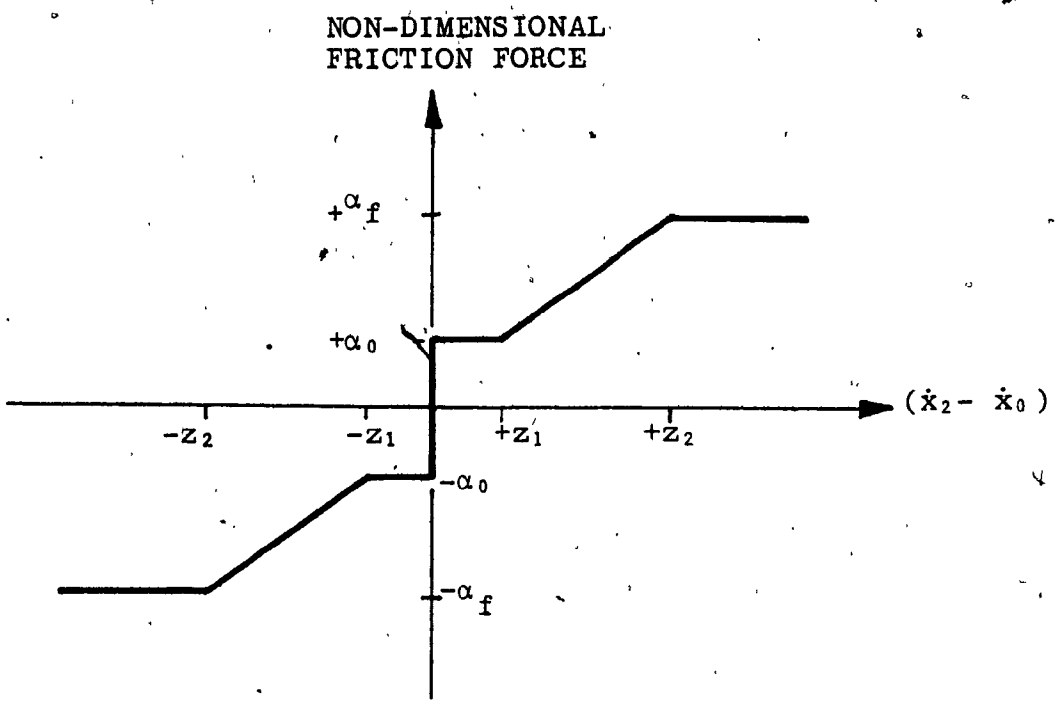

FIGURE 12: Coulomb Friction Characteristic for the Velocity-Increasing Friction Damper

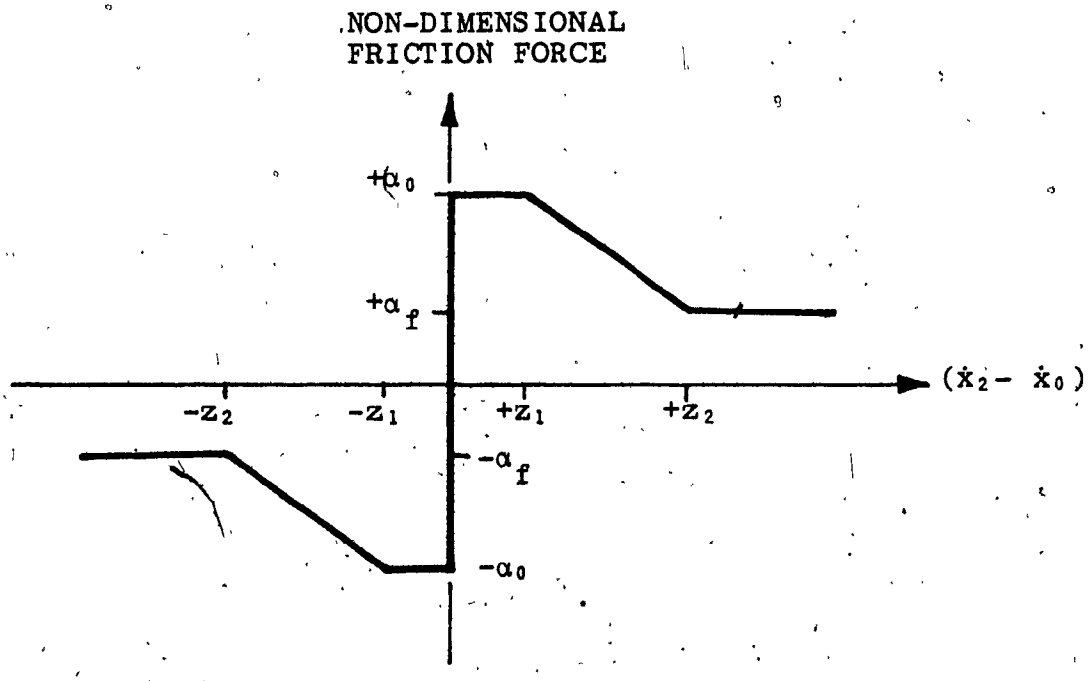

FIGURE 13: Coulomb Friction Characteristic for the Velocity-Decreasing Friction Damper

CHAPTER 3

BASE EXCITATION EQUATIONS

3.1 GENERAL BACKGROUND

Various types of transient base excitations which are described in terms of a time history of either force, acceleration, velocity or displacement, have been employed in the study of shock isolator systems. Acceleration time histories that are in the form of well defined pulse shapes, such as rectangular, saw-toothed, triangular, sine and versed sine pulses, are often used [8]. On the other hand, some studies [5], subject the system to complex shock pulses, consisting of several acceleration peaks, in order to better simulate the real environment.

When a system which has an initial velocity impacts the ground, causing its velocity to drop to zero in some prescribed function of time (such as during the landing of an aircraft), the base input is often modelled as a velocity pulse. In [7,12] an instantaneous step velocity pulse was used, whereas in [4] the effects due to rounded saw-tooth and step velocities were studied.

Displacement shocks occur when there is a sudden change in the position of the support foundation, such as when an automobile experiences a sudden depression in the road. In [2,3] various displacement inputs in the form of rounded pulses and steps, and oscillatory steps, were used. In this thesis, two displacement excitations are employed: the rounded pulse and the oscillatory pulse.

3.2 ROUNDED PULSE DISPLACEMENT

The rounded pulse applies a sudden displacement to the isolator base to a maximum value X_{in}, after which the base is returned to its original position at a somewhat lesser rate. The equations of the pulse are:

$$x_0(t) = 0 \qquad t \leq 0 \tag{64}$$

$$x_0(t) = X_{in}(e^2/4)(\nu\omega_n t)^2 e^{-(\nu\omega_n t)} \qquad t > 0 \tag{65}$$

where: X_{in} = the maximum displacement of the pulse

ν = the pulse severity

$e = 2.71828$

The severity of the pulse is defined in terms of duration of the pulse and the half period of the system's natural frequency:

$$\nu = (\frac{T}{2})/\tau = \frac{\pi}{\omega_n \tau} \tag{66}$$

where: $\frac{T}{2}$ = the half period of ω_n

τ = the duration of the pulse and is equal to the duration of an equivalent rectangular pulse of the same area but having a maximum displacement 17.6% greather than X_{in}.

The corresponding equations for the velocity and acceleration of the pulse are:

$$\dot{x}_0(t) = 0 \qquad t \leq 0 \tag{67}$$

$$\ddot{x}_0(t) = 0 \qquad t \leq 0 \tag{68}$$

and,

$$\dot{x}_0(t) = \omega_n X_{in} \left[(\frac{e^2\nu}{4})(e^{-\nu\omega_n t}) \times (2\nu\omega_n t - [\nu\omega_n t]^2) \right] \qquad t > 0 \tag{69}$$

$$\ddot{x}_0(t) = \omega_n^2 X_{in} \left[(\frac{e^2\nu^2}{2})(e^{-\nu\omega_n t}) \times (1 - 2\nu\omega_n t + \frac{1}{2}[\nu\omega_n t]^2) \right] \qquad t > 0 \tag{70}$$

Figure 14 shows the time histories of the normalized rounded pulse displacement, velocity and acceleration for $\nu = 5$. It can be seen that the base motion quantities are smooth, finite and continuous for all time values greater than zero.

3.3 OSCILLATORY PULSE DISPLACEMENT

In many shock situations the base disturbance does not consist of a single step or pulse, but rather, of a number of oscillations. An oscillatory step displacement was used in ref. [3] which was likened to that of an abrupt transient step which had been "filtered" by a resilient foundation prior to being applied to the isolator base. Three shock pulses of highly oscillating, varying amplitude accelerations were measured onboard a ship subjected to underwater explosions, and were used as base excitations of an adaptive isolator system [5]. With these studies in mind, an oscillatory pulse displacement was derived in order to investigate the effects of multiple base disturbances. The pulse is basically a seven peak oscillation, consisting of a series of four high frequency, constant amplitude peaks, followed by three exponentially decaying peaks of lower frequency. The equations of the pulse are:

$$x_0(t) = \frac{1}{2} X_{in} [1 - \cos \omega_1 t] \qquad 0 \leq t \leq T_1 \qquad (71)$$

$$x_0(t) = X_{in} [\cos \omega_2 (t-T_1)] \qquad T_1 < t \leq T_2 \qquad (72)$$

$$x_0(t) = X_{in} \begin{bmatrix} \cos \omega_3 (t-T_2) \\ (1-e^{-\beta\omega_3 (t-T_2)}) \end{bmatrix} \qquad T_2 < t \leq T_3 \qquad (73)$$

$$x_0(t) = XLAST [1 + \cos \omega_3 (t-T_3)] \qquad T_3 < t \leq T_4 \qquad (74)$$

$$x_0(t) = 0 \qquad t > T_4 \qquad (75)$$

where: $\omega_1 = 2\nu\omega_n$ $\quad T_1 = \frac{\pi}{\omega_1}$

$\omega_2 = \nu\omega_n$ $\quad T_2 = 13\frac{1}{2}\ T_1$

$\omega_3 = \frac{1}{4}\nu\omega_n$ $\quad T_3 = 61\ T_1$

$T_4 = 69\ T_1$

β = decay rate of the lower frequency oscillations

XLAST = amplitude of $x_0(t)$ at $t = T_3$

The pulse severity ν is defined as the ratio of the frequency of the pulse's initial oscillation ω_2 to the system's natural frequency ω_n. Figure 15 shows the time history of the pulse for $\nu = 5$.

The corresponding equations for the velocity of the pulse are:

$$\dot{x}_0(t) = \frac{1}{2} X_{in}\omega_1[\sin \omega_1 t] \qquad 0 \le t \le T_1 \qquad (76)$$

$$\dot{x}_0(t) = - X_{in}\omega_2[\sin \omega_2(t-T_1)] \qquad T_1 < t \le T_2 \qquad (77)$$

$$\dot{x}_0(t) = X_{in}\omega_3\left[\begin{matrix}-\sin \omega_3(t-T_2) \\ +e^{-\beta\omega_3(t-T_2)}\sin \omega_3(t-T_2) \\ +\beta e^{-\beta\omega_3(t-T_2)}\cos \omega_3(t-T_2)\end{matrix}\right] \quad T_2 < t \le T_3 \qquad (78)$$

$$\dot{x}_0(t) = \text{XLAST}\ [\omega_3 \sin \omega_3(t-T_3)] \qquad T_3 < t \le T_4 \qquad (79)$$

$$\dot{x}_0(t) = 0 \qquad t > T_4 \qquad (80)$$

The acceleration equations for the pulse are:

$$\ddot{x}_0(t) = \frac{1}{2} X_{in}\omega_1^2[\cos \omega_1 t] \qquad 0 \le t \le T_1 \qquad (81)$$

$$\ddot{x}_0(t) = - X_{in}\omega_2^2[\cos \omega_2(t-T_1)] \qquad T_1 < t \le T_2 \qquad (82)$$

$$\ddot{x}_0(t) = X_{in}\omega_3^2\left[\cos\omega_3(t-T_2)+e^{-\beta_3\omega_3(t-T_2)}\times\left[\begin{matrix}(1-\xi^2)\cos \omega_3(t-T_2) \\ (1+\xi)\sin \omega_3(t-T_2)\end{matrix}\right]\right] \quad T_2 < t \le T_3 \qquad (83)$$

$$\ddot{x}_0(t) = - \text{XLAST} \left[\omega_3^2 \cos \omega_3 (t-T_3)\right] \qquad T_3 < t \leq T_4 \qquad (84)$$

$$\ddot{x}_0(t) = 0 \qquad t > T_4 \qquad (85)$$

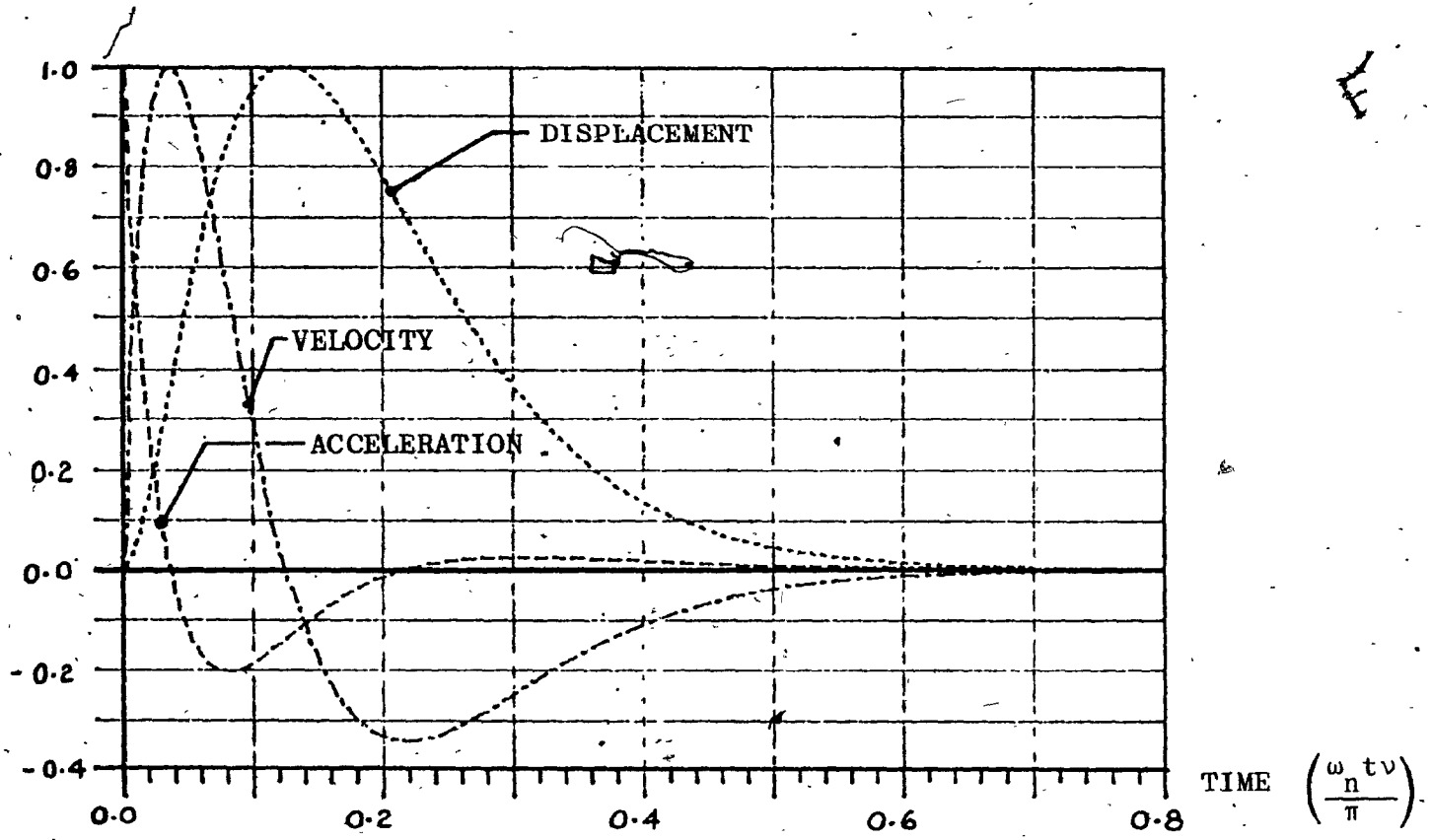

FIGURE 14: Rounded Pulse Displacement with its Corresponding Velocity and Acceleration ($\nu = 5$).

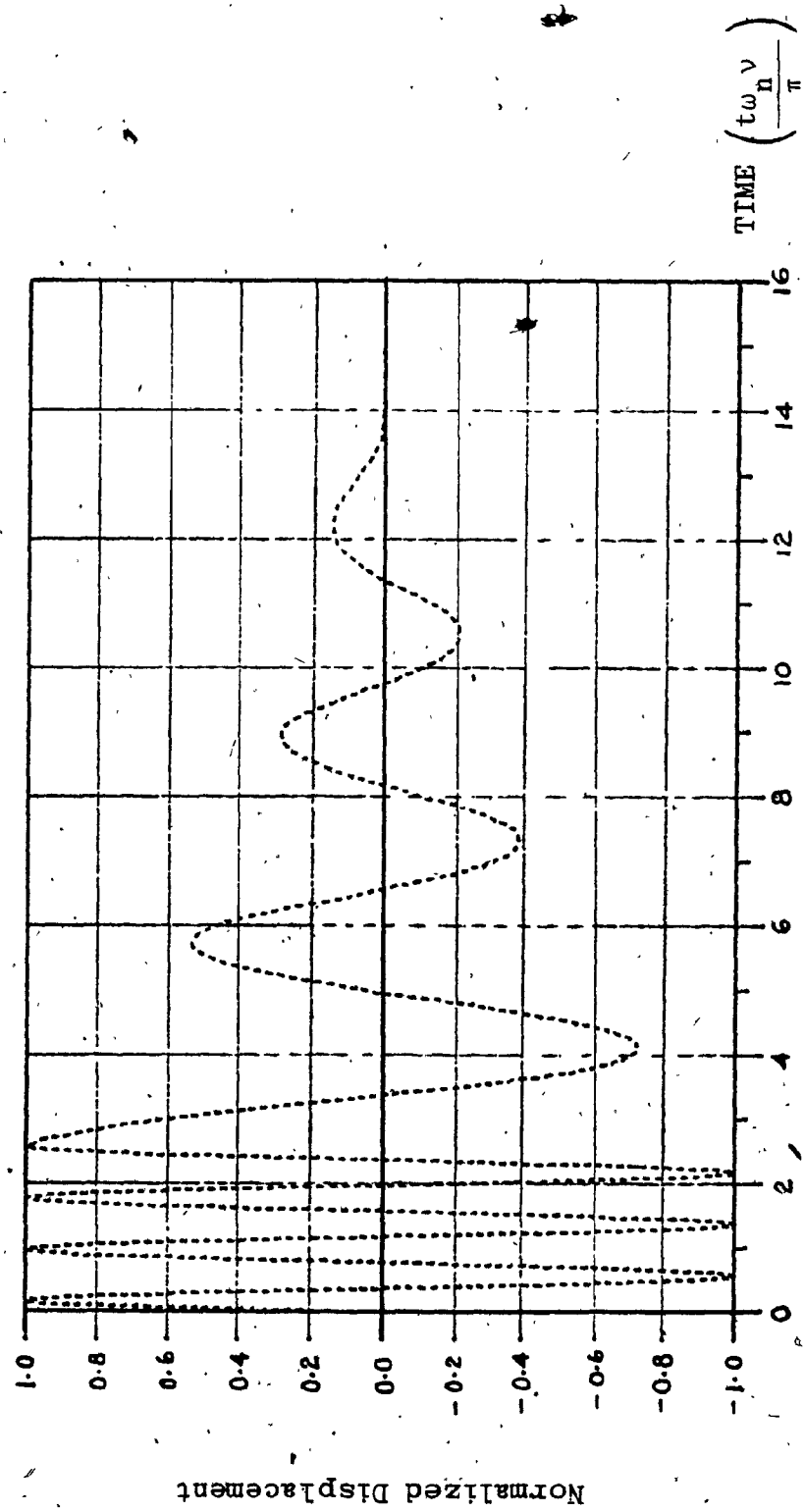

FIGURE 15: Oscillatory Pulse Displacement ($\nu = 5$).

CHAPTER 4

PERFORMANCE EVALUATION

4.1 PERFORMANCE CRITERIA OF ISOLATORS

To evaluate the effectiveness of an isolator, it is necessary to establish a performance criterion against which comparisons of different isolator systems can be made. An isolator's basic task is to reduce the base accelerations which are transmitted to the mass to be protected. This is achieved by allowing relative motion to occur across the isolator. The reduction of the base accelerations is important as the mass must be able to withstand without damage, the inertia forces which arise from the transmitted accelerations. On the other hand, physical considerations on the size and operating range of the isolator generally impose a maximum allowable relative displacement which can occur. It would be desirable to have an isolator which would produce both low transmitted acceleration and low relative displacements. However, it is more reasonable to expect that a trade-off exists between these two quantities. An isolator which is designed to transmit none of the base accelerations uses a large amount of space to absorb the base motions. However, an isolator which produces no relative motions (that is, one which rigidly connects the mass to the base) does not attenuate any base accelerations.

Various performance criteria for isolators based on the transmitted acceleration and relative displacement are found in the literature. In ref.[2] and [3], isolator performance was evaluated in terms of the shock acceleration ratio (SAR) and the relative displacement ratio (RDR). SAR was defined as the ratio of the maximum acceleration transmitted to the mass to the maximum acceleration of the base excitation. RDR was defined as the ratio of the maximum relative displacement experienced

by the isolator to the maximum amplitude of the base motion. Curves of SAR and RDR were plotted against the pulse severity ν for the various isolators. This type of presentation of isolator performance was not selected for this thesis as SAR does not allow for a direct comparison of the transmitted accelerations for different values of ν. Also the separate plots of SAR and RDR do not readily show the trade-off between acceleration and relative displacement.

A more direct manner of showing this trade-off is to plot the maximum acceleration experienced by the mass versus the maximum realtive displacement which occurred across the isolator. This type of plot was employed in many studies [4,7,9] and is used in this thesis. The plot is also useful in determining the sensitivity of the isolator's performance to changes in the parameters of the isolator or in the input excitation.

The maximum acceleration and maximum relative displacement are represented in this thesis as the non-dimensional quantities $\ddot{X}_2$ and RDR respectively, where:

$$\ddot{X}_2 = \frac{[\ddot{x}_2]_{max}}{X_{in}\,\omega_n^2} \tag{86}$$

$$RDR = \frac{[x_2 - x_0]_{max}}{X_{in}} \tag{87}$$

where $[\ ]_{max}$ denotes the maximum value of the bracketted variable which was experienced.

4.2 INFLUENCE OF TIME RESPONSE ON ISOLATOR PERFORMANCE

As outlined in the previous section, isolator performance is determined by two quantities: its maximum transmitted acceleration and its maximum relative displacement. However, there may be other criteria which are also important in determining isolator performance, such as how quickly the system returns to its equilibrium position after the external excitation has stopped. If a system is susceptible to damage due to cumulative accelerations, as in the case of metal fatigue, it may be desirable to reduce not only the maximum acceleration, but also any secondary acceleration peaks. Ref. [12] uses such a performance criterion. With these consideration in mind, the time responses of various selected isolators were examined to determine the effects of parameter variations.

CHAPTER 5

RESULTS AND DISCUSSION

5.1. METHOD OF CALCULATION

Three basic approaches can be used to solve the differential equations of motion of the isolator systems: they are analytical methods; analog simulation; and digital simulation. Analytical methods, either exact or approximate in form, can generally be applied only to simple systems subjected to simply defined excitations. Even so, the methods are often cumbersome to perform. Simulations using analog computers are able to handle larger sized systems, both linear and nonlinear, and are generally easy to implement. However set-up times are considered long due to requirements of hard-wiring and scaling. On the other hand, simulations of even large scale systems can generally run in a short time on a digital computer and the results can be stored for future use. Also optimization of system parameters can be easily accomplished using a digital computer. For these reasons, this last approach was taken to obtain the performance of the isolator systems.

Digital computer simulations use numerical methods which solve the equations of motion in small, discrete increments of time. One such method is the fourth-order Runge-Kutta technique, a description of which is given in Appendix B. This method was incorporated in a FORTRAN computer program which solved the equations of motion of the various isolator systems discussed in chapter 2 which were subjected to the base excitations of chapter 3. The program generated the time histories of the state variables and computed their maximum values which were used to evaluate the performance of the isolators. The program was written in an interactive mode which enabled the user to select any combination of isolator and excitation and to quickly run the simulation

and obtain the results. An iterating routine was also incorporated to permit studies of parameter sensitivity. Appendix C is a description on the use of the program and includes the terminal output from a typical computer run. A flowchart and listing of the program are given in Appendix D.

5.2 VISCOUS DAMPED ISOLATORS SUBJECTED TO ROUNDED PULSE BASE DISPLACEMENTS

Figures 16 through 22 are the performance curves of directly coupled, and types 1 and 2 elastically coupled viscous damped isolator systems, whose bases were subjected to rounded pulse displacements of various severities. Some typical time responses of selected systems are shown in figures 23 through 30.

5.2.1 PERFORMANCE OF THE DIRECTLY COUPLED VISCOUS ISOLATOR (DCVI)

Figure 16 shows the response of the DCVI having various degrees of damping and which was subjected to rounded pulse displacements of varying severities. Examining the curves of constant pulse severity, it is seen that for low severity (ν=1), the effect of increasing the damping ratio ξ was to decrease RDR, while $\ddot{X}_2$ was nearly independent of ξ. The opposite occurred for high pulse severity (ν=10) where $\ddot{X}_2$ markedly increased with higher damping while RDR was only slightly reduced. At intermediate severities, the influence of ξ was to trade-off RDR against $\ddot{X}_2$: by varying the damping, a greater or lesser maximum acceleration was transmitted to the mass, while the isolator sustained a corresponding smaller or larger maximum relative displacement.

Examining the curves of constant damping, it is seen that for low damping, the isolator's performance was nearly unaffected by pulse severity. However, at higher damping values $\ddot{X}_2$ and RDR increased directly with the pulse severity. The variations in $\ddot{X}_2$ and RDR were particularily high for (ξ=1.0).

In general it was found that the maximum transmitted acceleration increased with increases in either the pulse severity or damping ratio. Indeed the combination of both high severity and damping caused the viscous damper to become "stiff" and transmitted a large amount of the base acceleration to the mass. It was also found that RDR generally decreased with the damping ratio, the extent of which varied with the pulse severity. The best performance in terms of low RDR and $\ddot{X}_2$ was obtained with an isolator having high damping (ξ=1.0) and subjected to low severity pulse (ν=1). However this isolator gave high accelerations with increasing pulse severities.

5.2.2 PERFORMANCE OF ELASTICALLY COUPLED VISCOUS ISOLATORS (ECVI) TYPES 1 AND 2

Figures 17 and 18 show the influence of damping on the response of the ECVI types 1 and 2 systems subjected to rounded pulse base displacements. Generally their behaviours were similar to that of the DCVI system, in that at low pulse severity, the damping ratio primarily affected RDR, while at high severity, its influence was mainly on $\ddot{X}_2$. Table 1 shows a comparison of the three types of viscous isolators having the same damping ratio. It is seen that for (ν=1) the DCVI system had the lowest RDR. On the other hand, both ECVI types 1 and 2

systems had much less transmitted accelerations for higher values of ν for the same degree of viscous damping. This latter behaviour was due to the elastic coupling which by attenuating the base acceleration before it reached the damper, reduced the overall transmitted accelerations. In the ECVI type 2 system the elastic coupling also reduced the accelerations which were transmitted through the main isolator spring k_2, making it the most effective of the three configurations for reducing $\ddot{X}_2$ for a given amount of elastic coupling stiffness and damping ratio. However the penalty for this is an increase in the maximum relative displacement.

From Figures 17 and 18, it is seen that for the ECVI types 1 and 2 systems, at the lower pulse severities (ν=2 for types 1 and 2, and ν=3 for type 1), $\ddot{X}_2$ increased with increasing damping ratio, while RDR was found to decrease initially, reaching a minimum value, after which it increased with further increases in the damping. This behaviour in RDR can be explained by considering the equivalent viscous damping factor c_{eq}, and spring stiffness k_{eq}, of the system. It was shown in ref.[2] that for the ECVI type 1 system subjected to a sinusoidal base excitation having a frequency ω, the equivalent parameters c_{eq} and k_{eq} are given as:

$$c_{eq} = \frac{\omega c k_2}{k_2^2 k_1 + \omega^2 c^2 (k_1+k_2)} \qquad (88)$$

$$k_{eq} = \frac{k_1 k_2^2 + \omega^2 c^2 (k_1+k_2)}{k_2^2 + \omega^2 c^2} \qquad (89)$$

From equation (88) it can be shown that for either low or high values of ω, the system had zero equivalent damping. At intermediate values of ω, c_{eq} varied with ω and had a maximum value at the transition frequency ω_t, [2] where:

$$\omega_t = \frac{k_2}{c}\left[\frac{k_1}{k_1+k_2}\right]^{\frac{1}{2}} \qquad (90)$$

If one considered the rounded pulse as approximating a forced sinusoidal distrubance with a duration of one half a cycle, then it can be said in an analogous manner to the sinusoidal excitation, that for a ECVI type 1 system subjected to a rounded pulse, the equivalent damping of the system would vary with pulse severity. Maximum damping would occur when the duration of the rounded pulse matched the period of the transition frequency, which from equation (90), is dependent on the damping factor c. Hence, the minimum RDR response found for (ν=2) and (ν=3) correspond to the conditions of local maximum equivalent damping. Increasing or decreasing the viscous damping ratio caused a reduction in c_{eq} and thus increased RDR. For the higher pulse severities the transition frequency was not attained, so no minimum RDR phenomenon was observed. (Note that though equations (88) to (90) were derived for the ECVI type 1 system, the equations and above discussion are applicable to the ECVI type 2 system due to the dynamic equivalence of the two systems as given in section 2.1.4.).

Figures 19 and 20 show the influence of the elastic coupling N, on the response of ECVI types 1 and 2 systems subjected to rounded pulses of various severities, as compared to the response of a DCVI system.

It can be seen that the elastic coupling generally reduced the maximum transmitted acceleration while it increased the maximum relative displacement. Table 2 shows a comparison of the performance of the three types of viscous isolators for various values of the elastic coupling N, and the pulse severity ν. It is seen that at high severities, increasing N gave dramatic reductions in $\ddot{X}_2$ while only slightly increasing RDR. On the other hand, at low severities, increasing N only increased RDR, with little or no reductions in $\ddot{X}_2$.

The DCVI System (that is, N=0) gave the best performance for (ν=1) having the lowest values of RDR and $\ddot{X}_2$. However, it transmitted the highest acceleration with only a minor decrease in RDR for the case of (ν=10). As the amount of elastic coupling was increased, the differences between the performances at low and high pulse severities became smaller. This is desirable feature of an isolator system, as it can tolerate a wide variation in the severity of the base disturbance without degrading its performance. The penalty for this however, is high values of RDR.

As shown in Figure 19 there was a sudden increase of the RDR response of the ECVI type 1 at (ν=2). This was due to a resonant condition where the duration of the rounded pulse was approximately equal to half the natural period of the system.

Figures 21 and 22 show the combined influence of the elastic coupling ratio N and the viscous damping ratio ξ on the performance of the ECVI types1 and 2 subjected to a rounded pulse displacement (ν=5). It is seen that for 'stiff' elastic couplings (that is, low values of N), damping had a strong effect on the RDR and $\ddot{X}_2$ response, with high transmitted accelerations for large amounts of damping. However, for high values of

elastic coupling, the influence of damping was almost negligible and the transmitted accelerations were uniformly low. It can be seen that even moderate values of N gave remarkable reductions in $\ddot{X}_2$.

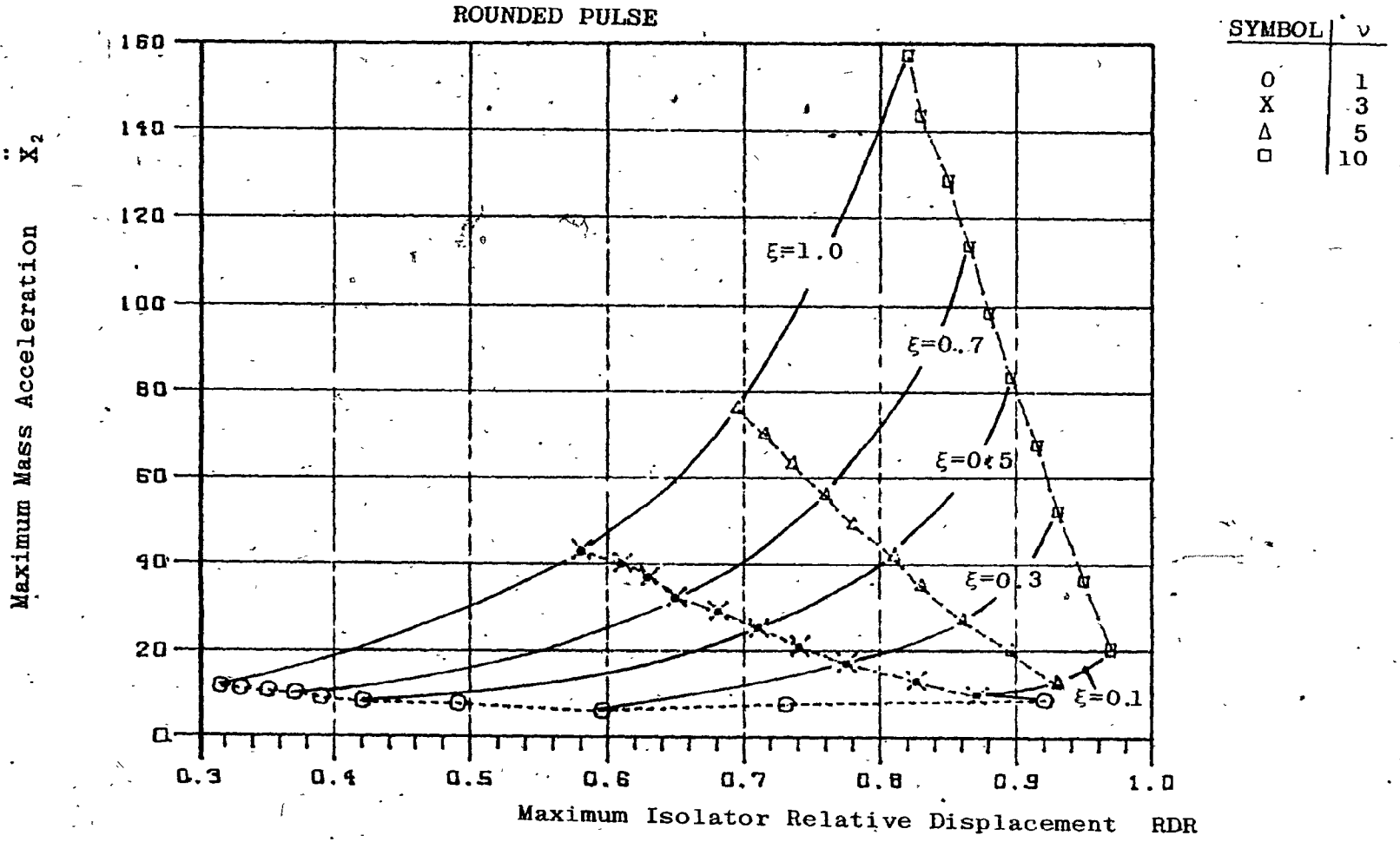

FIGURE 16: Performance of DCVI System for Various Damping Ratios ξ and Pulse Severities ν : $\omega_n = \pi$

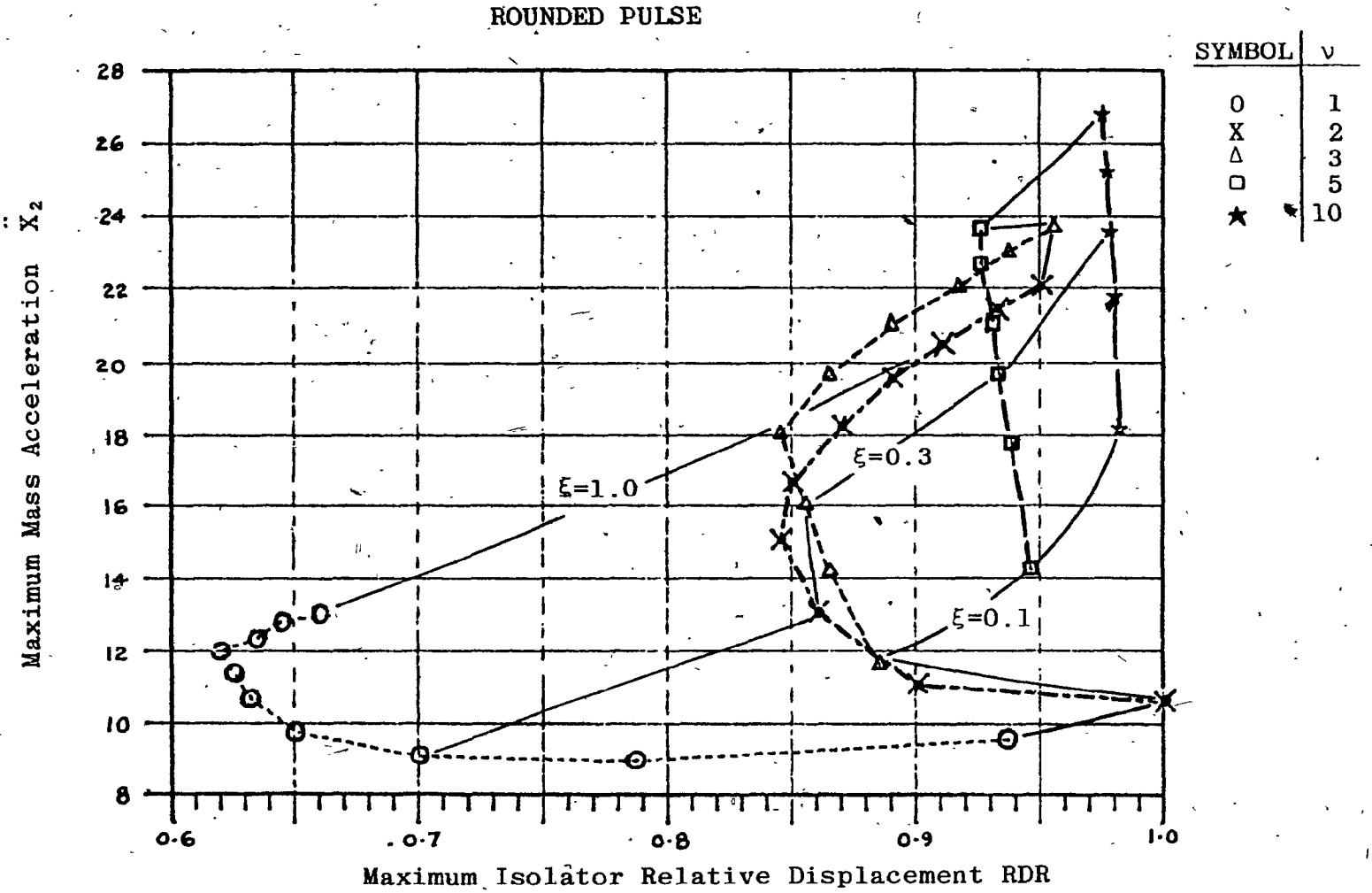

FIGURE 17: Performance of ECVI-1 System for Various Damping Ratios ξ and Pulse Severities ν : $\omega_n=\pi$ N = 0.5

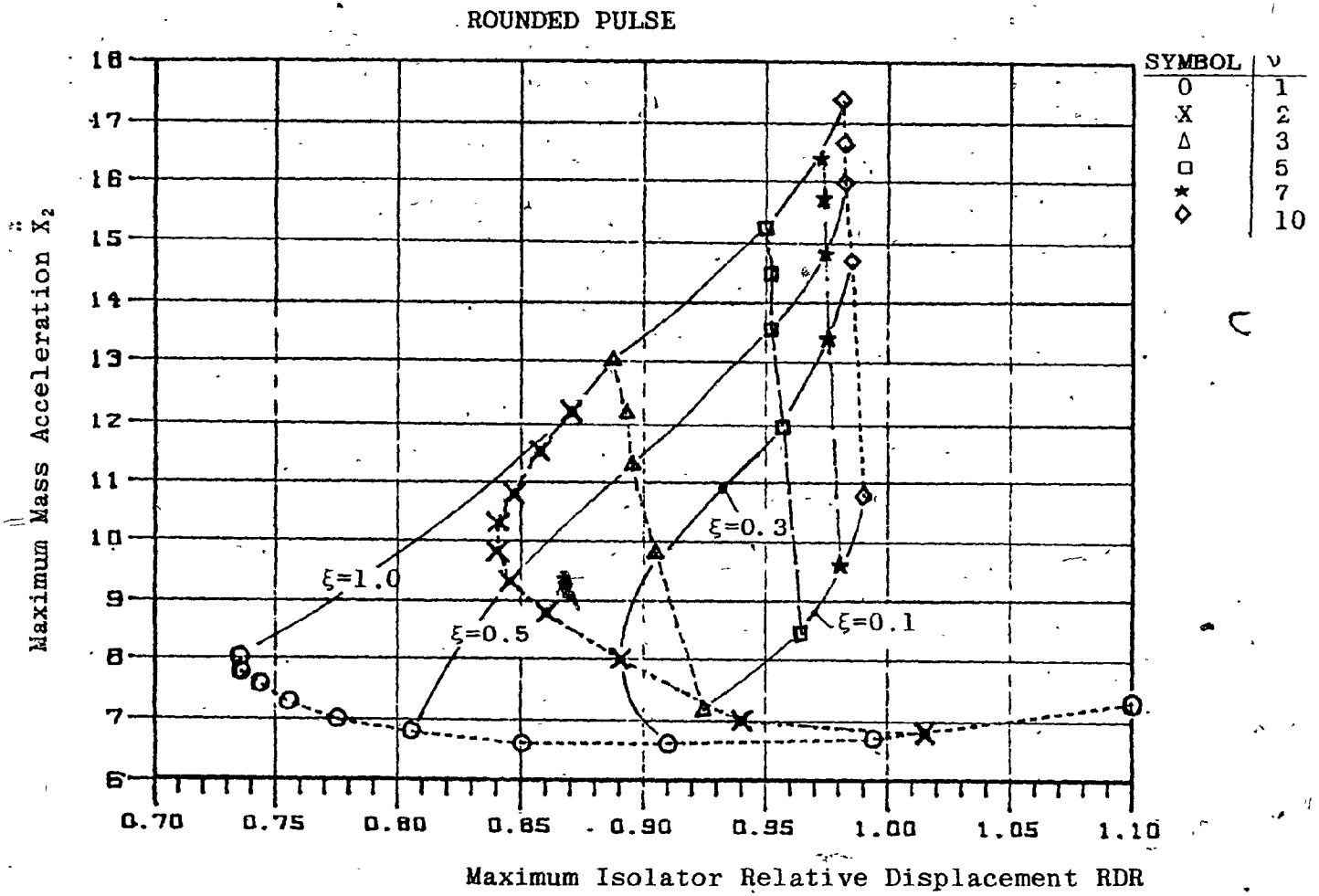

FIGURE 18: Performance of ECVI-2 System for Various Damping Ratios ξ and Pulse Severities ν: $\omega_n = \pi$ N=0.5

ROUNDED PULSE

ISOLATOR		ν = 1		ν = 5		ν = 10	
	ξ	RDR	$\ddot{X}_2$	RDR	$\ddot{X}_2$	RDR	$\ddot{X}_2$
DCVI	1.0	0.32	11	0.7	76	0.84	158
ECVI-1		0.66	13	0.925	24	0.97	27
ECVI-2		0.74	8	0.95	15	0.98	17.5
DCVI	0.5	0.49	7.5	0.83	35	0.90	84
ECVI-1		0.63	10.6	0.93	22	0.98	25
ECVI-2		0.81	6.8	0.96	14	0.99	16

TABLE 1: COMPARISON OF DCVI, ECVI TYPES 1 AND 2 SYSTEMS HAVING VARIOUS DAMPING RATIOS ; N=0.5 $\omega_n=\pi$

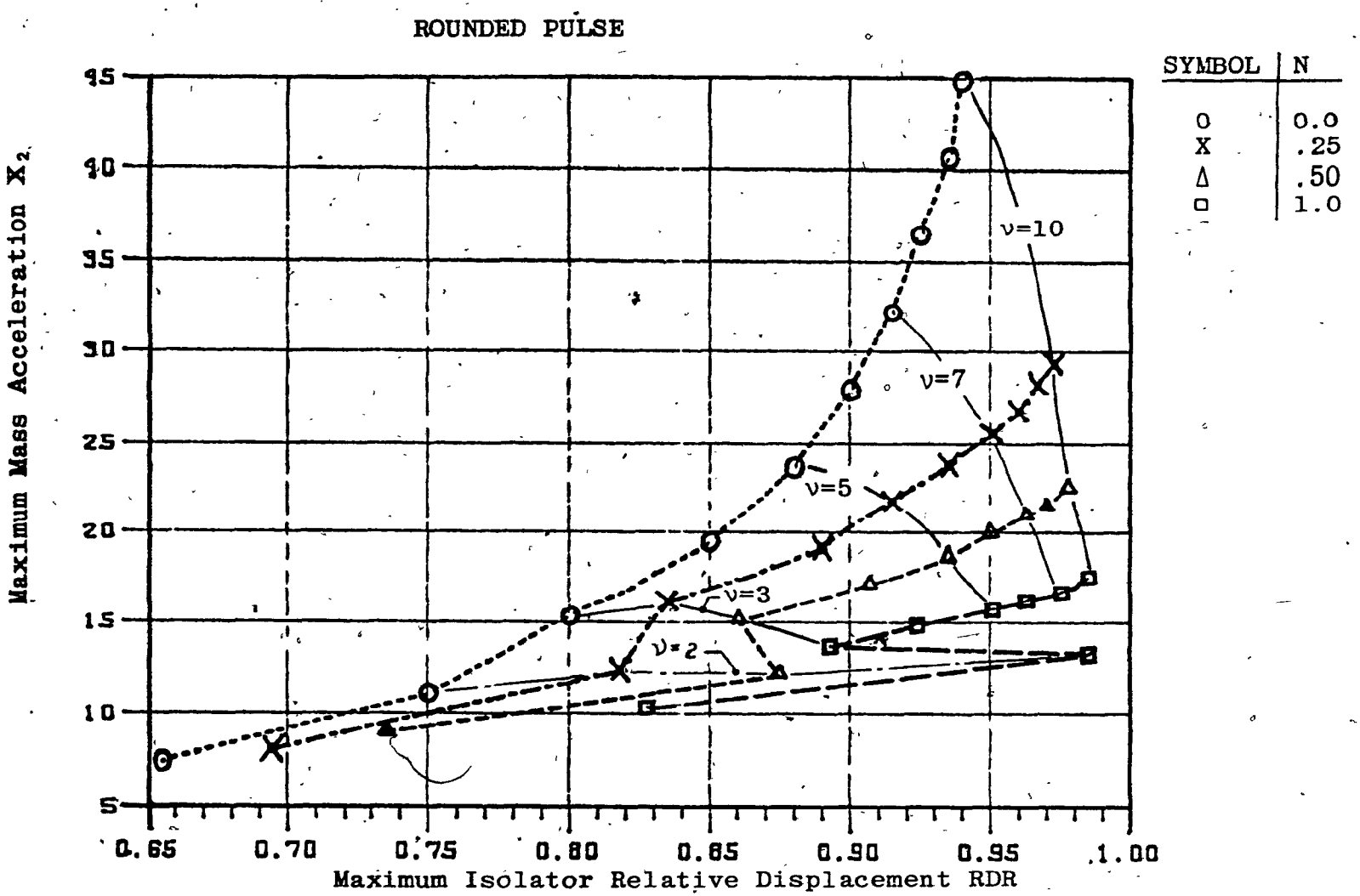

FIGURE 19: Performance of ECVI-1 System for Various Elastic Coupling Ratios N and Pulse Severities ν: $\omega_n=\pi$ $\xi=0.25$

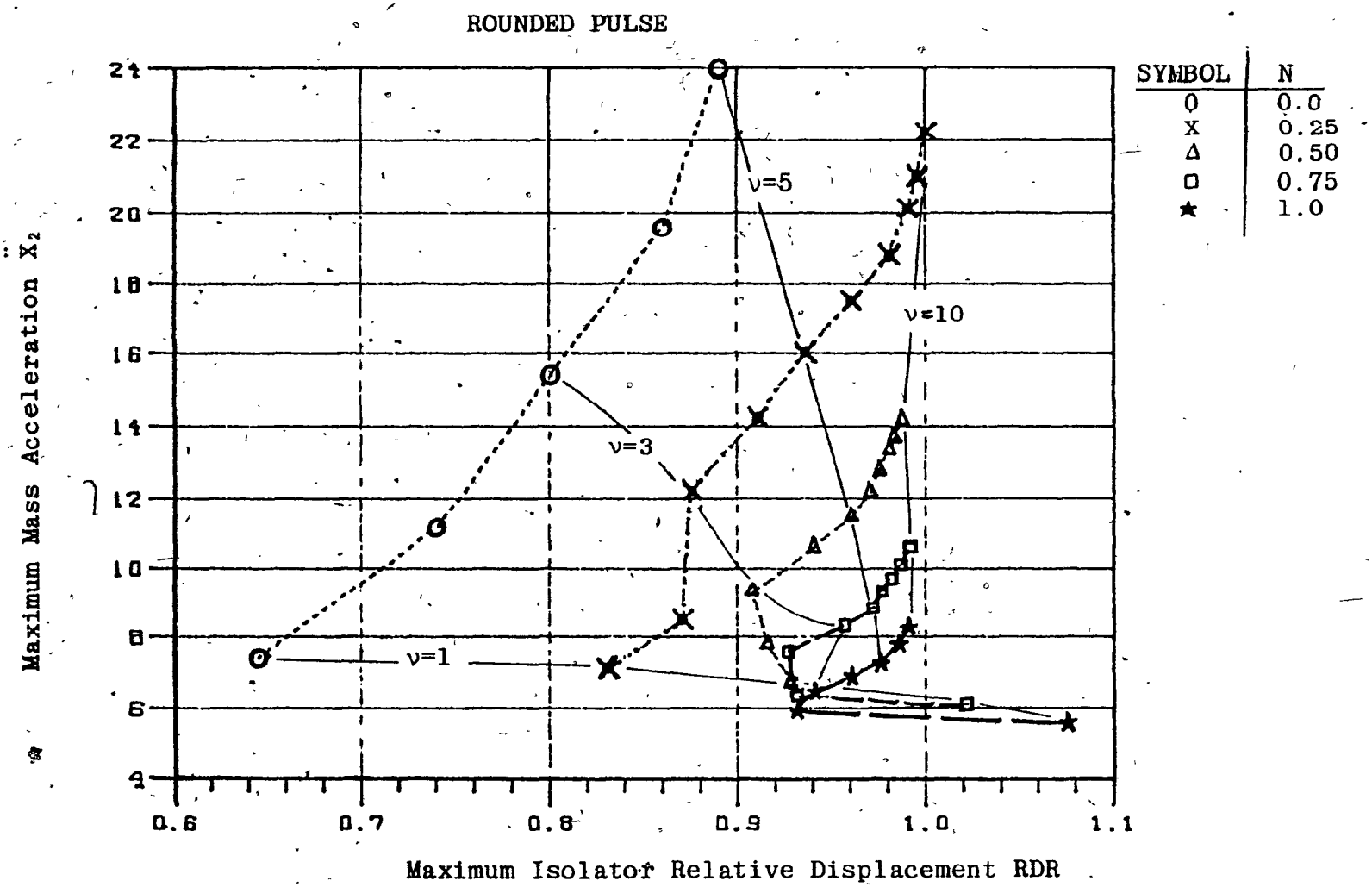

FIGURE 20: Performance of ECVI-2 System for Various Elastic Coupling Ratios N and Pulse Severities: $\omega_n=\pi$ $\xi=0.25$

ROUNDED PULSE

ISOLATOR		$\nu_o = 1$		$\nu = 5$		$\nu = 10$	
	N	RDR	$\ddot{X}_2$	RDR	$\ddot{X}_2$	RDR	$\ddot{X}_2$
DCVI	0	0.66	7.5	0.88	24	0.94	45
ECVI-1	.5	0.74	9.0	0.94	19	0.98	23
ECVI-2	1.0	0.83	10	0.95	15.7	0.99	17.5
DCVI	0	0.66	7.5	0.88	24	0.94	45
ECVI-1	.5	1.02	6.0	0.97	8.8	0.98	14
ECVI-2	1.0	1.08	5.5	0.98	7.25	0.99	8.3

TABLE 2: COMPARISON OF DCVI, ECVI TYPE 1 AND 2 SYSTEMS HAVING VARIOUS ELASTIC COUPLING RATIOS N: $\omega_n = \pi$ $\xi = 0.25$

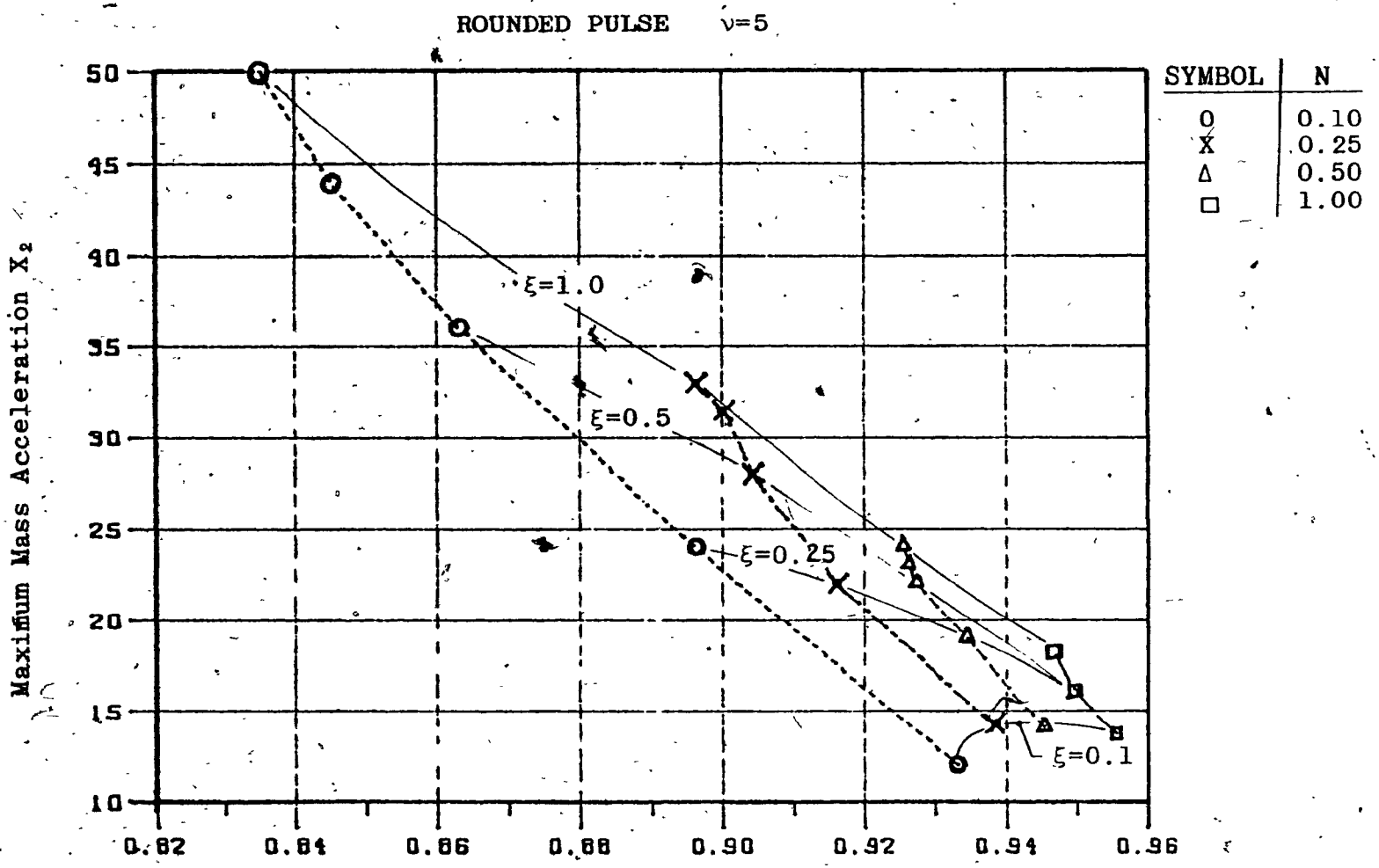

FIGURE 21: Performance of ECVI-1 System for Various Damping Ratios ξ and Elastic Coupling Ratios N : $\omega_n = \pi$

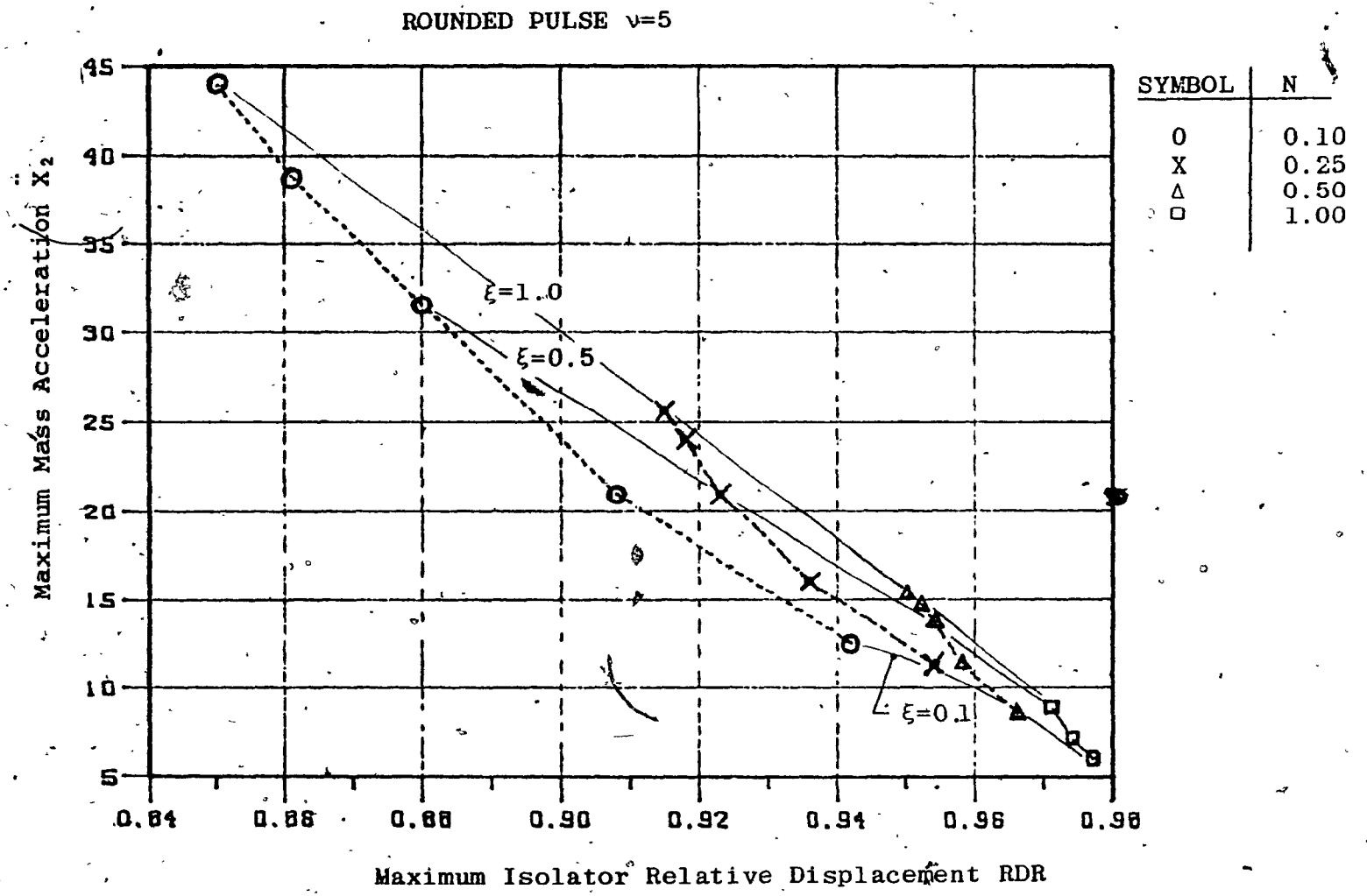

FIGURE 22: Performance of ECVI-2 System for Various Damping Ratios ξ and Elastic Coupling Ratios N: $\omega_n = \pi$

5.2.3. TIME RESPONSE OF VISCOUS DAMPED ISOLATORS

Figures 23 through 26 show the influence of the viscous damping ratio ζ on the time response of the normalized acceleration and relative displacement of the DCVI system subjected to rounded pulses of severity (ν=1) and (ν=5). From the relative displacement curves, Figures 23 and 24, it is seen that the number of oscillations which occurred across the isolator was inversely proportional to the amount of damping. Indeed at high damping, there were only three peaks - the first and second correspond to the initial displacement of the base and its return to the zero position, and the third, to a slight amount of overshoot. High damping also produced the lowest maximum relative displacements for the two pulse severities.

Figure 25 shows that for (ν=1), low damping was undersirable, as the acceleration levels were high not only for the maximum peak, but also for the subsequent secondary peaks. On the other hand, at (ν=5), it was high damping which was undersirable. As seen in Figure 26, both its first and second acceleration peaks were large amplitudes. In contrast, the acceleration response due to low damping, though it consisted of several oscillations, was of uniformily small amplitude.

Figure 27 and 28 show the comparison of the acceleration and relative displacement responses of the DCVI and ECVI types 1 and 2 systems having the same degree of damping and elastic coupling, subjected to a

rounded pulse of (ν=5). The general time responses of the three viscous damped systems were found to be similar. As seen in Figure 27, the DCVI system had the highest transmitted acceleration due to the direct coupling of the damper between the mass and the isolator base. The second acceleration peak was found, however, to be highest for the ECVI type 1 system. Figure 28 shows that during the second peak, the base excitation, x_0, had already ceased, which reduced the equivalent damping of the system, as given by c_{eq} in equation (88). This reduction in c_{eq} caused less energy to be removed from the system and thus increased the amplitude of the second acceleration peak. The ECVI type 2 system had the lowest maximum and second acceleration peaks of the three isolators. This was due to effectiveness of the elastic coupling which acted a second stage of isolation.

Figures 29 and 30 show the influence of the elastic coupling ratio N on the time response of the ECVI type 1 system. The relative displacement curves of Figure 29 show that except for stiffest amount of elastic coupling (N=0.1), the RDR response was generally unaffected by N. As seen by the subsequent relative displacement peaks, however, the influence of N was to reduce the effective damping of the system. Hence for (N=0.1), the system quickly returned to its zero steady position, whereas for a large degree of elastic coupling (N=1), the response was highly oscillatory. From Figure 30 it is seen that increasing the elastic coupling reduced the magnitudes of the first and second acceleration peaks. A similar reduction of the acceleration was achieved in the DCVI system by decreasing the viscous damping, as seen in Figure 23. However, a comparison of the acceleration peaks of a DCVI and ECVI type 1 having nearly the same $\ddot{X}_2$ as given in Table 3 shows that the amplitudes of the

secondary peaks were higher for the elastically coupled system. This was due to the reduction in effective damping c_{eq}, given by equation (88), which occurred once the base excitation had passed.

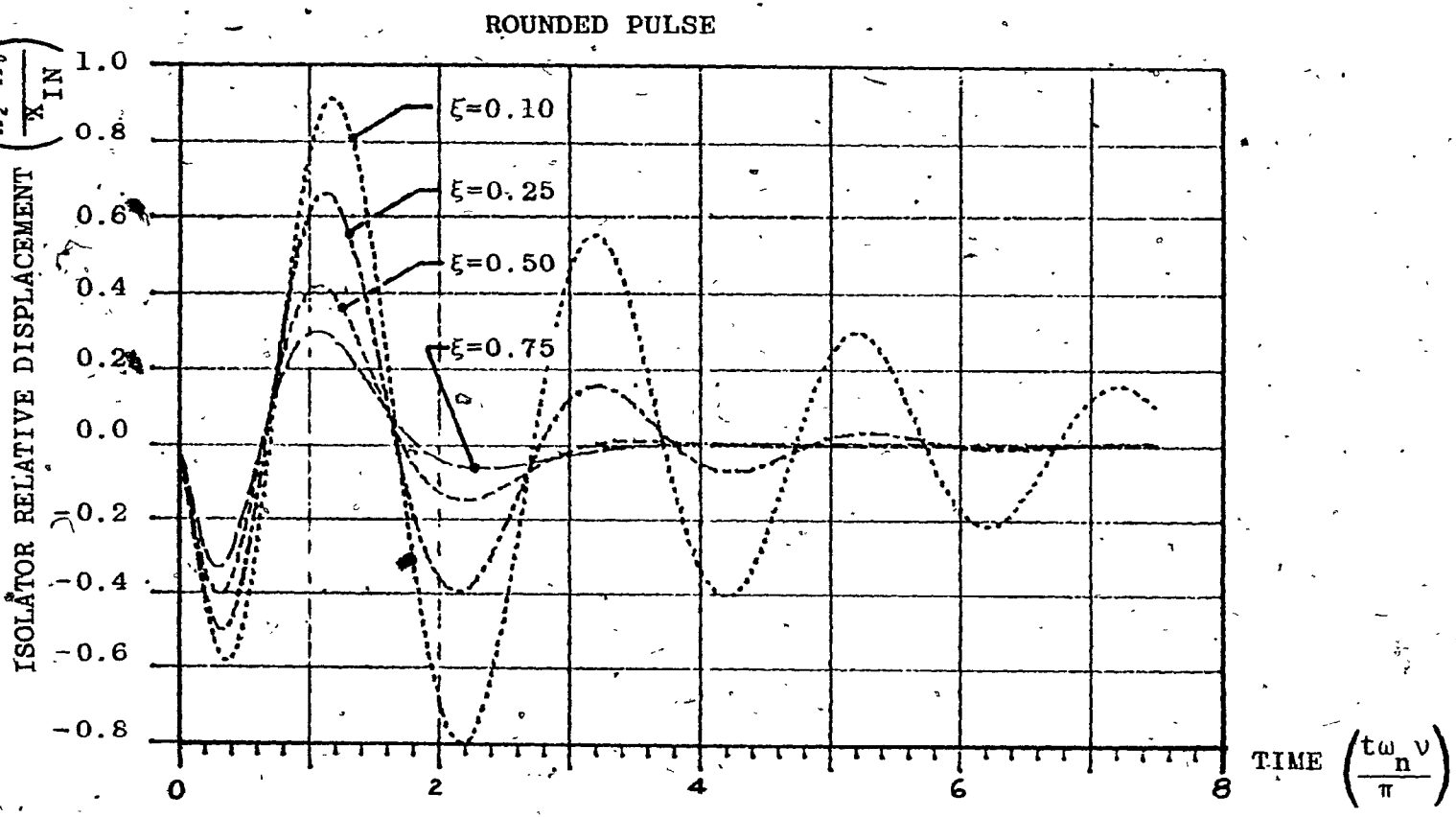

FIGURE 23: Isolator Relative Displacement Time Histories for DCVI System having 4 values of Damping: $\nu=1$ $\omega_n=\pi$

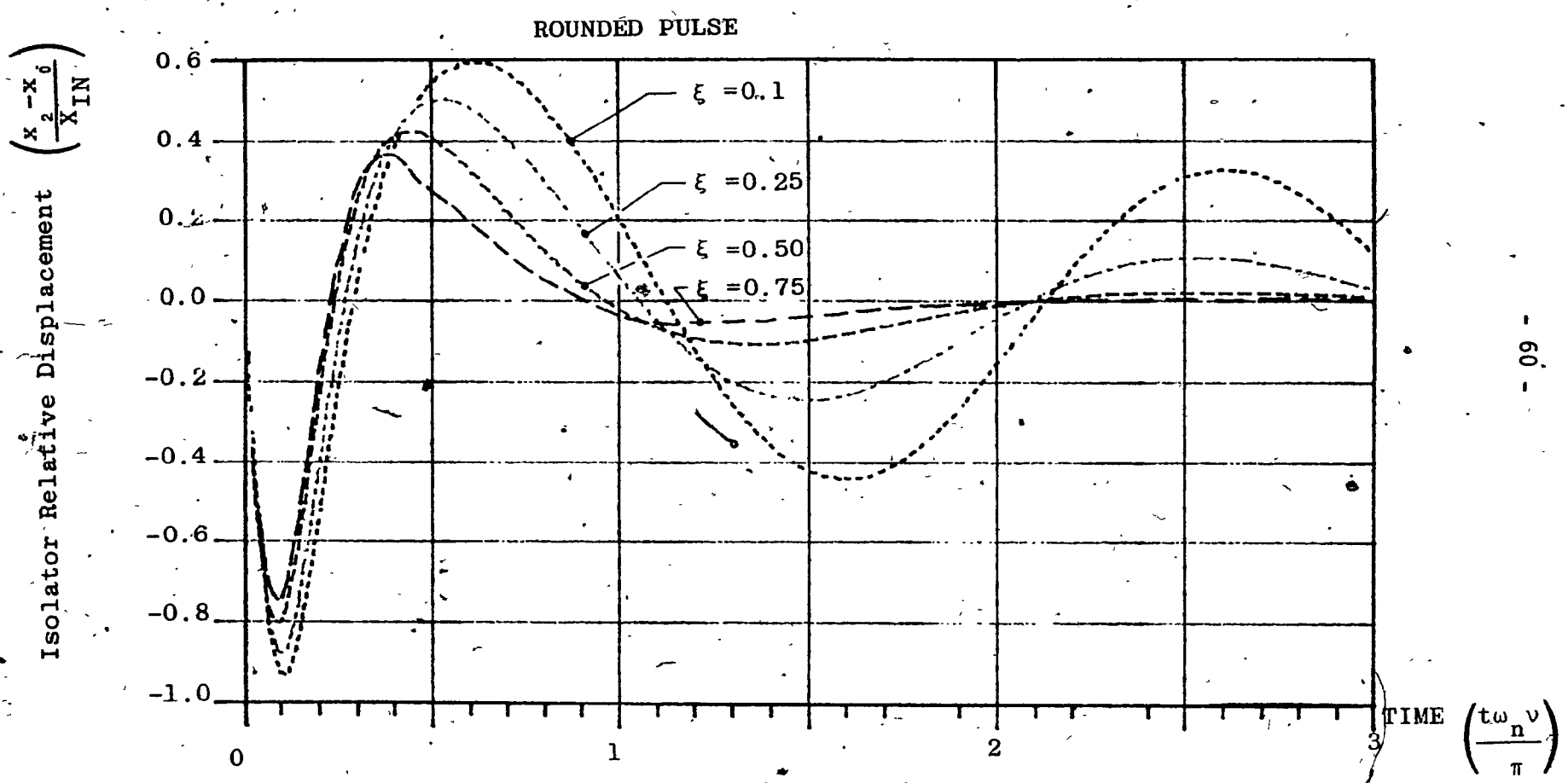

FIGURE 24: Isolator Relative Displacement Time Histories of DCVI System having 4 values of Damping: $\nu = 5$ $\omega_n = \pi$

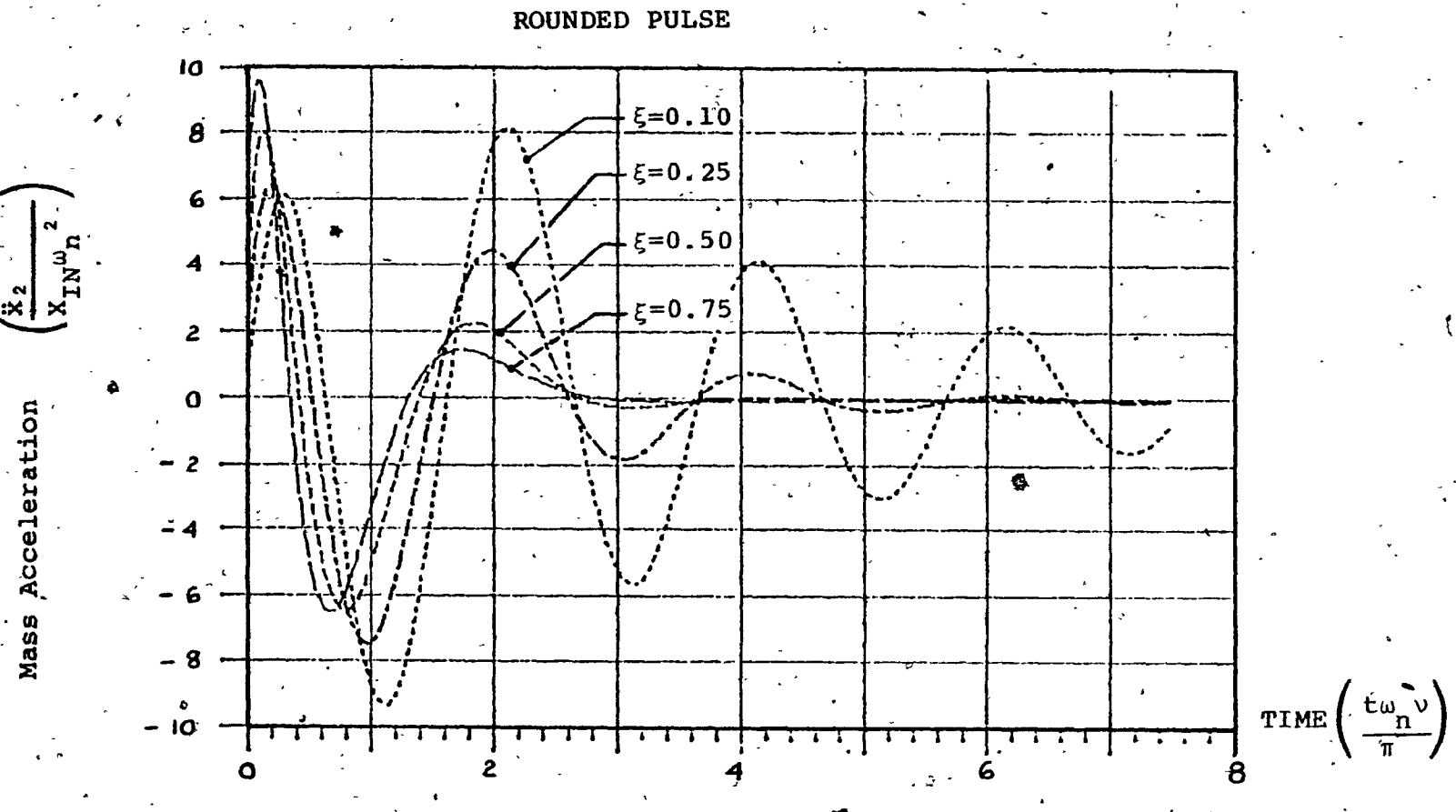

FIGURE 25: Mass Acceleration Time Histories of DCVI System having 4 values of Damping: $\nu=1$ $\omega_n = \pi$

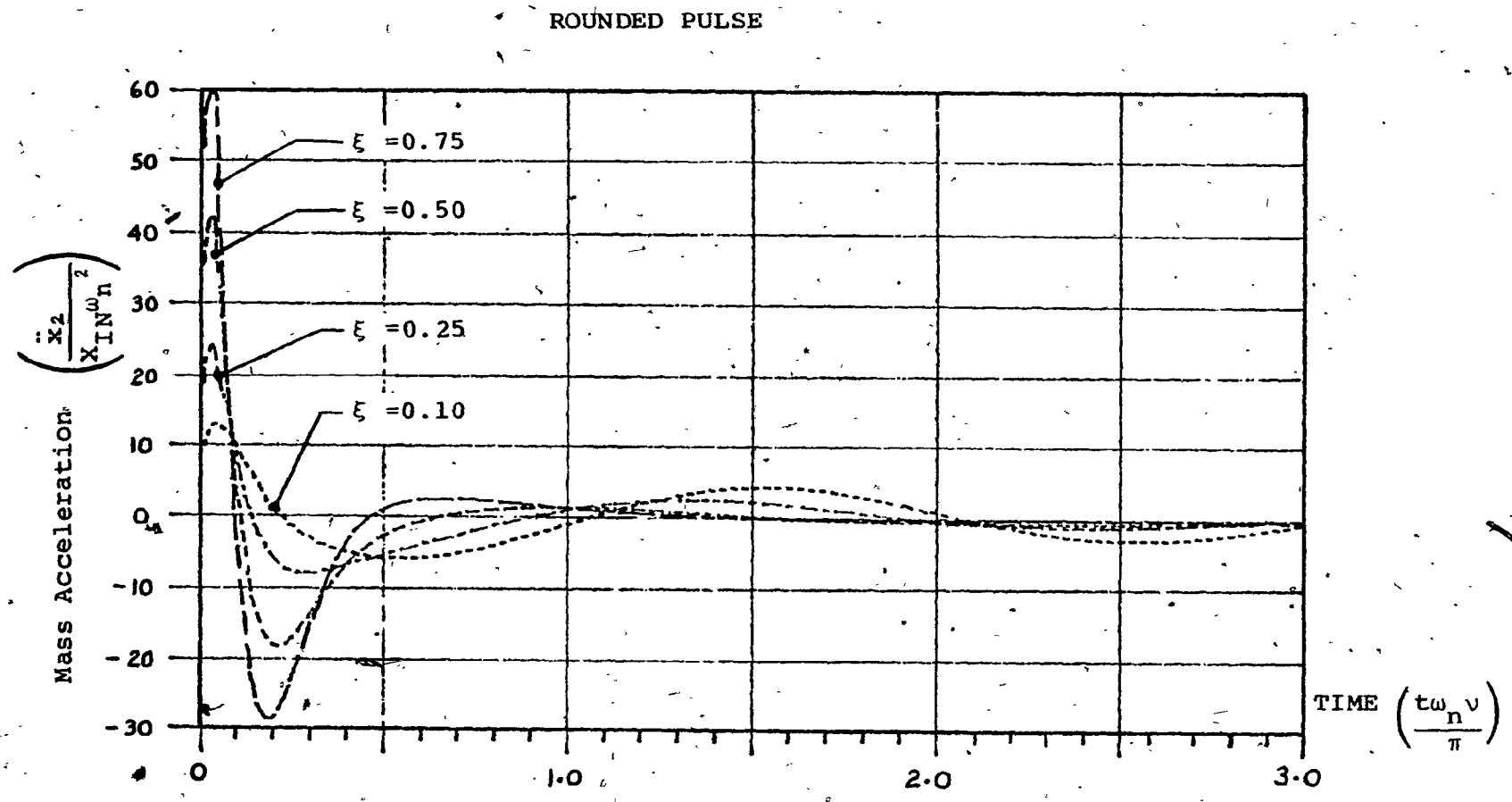

FIGURE 26: Mass Acceleration Time Histories for DCVI System having 4 values of Damping: $\nu = 5$ $\omega_n = \pi$

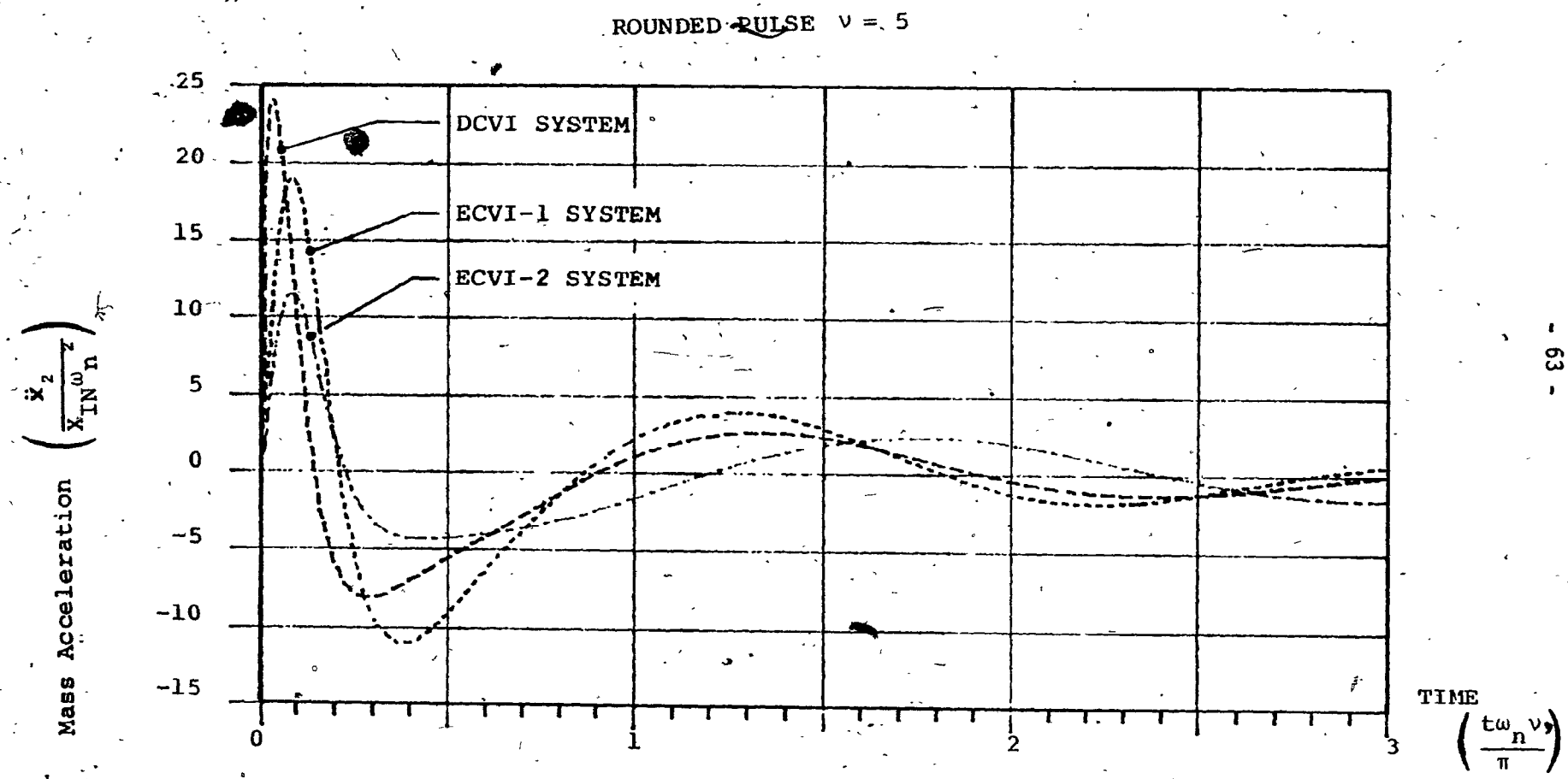

FIGURE 27: Comparison of Mass Acceleration Time Histories for DCVI and ECVI Types 1 and 2 Systems: $\omega_n=\pi$ $\xi=0.25$ N=0.25

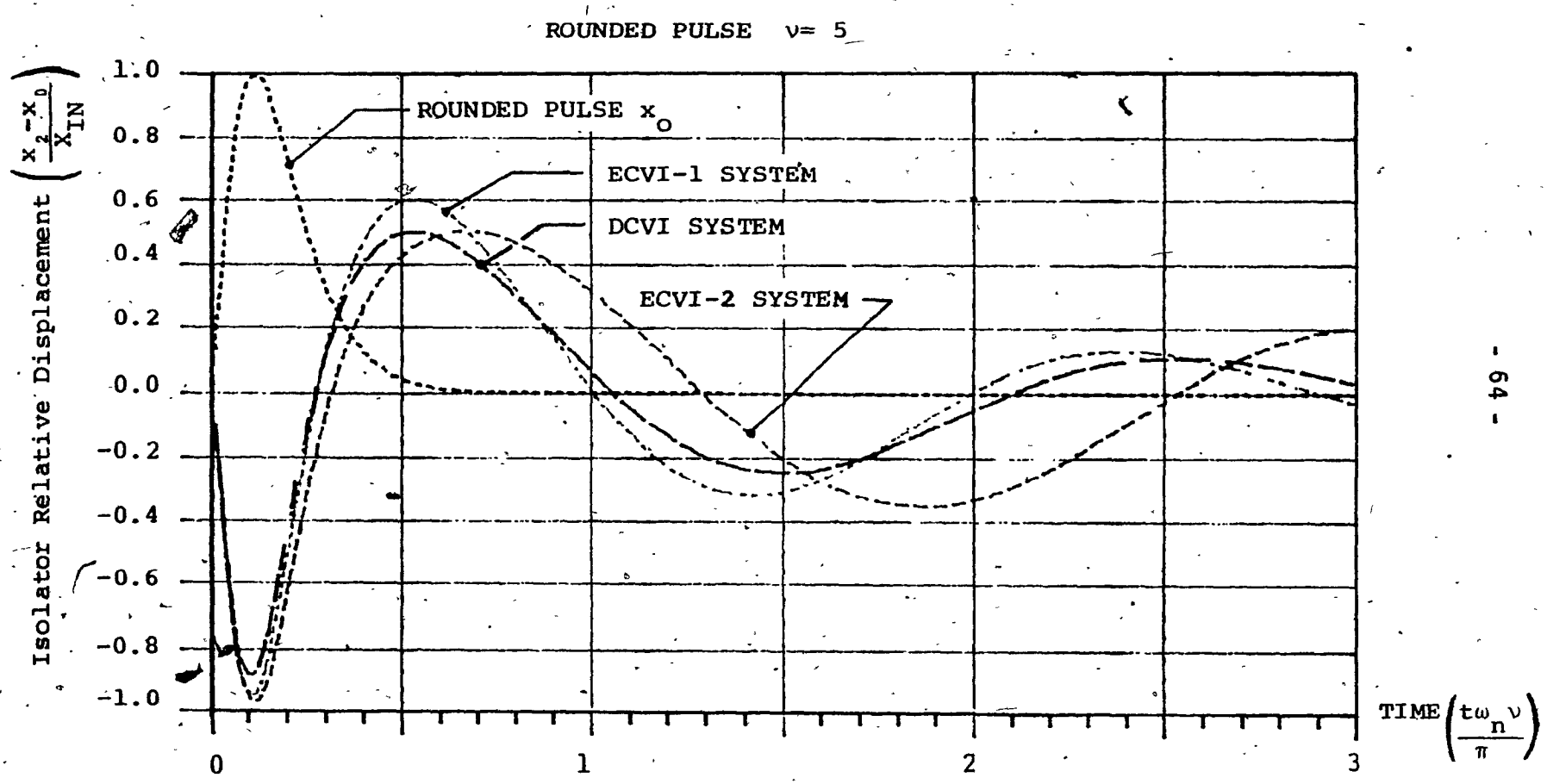

FIGURE 28: Comparison of Isolator Relative Displacement Time Histories for DCVI and ECVI Types 1 and 2 Systems: $\omega_n=\pi$ N=0.25 ξ=0.25

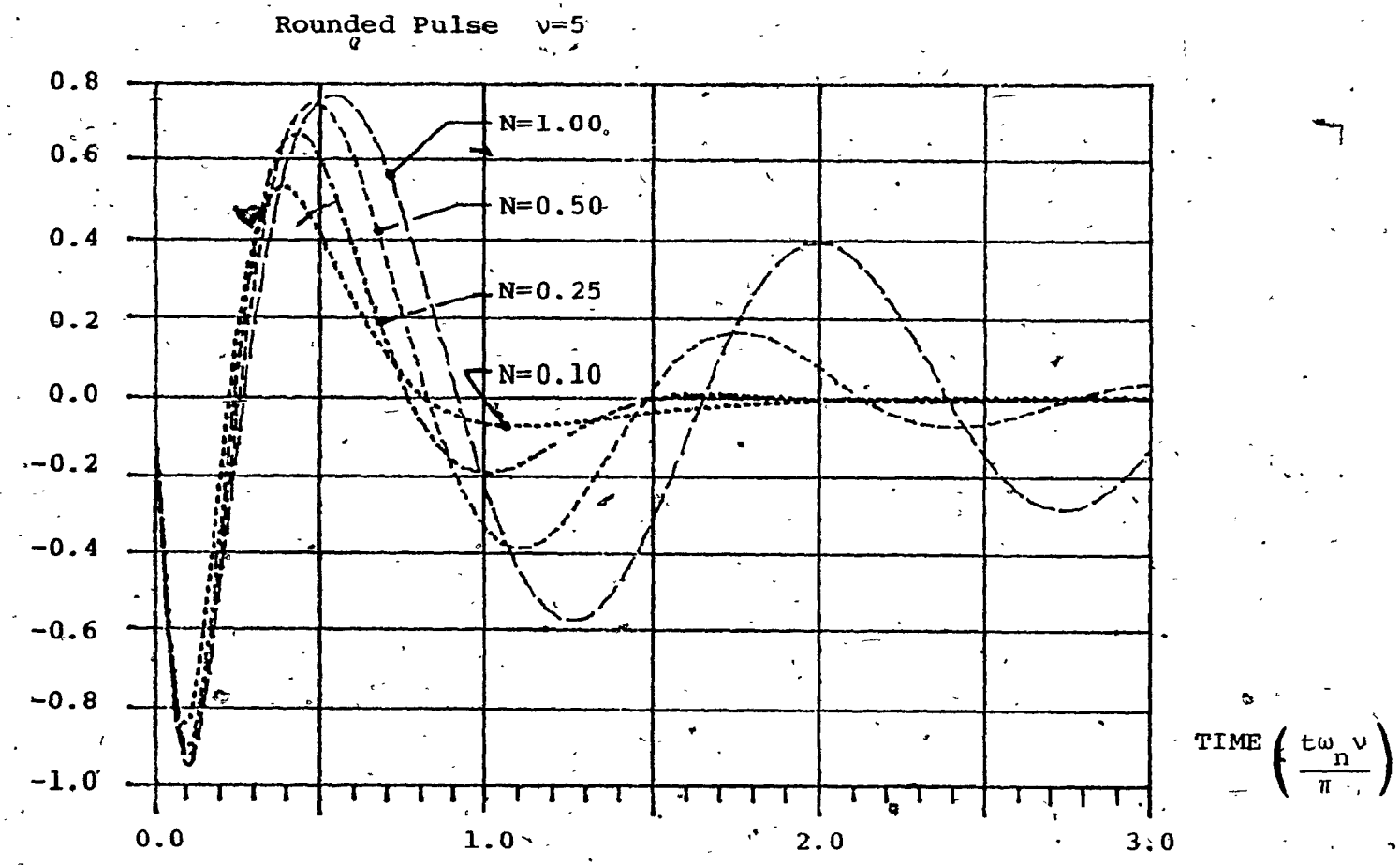

FIGURE 29: Isolator Relative Displacement Time Histories for ECVI-1 System having 4 Values of Elastic Coupling N.

: $\omega_n = \pi$ $\xi = 0.75$

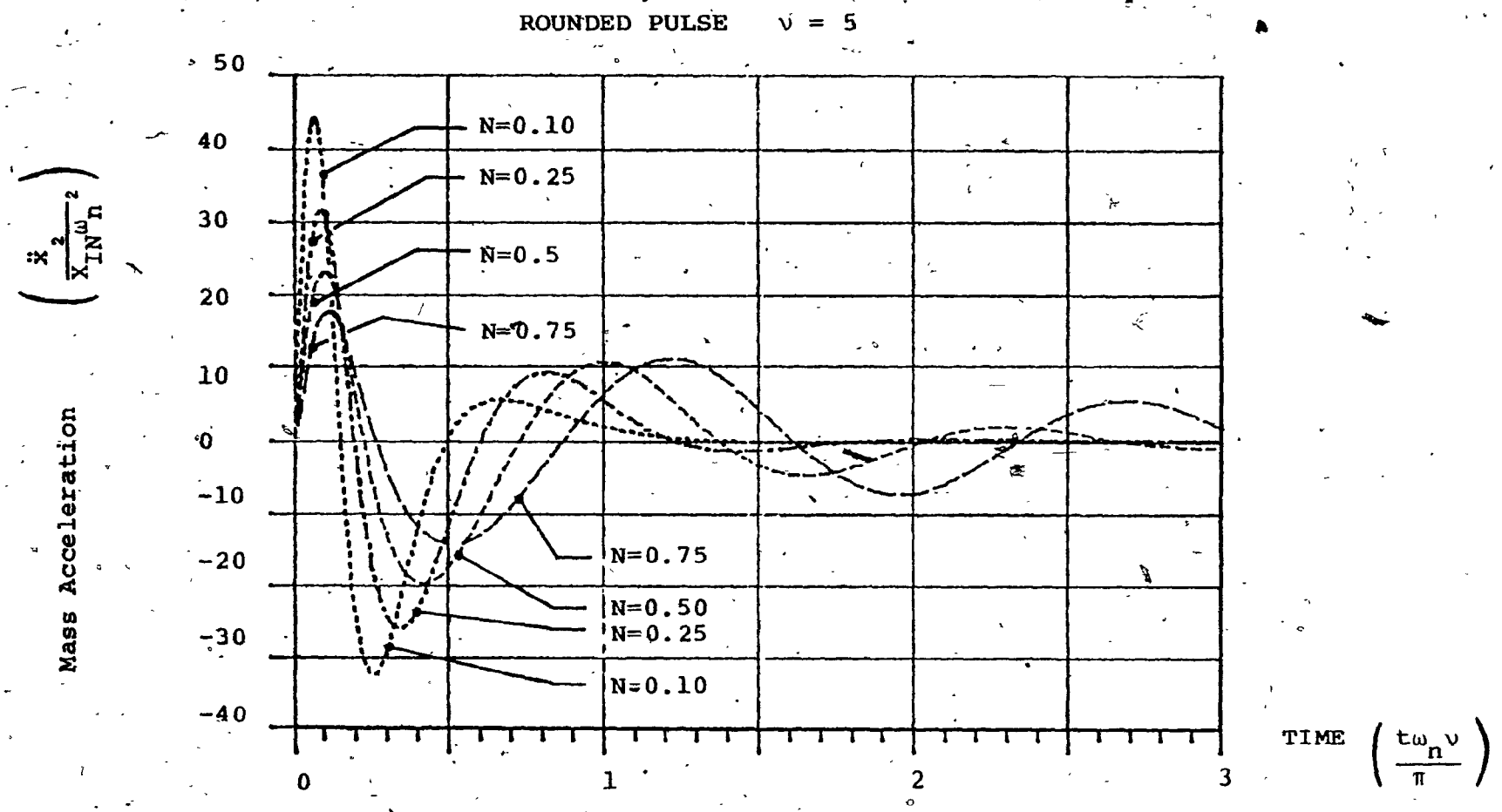

FIGURE 30: Mass Acceleration Time Histories for ECVI-1 System having 4 values of Elastic Coupling Ratio: $\omega_n=\pi$ $\xi=0.75$

ROUNDED PULSE $\nu = 5$

ISOLATOR	MASS ACCELERATION				
	1st PEAK $(\ddot{X}_2)$	2nd PEAK	3rd PEAK	4th PEAK	5th PEAK
DCVI $\xi = 0.25$ $\omega_n = \pi$	+25.5	-9	+3	-1.5	+0.1
ECVI-1 $\xi = 0.75$ $N = 0.50$ $\omega_n = \pi$	+24	-20	+11	-5	+2

TABLE 3: COMPARISON OF DCVI AND ECVI-1 SYSTEMS HAVING THE SAME MAXIMUM MASS ACCELERATION $\ddot{X}_2$.

5.3 COULOMB FRICTION DAMPED ISOLATORS SUBJECTED TO ROUNDED PULSE DISPLACEMENTS

Figures 31 through 42 are the performance curves of directly coupled, and types 1 and 2 elastically coupled coulomb friction damped isolator systems which were subjected to rounded pulse displacements at the isolator base. Typical time responses of some selected isolators are shown in Figures 43 through 49.

5.3.1. PERFORMANCE OF THE DIRECTLY COUPLED FRICTION ISOLATOR (DCFI)

Figure 31 shows the performance of the DCFI system for various degrees of coulomb damping ratio α and pulse severity ν. In general it was found that the maximum transmitted acceleration $\ddot{X}_2$ was governed by the amount of damping α, whereas the maximum relative displacement RDR was principally determined by the severity of the pulse. Only at (ν=1) and (ν=2) was RDR appreciably affected by increased damping and this was only for α up to 0.4.

It is seen that for low coulomb damping, (α=0.1) and (α=0.2), the response of the isolator in terms of RDR and $\ddot{X}_2$ was not highly influenced by pulse severity. At higher amounts of damping, the DCFI system showed steady increases in RDR and $\ddot{X}_2$ with increasing ν. As seen in Table 4, the increases in $\ddot{X}_2$ were small however, as compared with those for the DCVI system having approximately the same low severity performance. This was due to the coulomb damper, which being a force limiting device,

transmitted forces equal to or less than its breakout friction force. Hence RDR increased in order to absorb the base motion due to the higher pulse severity. This increase in RDR produced an increase in the transmitted force through the isolator spring k_2, which was reflected in the increased $\ddot{X}_2$.

5.3.2. PERFORMANCE OF THE ELASTICALLY COUPLED FRICTION ISOLATOR (ECFI) TYPES 1 AND 2

Figures 32 and 33 show the influence of coulomb damping on the response of the ECFI types 1 and 2 systems for various rounded pulse severities. Comparing these figures with Figure 31, it is seen that their performance trends were very similar to that of the DCFI system. Table 5 shows a comparison of the three types of coulomb damped isolators having the same amount of damping. The only major difference in the performances of the ECFI type 1 and DCFI system was for the case of low pulse severity (ν=1) with high coulomb damping (α=1.0), in which the elastically coupled system had much higher values of RDR and $\ddot{X}_2$. This particular combination of damping and pulse severity kept the friction damper locked and thus ineffective during most of the pulse. Hence the isolator behaved as an undamped system oscillating at its locked natural frequency (given in equation 34). Being undamped, it had a large RDR. The elastic coupling spring k_1 provided an additional path to transmit the base accelerations and produced an increase in $\ddot{X}_2$.

As seen from Table 5, the ECFI type 2 had the lowest maximum transmitted accelerations when compared to the ECFI type 1 and DCFI systems with the same degree of damping and pulse severity. This was due

to the elastic coupling spring k_1 which attenuated the base accelerations prior to the main isolator spring k_2 and the coulomb damper. It was also found that for low damping (α=.1), the ECFI type 2 system had the best RDR performance at (ν=2). This was a result of the spring k_1 which lowered the system's natural frequency and thus moved it away from the resonant condition. For the case of high coulomb damping (α=1.0) and low pulse severity (ν=1), there was a sudden degradation in the isolator performance with large increases in RDR and $\ddot{X}_2$. Similar to the ECFI type 1 system, the combination of low pulse severity with some degree of elastic coupling kept the force level across the damper below the break-out friction force during much of the pulse. This caused the isolator to behave like an undamped system with its poorer RDR and $\ddot{X}_2$ performance.

Figures 34 and 35 show the effect of various amounts of the elastic coupling ratio N on the performance of the ECFI types 1 and 2 systems. It can be seen from Figure 34 that N had little influence on the ECFI Type 1 system. This was due to the force limiting characteristic of the coulomb damper which predominated the response of the isolator. For the lower pulse severities, the effect of the elastic coupling was actually to degrade the performance by increasing both RDR and $\ddot{X}_2$ (though only by small amounts). This was due to the elastic coupling spring k_1 which had to be compressed in order to generate enough force to cause the friction device to break out. This compression of k_1 resulted in an additional compression of the primary spring k_2 and hence, an increase in RDR as compared with the DCFI system (that is, N=0). The additional compression of k_2 produced a higher spring force acting on

the mass and thus caused an increase in $\ddot{X}_2$. Indeed, the softer the elastic coupling (higher values of N), the poorer was the performance. For the higher pulse severities, this effect was not noticeable. In these cases the pulse was severe enough so that the additional spring compression became insignificant and hence N had no influence on the ECFI type 1 system performance.

In the ECFI type 2 system, the addition of the elastic coupling spring k_1 produced a second stage of isolation (the first being the parallel combination of the primary spring k_2 and the coulomb damper). Hence it would be expected that any variations in the elastic coupling ratio N would be directly reflected in maximum transmitted accelerations $\ddot{X}_2$. Examining Figure 35, it is seen that indeed this was true, and that $\ddot{X}_2$ decreased with increasing N. RDR was nearly independent of N with the exceptions of (ν=1) and (ν=2), in which there was a slight decrease in RDR for intermediate values of N.

Figures 36 and 37 show the combined effect of the coulomb damping factor α and the elastic coupling ratio N on the response of the ECFI types 1 and 2 systems subjected to a rounded pulse of severity (ν=5). It is seen from Figure 36 that the coulomb damping had a predominating influence on the ECFI type 1 system performance: increasing α produced higher values of $\ddot{X}_2$ but decreased RDR. For a given amount of damping, the elastic coupling caused a degradation of performance by increasing RDR without giving any reduction in $\ddot{X}_2$. The amount of degradation was small for low damping, but was quite substantial for high damping.

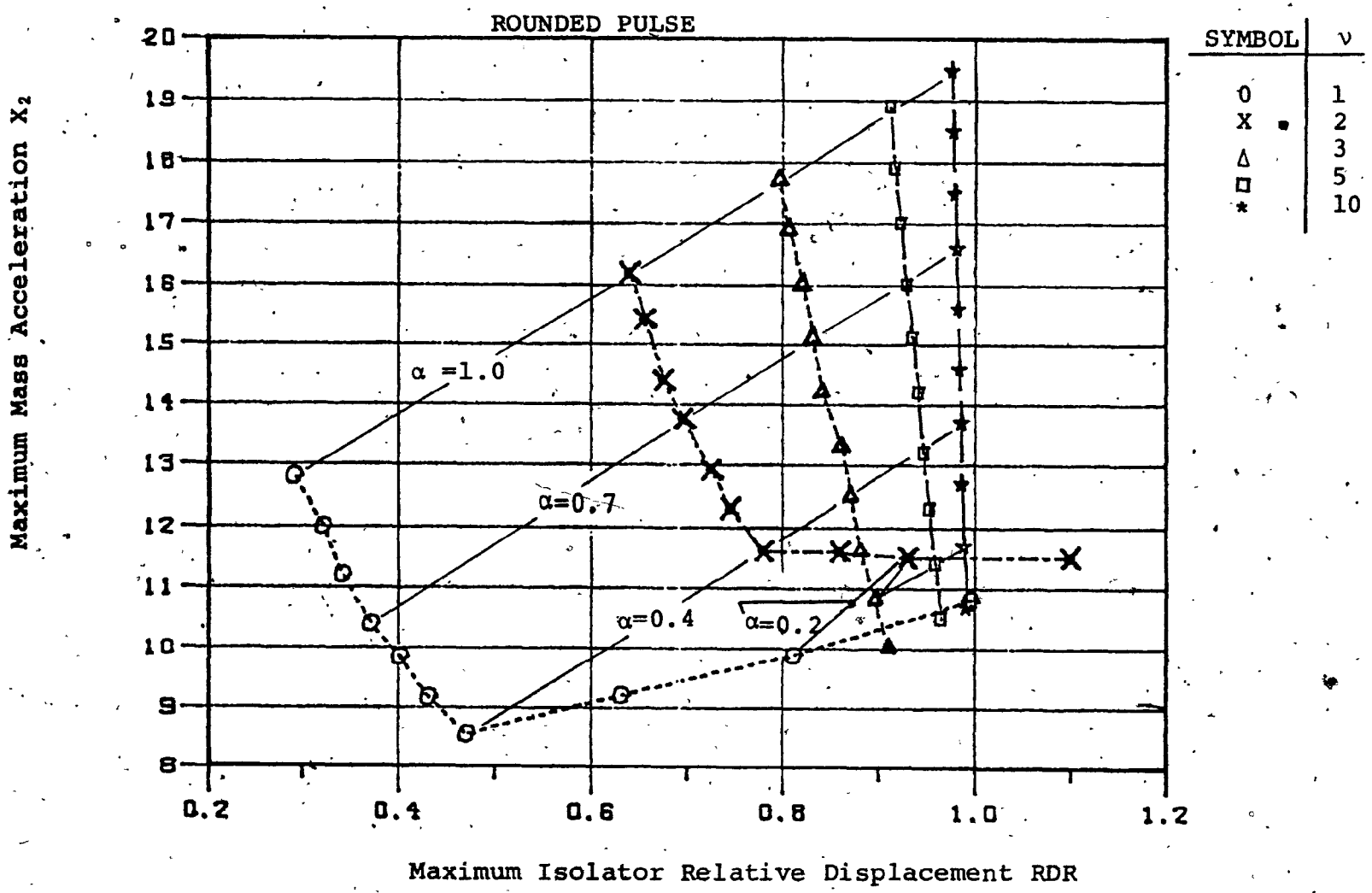

FIGURE 31: Performance of DCFI System for Various Damping Ratios α and Pulse Severities ν : $\omega_n = \pi$

ROUNDED PULSE

ISOLATOR	$\nu = 1$		$\nu = 3$		$\nu = 5$		$\nu = 10$	
	RDR	$\ddot{X}_2$	RDR	$\ddot{X}_2$	RDR	$\ddot{X}_2$	RDR	$\ddot{X}_2$
DCFI $\alpha = 1.0$	0.30	12.8	0.80	17.7	0.91	18.8	0.98	19.5
DCVI $\xi = 1.0$	0.32	12	0.58	43	0.70	75	0.82	158

TABLE 4: COMPARISON OF DCFI AND DCVI SYSTEMS HAVING THE SAME LOW PULSE SEVERITY RESPONSE: ($\nu = 1$)

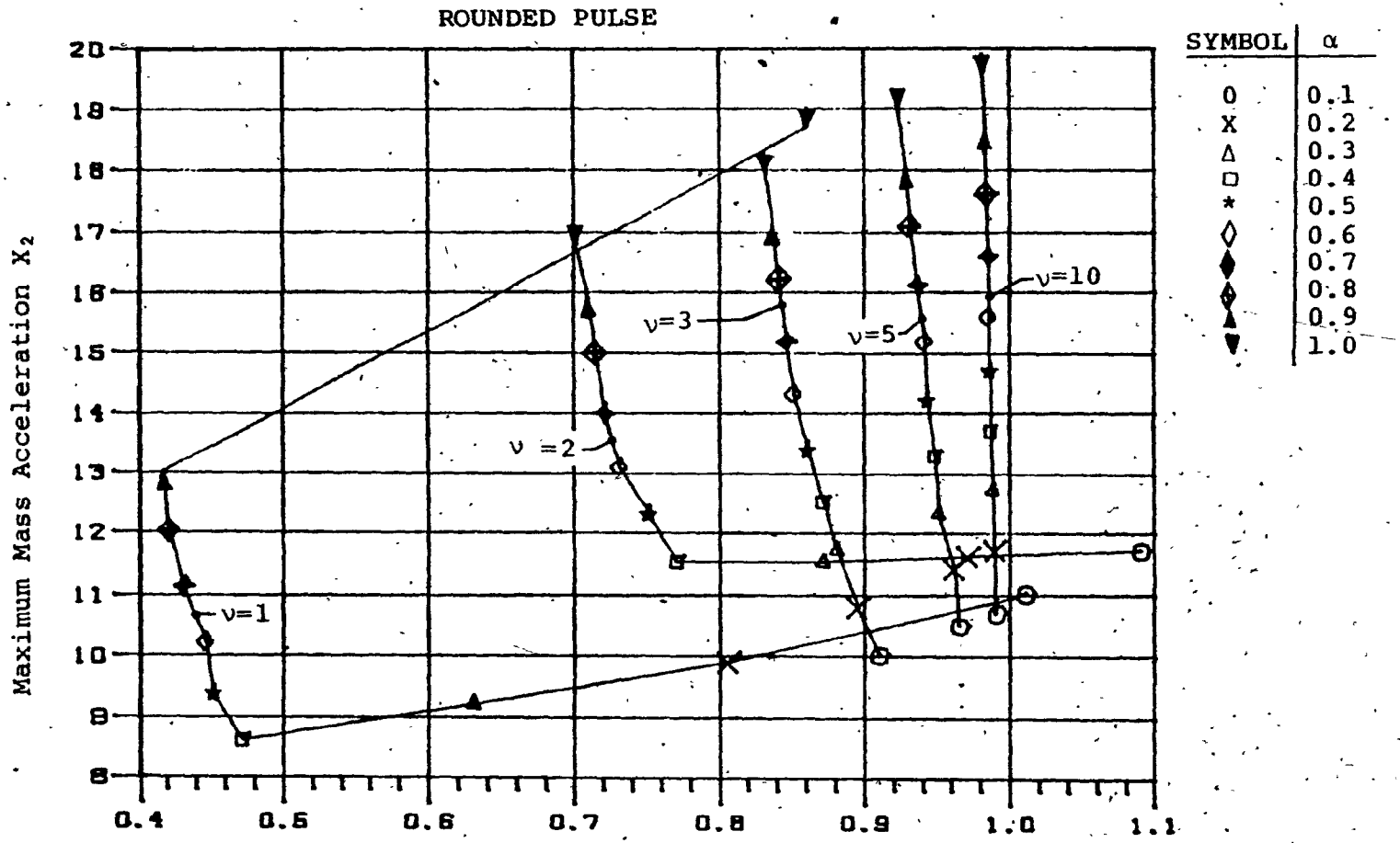

FIGURE 32: Performance of ECFI-1 System for Various Damping Ratios α and Pulse Severities ν : $\omega_n = \pi$ N=0.5

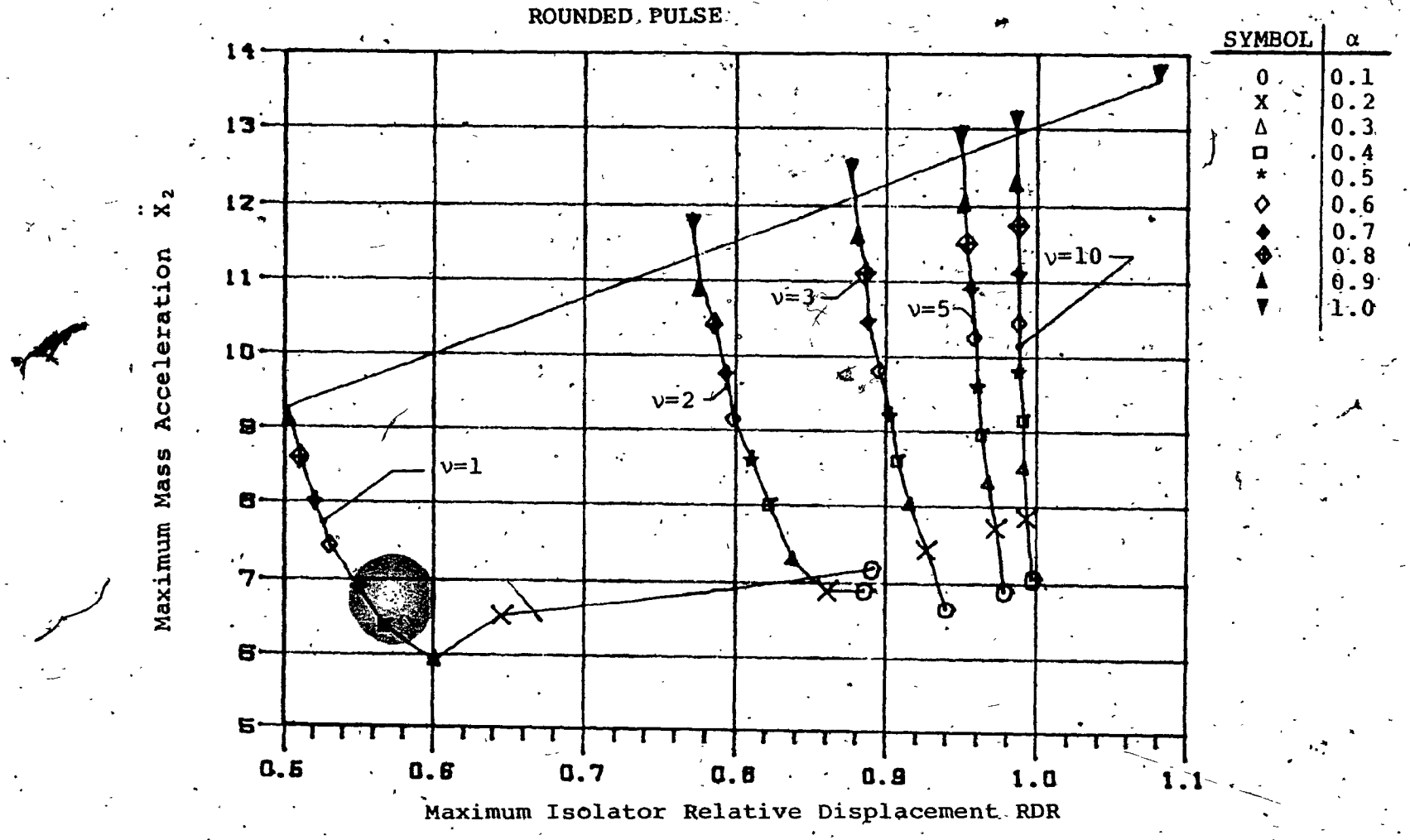

FIGURE 38: Performance of ECFI-2 System for Various Damping Ratios and Pulse Severities ν: $\omega_n=\pi$ N=0.5

ROUNDED PULSE

ISOLATOR		ν = 1		ν = 5		ν = 10	
	α	RDR	$\ddot{X}_2$	RDR	$\ddot{X}_2$	RDR	$\ddot{X}_2$
DCFI	1.0	0.30	12.8	0.91	18.8	0.97	19.5
ECFI-1		0.86	18.7	0.92	19	0.98	19.6
ECFI-2		1.08	13.7	0.95	12.2	0.99	12.4
DCFI	0.5	0.42	9.2	0.94	14.2	0.98	14.8
ECFI-1		0.45	9.4	0.94	14.2	0.98	14.8
ECFI-2		0.55	6.9	0.96	9.6	0.99	9.8

TABLE 5: COMPARISON OF DCFI, ECFI TYPES 1 AND 2 SYSTEMS HAVING THE SAME DAMPING RATIO α : $\omega_n = \pi$ N=0.5

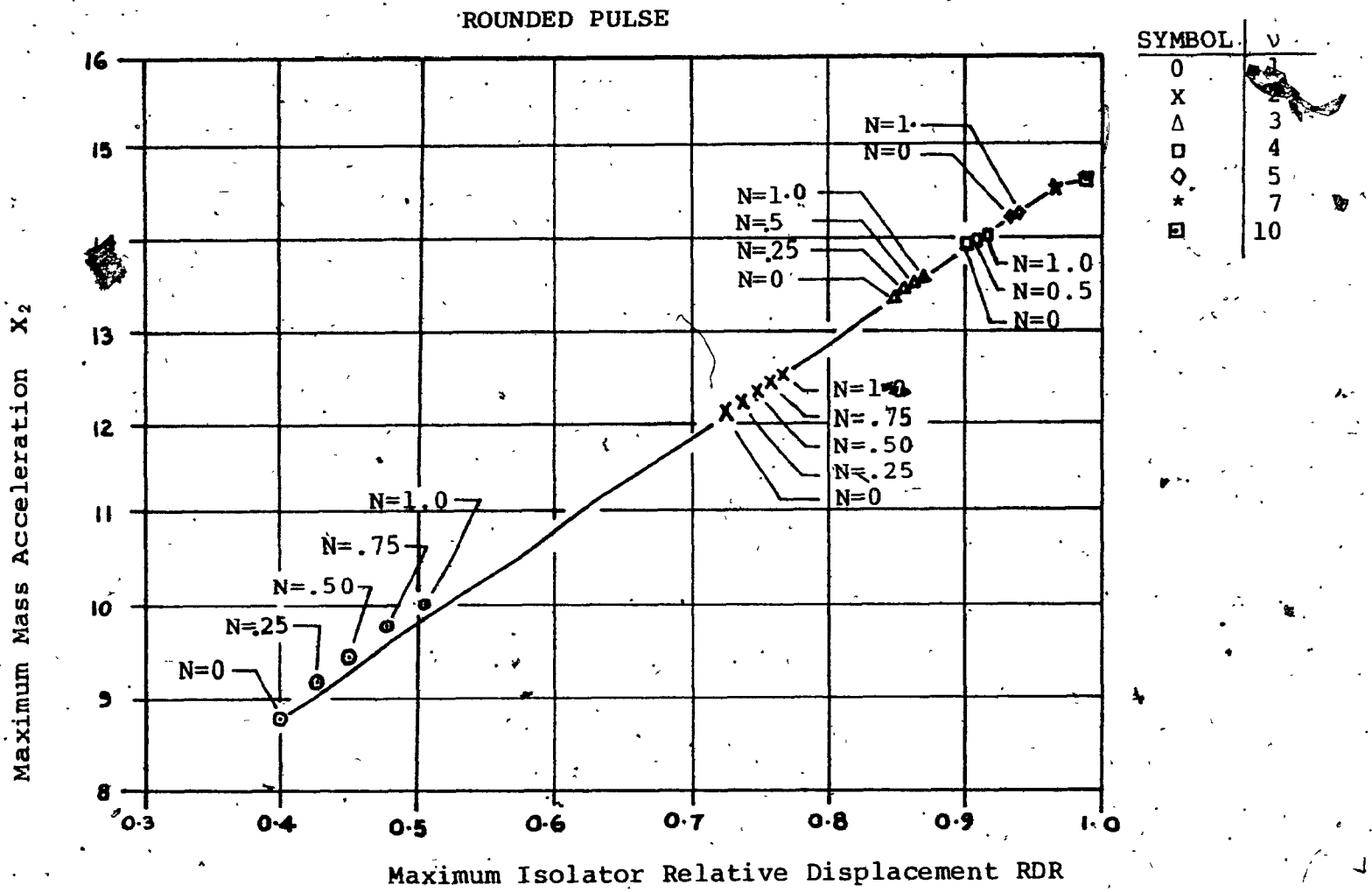

FIGURE 34: Performance of ECFI-1 System for Various Elastic Coupling Ratios N and Pulse Severities ν: $\omega_n=\pi$ $\alpha=0.50$

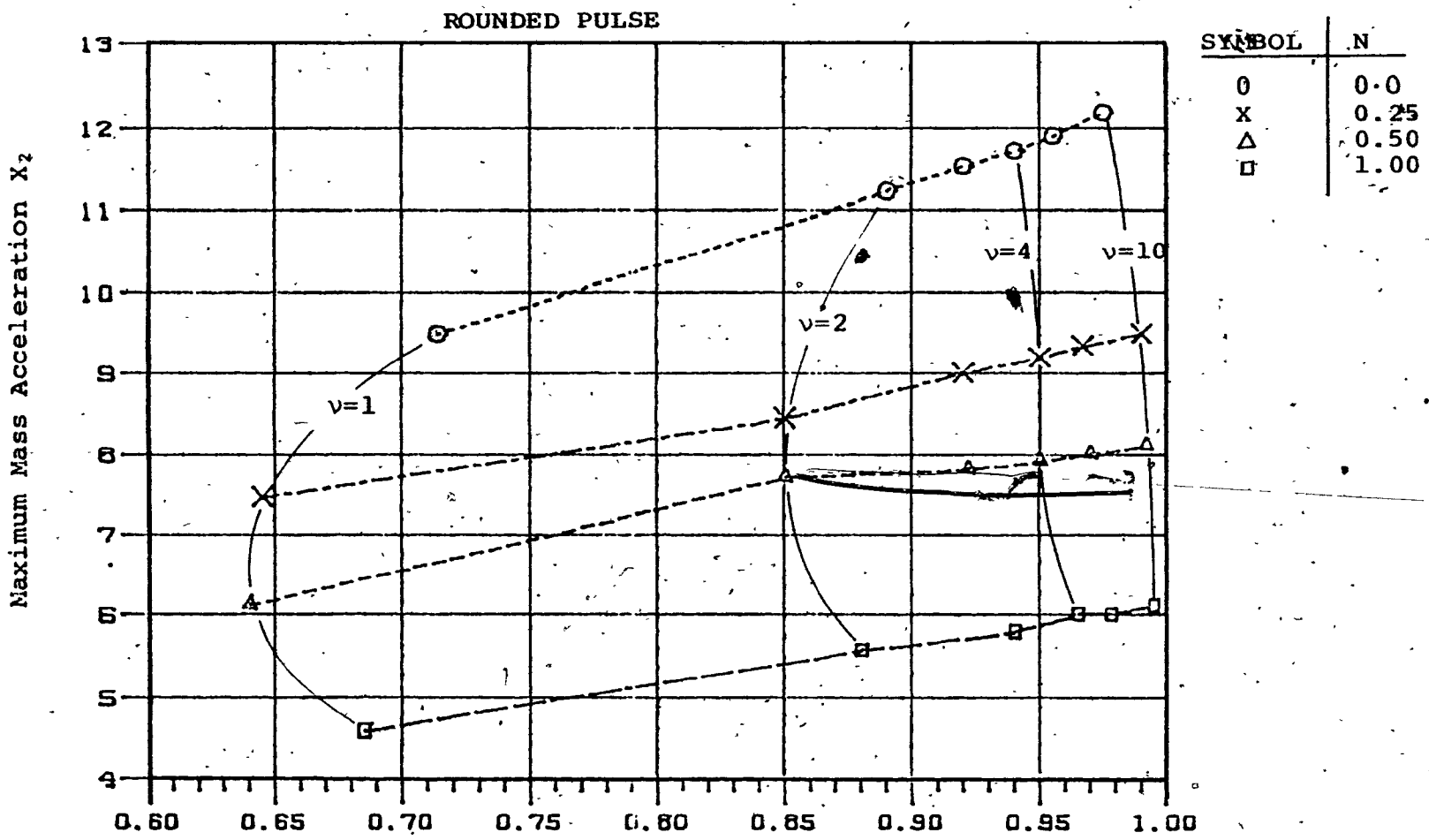

FIGURE 35: Performance of ECFI-2 System for Various Elastic Coupling Ratios N and Pulse Severities ν: $\omega_n = \pi$ $\alpha = 0.25$

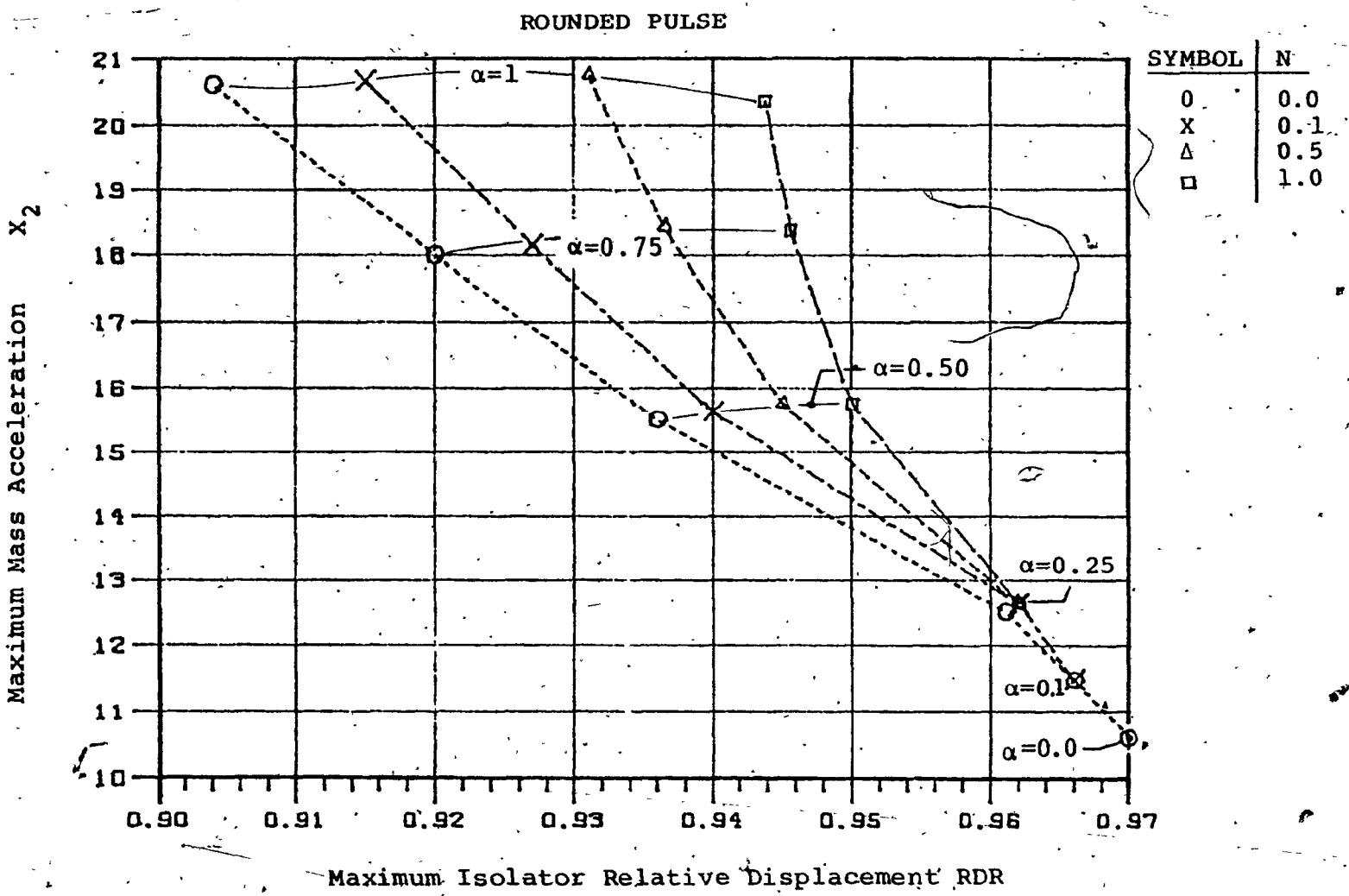

FIGURE 36: Performance of ECFI-1 System for Various Damping Ratios α and Elastic Coupling Ratios N : $\omega_n=\pi$ $\nu=5$

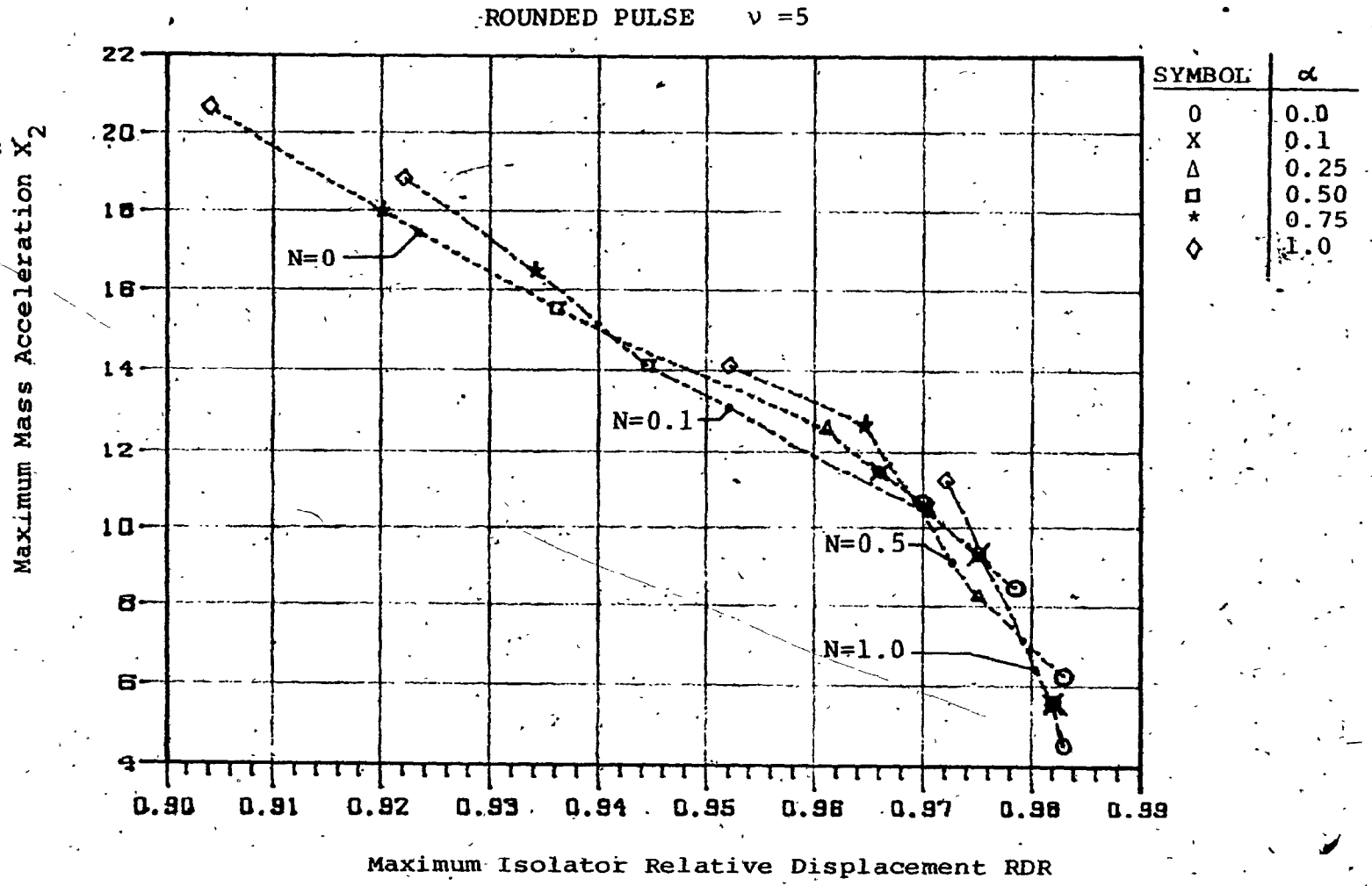

FIGURE 37: Performance of ECFI-2 System for Various Damping Ratios α and Elastic Coupling Ratios N: $\omega_n = \pi$

In Figure 37 it is seen that unlike the ECFI type 1 system, the elastic coupling ratio in the ECFI type 2 system reduced the maximum transmitted accelerations. This was due to the second stage of isolation which was produced by the elastic coupling spring k_1. As the second stage became 'softer' (increasing values of N), the variations in RDR and $\ddot{X}_2$ due to changes in the coulomb damping were lessened. The penalty for this however, was high values of RDR.

5.3.3. PERFORMANCE OF ADAPTIVE FRICTION ISOLATORS

Figures 38 through 42 are performance curves of the directly coupled friction isolator having adaptive friction dampers described in section 2.4, whose base was subjected to rounded pulse displacements of various severities. Figure 38 compares the four types of adaptive friction isolators having the same range of damping (α between 0.1 to 1.0) and the same break points (z_1= 0.1 and z_2= 1.0) to two fixed friction isolators (α=0.1 and 1.0). Recalling the discussion of section 5.3.1, it was found that for low damping, pulse severity had little influence on the performance of the fixed friction isolator: the transmitted accelerations being low, while the relative displacements were high. On the other hand, for high damping, $\ddot{X}_2$ and RDR increased with increasing pulse severity.

Figure 38 shows that the performance of the adaptive friction isolators laid between the limits set by the two fixed friction systems, with their response determined by the pulse severity ν. At low ν, the isolators tended to have a response predominated by damping values at the initial end of their damping range, whereas at high ν, the response was

determined by damping at the final end of their range. Hence, at (ν=10), the DIFI and VIFI systems had $\ddot{X}_2$ and RDR values equal to those of the fixed friction system with (α=1.0), while the DDFI system response was equal to the fixed friction (α=0.1) isolator. The VDFI system was also approaching the low fixed friction isolator performance. It is seen that the DDFI system had the best performance of any of the friction isolators, either fixed or adaptive. Its transmitted acceleration remained constant for increasing pulse severity, while RDR increased to absorb the base motions. The other isolators had either larger amounts of $\ddot{X}_2$ or RDR, or both, for the same pulse severity.

Figures 39 through 42 show the effect of break points, z_1 and z_2 on the performance of the four adaptive friction isolators. For the increasing friction systems, DIFI and VIFI, of Figures 39 and 40, the break points had the most influence at low pulse severities, with a wide variation in the $\ddot{X}_2$ and RDR response. Using the point (z_1= 0.1), z_2=1.0) as a reference response, it is seen that by advancing the break point z_2 (that is, lower values of z_2), the system had more damping and responded with larger $\ddot{X}_2$ but smaller RDR. On the other hand, by delaying the initial break point z_1 (higher values of z_1), there was less damping in the system which increased RDR. In the case of the DIFI system, a minimum $\ddot{X}_2$ was achieved at the reference point (z_1=0.1, and z_2=1.0) and $\ddot{X}_2$ increased with the delay of z_1. The minimum $\ddot{X}_2$ response had not yet been reached for the VIFI system and $\ddot{X}_2$ continued to decrease with z_1. At higher pulse severities, the isolator performance was little affected by the break points, the response of the increasing friction systems being determined by their final amounts of damping.

In the DDFI system, as shown in Figure 41, delaying of the break point z_1, that is increasing the value of z_1 with respect to the reference point (z_1=0.1, z_2=1.0), produced a general increase in the amount of damping for all pulse severities, and hence, increased $\ddot{X}_2$. By advancing the final break point z_2, a reduction in $\ddot{X}_2$ was achieved, though at the lower pulse severities, RDR was somewhat increased. Regardless of the value of the break points, however, a generally constant transmitted acceleration response which was independent of pulse severity, was attained.

The reference response of the VDFI system shown in Figure 42, had a low $\ddot{X}_2$ and RDR for (ν=1), both of which increased with increasing pulse severity. For ($\nu \geq 5$), however, $\ddot{X}_2$ began to decrease, as at these high severities, the system had effectively low damping. By advancing the final break point z_2, even further reductions in $\ddot{X}_2$ were achieved. Delaying the inital break point z_1 produced higher damping as compared to the reference response, and $\ddot{X}_2$ did not decrease at the high ν values.

At (ν=1), the opposite effect occurred, as the delay of z_1 improved the $\ddot{X}_2$ and RDR response as compared to the reference point. Advancing z_2 caused a deterioration to the reference response.

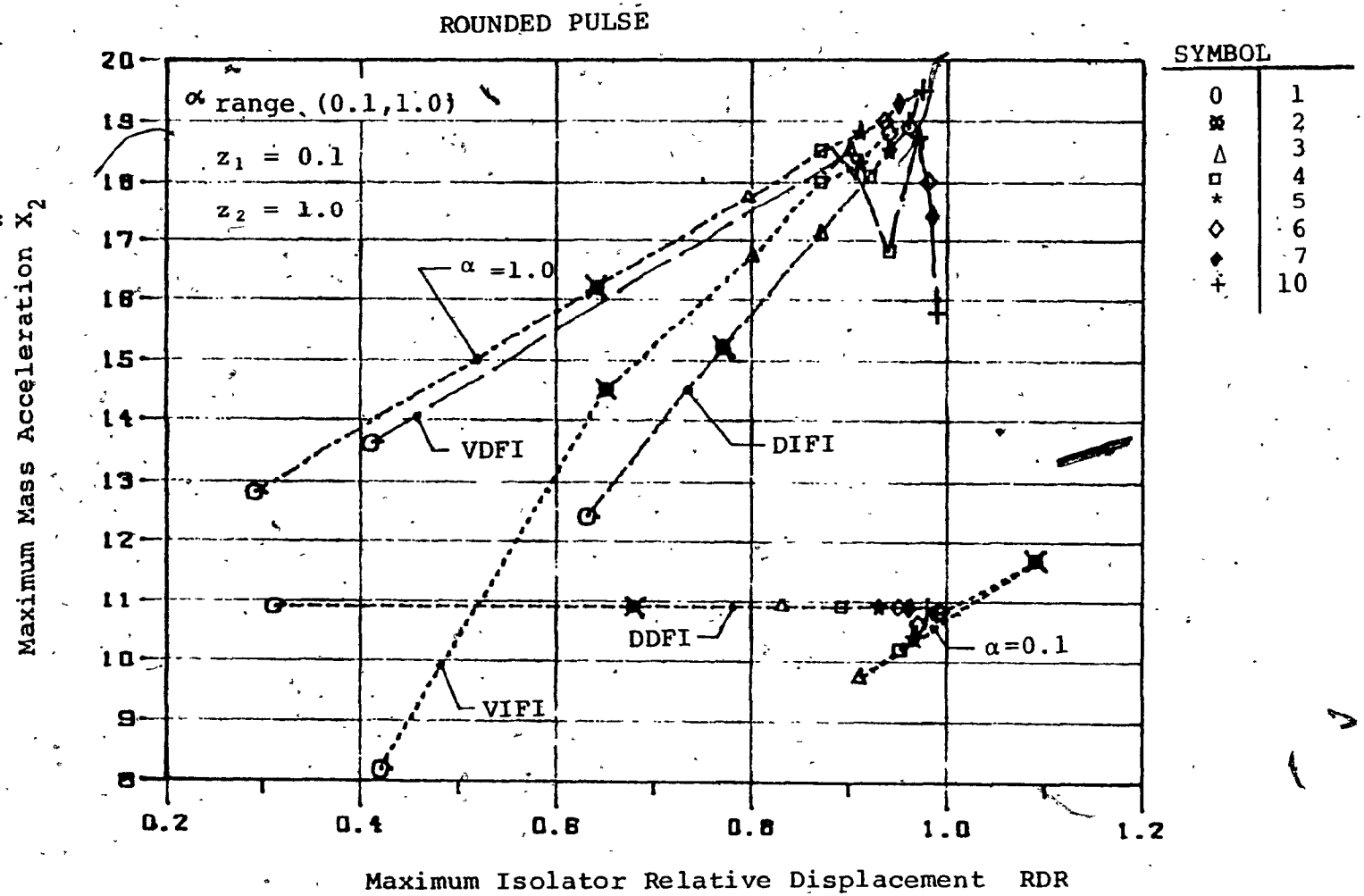

FIGURE 38: Comparison of Performance of DCFI System having Fixed and Adaptive Friction Devices for Various Pulse Severities: $\omega_n = \pi$

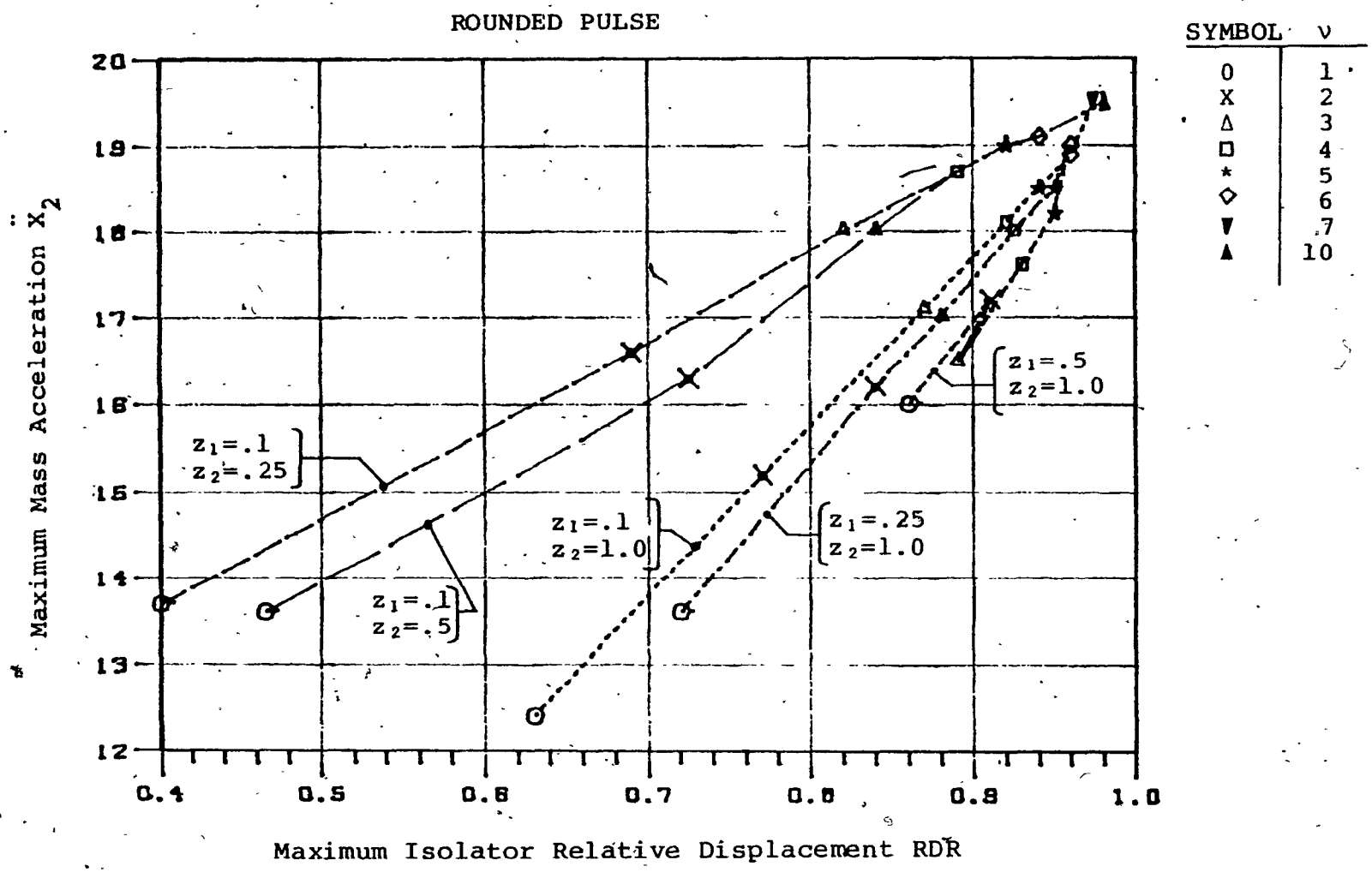

FIGURE 39: Performance of DCFI System having DIFI Device for Various Break Points and Pulse Severities: $\omega_n=\pi$ $\alpha_0=0.1$, $\alpha_f=1.0$

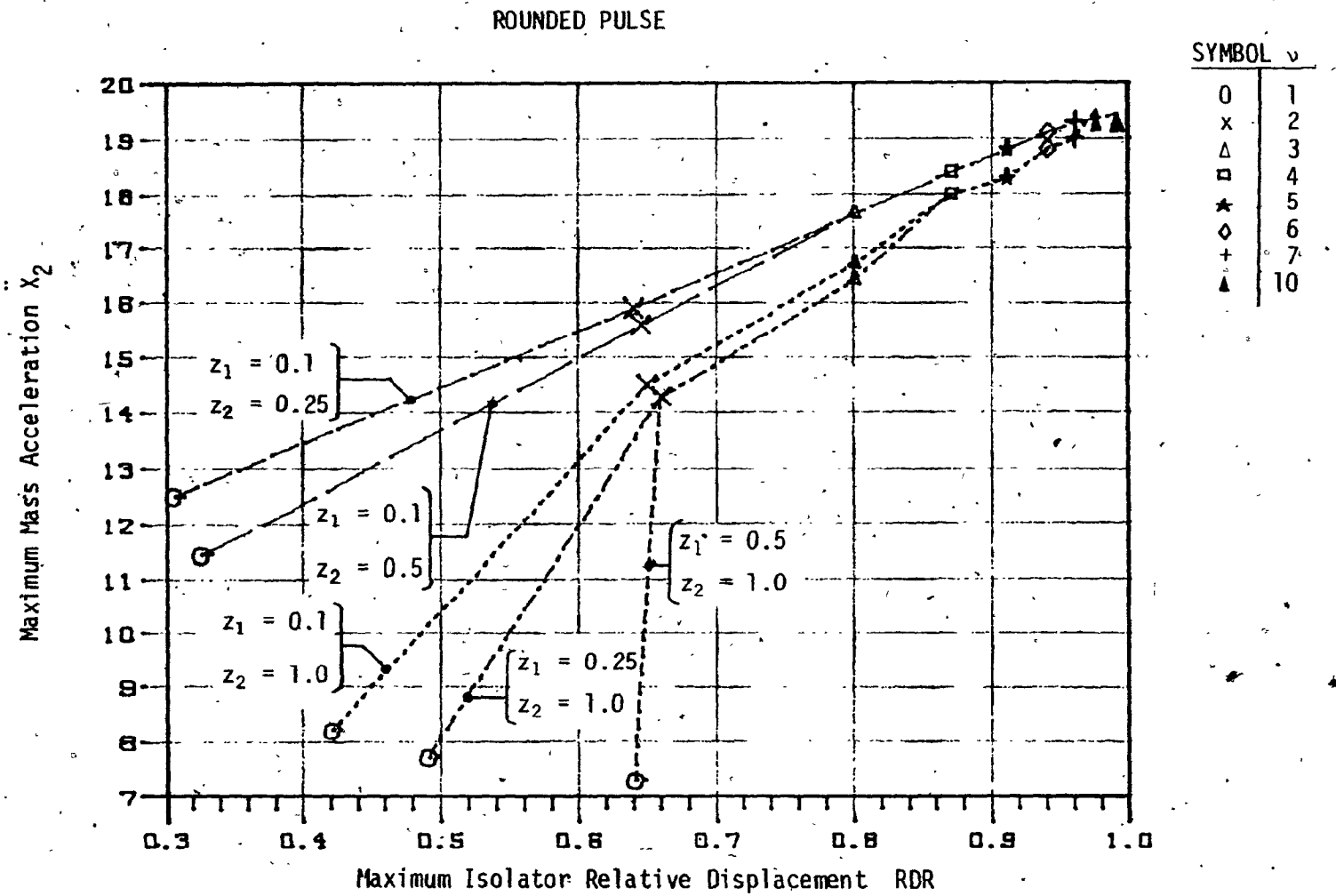

Figure 40. Performance of DCFI System Having VIFI Device for Various Break Points and Pulse Severities: $\omega_n = \pi$ $\alpha_o = .1$ $\alpha_f = 1.0$

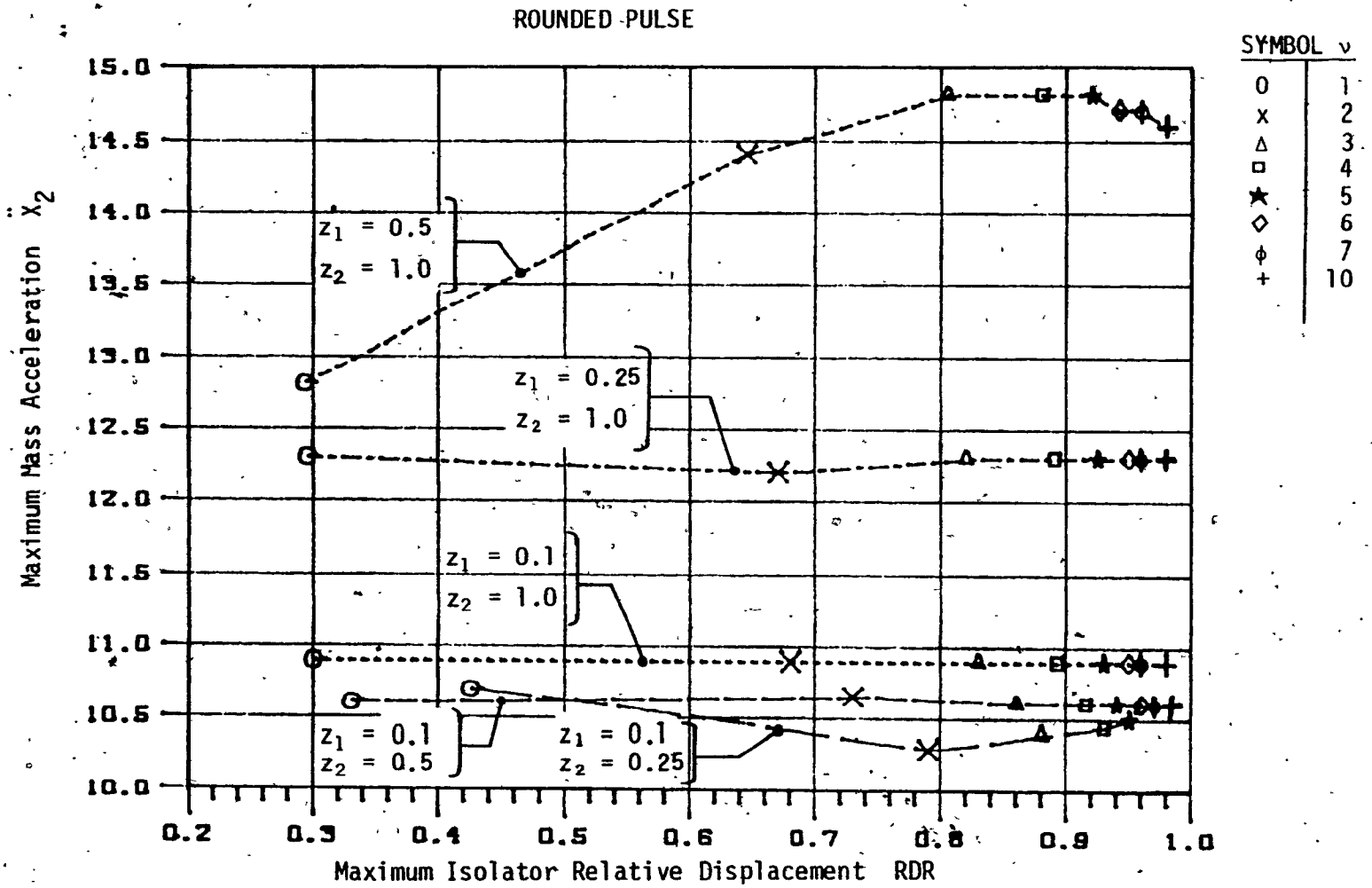

FIGURE 41. Performance of DCFI System having DDFI Device for Various Break Points and Pulse Severities: $\omega_n = \pi$ $\alpha_o = 1.0$ $\alpha_f = .1$

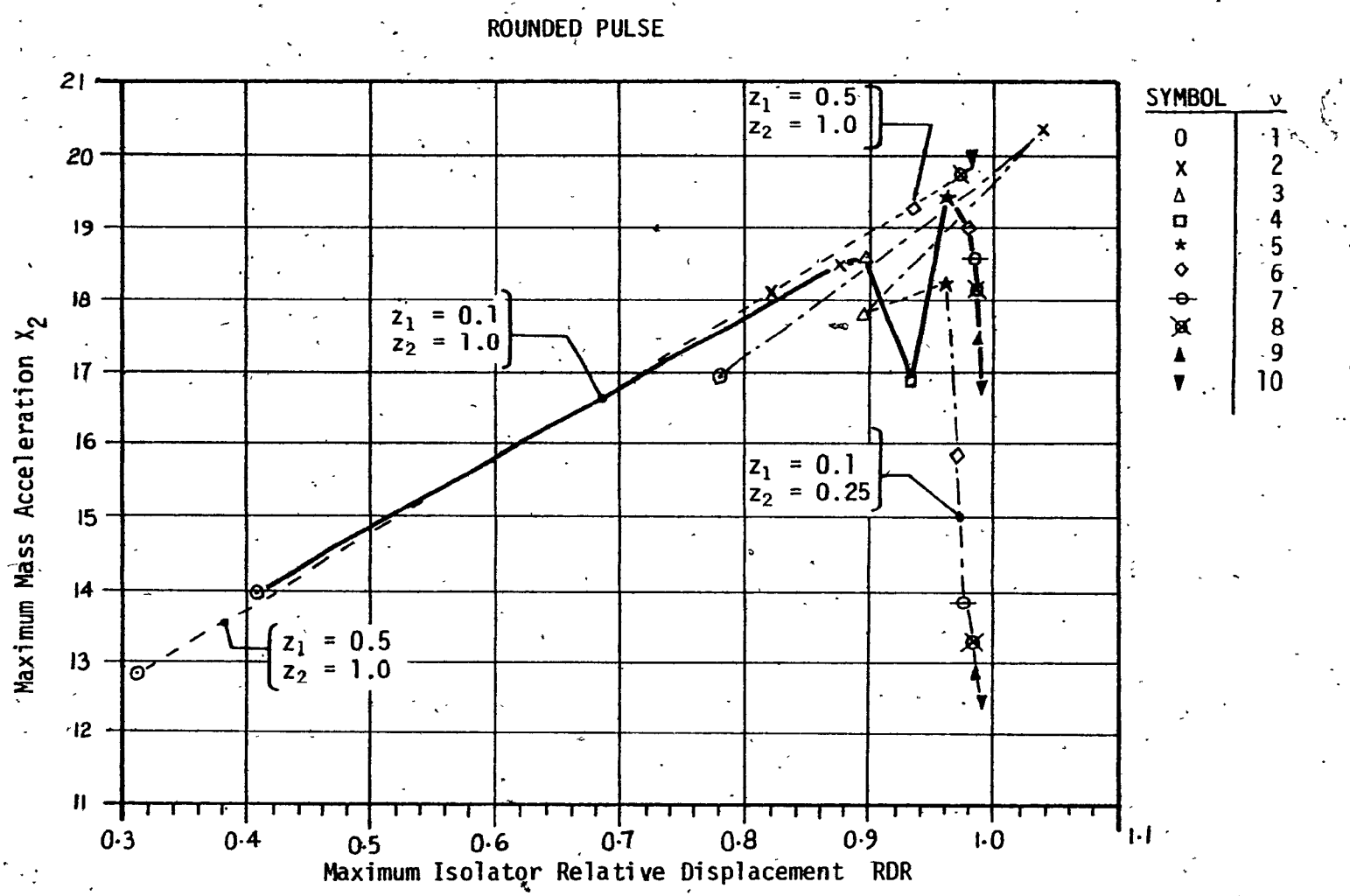

FIGURE 42. Performance of DCFI System having VDFI Device for Various Break Points and Pulse Severities: $\omega_n = \pi$ $\alpha_o = 1.0$, $\alpha_f = 0.1$

5.3.4 TIME RESPONSE OF COULOMB DAMPED FRICTION ISOLATORS

In this section the acceleration and relative displacement time responses of the DCFI system having constant and adaptive coulomb friction characteristics are discussed. The base excitation was a rounded pulse displacement of severity (ν=5). Figures 43 and 44 show the influence of the damping parameter α on the time responses for the constant coulomb friction isolator. It was found that α had only a small influence on the maximum relative displacement (RDR). However it had a large effect on the transmitted accelerations to the mass and the rate at which the system came to rest. It is seen from Figure 43 that the magnitudes of the first and second acceleration peaks were proportional to the degree of damping, and that at the higher damping levels, the system was quickly brought to rest. As seen in Figure 44, however, the relative displacement, particularily for high coulomb damping, did not return to its zero position. This was due to the friction damper which caused the isolator to lock-up when the external forces applied across the damper ends became less than the break-out friction force. (Note: the time histories of the elastically coupled friction isolators have not been presented, as there were large limit-cycle oscillations in the acceleration response after the pulse had ended. The $\ddot{X}_2$ and RDR responses, however, were found to be unaffected).

Figures 45 through 48 show the comparison of the transmitted acceleration time responses of the DCFI system having the four types of adaptive coulomb damping,to those of the constant friction isolator with low (α=0.1) and high (α=1.0) damping. The damping range and break points were the same for the four adaptive devices: (α between 0.1 and 1.0) and (z_1=0.1, z_2=1.0). From the figures, it is seen that the time response of the adaptive friction isolators varied between the limits set by the response of the two constant friction systems. All the adaptive systems brought the system to rest in a short time as compared to the low damped, constant friction isolator. Comparing the maximum acceleration values, it is seen that the DDFI system had the best performance of the adaptive systems, with its peak value, nearly equal to the low damped system.

Figure 49 shows the corresponding relative displacement time responses of the four adaptive friction and the two constant friction isolators. It is seen that the maximum relative displacement was nearly all the same for the six isolators. The DDFI, VDFI and the (α=1.0) fixed friction system showed a lock-up of the isolator prior to returning to their zero position. The VIFI and DIFI systems, having low damping around the zero velocity and zero displacement states respectively, had limited lock-up tendencies, and showed a convergence to the zero position.

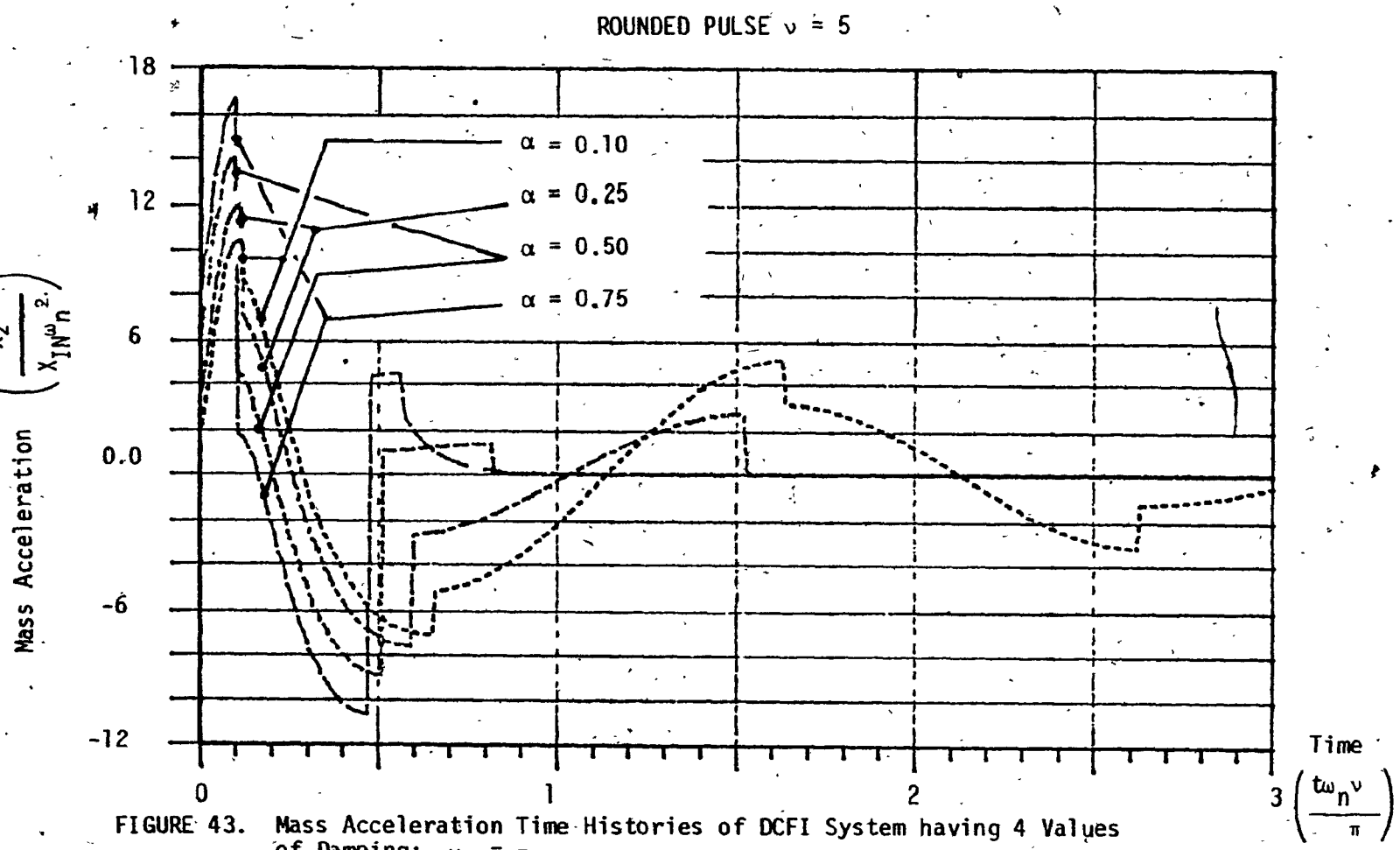

FIGURE 43. Mass Acceleration Time Histories of DCFI System having 4 Values of Damping: $\omega_n = \pi$

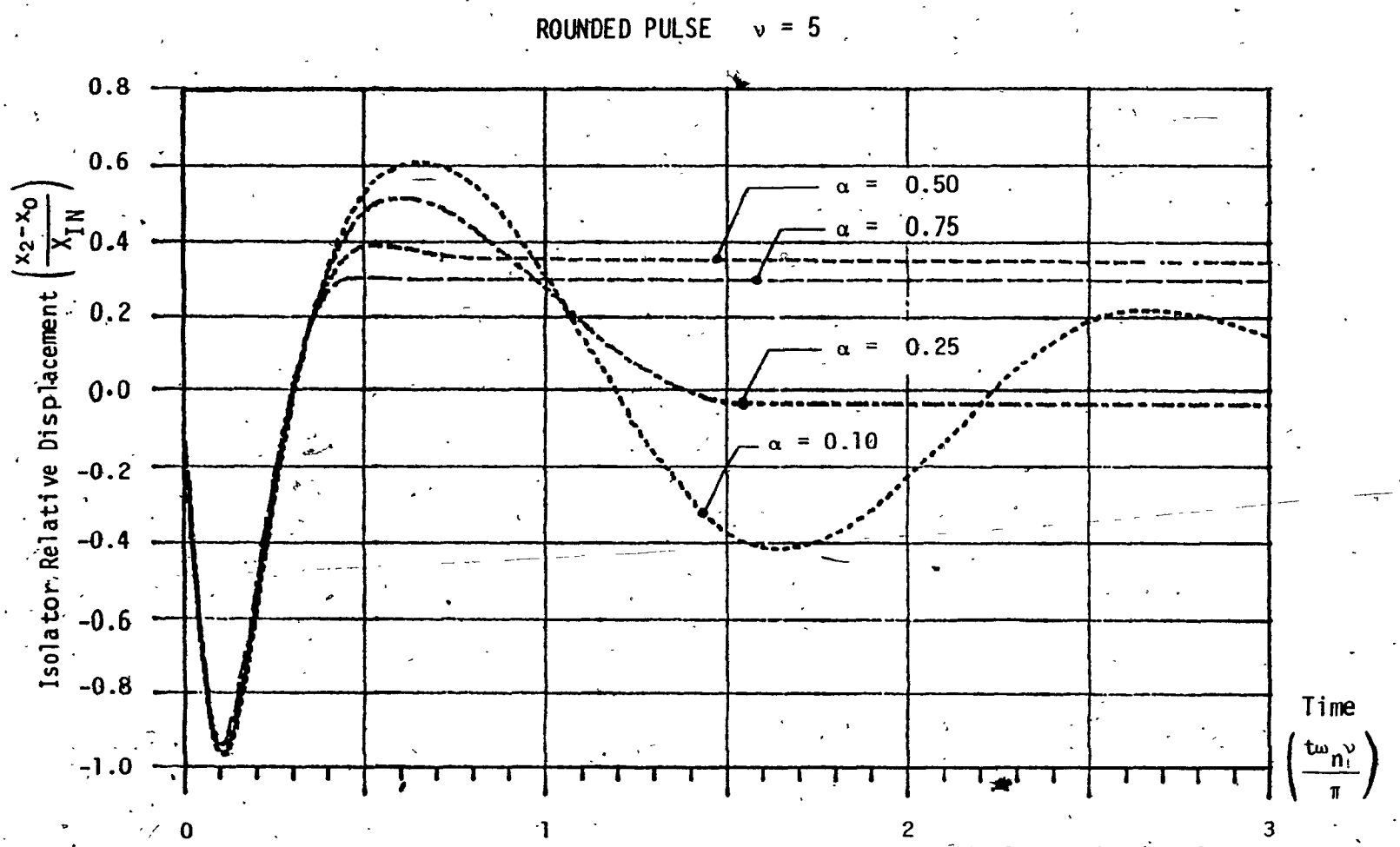

FIGURE 44. Isolator Relative Displacement Time Histories for DCFI System having 4 Values of Damping: $\omega_n = \pi$

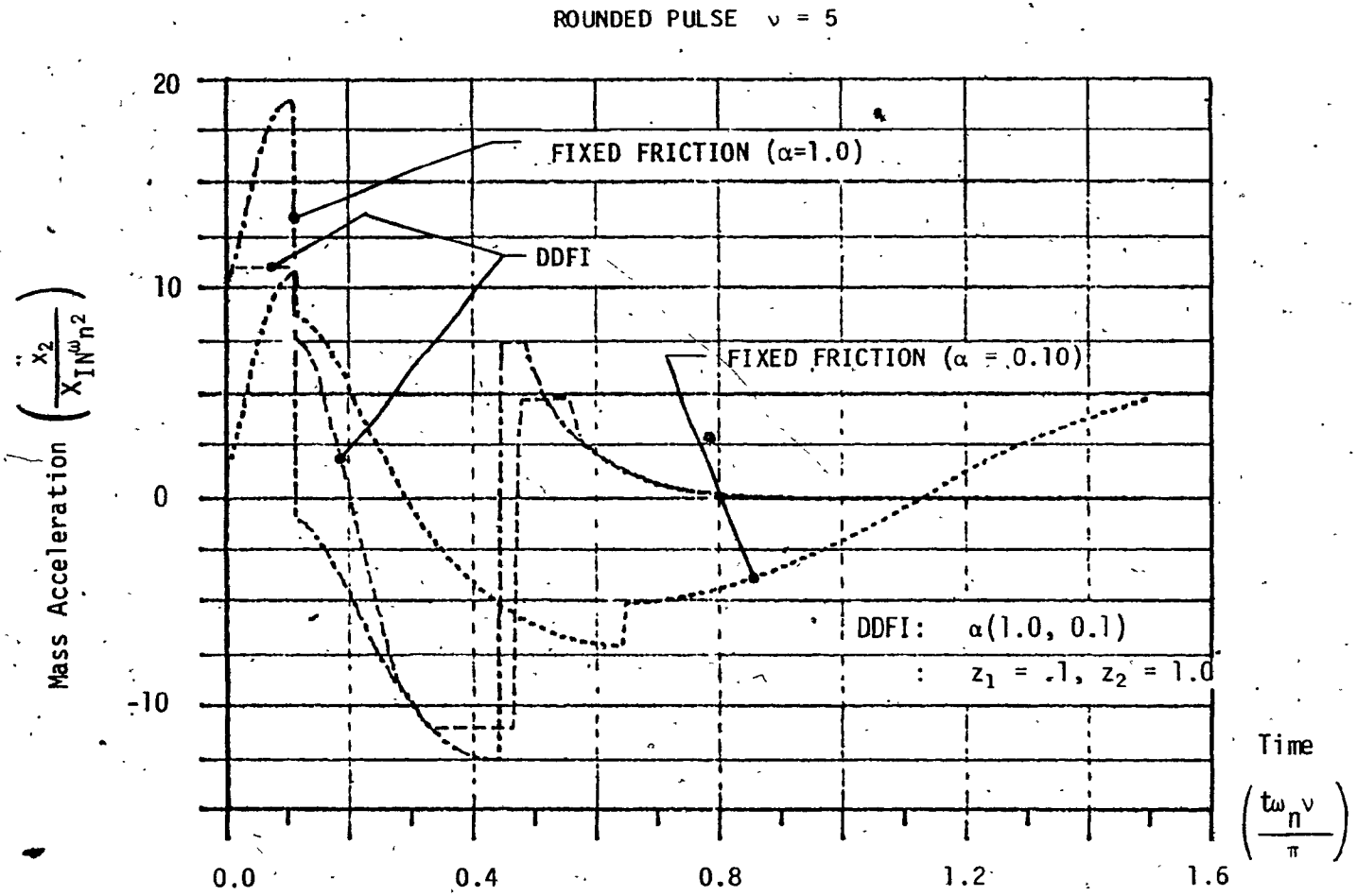

FIGURE 45. Comparison of Mass Acceleration Time Histories of DCFI Systems having DDFI and Fixed Friction: $\omega_n = \pi$

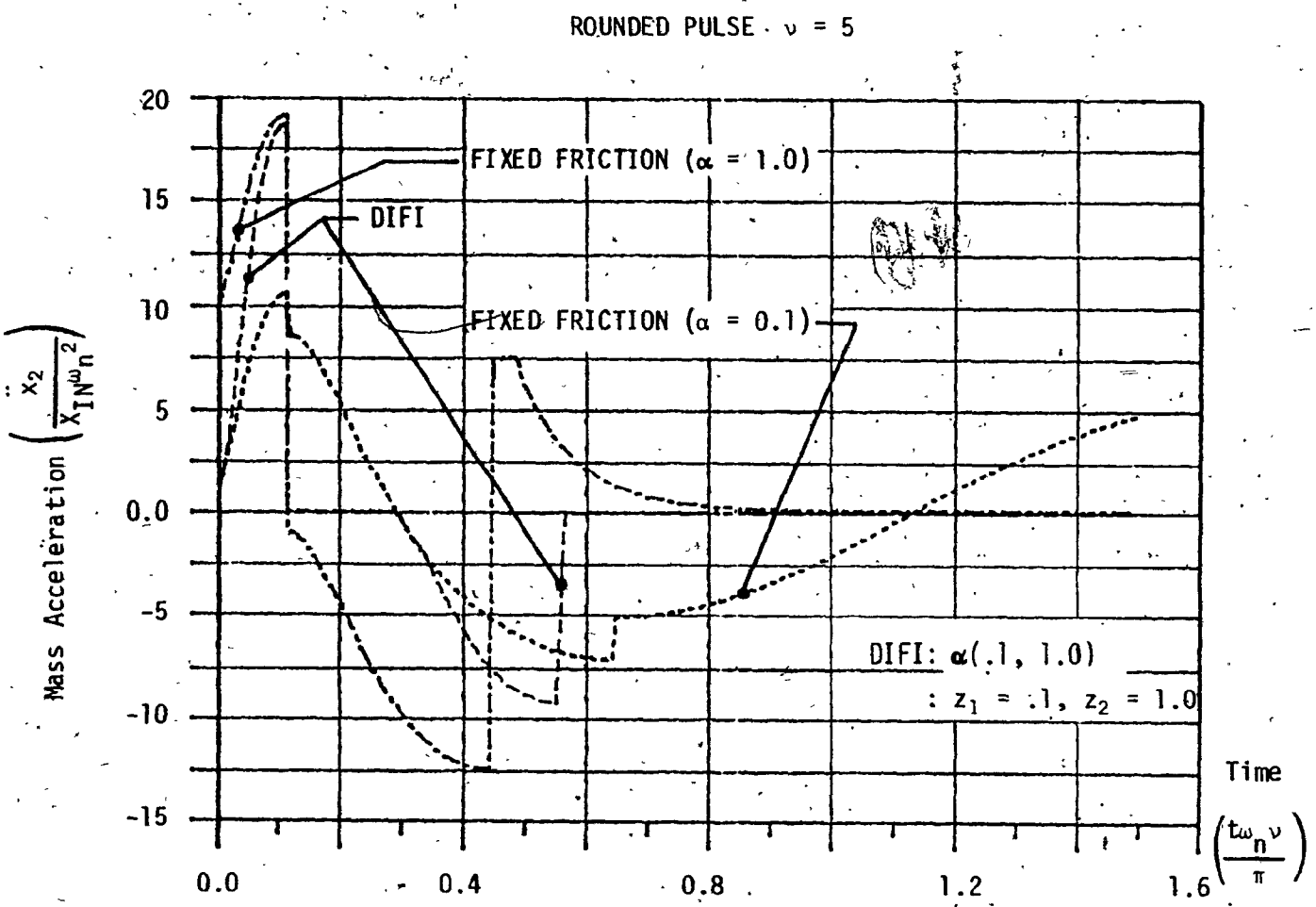

FIGURE 46. Comparison of Mass Acceleration Time Histories of DCFI Systems having DIFI and Fixed Friction: $\omega_n = \pi$

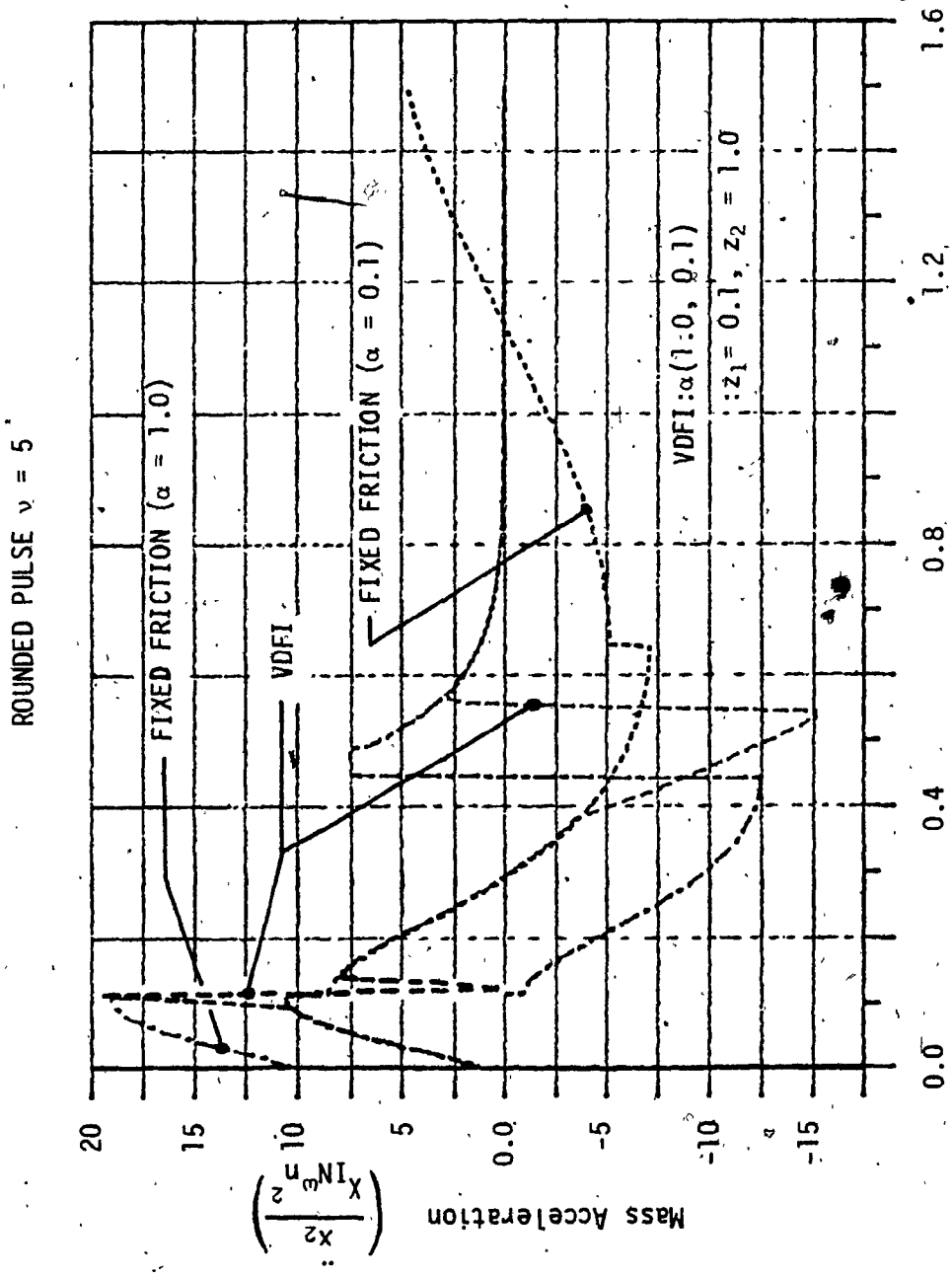

FIGURE 47. Comparison of Mass Acceleration Time Histories of DCFI Systems having VDFI and Fixed Friction: $\omega_n = \pi$

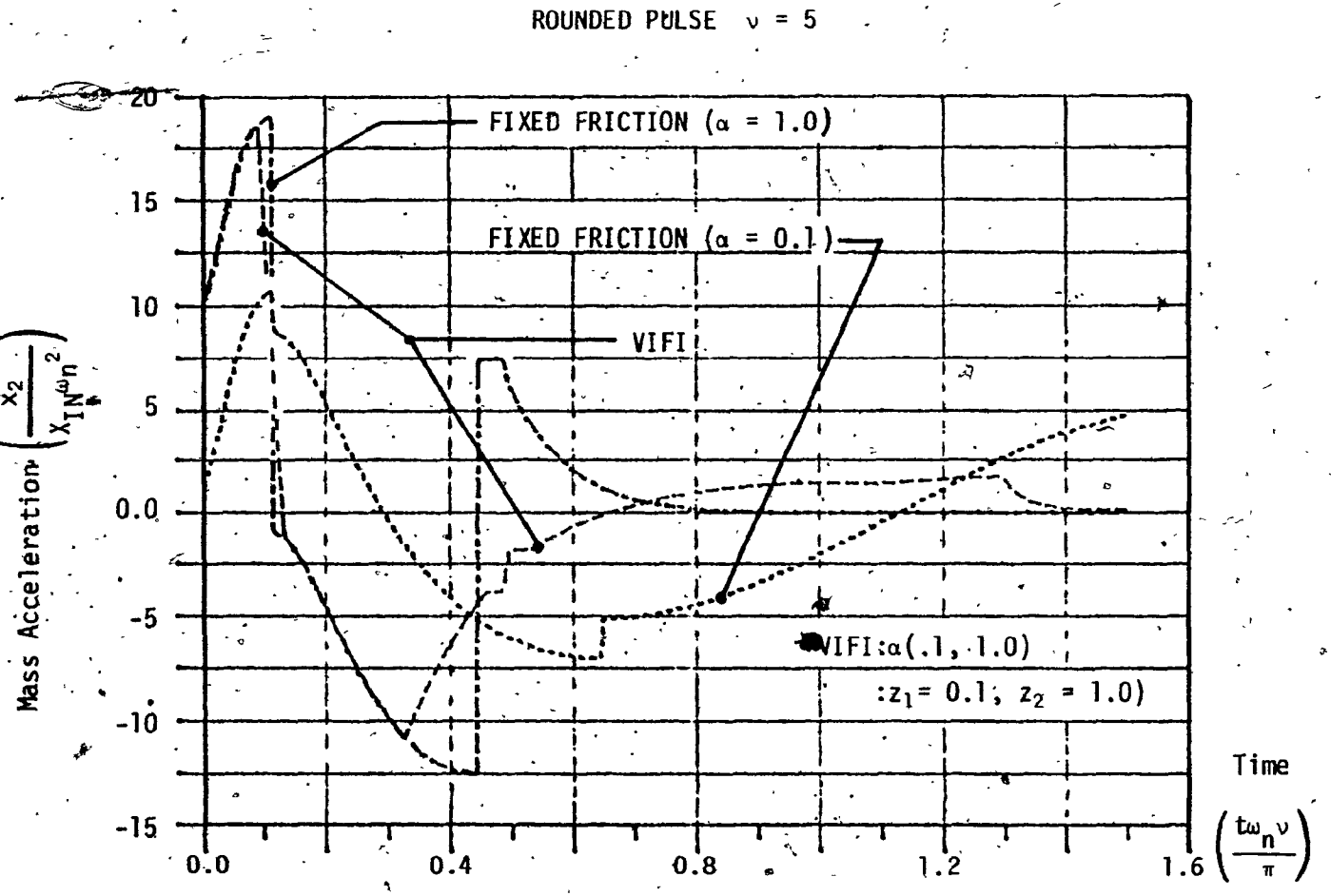

FIGURE 48. Comparison of Mass Acceleration Time Histories of DCFI Systems having VIFI and Fixed Friction: $\omega_n = \pi$

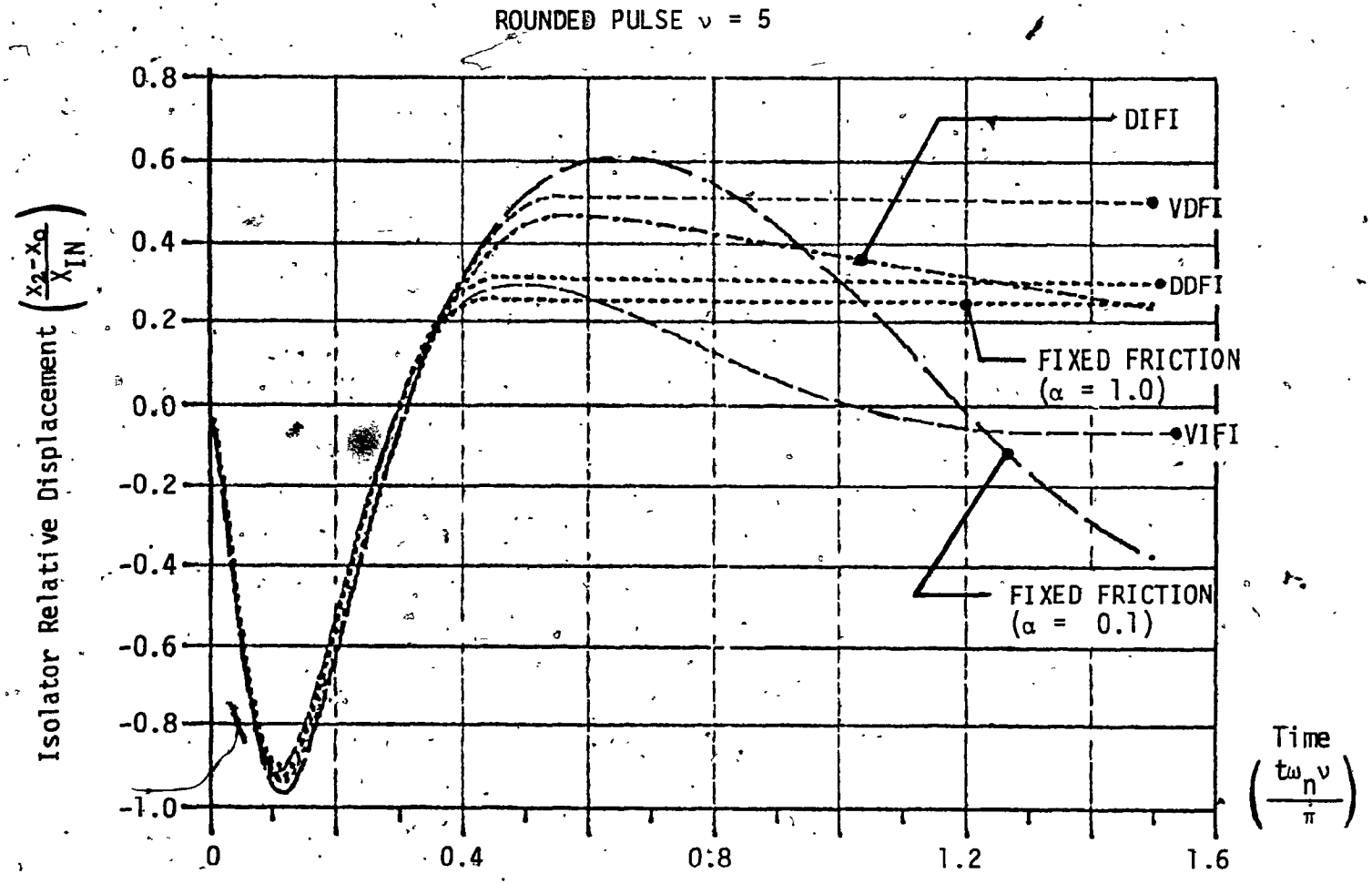

FIGURE 49. Comparison of Isolator Relative Displacement Time Histories of DCFI Systems having DDFI, DIFI, VDFI and VIFI and Fixed Friction.

5.4.1. COMBINED VISCOUS AND COULOMB DAMPED ISOLATORS (CVFI) SUBJECTED TO ROUNDED PULSE DISPLACEMENTS

Figures 50 through 56 are the performance curves of the combined viscous and coulomb damped isolator subjected to rounded pulse displacements of various severities. In Figures 50 and 51, the influence of the coulomb damping parameter α, on the response of the isolator having viscous damping ratios (ξ=0.25) and (ξ=0.50) is shown. For low coulomb damping, (α=0.1) and (α=0.25), the isolator behaved poorly at low pulse severities and had large values of RDR and $\ddot{X}_2$. This was due to the force limiting characteristic of the coulomb damper, which at low values of α, resulted in such low input velocities across the viscous damper, that the overall damping of the isolator was very small. A comparison of the responses of the CVFI system with low α and an undamped directly coupled system (ie. ξ=0), as given in Table 6, shows this to be the case. At the higher pulse severities, though the system remained substantiately undamped, the inertia of the mass was able to better control the behaviour of the system to give lower values of RDR and $\ddot{X}_2$.

For higher coulomb damping ($\alpha \geq 0.5$), the CVFI system had a much improved performance. At low pulse severity, it had low RDR and $\ddot{X}_2$, and as can be seen in Table 7, it approached the response of the DCVI system having the same degree of viscous damping. As the pulse severity increased so did RDR and $\ddot{X}_2$. However, at the high pulse severities the maximum transmitted acceleration leveled out, and the isolator responded in a similar manner as to a DCFI system (as shown in Table 7). It can be seen from Figures 50 and 51 that the amount of coulomb damping determined

the amount of $\ddot{X}_2$ at the high severities. To minimize $\ddot{X}_2$ it would be desirable to keep α small. However, this was found to have its drawbacks, as the CVFI system with low α gave poor performance at low severities. Hence a minimum value of α appears necessary: particularily if the isolator was to be subjected to pulse displacements of varying severities.

Figure 52 shows the influence of the viscous damping ratio ξ on the response of the CVFI system. For low ξ, the RDR behaviour was poor. As ξ was increased, the RDR performance improved, particularily at the lower severities, though there was a penalty in increased $\ddot{X}_2$. In Figure 52, it can be seen that all performance curves of the CVFI system plotted for variations in ξ with α =1.0 were completely bounded by the performance curve of the DCFI system with $\xi = \infty$.

Figure 53 shows the combined effect of viscous damping and coulomb damping on the performance of the CVFI system subjected to a rounded pulse displacement of severity (ν=5), and compares it to that of the DCVI and DCFI systems. It can be seen that the CVFI system had a poorer response compared to the other two systems, as it had higher RDR values for the same amount of $\ddot{X}_2$.

Figure 54 compares the performance of the CVFI system having adaptive friction devices versus constant coulomb friction dampers for various pulse severities. Two levels of constant coulomb friction were selected, (α=0.1) and (α=1.0), and the end points of the adaptive friction range were set to these two values. The values of z_1 and z_2, the limits in the adaptive friction dampers, were selected as z_1=.1 and z_2=1.0. It was found in general that the performances of the four types

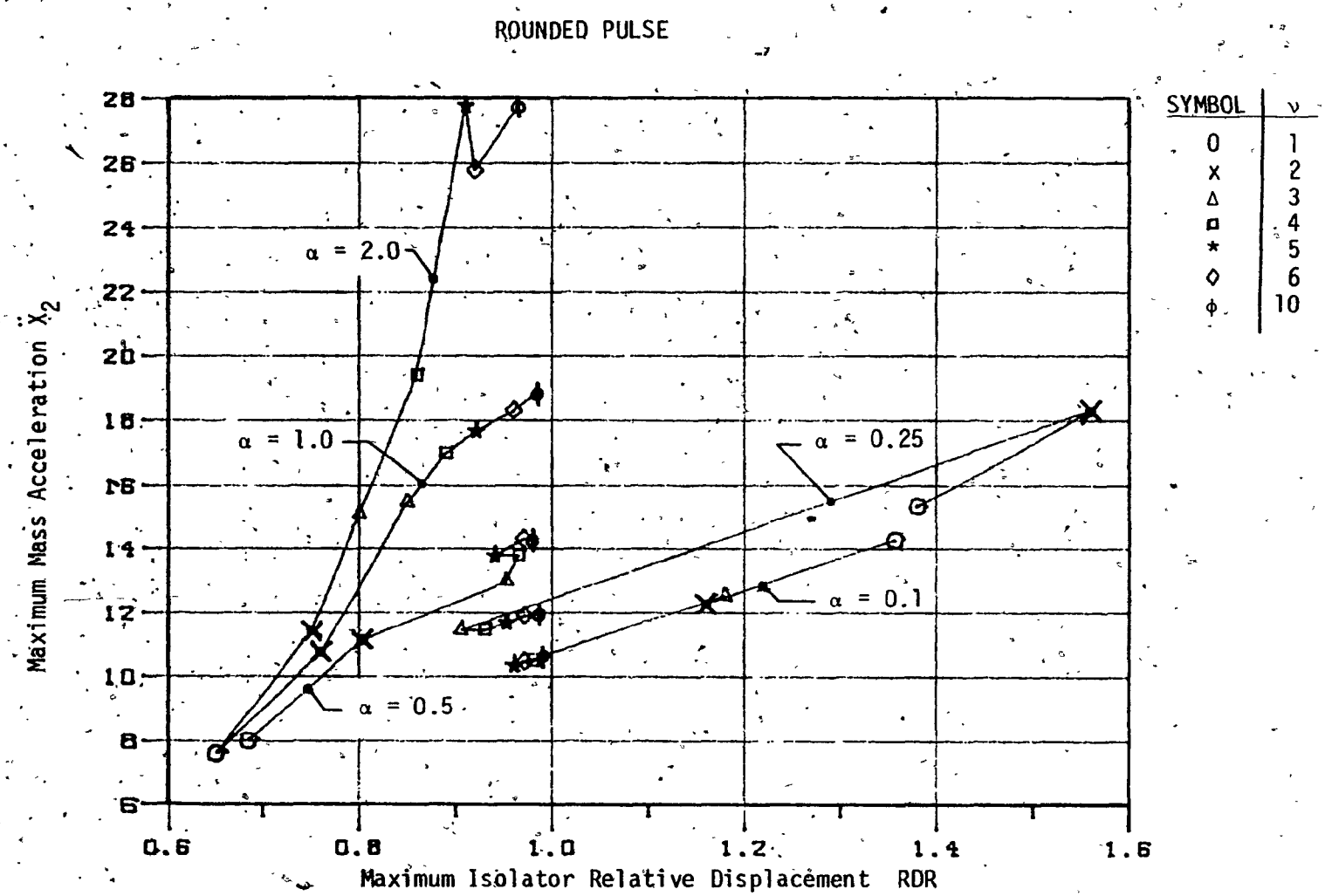

FIGURE 50. Performance of CVFI System for Various Coulomb Damping Ratios α and Pulse Severities: $\xi = 0.25$ $\omega_n = \pi$

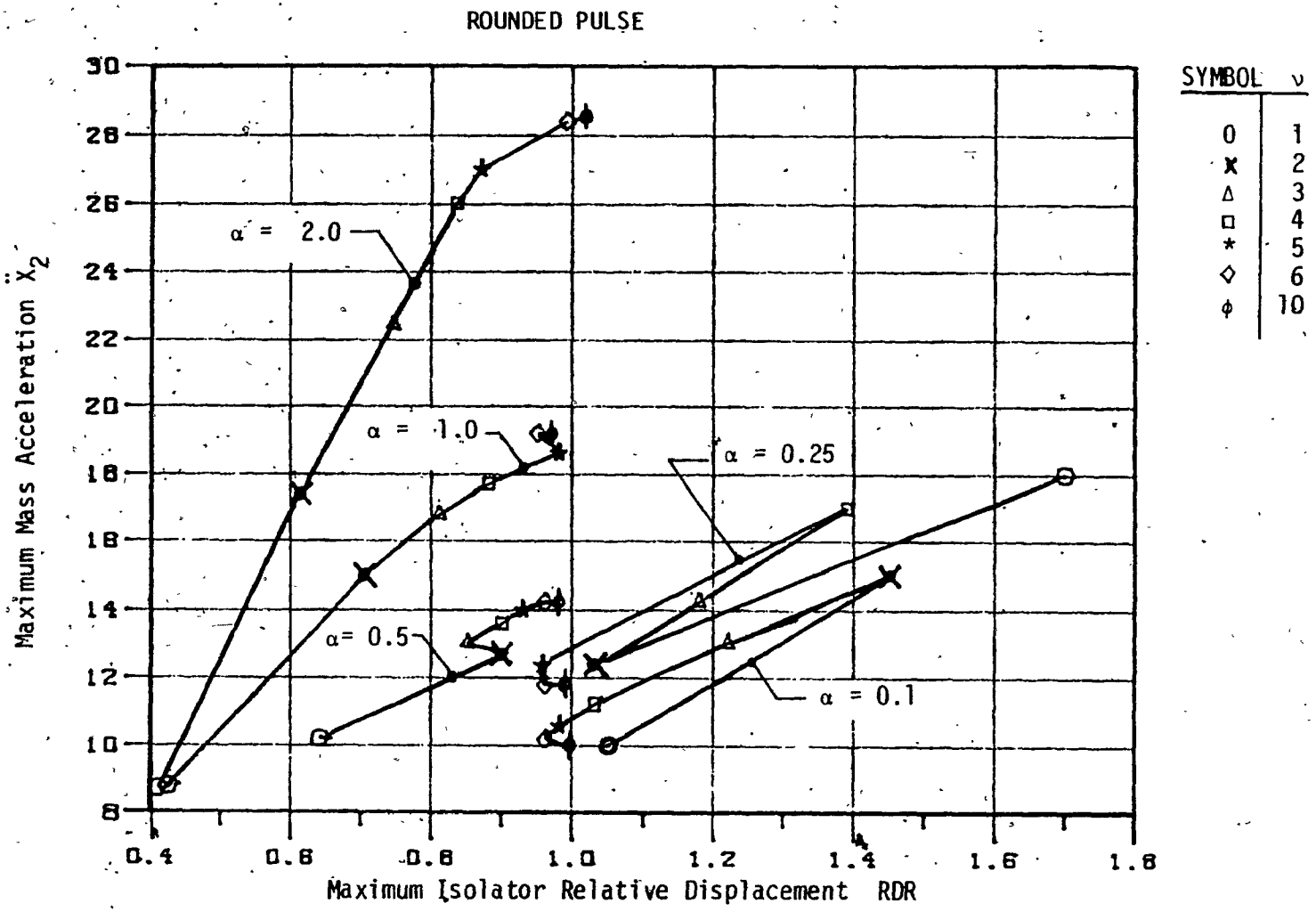

FIGURE 51. Performance of CVFI System for Various Coulomb Damping Ratios α and Pulse Severities: $\xi = 0.50$ $\omega_n = \pi$

ROUNDED PULSE

ISOLATOR $\omega_n = \pi$	$\nu = 1$		$\nu = 3$		$\nu = 5$		$\nu = 10$	
	RDR	$\ddot{X}_2$	RDR	$\ddot{X}_2$	RDR	$\ddot{X}_2$	RDR	$\ddot{X}_2$
CVFI $\alpha = 0.1$ $\xi = 0.25$	1.36	14	1.18	12.5	0.96	10.2	0.98	11
DCVI $\xi = 0$ (undamped)	1.33	13.17	1.05	10.37	0.97	9.57	0.99	9.78

TABLE 6: COMPARISON OF CVFI SYSTEM WITH LOW COULOMB DAMPING AND UNDAMPED DCVI SYSTEM.

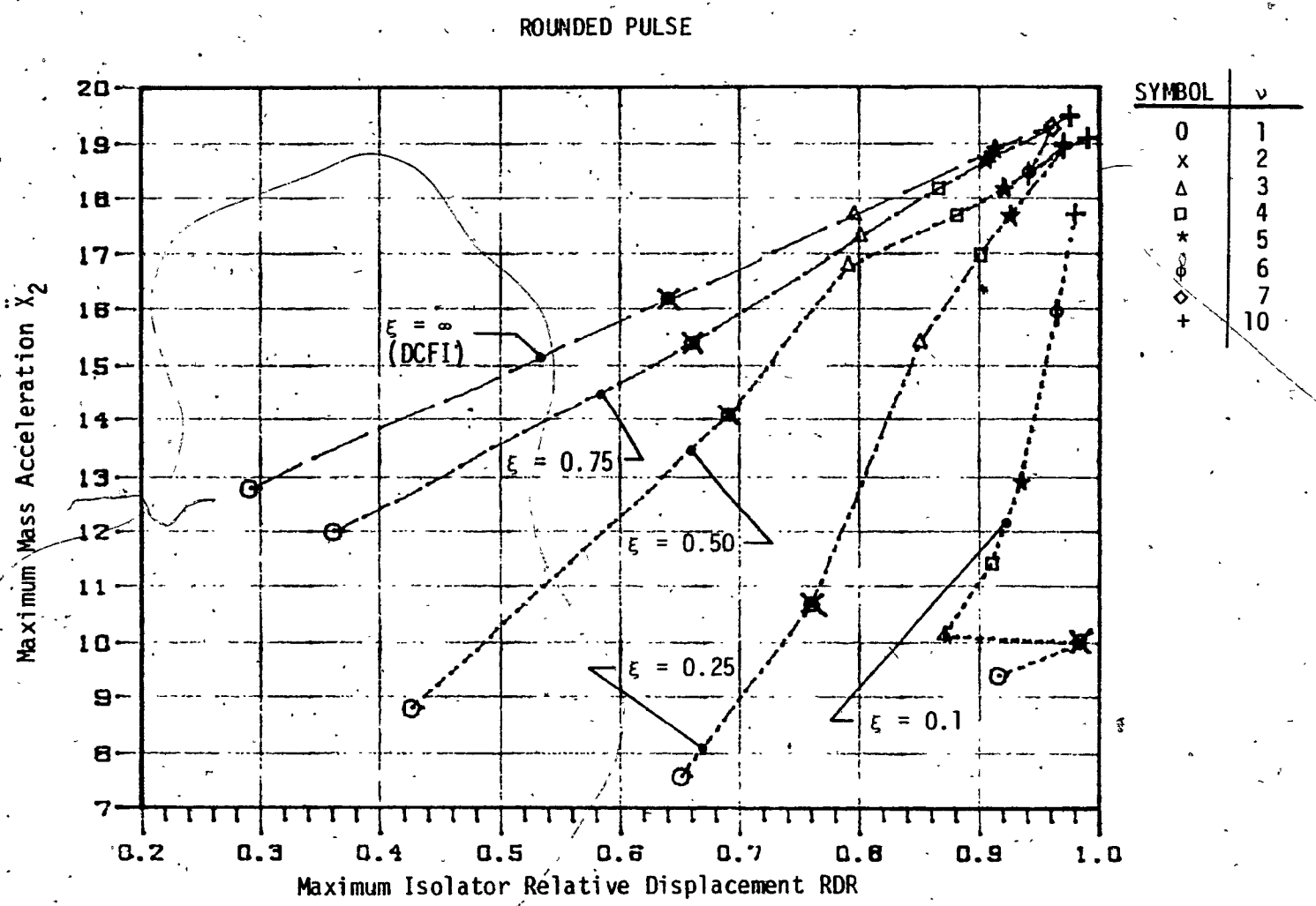

FIGURE 52. Performance of CVFI System for Various Viscous Damping Ratios ξ and Pulse Severities: $\alpha = 1$ $\omega_n = \pi$

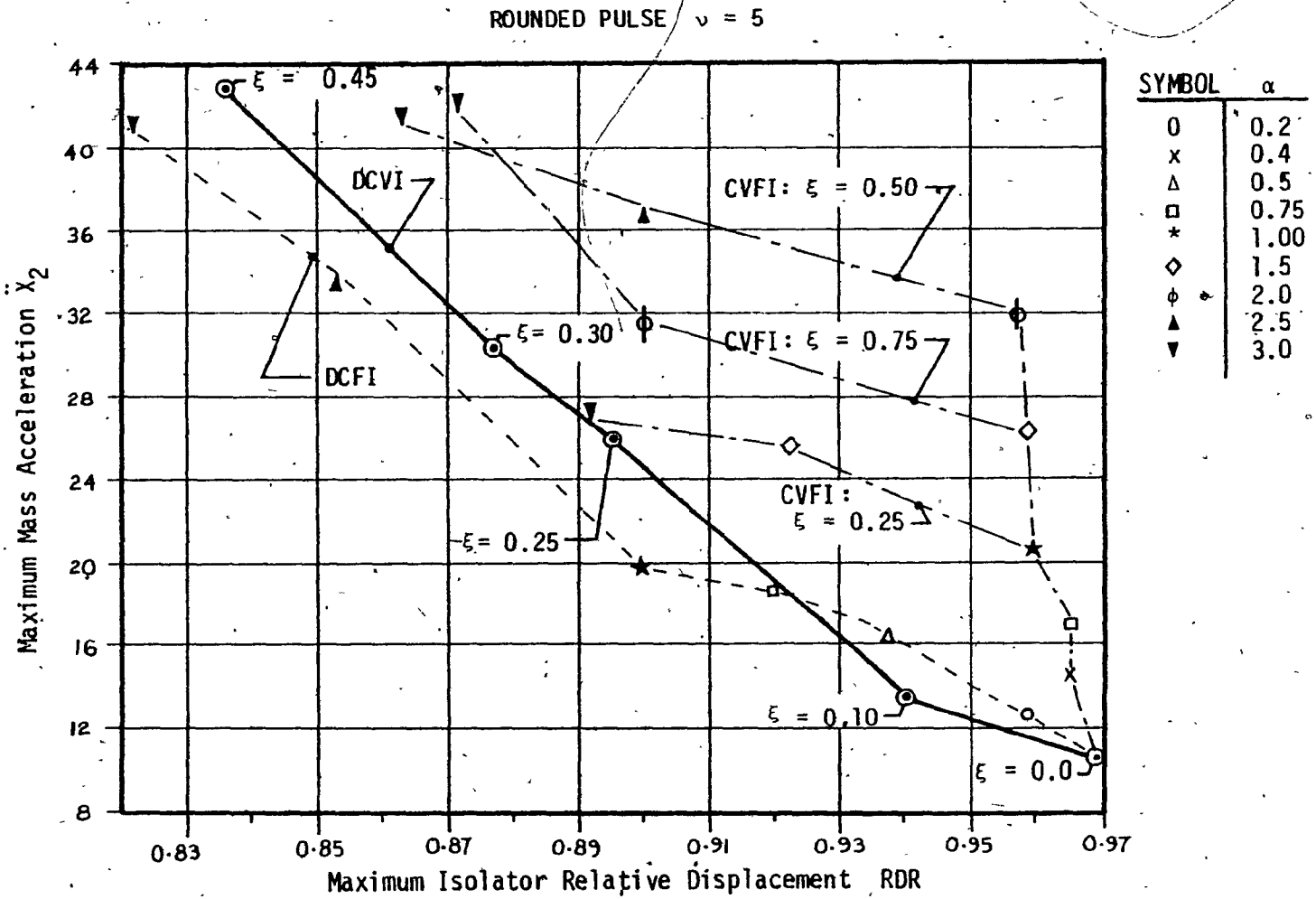

FIGURE 53. Comparison of Performance of DCVI, DCFI and CVFI Systems for Various Values of Damping ξ and α : $\omega_n = \pi$

ROUNDED PULSE

ISOLATOR $\omega_n = \pi$	$\nu = 1$		$\nu = 3$		$\nu = 5$		$\nu = 10$	
	RDR	$\ddot{X}_2$	RDR	$\ddot{X}_2$	RDR	$\ddot{X}_2$	RDR	$\ddot{X}_2$
CVFI $\xi = 0.25$ $\alpha = 0.50$	0.68	7.8	0.92	13	0.94	13.8	0.99	14.2
DCVI $\xi = 0.25$	0.66	7.5	0.80	15.4	0.88	24	0.94	45
DCFI $\alpha = 0.50$	0.43	9.1	0.87	13.2	0.94	14.2	0.98	14.7

TABLE 7: COMPARISON OF CVFI, DCVI AND DCFI SYSTEMS HAVING THE SAME VISCOUS AND COULOMB DAMPING.

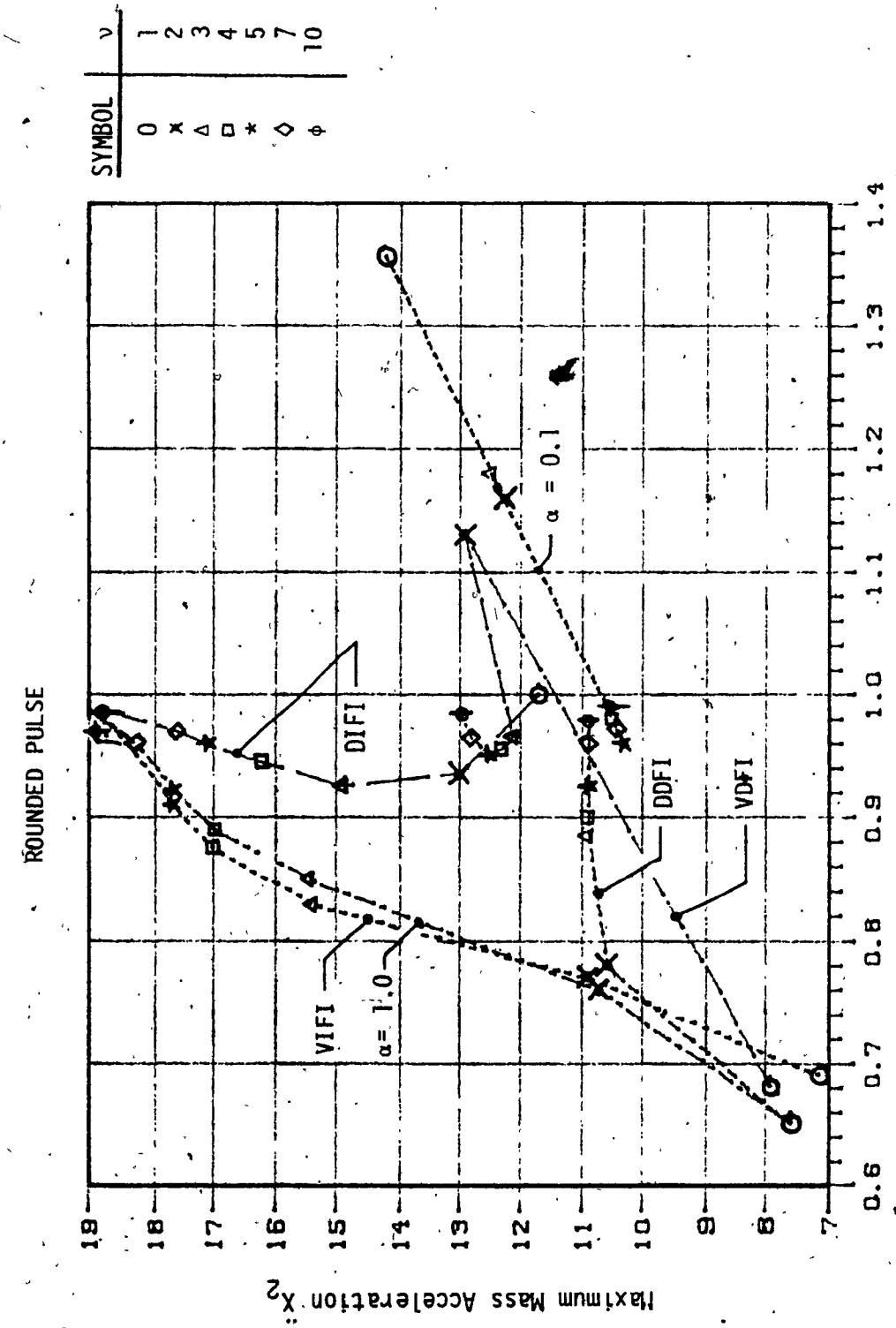

FIGURE 54. Comparison of Performance of CVFI System having Fixed and Adaptive Friction Devices for Various Pulse Severities: $\omega_n = \pi$ α range (-1, 1.0) $\xi = 0.25$: $z_1 = 0.1$ $z_2 = 1.0$

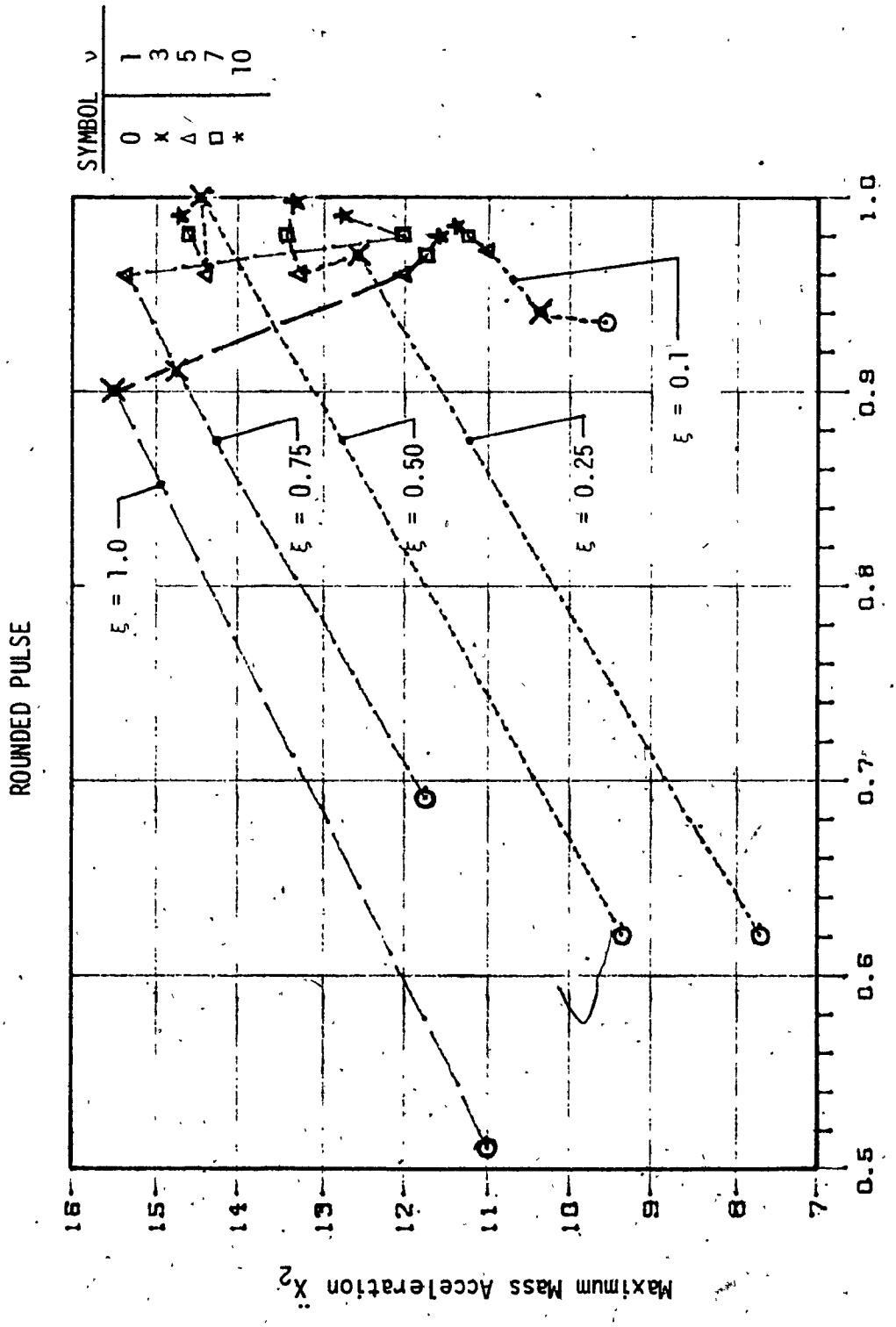

FIGURE 55. Performance of CVFI System having VDFI Device for Various Viscous Damping Ratios ξ and Pulse Severities: $\omega_n = \pi$ α range(1.0, 0.1) $z_1 = 0.1$ $z_2 = 1.0$

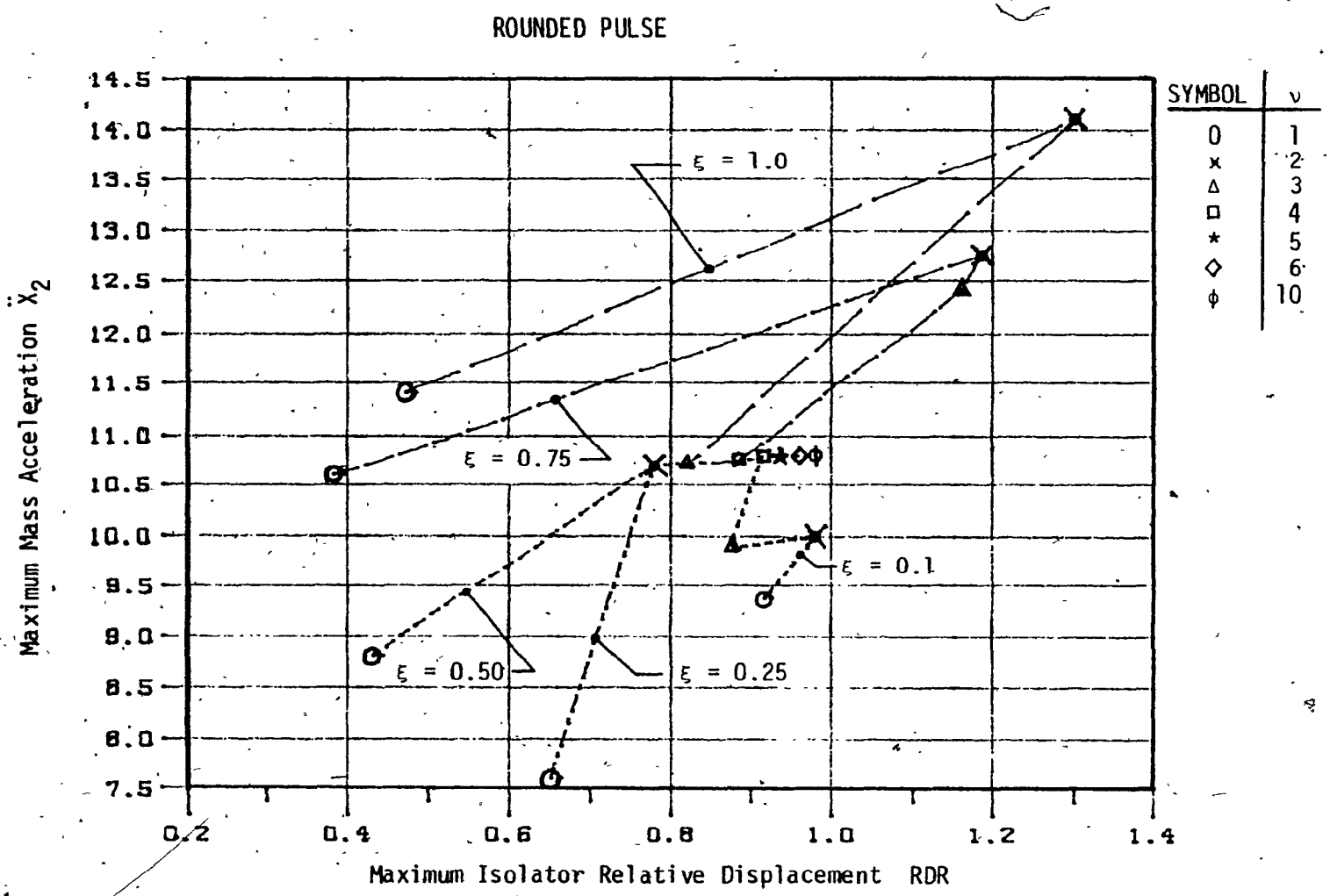

FIGURE 56. Performance of CVFI System having DDFI Device for Various Viscous Damping Ratios ξ and Pulse Severities: $\omega_n = \pi$ α range (1.0, 0.1) $z_1 = 0.1$ $z_2 = 1.0$

of adaptive friction CVFI were bounded by those of the constant friction CVFI systems, and that as the pulse severity increased, they tended to show a crossover response between the two bounds. (This behaviour was similar to that of the DCFI system having adaptive friction shown in Figure 38). Of the four adaptive isolators, the DDFI system was found to give the best performance: $\ddot{X}_2$ was nearly uniform throughout the range of ν, while RDR increased to absorb the additional base accelerations of the higher pulse severities. The VDFI system also showed low $\ddot{X}_2$ values, but its RDR response was somewhat higher. The VIFI and DIFI isolators had the poorest responses as $\ddot{X}_2$ and RDR increased with ν.

Figures 55 and 56 show the influence of the viscous damping ratio ξ on the response of the CVFI system with the VDFI and DDFI devices for various pulse severities. At (ν=1), increases in ξ for the two systems resulted in decreases of RDR and generally increases of $\ddot{X}_2$. For the DDFI system, except at the resonant condition at ν=2, the response at the higher pulse severities was determined by the adaptive coulomb damper and no differences due to ξ was found. On the other hand, for the VDFI system, the adaptive friction device and the viscous damper, which being both velocity sensitive, had an interdependence on ξ. Hence ξ had a noticeable influence on $\ddot{X}_2$ at the higher severities.

5.4.2. TIME RESPONSE OF THE COMBINED VISCOUS/COULOMB DAMPED ISOLATORS (CVFI)

Figures 57 through 60 show the influence of the viscous damping ratio ξ and the coulomb friction parameter α on the acceleration and relative displacement time responses of the CVFI system subjected to rounded pulse displacements of severity (ν=5). From Figures 57 and 58

it is seen that though the maximum relative displacements (RDR) were unaffected by changes in viscous or coulomb damping, there was a large influence in the subsequent oscillations of the system. At high ξ or α values, the amplitude of the secondary peaks was markedly reduced as the system was quickly brought to rest. For low values of α or ξ, the oscillations were nearly undamped and large excursions occurred.

From the acceleration curves of Figure 59, it was found that the maximum transmitted acceleration $\ddot{X}_2$, was proportional to the coulomb damping. However, in constrast to the DCVI and DCFI systems (as shown in Figures 26 and 43) the second acceleration peak decreased for higher values of α. From Figure 60 it is seen that except for the lowest value of ξ, the maximum acceleration $\ddot{X}_2$ was independent of the viscous damping ratio. This was due to the force limiting effect of the coulomb damper. During the subsequent oscillations the break-out force of the coulomb damper was not reached, and the time response was governed by the degree of viscous damping in the isolator.

Figures 61 and 62 show a comparison of the acceleration and relative displacement time responses to a rounded pulse displacement (ν=5) for the DCVI, DCFI and CVFI systems having the same amounts of viscous and coulomb damping. It is seen that the DCVI had the highest maximum acceleration $\ddot{X}_2$, while the coulomb damper in the CVFI limited its $\ddot{X}_2$ value to that of the DCFI system. After the base excitation had passed (which for ν = 5 was t>0.5) the time response of the CVFI system generally followed that of the viscous isolator. This was particularly

significant in terms of the relative displacement. As shown in Figure 62, the DCFI did not return to its initial zero position, whereas, for both the DCVI and CVFI systems, their relative displacements though still oscillating, were approaching zero.

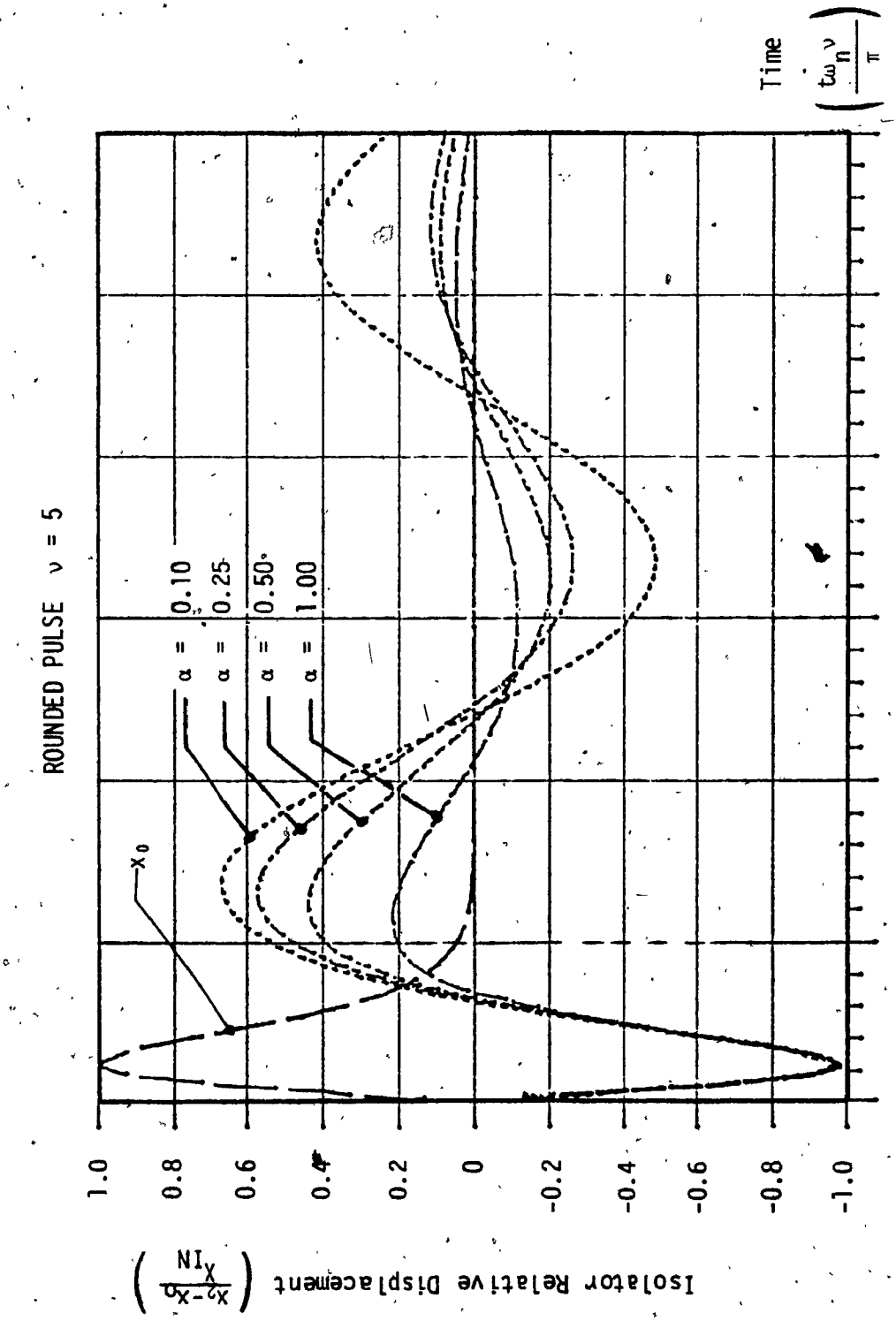

FIGURE 57. Isolator Relative Displacement Time Histories of CVFI System having 4 Values of Coulomb Damping: $\omega_n = \pi$ $\xi = 0.25$

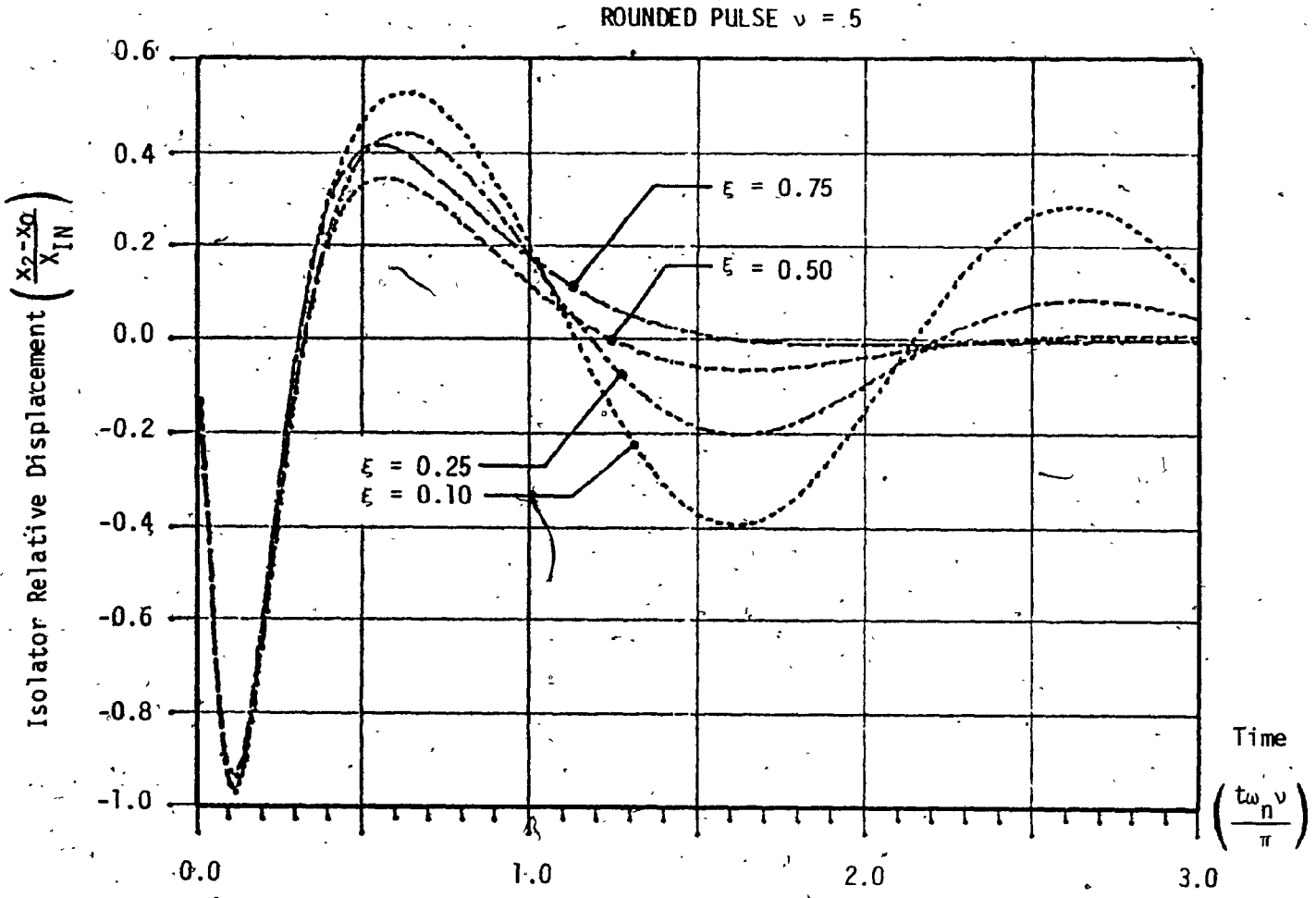

FIGURE 58. Isolator Relative Displacement Time Histories of CVFI System having 4 Values of Viscous Damping: $\omega_n = \pi$ $\alpha = 0.50$

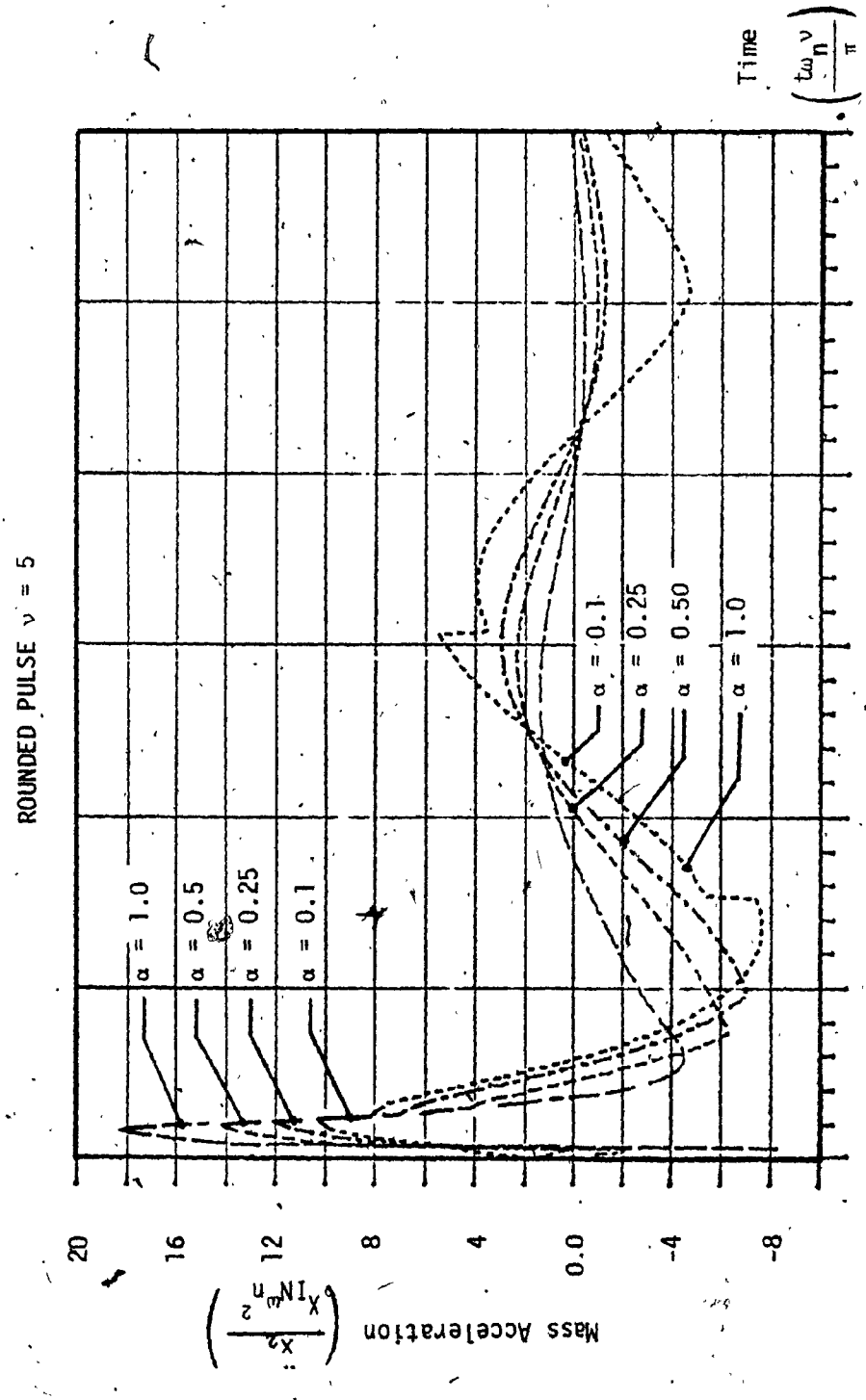

FIGURE 59. Mass Acceleration Time Histories of CVFI System having 4 Values of Coulomb Damping: $\omega_n = \pi$ $\xi = 0.25$

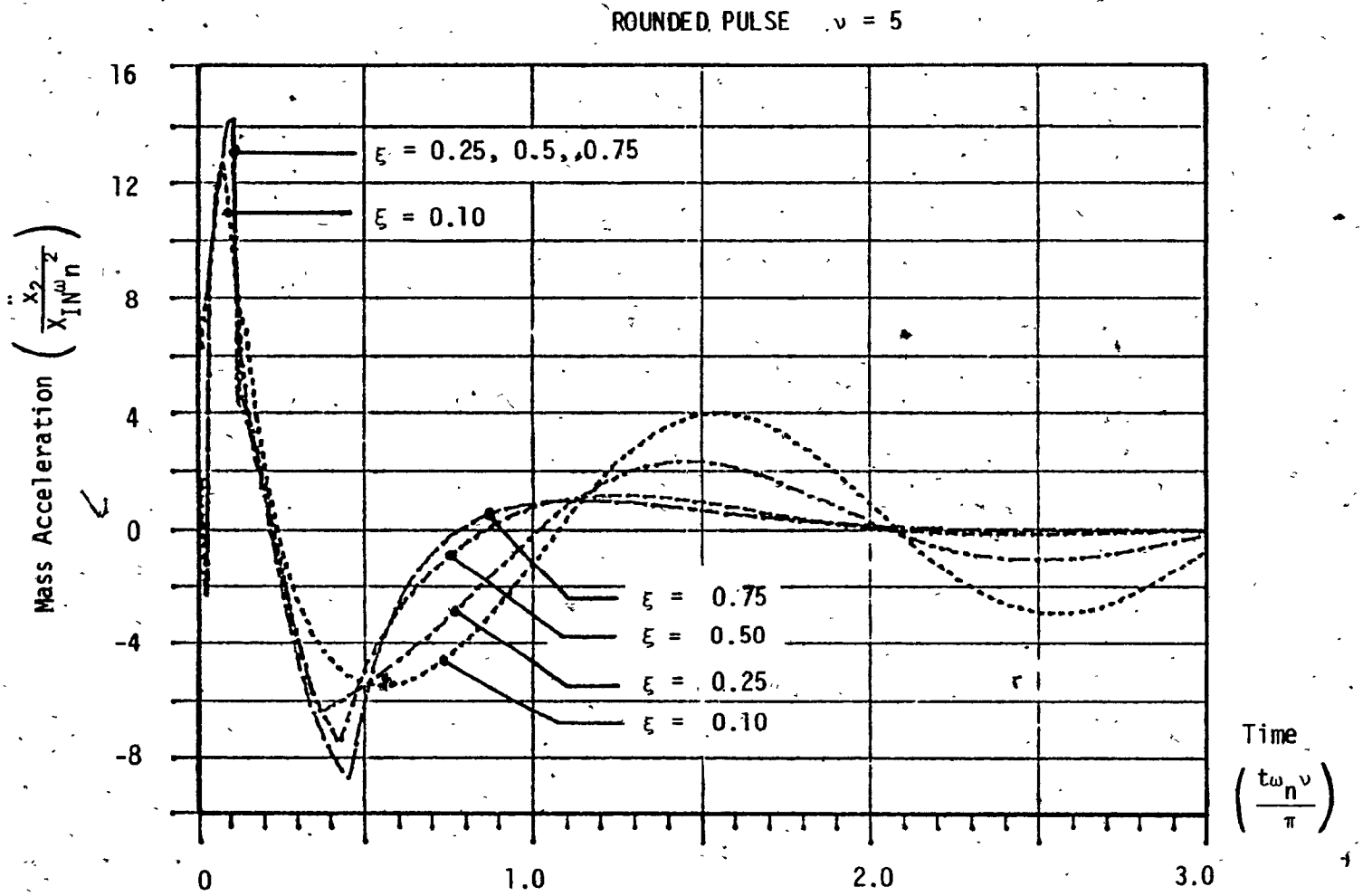

FIGURE 60. Mass Acceleration Time Histories of CVFI System having 4 Values of Viscous Damping: $\omega_n = \pi$ $\alpha = 0.5$

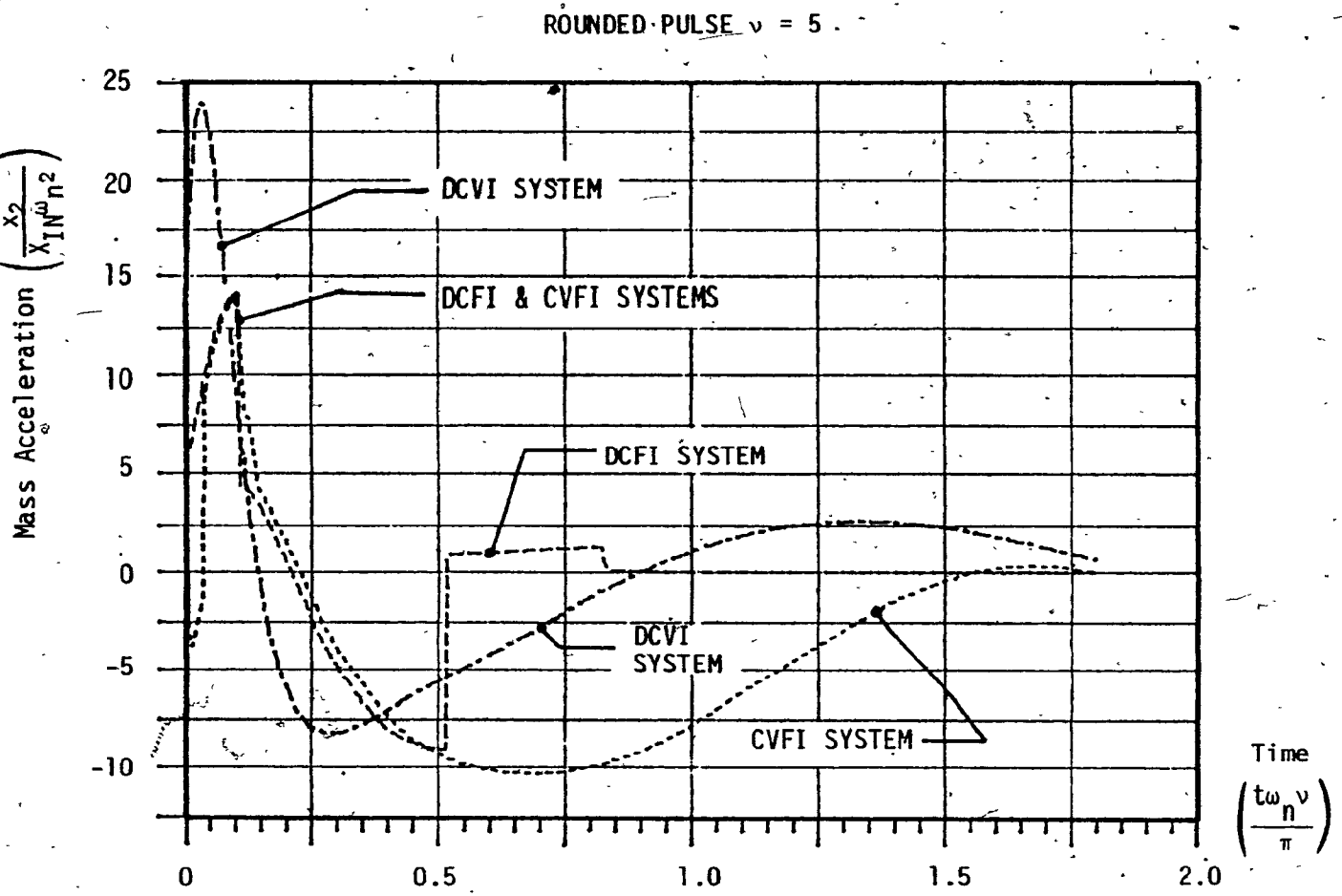

FIGURE 61. Comparison of Mass Acceleration Time Histories of DCVI, DCFI and CVFI Systems having the Same Viscous and Coulomb Damping: $\omega_n=\pi$ $\xi=0.25$ $\alpha=0.50$

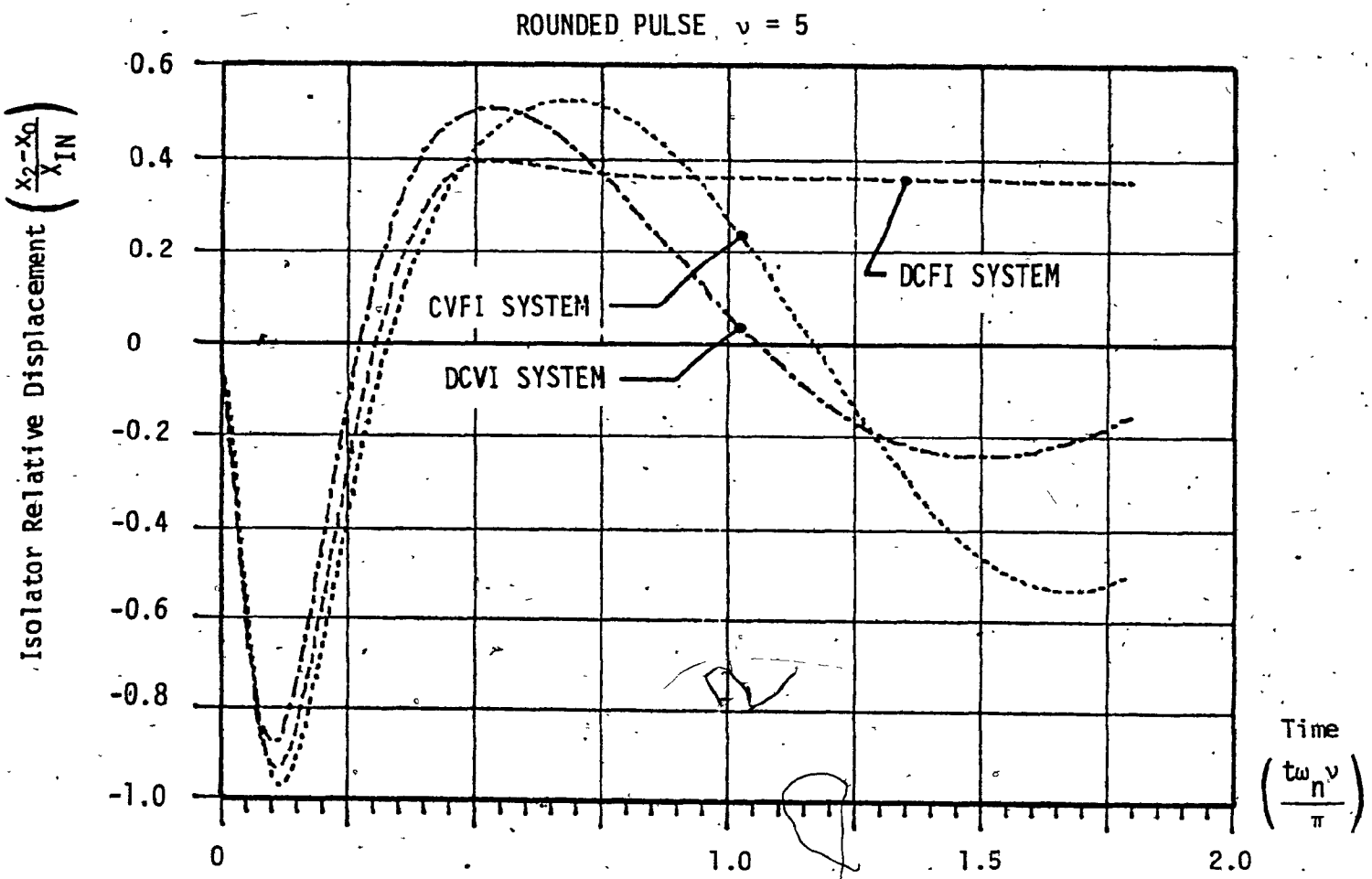

FIGURE 62. Comparison of Isolator Relative Displacement Time Histories of DCVI, DCFI and CVFI Systems having the Same Viscous and Coulomb Damping: $\omega_n=\pi$ $\xi=0.25$ $\alpha=0.50$

5.5 VARIOUS VISCOUS AND COULOMB DAMPED ISOLATORS SUBJECTED TO OSCILLATORY PULSE DISPLACEMENTS

Figures 63 through 67 are the performance curves for selected viscous, coulomb and combined viscous/coulomb damped isolator systems subjected to oscillatory pulse displacements. Typical time responses of some of the isolators are shown in Figures 68 through 75.

5.5.1 PERFORMANCE OF VISCOUS DAMPED ISOLATORS

Figure 63 shows the influence of the viscous damping ratio ξ on the DCVI system for various severities of the oscillatory pulse. It is seen that at low severities, increasing ξ primarily reduced both RDR and $\ddot{X}_2$ whereas at high severities, ξ increased $\ddot{X}_2$ with small changes in RDR. Except for (ν=1), RDR values for all other pulse severities were greater than unity. This was due to additive effects of the relative displacement during successive oscillations of the isolator base. This was particularily evident at (ν=3) where a resonant condition existed. It appears that there was an optimum degree of damping in terms of minimizing RDR, as seen in the curves of ν=1, 5 and 7.

For a constant amount of damping, $\ddot{X}_2$ increased with pulse severity. In terms of selecting a DCVI system having good performance for a wide range of pulse severities, one must trade-off the RDR response at (ν=3) against the $\ddot{X}_2$ response for ($\nu \geq 7$).

The effects of adding the type 1 elastic coupling to the viscous damped isolator subjected to an oscillatory pulse of severity (ν=5) is shown in Figure 64. The elastic coupling N produced a general degradation of both $\ddot{X}_2$ and RDR performance. Indeed, the addition of only a slight amount of elasticity (N=0.25), brought large increases in $\ddot{X}_2$, particularily with high viscous damping. Only by further increasing N, was $\ddot{X}_2$ able to be reduced to levels lower than the DCVI system, and only with penalties of larger RDR.

At low values of damping (ξ=0.1 and 0.20), the effect of N was primarily to increase RDR with only slight changes in $\ddot{X}_2$.

5.5.2 PERFORMANCE OF COULOMB DAMPED ISOLATORS

Figure 65 shows the performance of the DCFI system for various degrees of coulomb damping α and pulse severity ν. It is seen that, like the DCVI system (Figure 63), damping influenced primarily RDR at low severities and $\ddot{X}_2$ at high severities. However, for large values of α, $\ddot{X}_2$ at low severities was also affected by coulomb damping. This is seen at ($\alpha \geq 0.8$) at ν=1 and (α=2.0) at ν=3, where the friction became sufficiently high, so that large amounts of base accelerations were being transmitted.

Similar to the DCVI system, a resonant condition at (ν=3) occurred with high values of RDR. In constrast to the viscous isolator, however, for a fixed amount of damping, increasing of the pulse severity for ($\nu \geq 5$) did not greatly affect either RDR or $\ddot{X}_2$. This was due to the force limiting characteristic of the coulomb damper. Indeed, the RDR and $\ddot{X}_2$ response at (ν=10) was better than at (ν=5) for all values of damping.

Figure 66 shows the influences of the elastic coupling N and coulomb damping on the response of the ECFI type 1 system subjected to an oscillatory pulse of severity (ν=5). Similar to the ECVI type 1, a small amount of elasticity, (N=0.25), brought large increases in $\ddot{X}_2$ as compared to the directly coupled isolator (N=0). Increasing N further produced successive reductions in $\ddot{X}_2$.

For a fixed amount of elastic coupling, the effect of increased damping was primarily to reduce RDR and only slightly increase $\ddot{X}_2$. The curves show that the principal advantage of N is to be able to decrease RDR further than can be achieved with the DCFI system: for α=1.0, RDR is 1.31 for N=1.0, and RDR is 1.396 for N=0.

Tables 8 and 9 show a comparison of the peak $\ddot{X}_2$ and RDR responses of the DCFI system having fixed and adaptive coulomb friction for various oscillatory pulse severities. Two values of fixed friction were selected: (α=0.1) and (α=1.0). The same damping range and break points were used for the four adaptive devices: α between 0.1 and 1.0, z_1=.1 and z_2=1.0.

It was found that in terms of the RDR and $\ddot{X}_2$ responses, the isolators could be classified into two groups: low friction systems (α=.1, DDFI and VDFI) and high friction systems (α=1.0, DIFI and VIFI). For low pulse severities, ν=1 and ν=3, the high friction systems generally had the better performance: all but one value of RDR and two values of $\ddot{X}_2$ were lower than those of the low friction group. Indeed the VIFI system had the lowest RDR and $\ddot{X}_2$ for both ν=1 and ν=3.

At the higher pulse severities ($\nu \geq 5$), the low friction systems had lower $\ddot{X}_2$ with only slightly higher RDR. At $\nu=10$, the differences in RDR between the high and low friction systems were nearly negligible. Except for the VDFI system, the variation in $\ddot{X}_2$ performance within each group was small at the higher pulse severities.

The VDFI system showed a particular characteristic, in that it had both high values of RDR and $\ddot{X}_2$ at all pulse severities. This was because the isolator tends to transmit large amounts of base accelerations and displacements at low velocities (when its friction value is highest). However, it is precisely at these low velocities, that the base accelerations and displacements of the oscillatory pulse are high.

5.5.3 PERFORMANCE OF COMBINED VISCOUS/COULOMB DAMPED ISOLATORS (CVFI)

Figure 67 shows the performance of the CVFI system having $\xi=0.50$ for various degrees of coulomb damping and oscillatory pulse severities. Like the DCFI system, increasing the coulomb damping α reduced both RDR and $\ddot{X}_2$ at low pulse severities, and increased $\ddot{X}_2$ at high severities without much influence on RDR. The main difference between the DCFI and CVFI systems, is their response to low severity pulses for large amounts of coulomb damping. Both systems showed an initial insensitivity of $\ddot{X}_2$ for low values of α. However, after a certain value of damping was reached, $\ddot{X}_2$ increased with α in the DCFI system, whereas $\ddot{X}_2$ decreased in the CVFI system. This difference can be seen in the ($\nu=1$) and ($\nu=3$) curves of Figures 65 and 67, and was due to the viscous damper in the CVFI which, at high coulomb damping, limited the accelerations transmitted from the base.

Table 10 shows the comparison of the peak RDR and $\ddot{X}_2$ responses of the DCVI, DCFI and CVFI systems to oscillatory pulses of various severities. Two values of viscous damping and one value of coulomb damping were used. Comparing the DCFI to the two DCVI systems, it is seen that the coulomb damped isolator had a poorer performance at low severities ($\nu \leq 3$) and had high values of RDR and $\ddot{X}_2$. However, at high pulse severities, it showed a better performance, particularily when comparing its $\ddot{X}_2$ response to that of the DCVI system with ξ=1.0.

Of the two DCVI systems, the one with lower damping (ξ=0.25) generally showed the better performance having low maximum accelerations at all pulse severities. The only advantage of high damping was its better control of RDR at resonance (ν=3).

The CVFI systems had the best overall performance as they behaved like viscous isolators at low severities and friction isolators at high severities. Indeed, at the high severities, they even had slightly lower RDR and $\ddot{X}_2$ responses as compared to the DCFI system. These lower responses were due to the viscous damper which tended to provide a smoother transition in the damping force characteristic of the isolator when the velocity reversed its sign. The main disadvantage of the CVFI systems was that they responded like pure coulomb damped isolators at resonance (ν=3) and had large RDR and $\ddot{X}_2$ values. Increasing ξ produced a small decrease in RDR and $\ddot{X}_2$, but the response at resonance was still poorer than either of the DCVI systems.

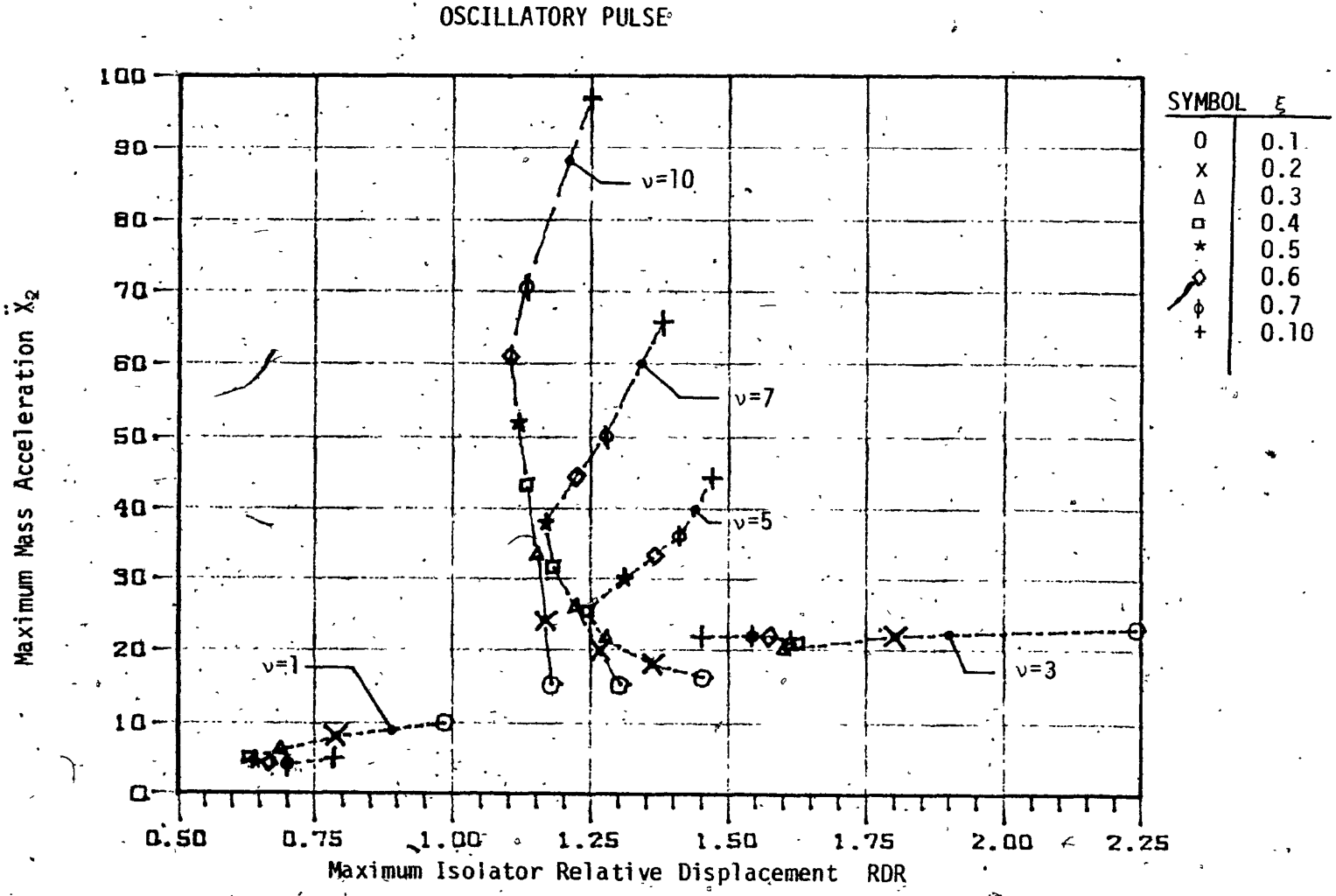

FIGURE 63. Performance of DCVI System for Various Damping Ratios ξ and Pulse Severities $\nu : \omega_n = \pi$

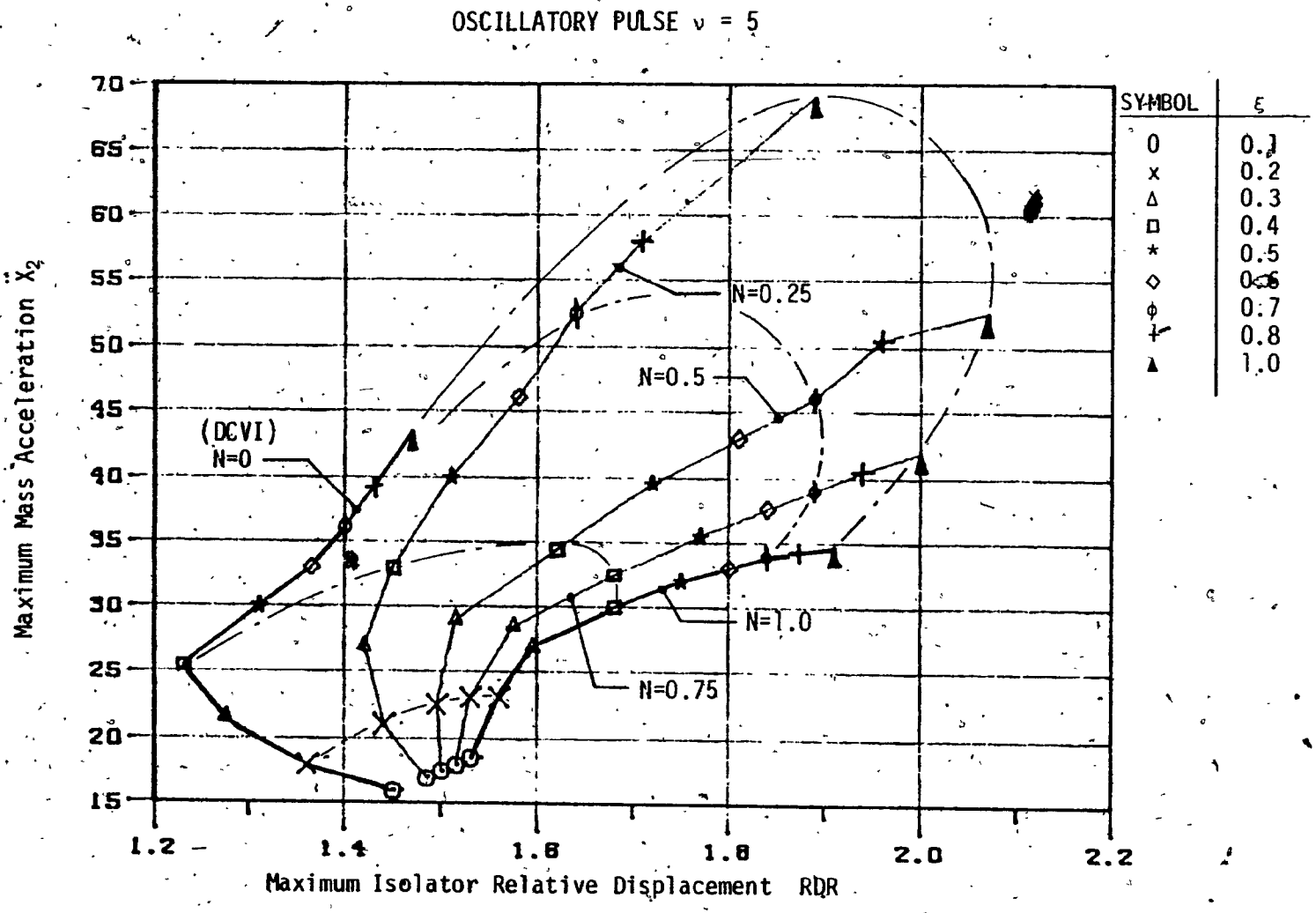

FIGURE 64. Performance of ECVI-1 System for Various Damping Ratios ξ and Elastic Coupling Ratios N : ω_n =

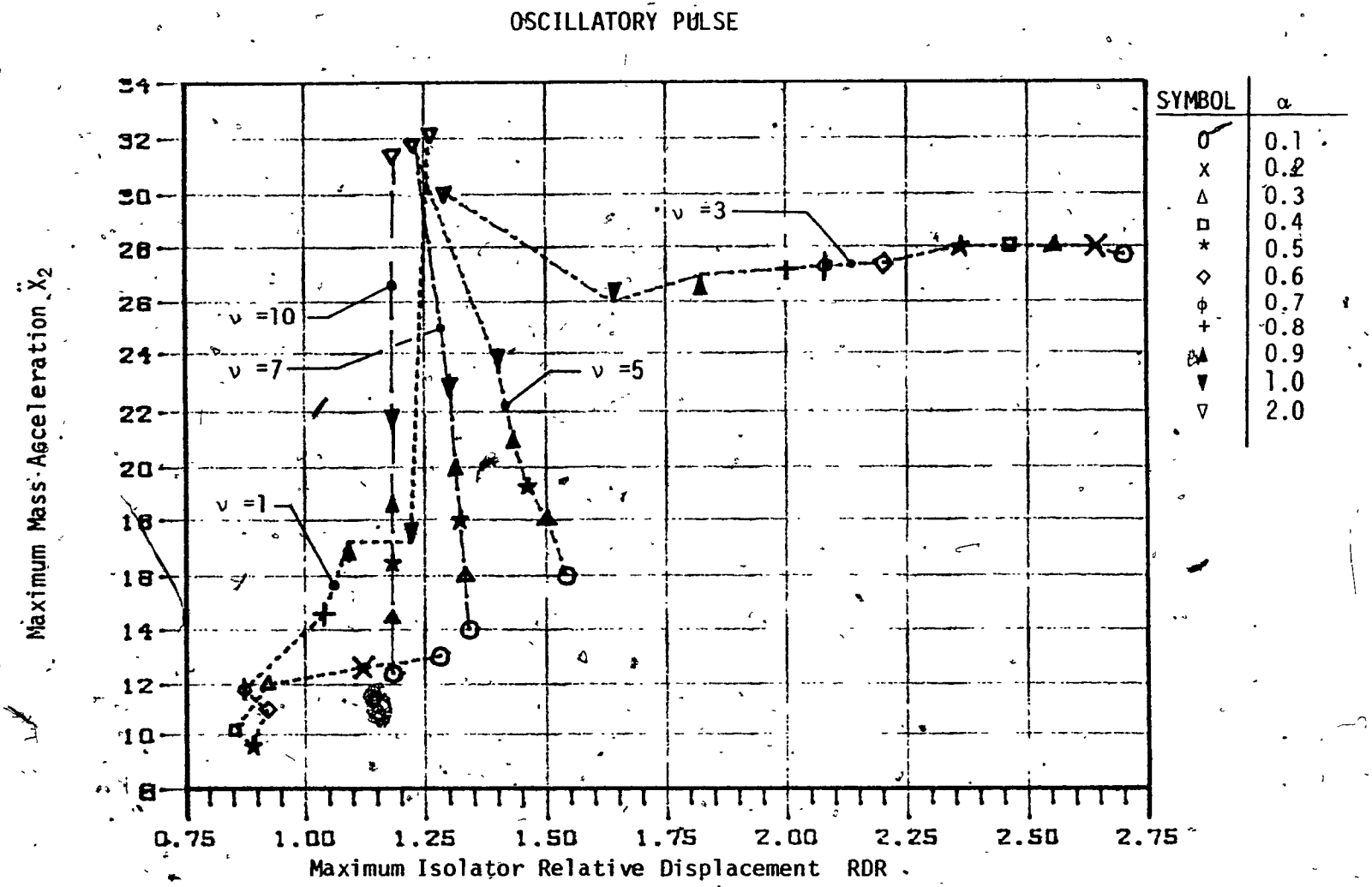

FIGURE 65. Performance of DCFI System having Various Damping Ratios α and Pulse Severities : $\omega_n = \pi$

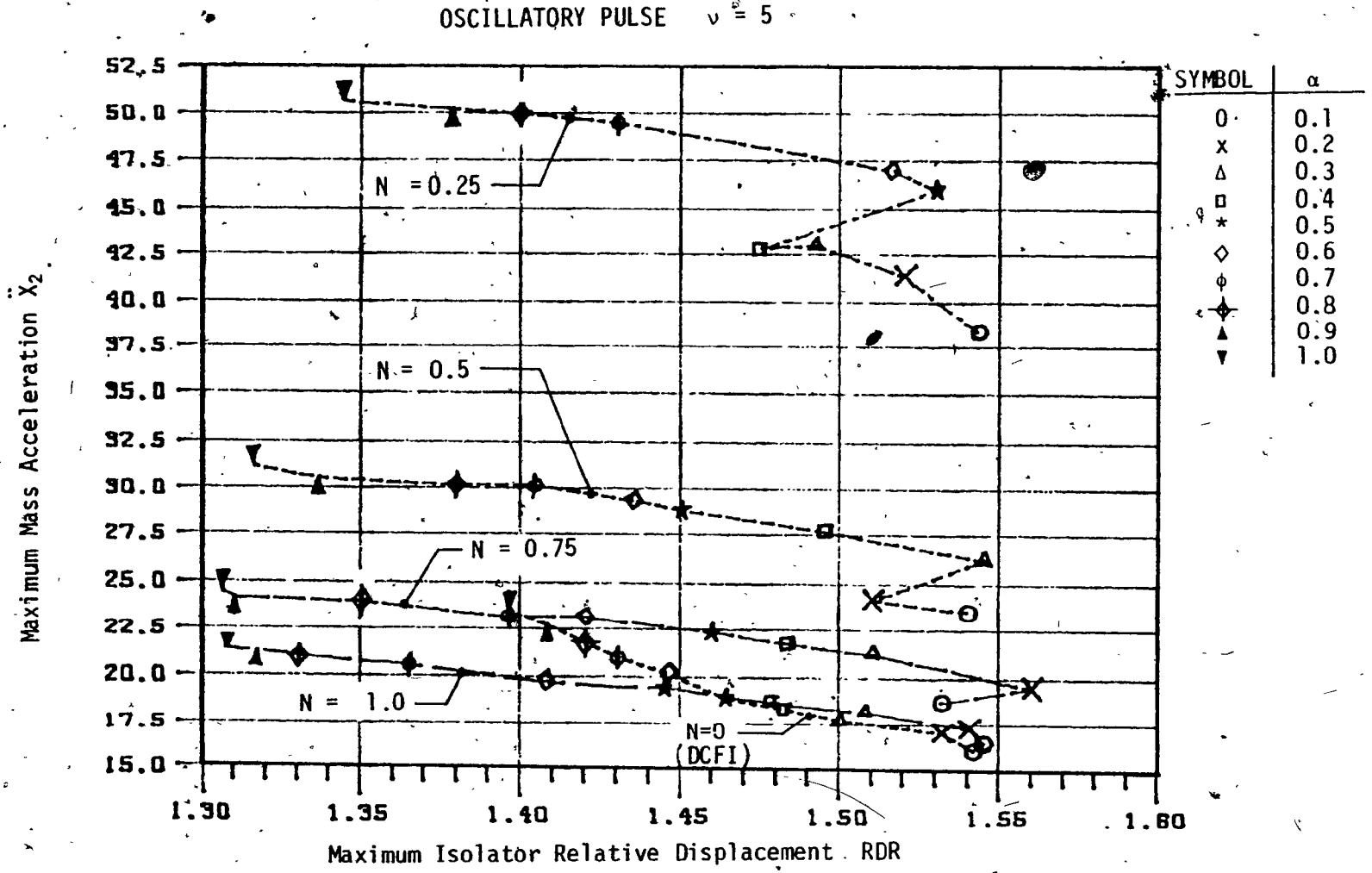

FIGURE 66. Performance of ECFI-1 System for Various Damping Ratios α and Elastic Coupling Ratios N: $\omega_n = \pi$

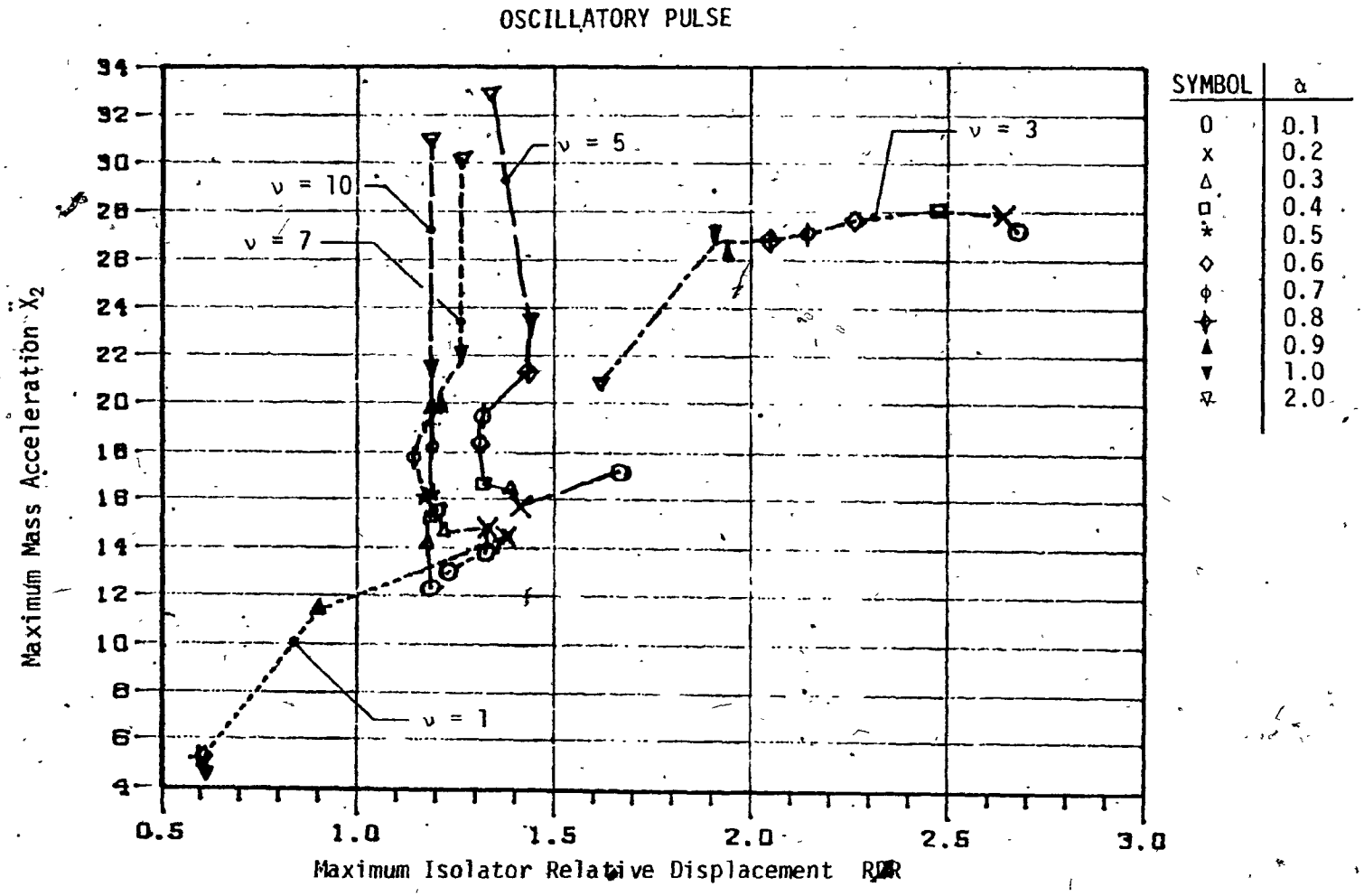

FIGURE 67. Performance of CVFI System for Various Coulomb Damping Ratios α and Pulse Severities ν : $\omega_n = \pi$ $\xi = 0.50$

OSCILLATORY PULSE

DCFI SYSTEM WITH:	RDR RESPONSE				
	$\nu = 1$	$\nu = 3$	$\nu = 5$	$\nu = 7$	$\nu = 10$
$\alpha = 0.1$	1.28	2.70	1.54	1.34	1.18
DDFI	1.09	2.75	1.52	1.35	1.20
VDFI	1.09	2.71	1.57	1.33	1.19
$\alpha = 1.0$	0.87	2.08	1.40	1.31	1.18
DIFI	1.28	1.86	1.39	1.29	1.16
VIFI	0.65	1.77	1.39	1.30	1.18

TABLE 8: COMPARISON OF RDR RESPONSE: DCFI SYSTEM WITH FIXED AND ADAPTIVE FRICTION: $\omega_n = \pi$ $\alpha_{range}(0.1, 1.0)$: $z_1 = 0.1$ $z_2 = 1.0$

OSCILLATORY PULSE

DCFI SYSTEM WITH:	$\ddot{X}_2$ RESPONSE				
	$\nu = 1$	$\nu = 3$	$\nu = 5$	$\nu = 7$	$\nu = 10$
$\alpha = 0.1$	13	27.7	16	14	12.4
DDFI	7.5	28.1	15.9	14.3	12.7
VDFI	18.7	36.4	24	22.6	21.5
$\alpha = 1.0$	11.8	27.3	23.5	20	21.5
DIFI	9.67	28.3	23.6	22.6	21.2
VIFI	4.88	25.5	22.6	22.0	21.2

TABLE 9: COMPARISON OF $\ddot{X}_2$ RESPONSE OF DCFI SYSTEM WITH FIXED AND ADAPTIVE FRICTION: $\omega_n = \pi$ $\alpha_{range}(0.1,1.0)$ $z_1 = 0.1$ $z_2 = 1.0$

OSCILLATORY PULSE

ISOLATOR	ν = 1		ν = 3		ν = 5		ν = 10	
$\omega_n = \pi$	RDR	$\ddot{X}_2$	RDR	$\ddot{X}_2$	RDR	$\ddot{X}_2$	RDR	$\ddot{X}_2$
DCFI :α= 0.50	0.92	11	2.36	28	1.46	19.2	1.19	16.6
DCVI								
:ξ= 0.25	0.74	7	1.62	20	1.32	19.5	1.16	28
:ξ= 1.00	0.79	5	1.45	21.5	1.38	66	1.25	97
CVFI (α=0.5)								
:ξ= 0.25	0.69	6.4	2.40	27.5	1.51	19.1	1.08	15.3
:ξ= 1.00	0.97	12.1	2.18	26.2	1.32	17.6	1.18	15.8

TABLE 10: COMPARISON OF DCVI, DCFI, AND CVFI SYSTEMS HAVING THE SAME VISCOUS AND COULOMB DAMPING.

5.5.4 TIME RESPONSE OF VARIOUS ISOLATORS

The relative displacement and acceleration time histories of the DCVI, DCFI having fixed friction, DCFI with displacement decreasing adaptive friction device and CVFI systems subjected to an oscillatory pulse of severity (ν=5), are shown in Figures 69 through 75.

It can be seen from the relative displacement curves that the response of the four isolators tended to follow the general pattern of the base input (Figure 15). During the high frequency portion of the pulse ($t\omega_n\nu/\pi < 2.5$), the DCVI and CVFI systems showed generally uniform amplitude peaks as compared to the systems having only friction damping. However, during the low frequency portion, the three systems having some form of friction damper, tracked the input more accurately. The viscous system (DCVI) showed an oscillation about a mean line which exponentially decayed to zero.

The acceleration time histories of Figures 72 through 75 show that during the high frequency portion of the pulse, the four isolators had similar acceleration responses, with the main differences being their amplitudes of the oscillations. However, there were marked variations in the four responses during the low frequency portion. The DCVI system oscillated about a decaying non-zero mean line. The DCFI system, with both fixed and displacement decreasing adaptive friction, showed sharp, jagged accelerations due to the stick/slip charactertistic of the coulomb damper. The CVFI system had the best low frequency response as it tracked the base input the most uniformly. Table 11 is a comparison of the acceleration peaks of the four isolator systems. It is seen that while the DCVI system had the highest accelerations during the high

frequency portion of the input, it had the lowest accelerations during the low frequencies. In contrast, the DCFI system with fixed friction, had low accelerations in the high frequency portion and high peaks in the low frequency range. The CVFI, however, had a response similar to the DCFI fixed friction system at high frequencies and the DCVI at low frequencies. The DCFI system with the displacement decreasing adaptive friction device, had the lowest accelerations of the four isolators during the high frequencies, as it tended to have a low friction value. This isolator also had the most uniform acceleration levels throughout the duration of the oscillatory pulse.

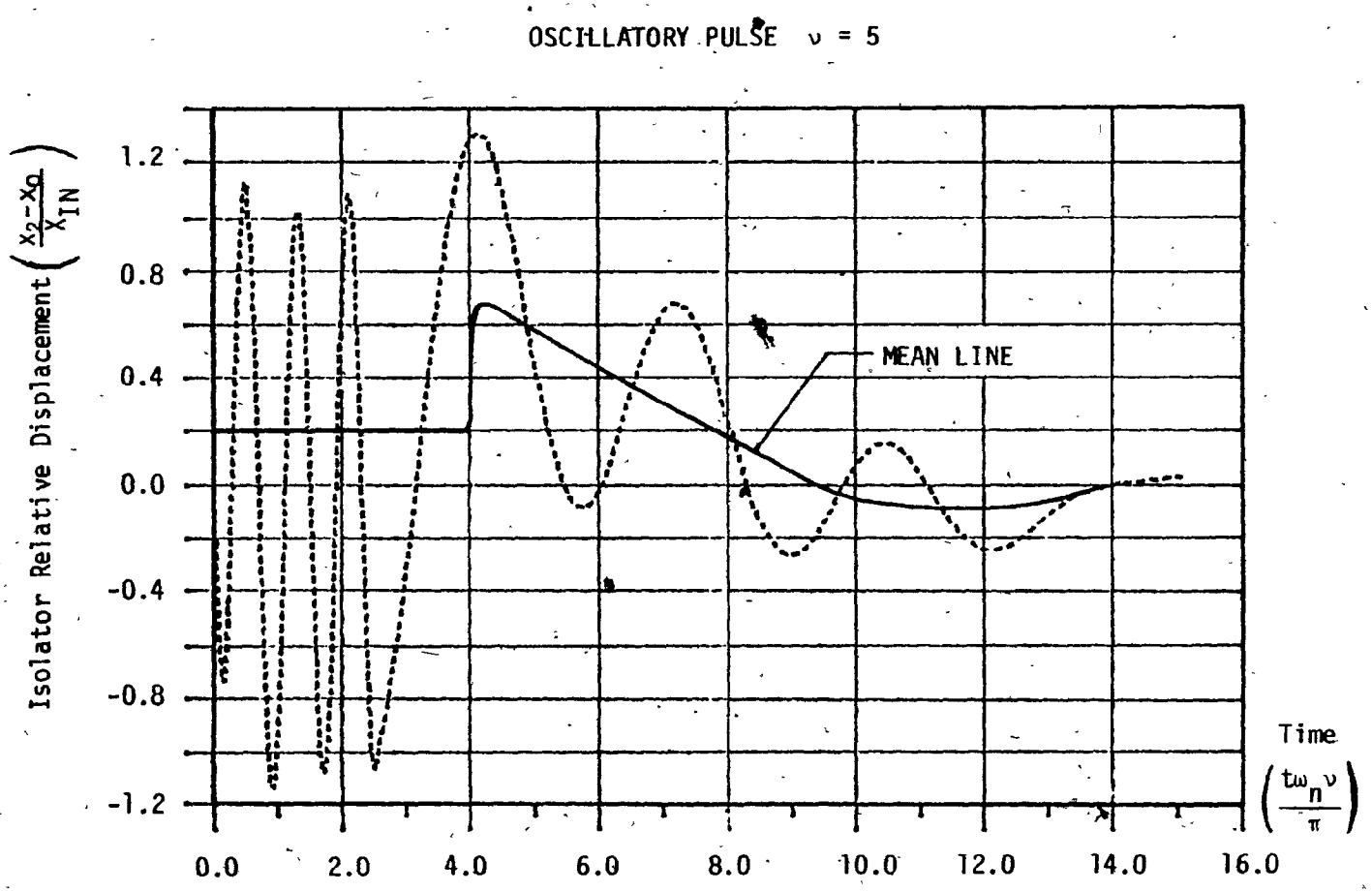

FIGURE 68. Isolator Relative Displacement Time History of DCVI System: $\omega_n = \pi$ $\xi = 0.50$

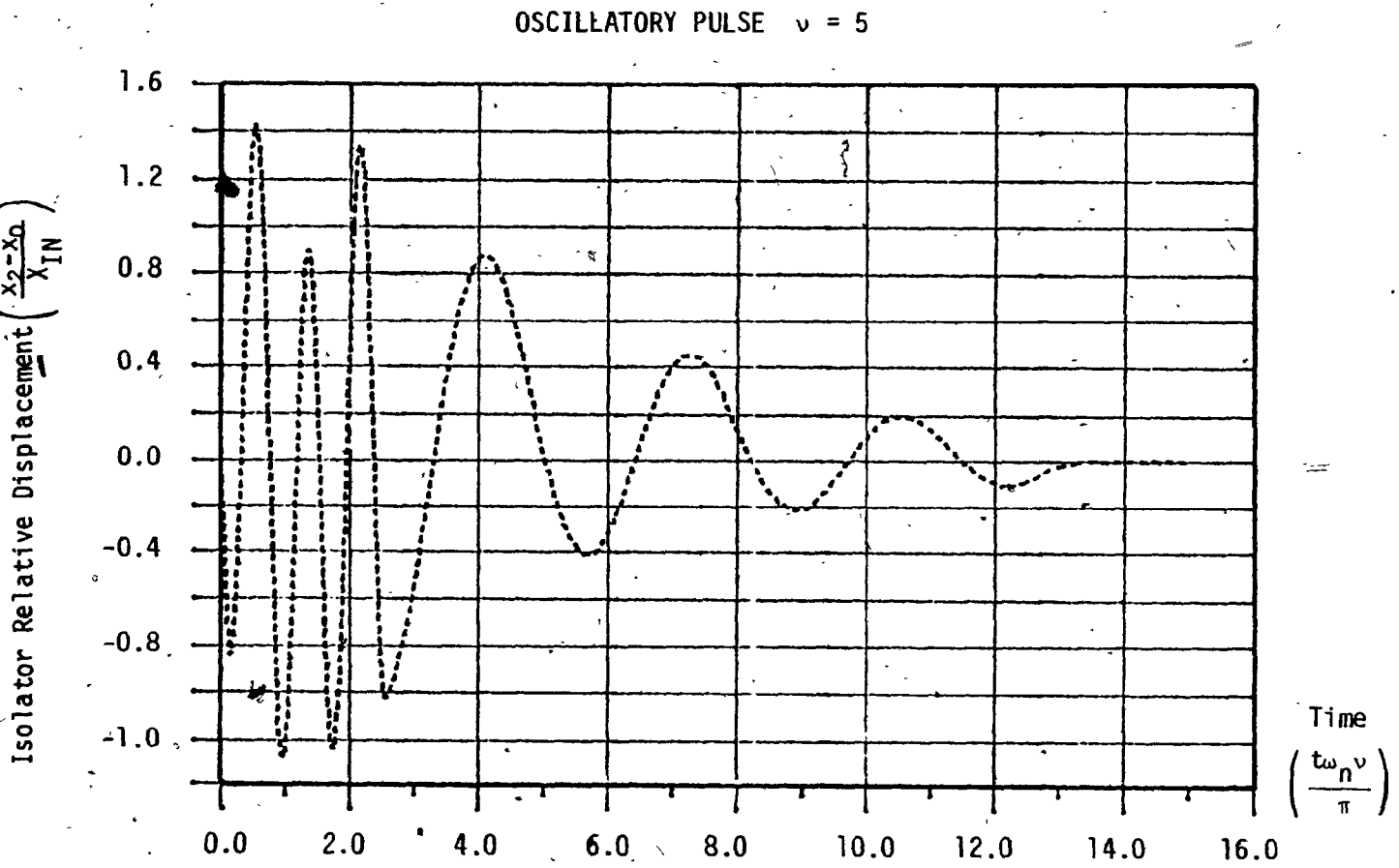

FIGURE 69. Isolator Relative Displacement Time History of DCFI System:
$\omega_n = \pi$ $\alpha = 0.75$

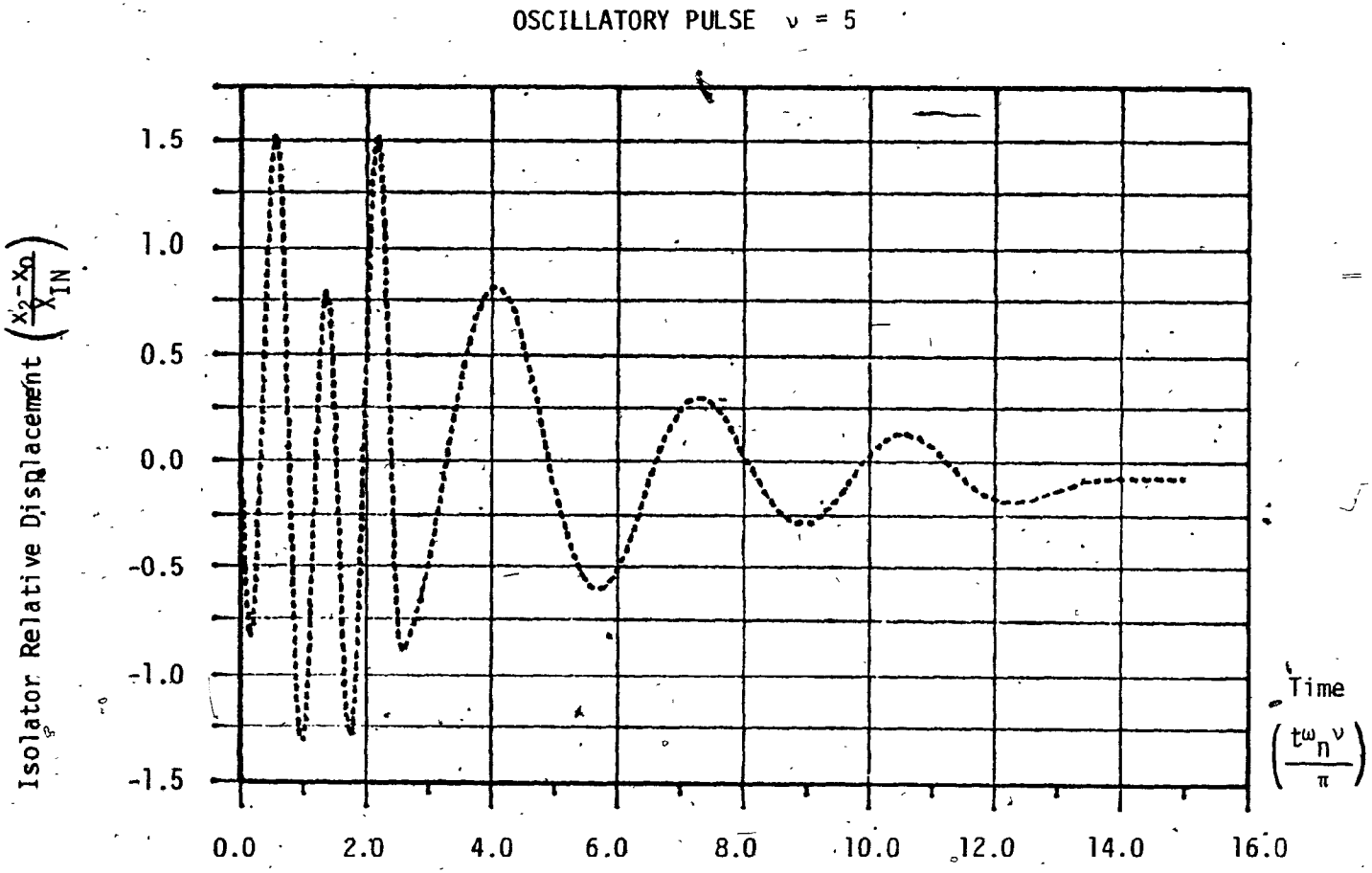

FIGURE 70. Isolator Relative Displacement Time History of DCFI System having DDFI Device: $\omega_n = \pi$ α range (1.0, 0.1)
$z_1 = 0.1$ $z_2 = 1.0$

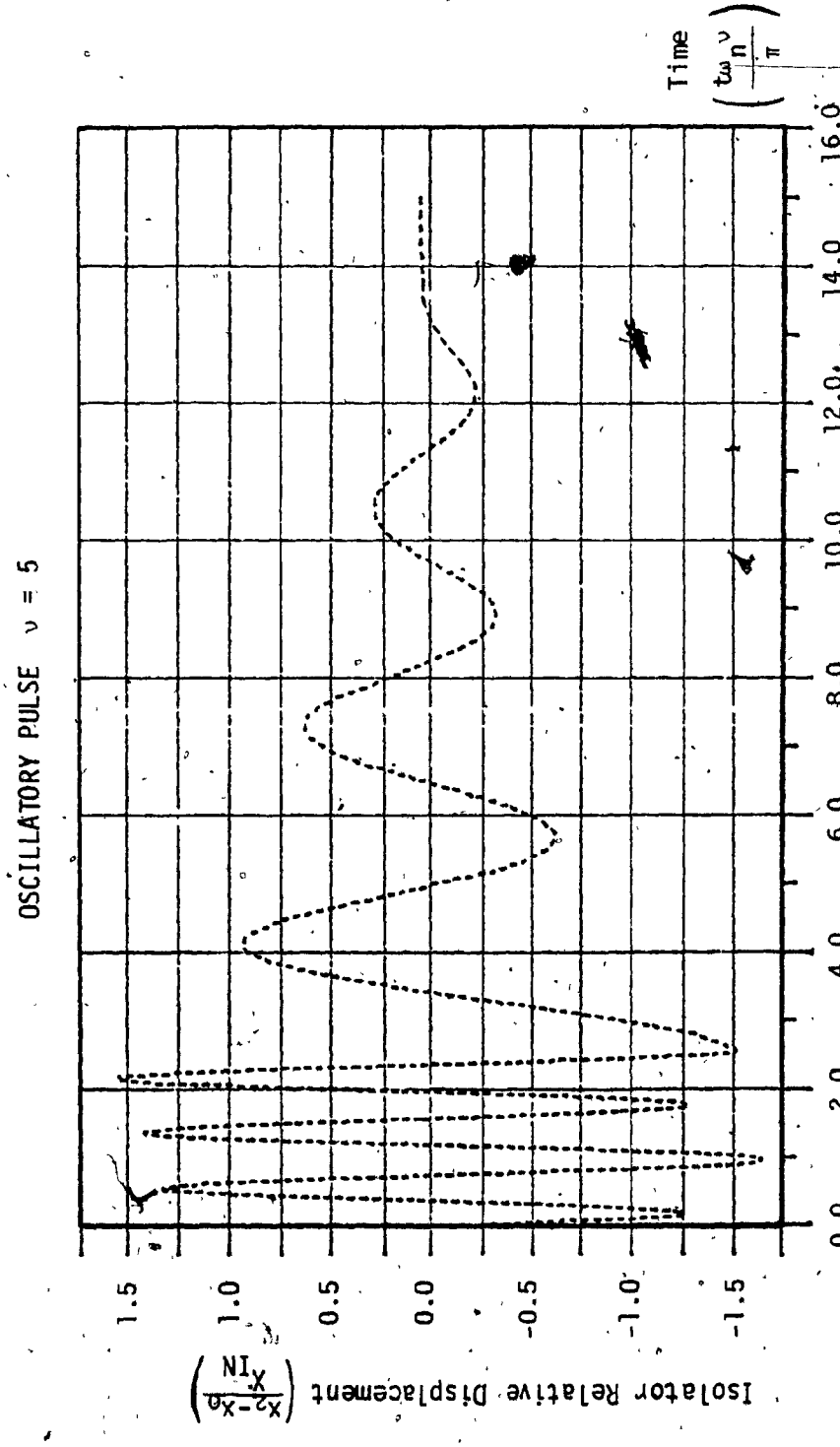

FIGURE 71. Isolator Relative Displacement Time History of CVFI System: $\omega_n = \pi$ $\xi = 0.50$ $\alpha = 0.75$

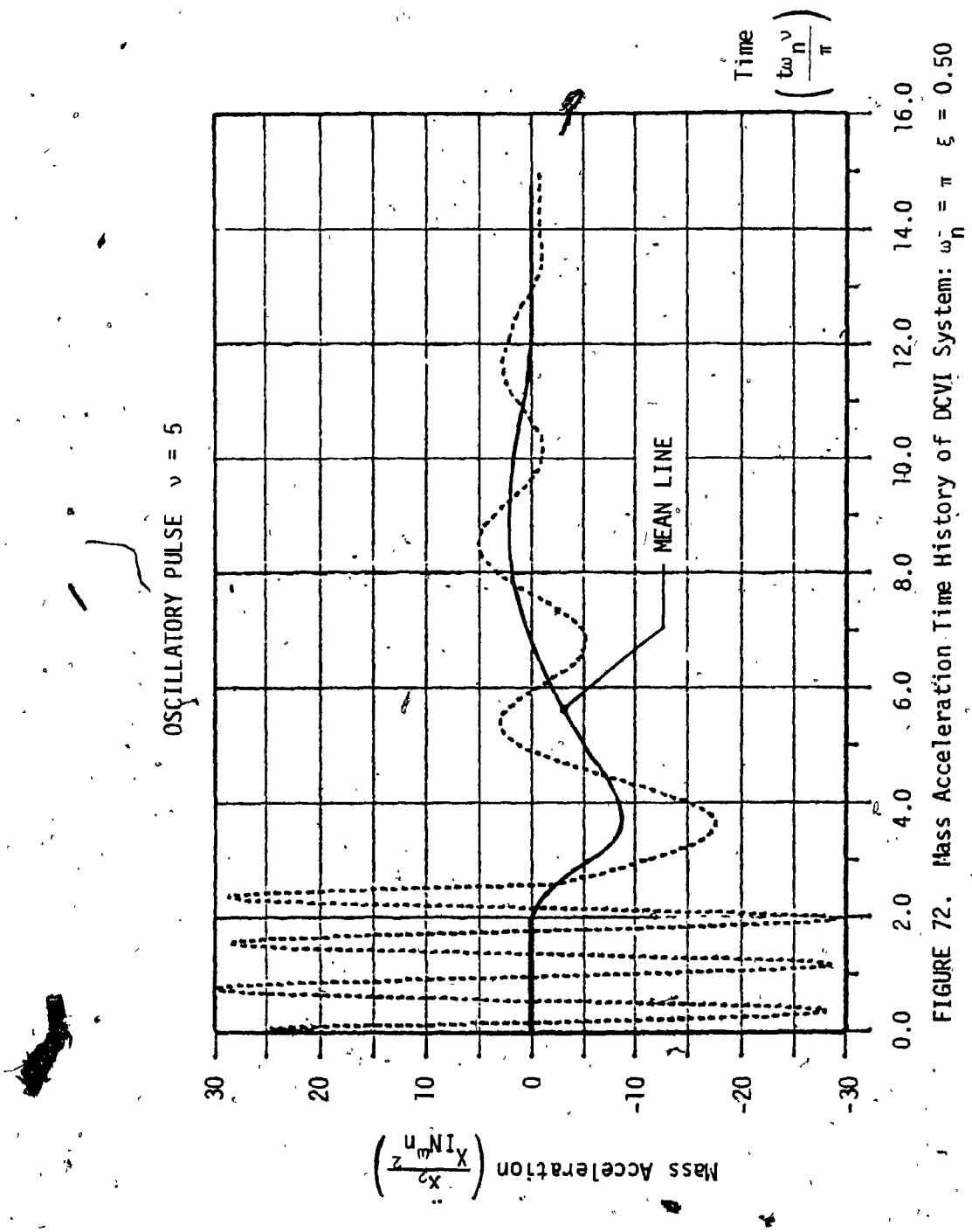

FIGURE 72. Mass Acceleration Time History of DCVI System: $\omega_n = \pi$ $\xi = 0.50$

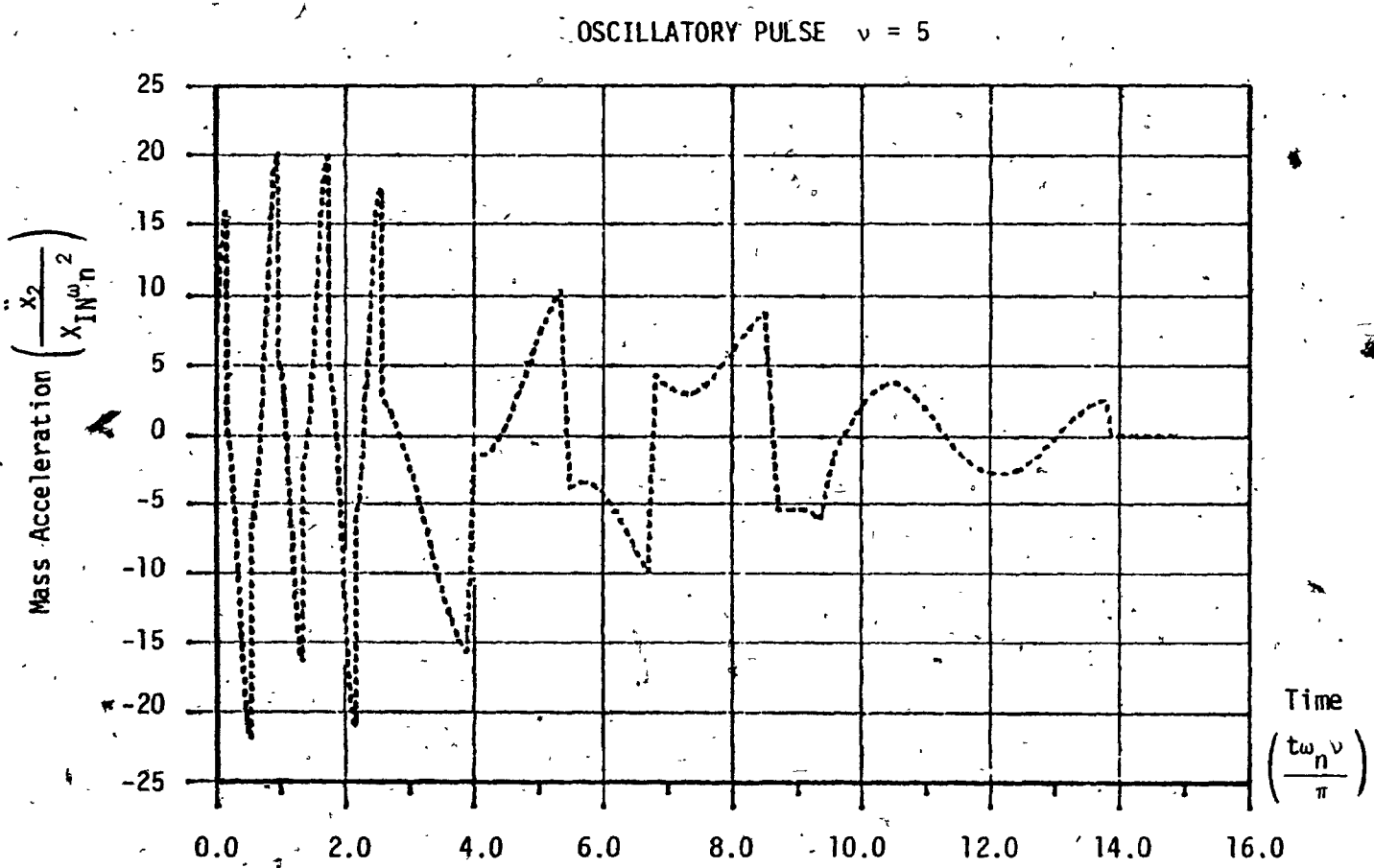

FIGURE 73. Mass Acceleration Time History of DCFI System: $\omega_n = \pi$ $\alpha = 0.75$

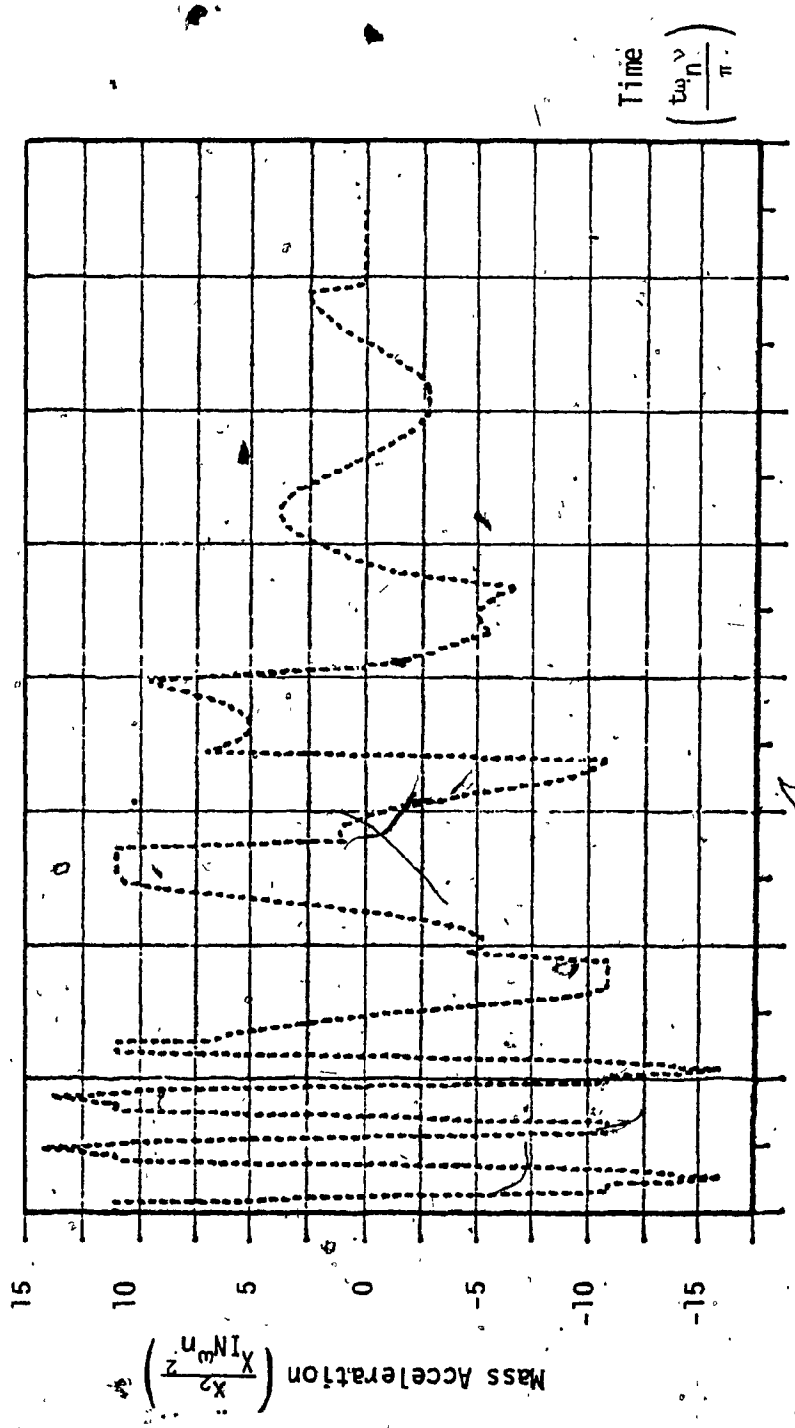

FIGURE 74. Mass Acceleration Time History of DCFI System having DDFI Device: $\omega_n = \pi$ arange (1.0,0.1)
$z_1 = 0.1$ $z_2 = 1.0$

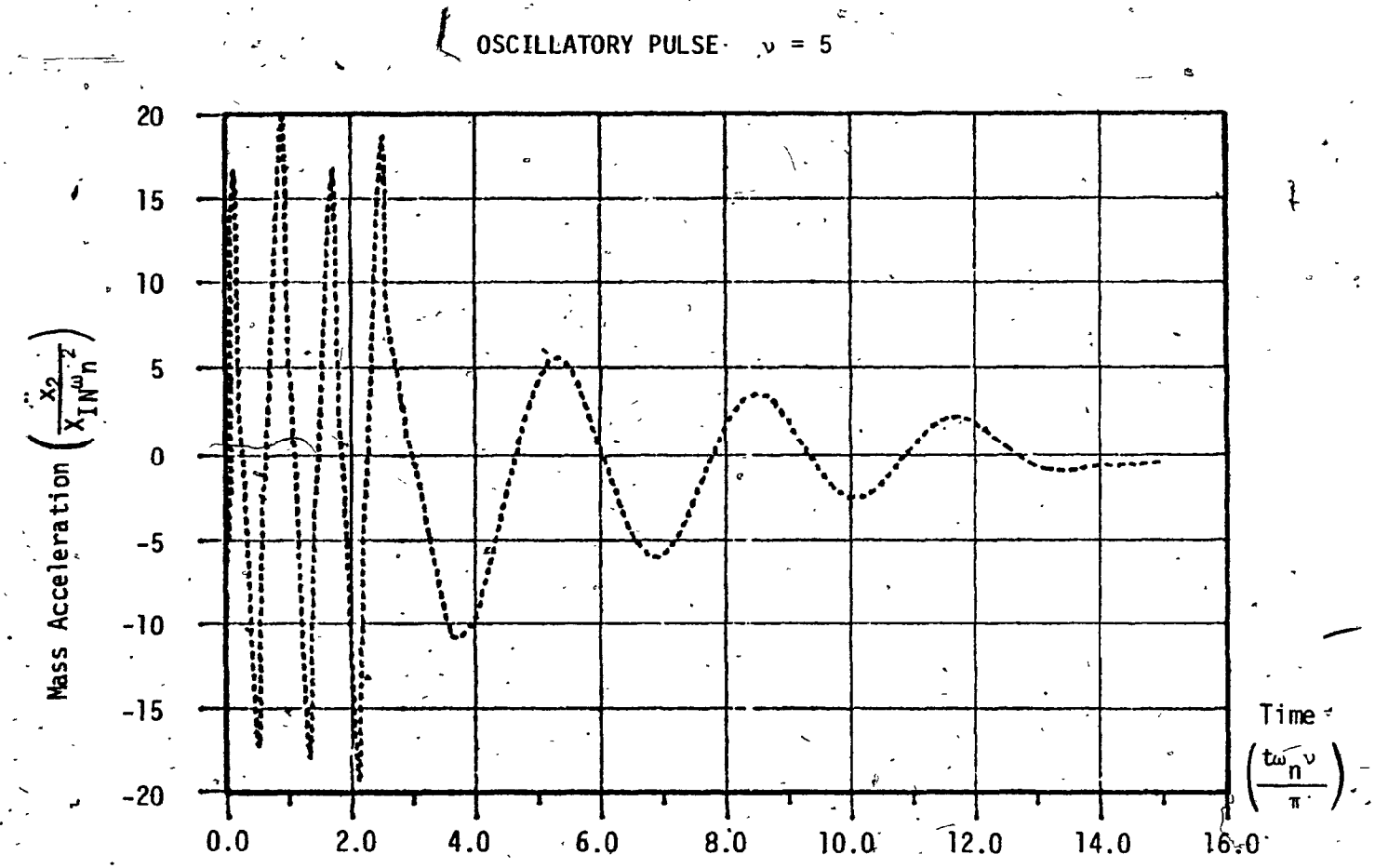

FIGURE 75. Mass Acceleration Time History of CVFI System: $\omega_n = \pi$ $\xi = 0.50$ $\alpha = 0.75$

OSCILLATORY PULSE $\nu = 5$

ACCELERATION PEAKS			
DCVI $\xi = 0.50$	DCFI $\alpha = 0.75$	DCFI with DDFI	CVFI $\xi = 0.50$ $\alpha = 0.75$
24.5	16	11	16.5
- 28	- 21.5	- 16	- 17
29.5	20	14	20
- 28.5	- 16	- 11	- 18
28	20	14	16.5
- 29	- 20.5	- 16	- 19
28	17.5	11	18.5
- 17.5	- 15.5	- 11	- 11
3	10	11	5.5
- 5	- 10	- 11	- 6
5	9	9.5	3.5
- 1	- 6	- 4.5	- 2.5
3	3.5	3.5	3

TABLE 11: COMPARISON OF ACCELERATION PEAKS OF DCVI, DCFI WITH FIXED α, DCFI WITH DDFI DEVICE, AND CVFI SYSTEMS.

: $\omega_n = \pi$ $\alpha_{range}(1.0, 0.1)$

$z_1 = 0.1$ $z_2 = 1.0$

CHAPTER 6

CONCLUSIONS AND RECOMMENDATIONS

6.0 CONCLUSIONS AND RECOMMENDATIONS

In this thesis, various isolator systems have been modelled and their responses to rounded and oscillatory pulse displacements have been studied. Seven isolator configurations were investigated: they incorporated a main return spring and a damping element. Three dampers were used: a viscous damper, a coulomb friction damper and a combined form of viscous and coulomb damper. The systems studied were directly and elastically coupled. Two forms of elastic coupling were employed: Type 1 which had one end of the damper connected to the base by an elastic spring, and Type 2 in which there was an elastic spring connecting the base to a directly coupled isolator. It was shown that the types 1 and 2 elastically coupled isolator systems, were dynamically equivalent for viscous and coulomb damping. However, both the type 1 and 2 systems were studied in order to examine the effect of the elastic coupling on the response of each system. Four devices having variable coulomb friction characteristics were also studied.

The performance of each isolator was determined in terms of the maximum acceleration transmitted to the mass ($\ddot{X}_2$) and the maximum relative displacement which occurred across the isolator (RDR). Though it is desirable to simultaneously have low values of $\ddot{X}_2$ and RDR, it was generally found that there was a trade-off between these two quantities. Comparative studies of isolator performance were made by plotting the $\ddot{X}_2$ versus RDR responses for various degrees of damping, elastic coupling and pulse severity for each isolator configuration. Comparisons in tabular form were also made between the performances of different isolator configurations. Time histories of the mass acceleration and isolator relative

displacements of selected isolator systems were also presented.

The following are specific conclusions on the performance of the isolators which were studied.

6.1 PERFORMANCE OF VISCOUS DAMPED ISOLATORS

- For the directly coupled viscous damped system (DCVI) subjected to either round or oscillatory pulses, low damping was desirable at high pulse severities in order to minimize $\ddot{X}_2$, while high damping was required to minimize RDR at low severities.
- The combination of high damping ξ and high severity ν was found to give the worst performance as very high accelerations were transmitted to the mass via the "stiff" damper, while there was little or no reduction in RDR.
- High damping was particularily effective in controlling the RDR response between the mass and base excitations at resonant conditions.
- The addition of either the type 1 or type 2 elastic coupling to the DCVI system, provided large reduction in the $\ddot{X}_2$ response to a rounded pulse displacement, particularily at high ν. The type 2 system had the lowest $\ddot{X}_2$ of the three systems for a given ν, N and ξ, as it provided a second stage of isolation.
- Depending on the severity of the rounded pulse and elastic coupling ratio N, there was an optimum value of damping which minimized RDR.
- For isolators subjected to variable shock environments (that is, varying levels of rounded pulse severities), the elastic coupled viscous isolator (ECVI) systems were found to offer more uniform $\ddot{X}_2$ responses as compared to the DCVI system.

- The addition of the type 1 elastic coupling however, was found to be detrimental to isolator performance for the case of an oscillatory pulse displacement of severity (ν=5), particularily for small values of the coupling ratio N. Both $\ddot{X}_2$ and RDR were increased, as compared to those of the DCVI system.
- The time histories showed that high damping quickly brought the DCVI system to rest, whereas several oscillations were required for the system with low damping to come to rest. Systems with large degrees of elastic coupling also required several oscillations to come to rest. For high pulse severities, these large number of oscillations were not considered damaging, as their magnitudes were small when compared with those with high damping. However, at low severities, the magnitudes for high and low damping were nearly the same, so it would be more desirable to have high viscous damping.

6.2 PERFORMANCE OF FRICTION DAMPED ISOLATORS

- It was found that for the directly coupled coulomb friction damped (DCFI) system, the degree of coulomb damping α desired was dependent on the pulse severity ν of the rounded and oscillatory pulses. At high severities, low damping produced good isolator performance, whereas at low ν, higher damping gave the best results.
- The type 1 elastic coupling (ECFI-1 system) gave no improvement in the response to rounded pulses as compared to the DCFI system. Indeed, at low severities, there was a slight degradation in performance.

- There was some reduction in $\ddot{X}_2$ with the ECFI Type 2 system as compared to the DCFI system: this is due, however, to the addition of a second stage of isolation which attenuated the input to the isolator's mid-frame.
- Both the ECFI type 1 and 2 systems showed markedly poorer performances for the combination of high coulomb damping and low rounded pulse severity, as compared to the DCFI system. In these cases the friction damper locked up throughout most of the duration of the pulse, causing the system to be practically undamped.
- Of the four types of adaptive friction devices which were used in the DCFI system, the DDFI device gave the best performance. It had a constant $\ddot{X}_2$ response which was independent of pulse severity, while its RDR response increased with severity in order to absorb the base motion. It was also found to give an improved performance over those of the fixed friction systems.
- Like the viscous damped system, the introduction of the type 1 elastic coupling produced a degradation in the $\ddot{X}_2$ response of the coulomb damped system subjected to an oscillatory pulse of severity (ν=5). "Stiff" elastic coupling springs (that is, small N) produced the worst performance. One benefit, however, was that RDR response was reduced at high damping values, as compared to the DCFI system.
- The time histories of the DCFI systems with fixed friction showed that except for very low coulomb damping, the mass was quickly brought to rest after the rounded pulse had passed. However, due to the lock-up of the friction device, the mass did not return to its zero position.

- The acceleration time histories of the DCFI system with adaptive friction devices were compared to the same system having two values of fixed friction; high and low. The end points of the damping range of the adaptive devices were set equal to these fixed friction values. The responses of the adaptive systems were found to be bounded by those of the fixed friction systems. The system with the DDFI device had the best performance, as during the pulse (when the base accelerations are high) it followed the low friction response, while after the pulse, it tracked the high friction response.
- In terms of the relative displacement time history, the system having the VIFI device was found the best. It brought the mass nearly to its zero position, which was achieved only by one other system (that with low fixed friction), and in a much shorter length of time.

6.3 PERFORMANCE OF COMBINED VISCOUS/COULOMB DAMPED ISOLATORS

- It was found that for the CVFI system subjected to rounded pulse displacements, in general had the viscous damping ratio ξ determine the system's performance at low pulse severities, while the coulomb damping ratio α determined its high severity response. By an appropriate selection of ξ and α , the system could have good performance for all values of ν , the pulse severity.
- A minimum amount of coulomb damping was required, as at low values of α, the system was virtually undamped and had very poor performance at low severities.

- Low values of ξ were also undesirable, since for low pulse severities, the RDR response was poor.

(Note: Though the response to oscillatory pulses was not fully studied, it is reasonable to expect that the above conclusions are also applicable to oscillatory pulses).

- The relative displacement time histories also confirmed that the low ξ or α values were undesirable, as in these cases, the system was highly undamped and several oscillations were required to bring the mass to rest.
- From the acceleration histories, it was found that at the higher pulse severities the coulomb damper determined the maximum acceleration transmitted to the mass (that is, $\ddot{X}_2$), while the viscous damper determined the values of the secondary and smaller acceleration peaks.
- Similar to the case of the directly coupled friction isolator, the DDFI device had the best performance of the four adaptive friction devices that were used in the CVFI system. This isolator system had low transmitted accelerations for all pulse severities. The other systems had either higher values of $\ddot{X}_2$ or RDR or both. There was an optimum value of viscous damping ξ associated with the DDFI device: low ξ gave high RDR values, while high ξ resulted in a poor resonant response (at $\nu=2$).

6.4 COMPARISONS OF THE VARIOUS ISOLATOR CONFIGURATIONS

- In terms of limiting the accelerations transmitted to the mass from rounded and oscillatory pulse displacements of varying severities, the DCFI and CVFI were found to be superior to the DCVI system. In the DCFI and CVFI, the accelerations were maintained at low levels by the force limiting behaviour of the friction damper. Indeed, when the DDFI device was used, the lowest and most uniform $\ddot{X}_2$ response was obtained. The viscous damper, which had a damping force proportional to the relative velocity across the damper, offered no such limiting characteristic in the DCVI system.
- The ECVI types 1 and 2 systems were also found superior to the DCVI system subjected to rounded pulses. This was because the elastic coupling spring reduced the relative velocities across the viscous damper, and hence limited $\ddot{X}_2$.
- The disadvantage of the two ECVI systems as compared to the DCVI, was their markedly poorer RDR response at the lower pulse severities, where their equivalent damping c_{eq} was found to be too low.
- The main disadvantage of the DCFI system was that because of the lock-up of the friction damper, it did not return the mass to its zero position after the base disturbance had ceased.
- One way of overcoming this disadvantage was to use adaptive friction dampers having low friction values near zero relative displacement or relative velocity. Indeed the VIFI device was found very effective in bringing the mass to its zero position.

- Another method of having the mass return to its equilibrium position, was to use the CVFI system. In this system, the return spring was de-coupled from the friction damper and hence was not affected by the lock-up.
- In summary, the CVFI system was found to offer generally the best overall performance to both rounded and oscillatory pulse displacements of varying severities. It maintained low values of $\ddot{X}_2$ for all pulse severities, while limiting its RDR response to that which was necessary to absorb the base motion. As shown in its relative displacement time histories, it would accurately track the motion of the base, and would quickly come to rest after the disturbance had passed. Unlike the DCFI system, it would not "lock-up" the mass and prevent it from returning to its zero position.

6.5 RECOMMENDATIONS FOR FUTURE WORK

The following is a list of recommendations for future areas of study:

1. Perform an optimization of the various isolator configurations based on an objective function which minimizes a weighted summation of RDR and $\ddot{X}_2$. In the present study, the comparative performances of isolator systems were analysed using parametric variations. However, no optimum performance was derived. It is suggested that the optimization be performed both for a single input of a given severity, and for a number of different inputs of various severities. This latter study is desirable for those isolator

systems which may be subjected to shock environments of varying intensities.

2. Examine the response of the isolator systems to other types of base excitations, such as various shaped velocity pulses. This may show that the above conclusions on isolator performance are valid for shock inputs in general, and are not unique to the two disturbances used in this study. Also a more in-depth study of the response to oscillatory pulse displacements would be desirable.

3. Further investigate the CVFI system in conjunction with adaptive friction devices using different Z parameters (ref. equations 61 to 63) to control the friction force: for example, having Z be the relative displacement across the viscous damper [5].

4. Investigate other mathematical models for the friction damper, such as the one used in ref. [13], in order to improve the accuracy of the simulation of the acceleration time history and particularily to stabilize the limit cycle behaviour found in the ECVI systems (see Appendix A).

5. Design and test an experimental CVFI system having fixed and adaptive friction devices, in order to validate the computer results.

REFERENCES

1. Ruzicka, J.E. and Derby, T.F.:"Influence of Damping in Vibration Isolation". The Shock & Vibration Information Center, United States Department of Defense, 1971.
2. Snowdon, J.C.: "Vibration and Shock in Damped Mechanical Systems". John Wiley & Sons, New York, 1968, pp. 33-36, 434-454.
3. Snowdon, J.C.: "Isolation from Mechanical Shock with a Mounting System Having Nonlinear Dual-Phase Damping". The Shock & Vibration Bulletin, no. 41 part 2, Dec. 1970.
4. Cornelius, K.: "A Study of the Performance of an Optimum Shock Mount". The Shock & Vibration Bulletin, no. 38 part 3, Nov. 1968.
5. Mercer, C.A. and Rees, P.L.: " An Optimum Shock Isolator". Journal of Sound and Vibration 18(4), 1971, pp. 511-520.
6. Sevin, E. and Pilkey, W.: "Optimum Shock and Vibration Isolation". The Shock & Vibration Information Center, United States Department of Defense, 1971.
7. Karnopp, D.C. and Trikha, A.K.: "Comparative Study of Optimization Techniques for Shock and Vibration Isolation". ASME, J. Eng. Ind. (91), Nov. 1969, pp. 1128-1132.
8. Derby, T.F. and Calcaterra, P.C.: "Response and Optimization of an Isolation System with Relaxation Type Damping". National Aeronautics and Space Administration, NASA CR-1542, May 1970.
9. Paul, I.L. and Fenoglio, B.F.:"Design and Computer Simulation of a Near-Optimum Active Vibration Isolation System". Dept. Mech. Eng. Massachusetts Institute of Technology, report DSR-76109-8, June 1968.

10. Boulden, L.L.:"Hydraulic Shock Absorbers, Putting a stop to shocking deceleration". Machine Design, Nov. 11, 1971, pp.140-144.

11. Mayne, R.W.:"The Effects of Fluid and Mechanical Compliance on the Performance of Hydraulic Shock Absorbers". ASME Paper no. 73-DET-1, presented at the Design Eng.Tech.Conf., Cincinatti, Ohio, Sept. 9-12, 1973.

12. Blake, R.E.: "Near-Optimum Shock Mounts for Protecting Equipment from Acceleration Pulses". The Shock & Vibration Bulletin, no. 35, Feb. 1966.

13. Heller, R., Tuten, J.M., Kadala, P.S. and Law, E.H.: "Analog and Digital Computer Simulation of Coulomb Friction". Dept. of Transportation, U.S.A., interim report no. FRA/ORD-78/07, Dec. 1977.

14. Hamming, R.W.: "Numerical Methods for Engineers and Scientists". McGraw-Hill, New York, 1962. pp. 212-213.

15. Den Hartog, J.P.: "Forced Vibrations with Coulomb and Viscous Friction", Transactions of ASME 53-9 (Applied Mechanics) 1931. pp. 107-115.

APPENDICES

APPENDIX A

FRICTION DAMPED ISOLATOR HAVING NO LINEAR VISCOUS BAND CHARACTERISTICS.

As discussed in Section 2.2.1, a modified coulomb friction force characteristic having a narrow linear viscous band was used in the DCFI system. The size of the viscous band $\Delta\dot{x}$ was selected to accurately simulate the acceleration response to conditions of free oscillation, while maintaining the basic friction characteristic during forced oscillations. As seen in Figures 76 and 77, the mass acceleration history for the systems having the "ideal" friction characteristic of Figure 5 had large high frequency oscillations during lock-up of the damper. The amplitude of these oscillations were proportional to the amount of the friction force. On the other hand, the systems with a friction characteristic having a linear viscous band, brought the mass acceleration to zero once the system was locked up, and had no high frequency oscillations. The figures show that the response of the systems with and without the viscous bands were identical prior to lock-up. The size of the viscous band $\Delta\dot{x}$ given in equation (A1) was determined in terms of the simulation parameters and was automatically selected by the computer program.

$$\Delta\dot{x} = \frac{(X_{in}\,\nu)\,(H_{mod})}{50\,\omega_n} \qquad (A1)$$

where H_{mod} = user selected step size modifier.

The types 1 and 2 ECFI systems did not employ the linear viscous band characteristic in their friction models, as it was believed that during lock-up of the dampers, the elastic coupling spring k_1 would control the mass acceleration response. However, this assumption was found to be erroneous, as the acceleration of these systems had the same type of oscillations during lock-up as the DCFI with no viscous band, despite attempts to eliminate the oscillations by decreasing the step size. $\ddot{X}_2$ and RDR however, were not affected by the oscillations. (Note: one of the recommendations of this thesis is to use different friction models with the ECFI systems in order to eliminate the oscillations).

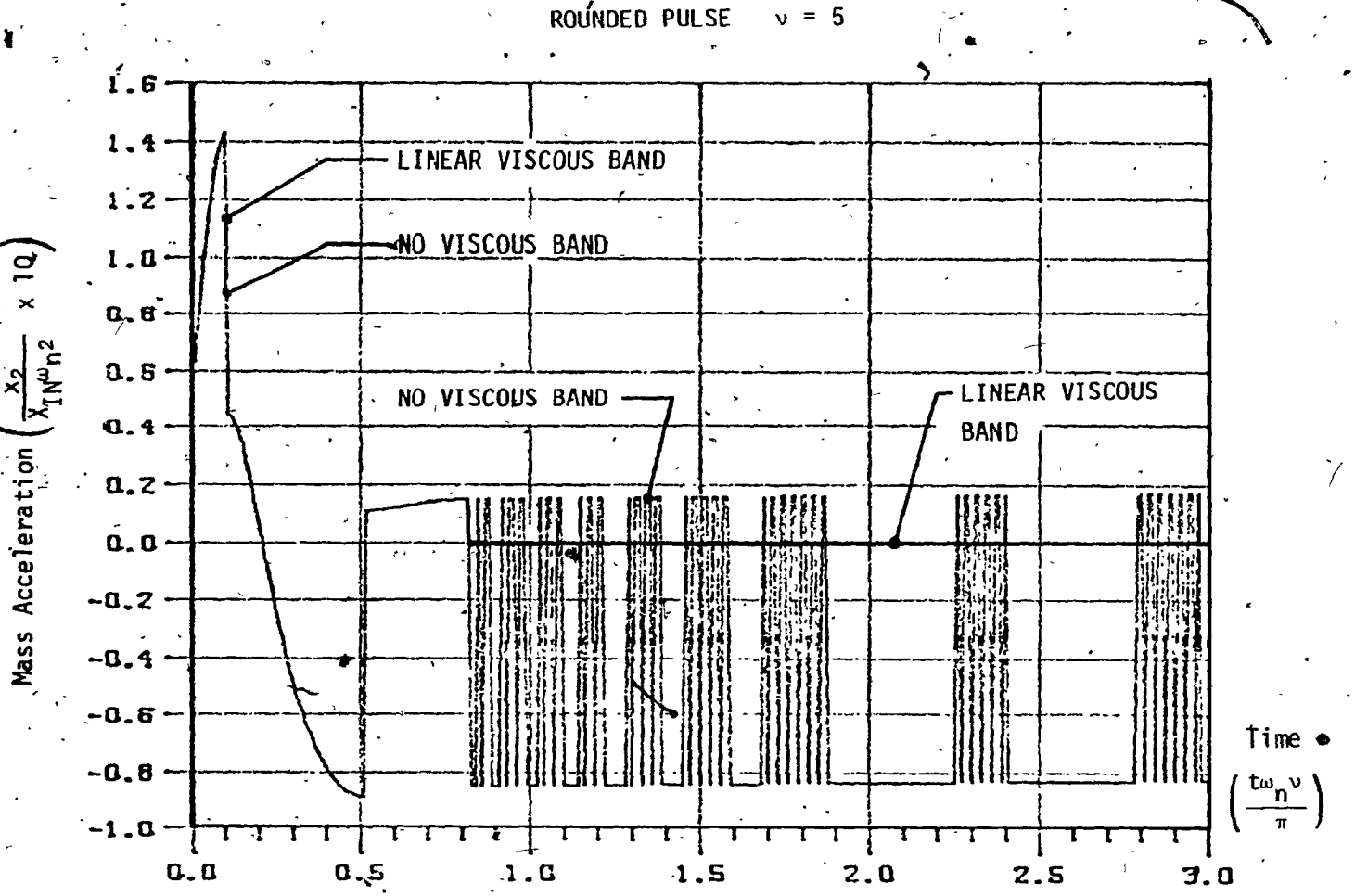

FIGURE 76. Comparison of Mass Acceleration Time Histories of DCFI System with and without Linear Viscous Band Friction Characteristic. $\alpha = 0.50$ $\omega_n = \pi$

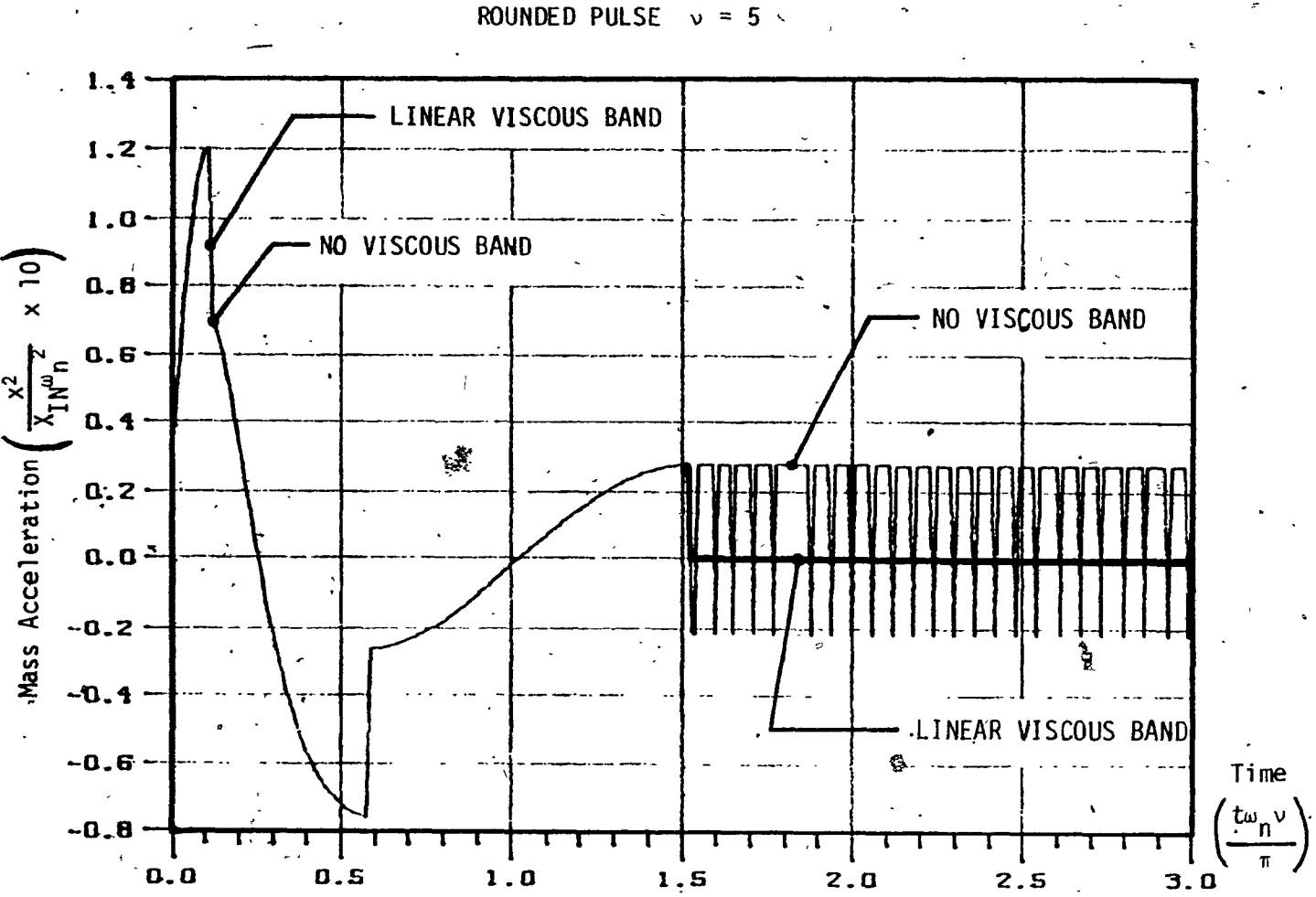

FIGURE 77. Comparison of Mass Acceleration Time Histories of DCFI System with and without Linear Viscous Band Friction Characteristic $\alpha = 0.25$: $\omega_n = \pi$

APPENDIX B

FOURTH-ORDER RUNGE-KUTTA METHOD OF SOLVING DIFFERENTIAL EQUATIONS [14]

This method solves for the dependent variable y_n in the differential equation (B1) for successive values of the independent variable X_n which is incremented in step sizes of h.

$$y' = f(x,y)$$

$$x_{n+1} = x_n + h \qquad \text{(B1)}$$

$$y_{n+1} = y_n + \Delta y$$

The method essentially expands the right hand side of (B1) in a fourth-order power series of h, by computing four sample slopes in the neighbourhood of the last step (x_n, y_n), and then averaging the slopes using weighting factors (1/6, 2/6, 2/6 and 1/6) to determine the next step at (x_{n+1}, y_{n+1}). The slopes are given as:

$$k_1 = [f(x_n,y_n)]\,[h] \qquad \text{(B2)}$$

$$k_2 = [f(x_n + \tfrac{h}{2}, y_n + \tfrac{k_1}{2})]\,[h] \qquad \text{(B3)}$$

$$k_3 = [f(x_n + \tfrac{h}{2}, y_n + \tfrac{k_2}{2})]\,[h] \qquad \text{(B4)}$$

$$k_4 = [f(x_n + h, y_n + k_3)]\,[h] \qquad \text{(B5)}$$

The average slope is given as:

$$\Delta y = \frac{1}{6}[k_1 + 2k_2 + 2k_3 + k_4] \qquad \text{(B6)}$$

The geometric representation of the method is shown in Figure 78.

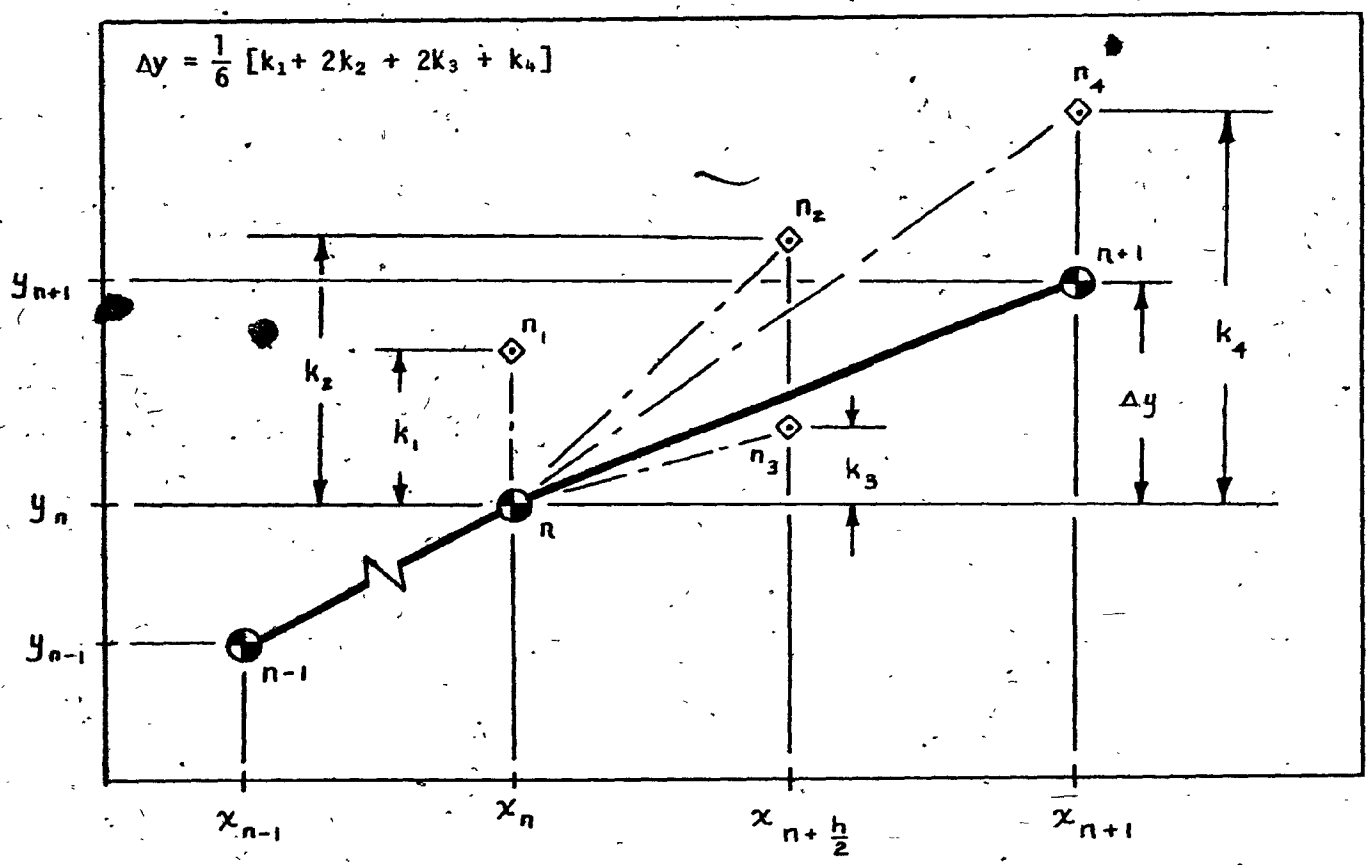

FIGURE 78: Geometric Representation of the Fourth-Order Runge-Kutta Method.

APPENDIX C

DESCRIPTION OF THE USE OF THE COMPUTER PROGRAM

The digital computer FORTRAN program was written in an interactive mode which allows the user to select any of the isolators discussed in Chapter 2 and to determine its response to either of the base excitations of Chapter 3. The following is a description of the use of the program.

The user first selects the type of damper in the system: viscous, friction or combined viscous and friction. The isolator configuration is then inputted; either directly or elastically coupled. If a friction device is involved, then the program asks for its characteristics: either fixed or adaptive, and whether or not, the linear viscous band is to be used. Having defined the isolator system, the user then inputs the values of the system parameters.

The program follows by asking for the type of base excitation (six types are available, though only rounded pulse -1- and oscillatory pulse B -4- were studied in this thesis). The user then enters the amplitude of the excitation - XIN - and its severity - D.

Based on the values of system and excitation parameters, the program automatically selects the iteration step size and the time duration of the simulation. In general, a fixed step size is used, though for friction isolators, it is reduced to a tenth in the neighbourhood of the lock-up condition. This is to prevent overshooting the region of lock-up. During the low frequency of the oscillatory pulse, the step size was increased to minimize the CPU time required for the run. However, the program allows the user to either increase or

decrease the step size and time duration by setting the values of HMOD and LIMOD to values larger or smaller than unity.

The program also lets the user select the type of output from the simulation and where it will be displayed - on the terminal and/or in a file to be hard copied. All the values of the state variables may be stored, or only their nondimensional maximum values (SAR, AMAX, RDR, SDR) with their corresponding time values. The user can also select any of the state variables to later be plotted as a time history.

The program incorporates an iterating routine by which the user can select one parameter of the simulation to successively take on a series of values, either in constant increments or having user-selected values. At the end of the run, the user can change any or all of the parameter values, review the status of the parameters and rerun the simulation.

On the following two pages a typical terminal display from an isolator system simulation is shown. The first page is the user/program dialogue; the CVFI system ($\omega_n = \pi$) having a DIFI adaptive friction device (α_0=0.25, α_f=1.0, z_1=.1, z_2=1.0) was selected. The base excitation was a rounded pulse (X_{in}=1, ν=5), and the program was run for two values of ξ (dampv=0.5 and 1.0). The results from the runs are shown on the second page, along with the status of the parameters of the second run.

```
 ENTER USER,  0 FOR SANKAR, 1 FOR BOB
? 0

 ENTER 0 FOR VISCOUS, 1 FOR FRICTION, 2 FOR COMBINED DAMP
? 2

 ENTER 6 FOR SIMPLE COMBINED, 7 FOR DUAL K  - COMBINED
? 6

 ENTER 0 FOR FIXED FRICTION, 1 FOR VARIABLE, REL. DISPL
       2 FOR VARIABLE FRICTION, REL. VELOCITY
? 1

 ENTER 1 FOR NO LINEAR VISCOUS BAND, 0 FOR L.V.BAND
? 0

 ENTER FRICTION PARAMETERS... DAMP, XN1, XN2, DMAX
? .25      .1      1.0      1.0

 ENTER  FREQ, N  .......SYSTEM PARAMETERS
? 3.14159     1

 ENTER DAMPV  .... VISCOUS DAMPING RATIO
? .5

 ENTER 0 FOR STEP, 1 FOR PULSE, 2 FOR MASS INPUT
       3 FOR OSCIL. PULSE A, 4 FOR OSCIL. PULSE B
       5 FOR VELOCITY PULSE
? 1

 ENTER XIN,D,HMOD,LIMOD ..... INPUT PARAMETERS
? 1   5       1     1

 ENTER 0 FOR ALL VALUES PRINTED, 1 FOR PEAK VALUES
       2 FOR NO TERMINAL OUTPUT  PEAK VALUES
? 1

 ENTER 0 FOR DATA STORED, 1 FOR NO STORAGE
? 1

 ENTER NAME OF ITERATED PARAMETER, -NO- FOR NO ITERATION
? dampv

 ENTER 0 FOR CONSTANT INCREMENT, 1 FOR VARIABLE INCREMENT
? 1

 ENTER -N- NUMBER OF ITERATIONS AND -N- VARIABLE VALUES
?      2                    .5     1.0
```

```
 MODEL AND SYSTEM VALUES DEFINED...ITERATION NO     1

VALUE OF S.A.R.          .01976        TIME OF S.A.R.          .12600
VALUE OF A.MAX.        18.01162        NO. OF PEAKS             7
VALUE OF R.D.R.          .94814        TIME OF R.D.R.          .08800
VALUE OF S.D.R.          .42367        TIME OF S.D.R.          .51800
VALUE OF A.RMS.         2304.685       LAST TIME VALUE        5.99800
STEP SIZE                .02000        TIME LIMIT             6.00000

 MODEL AND SYSTEM VALUES DEFINED...ITERATION NO     2

VALUE OF S.A.R.          .01908        TIME OF S.A.R.          .12000
VALUE OF A.MAX.        17.38905        NO. OF PEAKS             5
VALUE OF R.D.R.          .96052        TIME OF R.D.R.          .08000
VALUE OF S.D.R.          .39059        TIME OF S.D.R.          .49000
VALUE OF A.RMS.          776.755       LAST TIME VALUE        5.99600
STEP SIZE                .02000        TIME LIMIT             6.00000

 ENTER VARIABLE TO BE CHANGED - NOMORE TO STOP
? status


 COMBINED VISCOUS - FRICTION    - 6
 VARIABLE FRICTION - DAMP-       .25
 - DMAX -     1.
 VISCOUS DAMP  - DAMPV -     1.
  - FREQ -      3.14159
 VALUE OF ELASTIC COUPLING - N -  1.
  - INPUT -    PULSE     1
 INPUT AMPLITUDE  - XIN -      1.
 TRANS TIME RATIO   - D -       5.
 NUMERICAL SOLN VARIABLES
 STEP MOD    - H -     1.
 LIMIT MOD    - LIMOD -    1.
 STEP SIZE  - H -       .02000
 END OF TIME    - LIMIT -       6.0000
 DATA STORED -GRAPH-  =0,   YES-  SET TO 1
 ALL VALUES=0  ,PEAK VALUES=1   -PRINT-   1.
 ENTER -RETURN- TO RUN    ,    -NAME-  OF NEW VARIABLE
? nomore
```

APPENDIX D

FLOWCHART AND LISTING OF COMPUTER PROGRAM

The computer program comprises the main program EQS and three major subroutines DIFEQS, EVF and PULSE. EQS is the user interactive portion of the program and contains the prompt commands to select the isolator, base excitation, values of the system parameters and type of output. The program then calculates the step size and time duration of the simulation, and the co-efficients of the equations of motion.

Subroutine DIFEQS contains the Runge-Kutta numerical method package which solves the equations of motion. It also calculates the peak values of the state variables and stores the data in various files for either terminal display, hard-copy or for a plotting package.

Subroutine EVF contains the equations of motion for the isolator systems while PULSE generates the base excitation for each increment of time.

Figure 79 is a flowchart of the entire program, followed by the program listing.

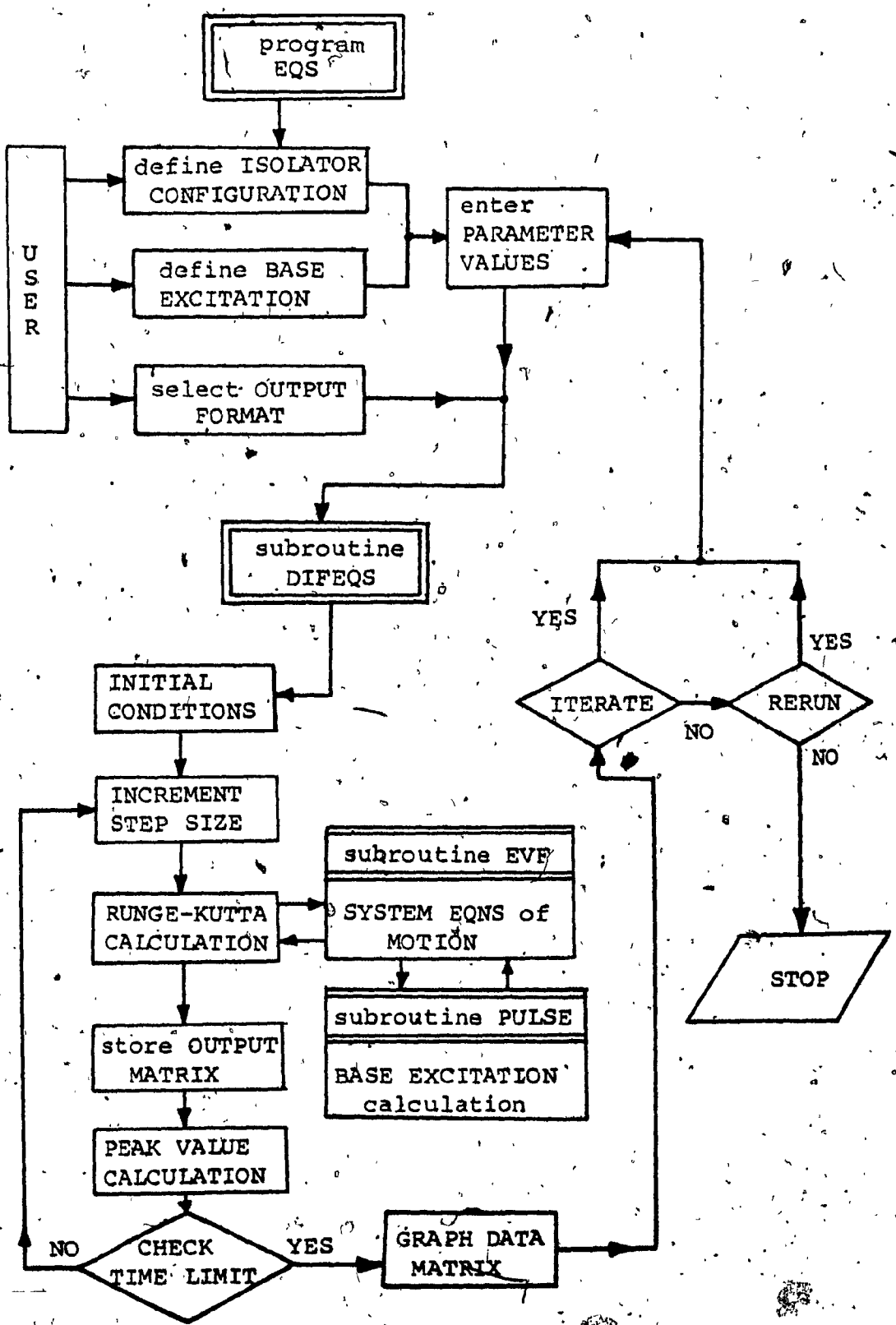

FIGURE 79: Flowchart of Isolator Simulation Program

```
      PROGRAM EQS(TAPE1,OUTPUT,TAPE6=OUTPUT,INPUT,
     *    TAPE5=INPUT,TAPE8,TAPE9)
      DOUBLE PRECISION DEP(20),RSLT(20),H,INDEP,LIMIT
      REAL FREQ,DMAX,XIN,ZN,DAMP
      DIMENSION COEFF(15),VNEW(10
      INTEGER N,CHECK
      IVARNO=1

      PRINT*,"ENTER USER,  0 FOR SANKAR, 1 FOR BOB"
      READ*,MODE
      PRINT*,"ENTER 0 FOR VISCOUS, 1 FOR FRICTION,
     *    2 FOR COMBINED DAMP*
      READ*,DAMPER
      IF(DAMPER.EQ.1) GO TO 100
      IF(DAMPER.EQ.2) GO TO 101
      PRINT*,"ENTER 0 FOR MODEL A, 1 FOR MODEL E"
      PRINT*,"      2 FOR SIMPLE - VISCOUS"
      GO TO 105
  100 PRINT*,"ENTER 3 FOR MODEL A, 4 FOR MODEL E"
      PRINT*,"      5 FOR SIMPLE - FRICTION"
      GO TO 105
  101 PRINT*,"ENTER 6 FOR SIMPLE COMBINED, 7 FOR DUAL K"
  105 READ*,MODEL
      IF(DAMPER.LT.1) GO TO 102
      PRINT*,"ENTER 0 FOR FIXED, 1 FOR VARIABLE, REL DISPL"
      PRINT*,"      2 FOR VARIABLE FRICTION, REL. VELOCITY"
      READ*,IFRICN
      PRINT*,"ENTER 1 FOR NO LIN VISC BAND, 0 FOR L.V.BAND"
      READ*,LVB
      IF(IFRICN.LT.1) GO TO 102
      PRINT*,"ENTER FRICTION PARAMETERS...DAMP,XN1,XN2,DMAX"
      READ*,DAMP,XN1,XN2,DMAX
      PRINT*,"ENTER  FREQ, N  .......SYSTEM PARAMETERS"
      READ*,FREQ,ZN
      GO TO 107
  102 PRINT*,"ENTER DAMP, FREQ, AND N .. SYSTEM PARAMETERS"
      READ*,DAMP,FREQ,ZN
  107 IF(DAMPER.NE.2) GO TO 103
      PRINT*,"ENTER DAMPV  .... VISCOUS DAMPING RATIO"
      READ*,DAMPV
  103 PRINT*,"ENTER 0 FOR STEP, 1 FOR PULSE, 2 FOR MASS "
      PRINT*,"      DISPL., 4 FOR OSCIL. PULSE B"
      PRINT*,"      5 FOR VELOCITY PULSE"
      READ*,INPUT
      IF(INPUT.NE.5) GO TO 104
      PRINT*,"SELECT VELOCITY TYPE,  6 FOR TRIANGLE, "
      PRINT*,"      7 FOR SINE, 8 FOR VERSED SINE"
      READ*,INPUT
      IF(INPUT.NE.6) GO TO 106
      PRINT*,"ENTER VIN,D,DRATIO,HMOD,LIMOD... INPUT PARAM"
      READ*,VIN,D,DRATIO,HMOD,FMOD
      TAO=3.1415926/(FREQ*D)
      XIN=VIN*TAO/2.
```

```
      PRINT*,"VALUE OF XIN   ",XIN
      GO TO 108
105   PRINT*,"ENTER VIN,D,HMOD,LIMOD . .. INPUT PARAMETERS"
      READ*,VIN,D,HMOD,FMOD
      TAO=3.1415926/(FREQ*D)
      IF(INPUT.EQ.7) XIN=VIN*TAO/1.570796
      IF(INPUT.EQ.8) XIN=VIN*TAO/2.
      PRINT*,"VALUE OF XIN    ",XIN
      GO TO 108
104   PRINT*,"ENTER XIN,D,HMOD,LIMOD ... INPUT PARAMETERS"
      READ*,XIN,D,HMOD,FMOD
108   PRINT*,"ENTER 0 FOR ALL VALUES PRINTED, 1 FOR PEAK"
      PRINT*,"      VALUES, 2 FOR NO TERMINAL OUTPUT "
      READ*,PRINT
      PRINT*,"ENTER 0 FOR DATA STORED, 1 FOR NO STORAGE"
      READ*,GRAPH
      PRINT*,"ENTER NAME OF ITERATED PARAMETER"
      PRINT*,"      -NO- FOR NO ITERATION"
      READ(5,601) VARITE
      IF((MODEL.EQ.2).OR.(MODEL.EQ.5).OR.(MODEL.EQ.6)) ZV=1
      IF(VARITE.EQ."NO") GO TO 606
      PRINT*,"ENTER 0 FOR CONSTANT INCREMENT"
      PRINT*,"      1 FOR VARIABLE INCREMENT"
      READ*,INCRMT
      IF(INCRMT.NE.0) GO TO 109
      PRINT*,"ENTER STEP SIZE OF ITERATION AND NUMBER"
      READ*,VARSE,IVARNO
      DO 111 I=1,IVARNO
      VNEW(I)=I*VARSE
111   CONTINUE
      GO TO 606
109   PRINT*,"ENTER -N- NUMBER OF ITERATIONS AND "
      PRINT*,"     -N- VARIABLE VALUES"
      READ*,IVARNO
      DO 110 I=1,IVARNO
      READ*,VNEW(I)
110   CONTINUE
      GO TO 606

600   READ(5,601)VAR
601   FORMAT(A6)
602   IF(VAR.EQ."NOMORE") GO TO 1000
      IF(VAR.NE."STATUS") GO TO 607


      IF(MODEL.EQ.0) PRINT*,"MODEL A VISCOUS    ",MODEL
      IF(MODEL.EQ.1) PRINT*,"MODEL E VISCOUS    ",MODEL
      IF(MODEL.EQ.2) PRINT*,"SIMPLE VISCOUS     ",MODEL
      IF(MODEL.EQ.3) PRINT*,"MODEL A FRICTION -  ",MODEL
      IF(MODEL.EQ.4) PRINT*,"MODEL E FRICTION -  ",MODEL
      IF(MODEL.EQ.5) PRINT*,"SIMPLE FRICTION     ",MODEL
      IF(MODEL.EQ.6) PRINT*,"COMB VISCOUS/FRICTION ",MODEL
      IF(MODEL.EQ.7) PRINT*,"COMB DAMP - DUALI K   ",MODEL
```

```
      IF(MODEL.EQ.0) GO TO 608
      IF(MODEL.EQ.1) GO TO 608
      IF(MODEL.EQ.2) GO TO 608
      IF(MODEL.EQ.10) GO TO 608
      IF(MODEL.EQ.11) GO TO 608
      IF(IFRICN.EQ.1) GO TO 609
      PRINT*,"CONST FRICT - DAMP-     ",DAMP
      GO TO 610
609   PRINT*,"VARIABLE FRICTION - DAMP-       ",DAMP
      PRINT*,"- DMAX -     ",DMAX
610   IF(MODEL.EQ.5)PRINT*,"VISCOUS DAMP - DAMPV- ",DAMPV
      IF(MODEL.EQ.7)PRINT*,"VISCOUS DAMP  -DAMPV- ",DAMPV
      GO TO 611
608   PRINT*,"VISCOUS  - DAMP -      ",DAMP
611   PRINT*,"- FREQ -      ",FREQ
      PRINT*,"VALUE OF ELASTIC COUPLING  - N -    ",ZN
      IF(INPUT.EQ.0) PRINT*,"- INPUT -   STEP  ",INPUT
      IF(INPUT.EQ.1) PRINT*,"- INPUT -   PULSE ",INPUT
      IF(INPUT.EQ.2) PRINT*,"- INPUT - MASS DISP  ",INPUT
      IF(INPUT.EQ.3) PRINT*,"- INPUT - OSCIL PULSE  ",INPUT
      PRINT*,"INPUT AMPLITUDE  - XIN -     ",XIN
      PRINT*,"TRANS TIME RATIO   - D -      ",D
      PRINT*,"NUMERICAL SOLN VARIABLES"
      PRINT*,"STEP MOD    - H -     ",HMOD
      PRINT*,"LIMIT MOD    - LIMOD -    ",FMOD
      PRINT*,"STEP SIZE   - H -      ",H
      PRINT*,"LAST OF TIME    - LIMIT -       ",LIMIT
      PRINT*,"DATA STORED -GRAPH-  =0,   YES-  SET TO 1"
      PRINT*,"ALL VALUES=0  ,PEAK VALUES=1 -PRINT- ",PRINT
      GO TO 605


607   PRINT*,"ENTER VALUE OF CHANGED VARIABLE"
      READ*,VALUE
      IF(VAR.NE."IFRICN") GO TO 604
      IFRICN=VALUE
      IF(IFRICN.NE.0) GO TO 603
      PRINT*,"ENTER VALUE OF FIXED DAMP"
      READ*,DAMP
      GO TO 605
603   PRINT*,"ENTER VALUES OF DAMP, XN1, XN2, DMAX"
      READ*,DAMP,XN1,XN2,DMAX
      GO TO 605
604   IF(VAR.EQ."MODEL")MODEL=VALUE
      IF(VAR.EQ."INPUT")INPUT=VALUE
      IF(VAR.EQ."DAMP") DAMP=VALUE
      IF(VAR.EQ."DAMPV") DAMPV=VALUE
      IF(VAR.EQ."XN1") XN1=VALUE
      IF(VAR.EQ."XN2") XN2=VALUE
      IF(VAR.EQ."DMAX") DMAX=VALUE
      IF(VAR.EQ."FREQ") FREQ=VALUE
      IF(VAR.EQ."XIN") XIN=VALUE
      IF(VAR.EQ."D") D=VALUE
      IF(VAR.EQ."N") ZN=VALUE
```

```
      IF(VAR.EQ."H") HMOD=VALUE
      IF(VAR.EQ."LIMOD") FMOD=VALUE
      IF(VAR.EQ."PRINT") PRINT=VALUE
  605 PRINT*,"ENTER -RETURN- TO RUN, -NAME- OF NEW VARIABLE"
      READ(5,601)VAR
      IF(VAR.EQ."RETURN") 606,602


  606 DO 999 ITER=1,IVARNO
      IF(VARITE.EQ."NO") GO TO 701
      IF(VARITE.EQ."DMAX") DMAX=VNEW(ITER)
      IF(VARITE.EQ."XN1")  XN1=VNEW(ITER)
      IF(VARITE.EQ."XN2")  XN2=VNEW(ITER)
      IF(VARITE.EQ."DAMP") DAMP=VNEW(ITER)
      IF(VARITE.EQ."FREQ") FREQ=VNEW(ITER)
      IF(VARITE.EQ."N")    N=VNEW(ITER)
      IF(VARITE.EQ."D")    D=VNEW(ITER)
      IF(VARITE.EQ."DAMPV") DAMPV=VNEW(ITER)
      IF(ITER.EQ.1) GO TO 701

      WRITE(1,726)
  726 FORMAT(////,T5,*ITERATED PARAMETER*,T38,*NEW VALUE*,)
      WRITE(1,728)
  728 FORMAT(T3,*_____*,/)
      WRITE(1,727) VARITE,VNEW(ITER)
  727 FORMAT(10X,A6,15X,F15.5)
  999 CONTINUE

  701 INDEP=0.0
      DEP(1)=0.0
      DEP(2)=0.0
      DEP(3)=0.0

      N=3
      CHECK=0
      H=0.31415926*HMOD/(FREQ*D)
      LIMIT=300*H*FMOD
      IF(INPUT.EQ.4) LIMIT=10*LIMIT

*  CALCULATION OF EQUATION COEFFICIENTS  *

*  FRICTION COEFFICIENTS  *

      IF(IFRICN.EQ.0) GO TO 702
      COEFF(5)=(DMAX-DAMP)*XIN*FREQ**2
      COEFF(6)=(DMAX-DAMP)*XIN*ZN
      IF(MODEL.EQ.5) COEFF(6)=0.0
      IF(MODEL.EQ.6) COEFF(6)=(DMAX-DAMP)*XIN*FREQ/(2*DAMPV)
      IF(MODEL.EQ.7) COEFF(6)=(DMAX-DAMP)*XIN
      COEFF(7)=XN1*XIN
      COEFF(8)=XN2*XIN
      COEFF(9)=XN1*XIN*FREQ
      COEFF(10)=XN2*XIN*FREQ
      COEFF(11)=COEFF(5)/(COEFF(8)-COEFF(7))
```

```
      COEFF(12)=COEFF(6)/(COEFF(8)-COEFF(7))
      COEFF(13)=COEFF(5)/(COEFF(10)-COEFF(9))
      COEFF(14)=COEFF(6)/(COEFF(10)-COEFF(9))
      GO TO 703
702   DO 705 I=5,12,1
      COEFF(I)=0.0
705   CONTINUE

*  MODEL COEFFICIENTS  *

703   COEFF(4)=0.0
      IF(MODEL.EQ.3) GO TO 9
      IF(MODEL.EQ.4) GO TO 12
      IF(MODEL.EQ.5) GO TO 130
      IF(MODEL.EQ.6) GO TO 121
      IF(MODEL.EQ.7) GO TO 131

*  VISCOUS ISOLATOR MODELS  *

      COEFF(1)=2.*DAMP*FREQ
      COEFF(2)=FREQ**2.

      IF(MODEL.EQ.1) GO TO 115
      IF(MODEL.EQ.0) GO TO 118
      COEFF(3)=0.0
      N=2
      IF(ITER.GT.1) GO TO 70
      WRITE(1,116)
116   FORMAT(1H1,///,T5,*CONFIGURATION - SIMPLE VISCOUS
     *   ISOLATOR*,//)
      GO TO 31

115   COEFF(3)=FREQ/(2.*DAMP)
      IF(ITER.GT.1) GO TO 70
      WRITE(1,117)
117   FORMAT(1H1,///,T5,*CONFIGURATION -  VISCOUS
     * ELASTICALLY COUPLED ISOLATOR - MODEL E*,//)
      GO TO 20

118   COEFF(3)=FREQ/(2.*DAMP*ZN)
      IF(ITER.GT.1) GO TO 70
      WRITE(1,119)
119   FORMAT(1H1,///,T5,*CONFIGURATION -  VISCOUS
     * ELASTICALLY COUPLED ISOLATOR - MODEL A*,//)
      GO TO 20

*  FRICTION ISOLATOR MODELS  *

130   N=2
      COEFF(3)=0.0
      COEFF(2)=FREQ**2.
```

```
      COEFF(1)=DAMP*XIN*FREQ**2.
      IF(ITER.GT.1) GO TO 70
      WRITE(1,6)
    6 FORMAT(1H1,///,T5,*CONFIGURATION   SIMPLE FRICTION
     * ISOLATOR*,//)
      GO TO 31
    9 COEFF(3)=DAMP*XIN*ZN
      COEFF(2)=FREQ**2.
      COEFF(1)=DAMP*XIN*FREQ**2.
      IF(ITER.GT.1) GO TO 70
      WRITE(1,10)
   10 FORMAT(1H1,///,T5,*CONFIGURATION    ELASTICALLY
     * COUPLED FRICTION ISOLATOR  -  MODEL A*,//)
      GO TO 20

   12 COEFF(3)=XIN*DAMP*ZN
      COEFF(2)=FREQ**2.
      COEFF(1)=DAMP*XIN*FREQ**2.
      IF(ITER.GT.1) GO TO 70
      WRITE(1,15)
   15 FORMAT(1H1,///,T5,*CONFIGURATION    ELASTICALLY
     * COUPLED FRICTION ISOLATOR  -  MODEL E*,//)
      GO TO 20

*  COMBINED VISCOUS/FRICTION ISOLATOR MODELS  *

  121 COEFF(1)=DAMP*XIN*FREQ**2.
      COEFF(2)=FREQ**2.
      COEFF(3)=DAMP*FREQ*XIN/(2.*DAMPV)
      COEFF(4)=2.*DAMPV*FREQ
      IF(ITER.GT.1) GO TO 70
      WRITE(1,122)
  122 FORMAT(1H1,///,T5,*CONFIGURATION  - COMBINED FRICTION
     * AND VISCOUS DAMPED ISOLATOR*,//)

      WRITE(1,123)
  123 FORMAT(T27,*FRICTION PARAMETER*,T58,*VISCOUS RATIO*
     *    ,T90,*NATURAL FREQUENCY*,/)
      IF(IFRICN.EQ.1) GO TO 124
      IF(IFRICN.EQ.2) GO TO 114
      WRITE(1,30) DAMP,DAMPV,FREQ
      GO TO 924
  124 WRITE(1,717) DAMPV,FREQ
      GO TO 708
  114 WRITE(1,712) DAMPV,FREQ
      GO TO 708

      COEFF(2)=FREQ**2.
      COEFF(3)=DAMP*XIN
      COEFF(4)=2.*DAMPV*FREQ/(ZN**.5)
      IF(ITER.GT.1) GO TO 70
      WRITE(1,132)
  132 FORMAT(1H1,//,T5,*CONFIGURATION  - COMBINED FRICTION
     * AND VISCOUS DAMPED ISOLATOR  -  DUAL SPRINGS*,//)
```

```
      WRITE(1,133)
  133 FORMAT(T8,*FRICTION PARAMETER*,T39,*VISCOUS RATIO*,
     *  T67,*NATURAL FREQUENCY*,T99,*SPRING RATIO*,/)
      IF(IFRICN.EQ.1) GO TO 135
      IF(IFRICN.EQ.2) GO TO 137
      WRITE(1,134) DAMP,DAMPV,FREQ,ZN
  134 FORMAT(D20.5,9X,D20.5,10X,D20.5,10X,D20.5)
      GO TO 924
  135 WRITE(1,136) DAMPV,FREQ,ZN
  136 FORMAT(T4,*DISPLACEMENT VARIABLE*,5X,D20.5,10X,D20.5,
     *     10X,D20.5)
      GO TO 708
  137 WRITE(1,138) DAMPV,FREQ,ZN
  138 FORMAT(T4,*    VELOCITY VARIABLE*,5X,D20.5,10X,D20.5,
     *     10X,D20.5)
      GO TO 708


*  SYSTEM PARAMETERS  *

   20 WRITE(1,25)
   25 FORMAT(T30,*DAMPING RATIO*,T60,*NATURAL FREQUENCY*,
     *   T90,*SPRING RATIO*,/)
      IF(IFRICN.EQ.1) GO TO 704
      IF(IFRICN.EQ.2) GO TO 711
      WRITE(1,30)DAMP,FREQ,ZN
   30 FORMAT(10X,3D30.5)
      GO TO 924
  704 WRITE(1,717) FREQ,ZN
  717 FORMAT(T29,*DISPLACEMENT VARIABLE*,D20.5,D30.5)
      GO TO 708
  711 WRITE(1,712) FREQ,ZN
  712 FORMAT(T33,*VELOCITY VARIABLE*,D20.5,D30.5)
      GO TO 708


   31 WRITE(1,32)
   32 FORMAT(T30,*DAMPING RATIO*,T58,*NATURAL FREQUENCY*,/)
      IF(IFRICN.EQ.1) GO TO 706
      IF(IFRICN.EQ.2) GO TO 713
      WRITE(1,33) DAMP,FREQ
   33 FORMAT(10X,2D30.5)
      GO TO 924
  706 WRITE(1,707) FREQ
  707 FORMAT(T29,*DISPLACEMENT VARIABLE*,D20.5)
      GO TO 708
  713 WRITE(1,714) FREQ
  714 FORMAT(T33,*VELOCITY VARIABLE*,D20.5)


  708 WRITE(1,709)
  709 FORMAT(/,T13,*INITIAL DAMPING*,T39,*BREAK POINT ONE*
     *     ,T64,*LIMIT OF DAMPING*,T90,*BREAK POINT TWO*,/)
```

```
      WRITE(1,710) DAMP,XN1,DMAX,XN2
710   FORMAT(4D25.5)

924   WRITE(1,900)
900   FORMAT(//,T11,*EQUATION CO-EFF   - C3,    C2,    C1*)
      WRITE(1,901) COEFF(3),COEFF(2),COEFF(1)
901   FORMAT(/,3D20.5)
      IF(COEFF(1).LT.1000) GO TO 902
      H=.5*H
      LIMIT=.5*LIMIT
902   CONTINUE

*  INPUT DESCRIPTION  *

      IF(INPUT.NE.8) GO TO 927
      WRITE(1,928)
928   FORMAT(//,T5,*INPUT IS VERBED SINE VELOCITY PULSE*,//)
      GO TO 929

927   IF(INPUT.NE.7) GO TO 930
      WRITE(1,931)
931   FORMAT(///,T5,*INPUT IS SINE VELOCITY PULSE*,//)
929   WRITE(1,938)
938   FORMAT(T24,*INPUT VELOCITY*,T50,*TRANS. TIME RATIO*,
     *  T78,*STEP SIZE*,T104,*LIMIT*,/)
      WRITE(1,65) VIN,D,H,LIMIT
      GO TO 38

930   IF(INPUT.NE.6) GO TO 935
      WRITE(1,932)
932   FORMAT(//,T5,*INPUT IS TRIANGULAR VELOCITY PULSE*,//)
      WRITE(1,933)
933   FORMAT(T5,*INPUT VELOCITY*,T24,*RISE TIME*,T50,
     *  *TRANS. TIME RATIO*,T78,*STEP SIZE*,T104,*LIMIT*,/)
      WRITE(1,934) VIN,DRATIO,D,H,LIMIT
934   FORMAT(5D20.5)
      GO TO 38

935   IF(INPUT.NE.4) GO TO 936
      WRITE(1,937)
937   FORMAT(///,T5,*INPUT IS VARIABLE FREQUENCY
     *    OSCILLATORY PULSE*,//)
      GO TO 50

936   IF(INPUT.NE.3) GO TO 36
      WRITE(1,925)
925   FORMAT(///,T5,*INPUT IS FIXED FREQUENCY OSCILLATORY
     *  PULSE*,//)
      GO TO 50

36    IF(INPUT.NE.2) GO TO 34
      WRITE(1,921)
921   FORMAT(//,T5,*INPUT IS DISPLACED MASS AT TIME T=0*,//)
      WRITE(1,922)
```

```
922     FORMAT(T24,*INITIAL MASS DISPLACEMENT*,T60,*STEP
     *      SIZE*,T90,*LIMIT*,/)

        DEP(1)=XIN
        WRITE(1,923) XIN,H,LIMIT
923     FORMAT(10X,3D30.5)
        GO TO 38

34      IF(INPUT.GE.1) GO TO 40
        WRITE(1,35)
35      FORMAT(//,T5,*INPUT IS ROUNDED STEP DISPLACEMENT*,//)
        GO TO 50
40      WRITE(1,45)
45      FORMAT(//,T5,*INPUT IS ROUNDED PULSE DISPLACEMENT*,//)
        GO TO 50
70      IF(VARITE.NE."D") GO TO 71
50      WRITE(1,55)
55      FORMAT(/,T14,*INPUT AMPLITUDE*,T40,*TRANS. TIME
     *      RATIO*,T58,*STEP SIZE*,T94,*LIMIT*,/)
        WRITE(1,65) XIN,D,H,LIMIT
65      FORMAT(4D25.5)
38      IF(PRINT.GE.1.) GO TO 71
        WRITE(1,69)
69      FORMAT(//,T5,*INDEP. VAR.*,T30,*X*,T43,*D(X)/DT*,T59
     *    ,*D2(X)/DT2*,T75,*X RELAT*,T95,*X0*,T114,*VREL*,/)


71      IF(PRINT.EQ.2) GO TO 72
        PRINT*,"     "
        WRITE(6,73) ITER
73      FORMAT(T2,*MODEL AND SYSTEM VALUES DEFINED...
     * ITERATION NO*,2X,I4)

*  ENTER RUNG-KUTTA ROUTINE  *

72      CALL DIFEQS(DEP,INDEP,RSLT,H,N,CHECK,LIMIT,FREQ,XIN,
     *    D,COEFF,INPUT,MODEL,ZN,PRINT,IFRICN,GRAPH,LVB,VIN,
     *   DRATIO,DAMP,MODE,DMAX)


999     CONTINUE
        PRINT*,"ENTER VARIABLE TO BE CHANGED - NOMORE TO STOP"
        GO TO 600
1000    STOP
        END
```

```
      SUBROUTINE DIFEQS(DEP,INDEP,RSLT,H,N,CHECK,LIMIT,
     * FREQ,XIN,D,COEFF,INPUT,MODEL,ZN,PRINT,IFRICN,GRAPH,
     *   LVB,DRATIO,DAMP,MODE,DMAX)

      DOUBLE PRECISION DEP(20),RSLT(20),H,INDEP,LIMIT,
     * INDEPT,DEPT(20),K1(20),K2(20),K3(20),K4(20),
     *  ERRSAVE(20),ERROR,XO,XOP,XTIME,VTIME,ATIME
      REAL FREQ,XIN,D
      INTEGER N,CHECK,ON,OFF,I,INPUT
      DIMENSION COEFF(15),XVALUE(450),YVALUE(450,8)
      DIMENSION YPEAK(100,4),NPEAK(4),YMAX(4),JMAX(4)

      DATA ON,OFF/1,0/
      COUNT=0
      IC=0
      ISTEP=0
      STEPMOD=0
      RMSA=0.0
      RMAX=0.0
      XMAX=0.0
      VMAX=0.0
      AMAX=0.0
      RTIME=0.0
      XTIME=0.0
      VTIME=0.0
      ATIME=0.0
      IXNUM=0.0
      ITNUM=0
      XVALUE(1)=0.0
      YVALUE(1,1)=DEP(1)
      DO 5 I=2,5
    5 YVALUE(1,I)=0.0

C     * MAXIMUM INPUT VALUES  *

      IF(INPUT.NE.8) GO TO 6
      XOPMAX=VIN
      XPPMAX=VIN*3.1415926/D
      GO TO 15
    6 IF(INPUT.NE.7) GO TO 7
      XOPMAX=VIN
      XPPMAX=VIN*3.1415926/D
      GO TO 15
    7 IF(INPUT.NE.6) GO TO 8
      XOPMAX=VIN
      IF(DRATIO.LT.(0.5)) XPPMAX=VIN/(DRATIO*D)
      IF(DRATIO.GE.(0.5)) XPPMAX=VIN/((1-DRATIO)*D)
      GO TO 15
    8 IF(INPUT.NE.4) GO TO 9
      XOPMAX=XIN*FREQ*D/2.
      XPPMAX=XIN*(FREQ*D)**2./2.
      GO TO 15
```

```
9       IF(INPUT.NE.3) GO TO 11
        XOPMAX=3.1415926*XIN
        XPPMAX=9.8596044*XIN
        GO TO 15
11      IF(INPUT.GE.1) GO TO 10
        XOPMAX=0.35798*D
        XPPMAX=XIN*D*D
        GO TO 15
10      XOPMAX=0.85198*D*FREQ
        XPPMAX=3.69453*XIN*(D*FREQ)**2
15      CONTINUE
        XO=0.0
        XOP=0.0
        XDMAX=FREQ*XIN
        XDDMAX=XIN*FREQ**2.

        TOGGLE=ON
        XSTEP=.025/ZN
        IF(ZN.GT.1) XSTEP=.025
        IF(MODE.EQ.0) XSTEP=0.1
20      ITNUM=ITNUM+1
        IF(STEPMOD.EQ.0) HCHANGE=1
        IF(STEPMOD.EQ.1) HCHANGE=6
        IF(ISTEP.EQ.1) HO=XSTEP*H
        IF(ISTEP.EQ.0) HO=H
        IF((MODEL.EQ.5).AND.(LVB.EQ.1)) HO=H
        INDEP=INDEP+HO*HCHANGE


25      CALL EVF(DEP,INDEP,RSLT,N,FREQ,XIN,D,XO,XOP,COEFF,
     *       INPUT,MODEL,ZN,IFRICN,ISTEP,LVB,VIN,DRATIO,
     *   DAMP,DMAX,STEPMOD)
        DO 30 I=1,N,1
        K1(I)=HO*RSLT(I)
        DEPT(I)=DEP(I)+0.5*K1(I)
30      CONTINUE

        INDEPT=INDEP+0.5*HO
        CALL EVF(DEPT,INDEPT,RSLT,N,FREQ,XIN,D,XO,XOP,COEFF,
     *      INPUT,MODEL,ZN,IFRICN,ISTEP,LVB,VIN,DRATIO
     *   ,DAMP,DMAX,STEPMOD)
        DO 40 I=1,N,1
        K2(I)=HO*RSLT(I)
        DEPT(I)=DEP(I)+0.5*K2(I)
40      CONTINUE

        CALL EVF(DEPT,INDEPT,RSLT,N,FREQ,XIN,D,XO,XOP,COEFF,
     *    INPUT,MODEL,ZN,IFRICN,ISTEP,LVB,VIN,DRATIO,DAMP
     *     ,DMAX,STEPMOD)
        DO 50 I=1,N,1
        K3(I)=HO*RSLT(I)
        DEPT(I)=DEP(I)+K3(I)
50      CONTINUE
        INDEPT=INDEP+HO
```

```
      CALL EVF(DEPT,INDEPT,RSLT,N,FREQ,XIN,D,XO,XOP,COEFF
     *    ,INPUT,MODEL,ZN,IFRICN,ISTEP,LVB,VIN,DRATIO,DAMP
     *      ,DMAX,STEPMOD)
      IF((CHECK.EQ.ON).AND.(TOGGLE.EQ.OFF))GO TO 70
      DO 60 I=1,N,1
      K(4)=HO*RSLT(I)
      DEP(I)=+0.166666666*(K1(I)+2.0*K2(I)+
     *       2.0*K3(I)+K4(I))
   60 CONTINUE

      RVALUE=DABS(DEP(1)-XO)
      IF(RMAX.GT.RVALUE) GO TO 700
      RMAX=RVALUE
      RTIME=(INDEP-H)*FREQ/3.1415926

  700 DVALUE=DABS(DEP(1))
      IF(XMAX.GT.DVALUE) GO TO 701
      XMAX=DVALUE
      XTIME=(INDEP-H)*FREQ/3.1415926

  701 VVALUE=DABS(DEP(2))
      IF(VMAX.GT.VVALUE) GO TO 702
      VMAX=VVALUE
      VTIME=(INDEP-H)*FREQ/3.1415926

  702 AVALUE=DABS(RSLT(2))
      RMSA=AVALUE**2.+RMSA
      IF(AMAX.GT.AVALUE) GO TO 703
      AMAX=AVALUE
      ATIME=(INDEP-H)*FREQ/3.1415926


  703 IF(CHECK.EQ.OFF)GO TO 80
      IF(TOGGLE.EQ.OFF)GO TO 70
      TOGGLE=OFF
      HO=2.0*HO
      GO TO 25

   70 TOGGLE=ON
      DO 90 I=1,N,1
      K4(I)=HO*RSLT(I)
      ERROR=0.055566667*(DEP(I)+0.1666666667*(K1(I)+
     *       2.0*K2(I)+2.0*K3(I)+K4(I))-DEP(I))
      ERRSAVE(I)=ERROR
      DEP(I)=DEP(I)-ERROR
   90 CONTINUE

   80 CONTINUE
      PEAK=1
      IF((GRAPH.NE.0).AND.(PRINT.NE.0).AND.(PEAK.NE.1))
     *   GO TO 100
      IF(IXNUM.EQ.450) GO TO 604
      IF(IXNUM.GT.450) GO TO 605
      IF(ISTEP.EQ.0) GO TO 607
```

```
      IF((ISTEP.EQ.1).AND.(COUNT.EQ.0)) IC=0
      IC=IC+1
      IF(IC.LT.(1/XSTEP)) GO TO 606
  607 IXNUM=IXNUM+1
      XVALUE(IXNUM)=INDEP*FREQ/3.1415926
      YVALUE(IXNUM,1)=DEP(1)/XIN
      YVALUE(IXNUM,2)=DEP(2)/XDMAX
      YVALUE(IXNUM,3)=RSLT(2)/XDDMAX
      YVALUE(IXNUM,4)=DEP(1)/XIN-XO/XIN
      YVALUE(IXNUM,5)=XO/XIN
      YVALUE(IXNUM,6)=(DEP(2)-XOP)/XDMAX
      YVALUE(IXNUM,7)=XOP/XOPMAX
      TIME=D*FREQ*INDEP
      ZEXP=2.7182818
      YVALUE(IXNUM,8)=XIN*(FREQ*ZEXP*D)**2*(1-2*TIME+0.5*
     *  TIME**2)/((2*ZEXP**TIME)*(XPPMAX))
      COUNT=0
      GO TO 605
  606 COUNT=1
      GO TO 605
  604 PRINT*,"OVERFLOW OF ARRAY SIZE"
  605 CONTINUE

  100 IF(MODE.NE.0) GO TO 107
      IF(ITNUM.LE.3000) GO TO 105
      PRINT*,"  ITNUM. REACHED 3000"
      GO TO 106
  107 IF(ITNUM.LE.1000) GO TO 105
      PRINT*,"  ITNUM. REACHED 1000"
      GO TO 106
  105 IF(INDEPT.LE.LIMIT) GO TO 20

  106 IF(PRINT.GE.1) GO TO 110
      WRITE(1,1111) (XVALUE(I),YVALUE(I,1),YVALUE(I,2),
     *  YVALUE(I,3),YVALUE(I,4),YVALUE(I,5),YVALUE(I,6),
     *     I=1,IXNUM)
 1111 FORMAT(7D17.5)

  110 RMSA=RMSA/LIMIT
      SDR=XMAX/XIN
      RDR=RMAX/XIN
      SVR=VMAX/XOPMAX
      SAR=AMAX/XPPMAX

      IF(PEAK.NE.1) GO TO 618
      DO 611 K=1,4
      J=0
      DO 614 I=1,IXNUM
      SEEK1=SGN(YVALUE(I,K))
      SEEK2=SGN(YVALUE((I+1),K))
      IF((SEEK1-SEEK2).EQ.0) GO TO 614
```

```
      J=J+1
      YPEAK(J,K)=YVALUE(I,K)
      IF(YMAX(K).GT.(ABS(YPEAK(J,K)))) GO TO 705
      YMAX(K)=ABS(YPEAK(J,K))
      JMAX(K)=J
  705 CONTINUE
  614 CONTINUE
      NPEAK(K)=J
  611 CONTINUE
      WRITE(1,1112)
      WRITE(1,1113) SAR,ATIME
      WRITE(1,1114) AMAX,NPEAK(3),JMAX(3),YVALUE(IXNUM,3)
      WRITE(1,1115) RDR,RTIME,NPEAK(4),JMAX(4),YVALUE
     *    (IXNUM,4)
      WRITE(1,1116) SDR,XTIME,NPEAK(1),JMAX(1),YVALUE
     *    (IXNUM,1)
      WRITE(1,1117) SVR,VTIME
      WRITE(1,1118) VMAX,NPEAK(2),JMAX(2),YVALUE(IXNUM,2)
      WRITE(1,1119) INDEP
 1112 FORMAT(///,T42,* VALUE*,17X,*TIME*,10X,*NO. OF *,5X,
     * *OCCURS AT*,9X,*LAST VALUE*,/,T79,*PEAKS*,7X,*PEAK
     *  NO.*,/)
 1113 FORMAT(T5,*SHOCK ACCELERATION RATIO*,T38,D12.5,T60,
     *   D12.5)
 1114 FORMAT(T5,*MAXIMUM ACCELERATION*,T38,D12.5,T78,I4,7X
     *  ,I4,T107,D12.5)
 1115 FORMAT(T5,*RELATIVE DISPLACEMENT RATIO*,T38,D12.5,
     *   T60,D12.5,T78,I4,7X,I4,T107,D12.5)
 1116 FORMAT(T5,*SHOCK DISPLACEMENT RATIO*,T38,D12.5,T60,
     *  D12.5,T78,I4,7X,I4,T107,D12.5)
 1117 FORMAT(T5,*SHOCK VELOCITY RATIO*,T38,D12.5,T60,D12.5)
 1118 FORMAT(T5,*MAXIMUM VELOCITY*,T38,D12.5,T78,I4,7X,I4,
     *  T107,D12.5)
 1119 FORMAT(T5,*LAST TIME VALUE*,T38,D12.5)

      IF(MODE.EQ.0) GO TO 618
      DO 616 K=1,4
      IPEAK=NPEAK(K)
      WRITE(1,617) (YPEAK(I,K),I=1,IPEAK)
  617 FORMAT(T5,F10.5)
      WRITE(1,612)
  612 FORMAT(//)
  615 CONTINUE

  618 IF(GRAPH.NE.0.0) GO TO 603
      WRITE(9,602) IXNUM,(XVALUE(I),I=1,IXNUM)
  601 PRINT*,"ENTER CURVE DATA - 1=X, 2=VEL, 3=ACC, 4=XREL,
     * 5=XO,  6=VREL,  7=XOP   8=XOPP   0=NO MORE DATA"
      READ*,J
      IF(J.NE.0) GO TO 9999
      ENDFILE 8
      ENDFILE 9
```

```
      GO TO 603
 9999 WRITE(8,602) IXNUM,(YVALUE(I,J),I=1,IXNUM)
  602 FORMAT(I3,30(10E12.4/))
      GO TO 601

  603 IF(PRINT.EQ.2) RETURN
      PRINT*,"   "
      WRITE(6,1234) SAR,ATIME,JMAX(3)
      WRITE(6,1235) AMAX,NPEAK(3),YVALUE(IXNUM,3)
      WRITE(6,1236) RDR,RTIME
      WRITE(6,1237) SDR,XTIME
      WRITE(6,1238) RMSA,INDEP
      WRITE(6,1239) H,LIMIT

 1234 FORMAT(*VALUE OF S.A.R.*,5X,F10.5,10X,*TIME OF S.A.R.*
     *   ,5X,F10.5,10X,*OCCURS AT PEAK NO.*,3X,I4)
 1235 FORMAT(*VALUE OF A.MAX.*,5X,F10.5,10X,*NO. OF PEAKS*
     *   ,9X,I4,4X,*ALAST*,2X,F10.5)
 1236 FORMAT(*VALUE OF R.D.R.*,5X,F10.5,10X,*TIME OF R.D.R.*
     *   ,5X,F10.5)
 1237 FORMAT(*VALUE OF S.D.R.*,5X,F10.5,10X,*TIME OF S.D.R.*
     *   ,5X,F10.5)
 1238 FORMAT(*VALUE OF A.RMS.*,5X,F12.3,8X,*LAST TIME VALUE*
     *   ,4X,F10.5)
 1239 FORMAT(*STEP SIZE      *,5X,F10.5,10X,*TIME LIMIT  *
     *   ,7X,F10.5)
      PRINT*,"   "
      RETURN
      END
```

```
      FUNCTION SGN(X)

      IF(X.GE.0.0) GO TO 2
      SGN=-1.0
      RETURN
    2 SGN=+1.0
      RETURN
      END
```

```
      SUBROUTINE EVF(DEP,INDEP,RSLT,N,FREQ,XIN,D,XO,XOP,
     * COEFF,INPUT,MODEL,ZN,IFRICN,ISTEP,LVB,VIN,DRATIO,
     *   DAMP,DMAX,STEPMOD)
      DOUBLE PRECISION DEP(20),RSLT(20),INDEP,XO,XOP,BREAK
      DIMENSION COEFF(15)
      INTEGER N,INPUT

      CALL PULSE(STEPMOD,XIN,FREQ,D,INPUT,VIN,DRATIO,XO,
     *   XOP,INDEP)

      IF(IFRICN.NE.2) GO TO 11
      VREL=DABS(DEP(2)-XOP)
      IF(VREL.LT.COEFF(10)) GO TO 12
      DELTFN=COEFF(5)
      DELTBK=COEFF(6)
      GO TO 13
   12 IF(VREL.LT.COEFF(9)) GO TO 14
      DELTFN=COEFF(13)*(VREL-COEFF(9))
      DELTBK=COEFF(14)*(VREL-COEFF(9))
      GO TO 13
   11 IF(IFRICN.NE.1) GO TO 14
      XREL=DABS(DEP(1)-XO)
      IF(XREL.LT.COEFF(8)) GO TO 15
      DELTFN=COEFF(5)
      DELTBK=COEFF(6)
      GO TO 13
   15 IF(XREL.LE.COEFF(7)) GO TO 14
      DELTFN=COEFF(11)*(XREL-COEFF(7))
      DELTBK=COEFF(12)*(XREL-COEFF(7))
      GO TO 13
   14 DELTFN=0.0
      DELTBK=0.0
   13 CONTINUE
      C4=COEFF(4)
      C3=COEFF(3)+DELTBK
      C2=COEFF(2)
      C1=COEFF(1)+DELTFN

      IF(MODEL.EQ.6) GO TO 25
      IF(MODEL.EQ.5) GO TO 60
      IF(MODEL.EQ.4) GO TO 35
      IF(MODEL.EQ.3) GO TO 50
      IF(MODEL.EQ.2) GO TO 100
      IF(MODEL.EQ.1) GO TO 110
      IF(MODEL.EQ.0) GO TO 120

* MODEL 7 EQUATIONS -  COMBINED DAMP ISOLATOR, DUAL SPRINGS*

      BREAK=DABS((C4/C2)*(RSLT(3)-XOP)+(DEP(3)-XO)/ZN-
     *      (DEP(1)-DEP(3)))
      RSLT(1)=DEP(2)
      IF(BREAK.GE.(1.5*C3)) ISTEP=0
      IF(BREAK.LT.(1.5*C3)) ISTEP=1
```

```
      IF(BREAK.LE.(0.5*C3)) ISTEP=0
      IF(BREAK.GE.C3) GO TO 26
      RSLT(2)=-C2*ZN*(DEP(3)-XO)-C4*(RSLT(3)-XOP)
      RSLT(3)=DEP(2)
      RETURN
26    RELV=DEP(2)-RSLT(3)
      RSLT(2)=-C2*(DEP(1)-DEP(3))-C1*SGN(RELV)
      RSLT(3)=XOP+(C2/C4)*(C3*SGN(RELV)+(DEP(1)-DEP(3))
     *          -(DEP(3)-XO)/ZN)
      RETURN

* MODEL 6 EQUATIONS  -  COMBINED DAMPERS ISOLATOR  *

25    BREAK=DABS(RSLT(3)-XOP)
      RSLT(1)=DEP(2)
      IF(BREAK.GE.(1.5*C3)) ISTEP=0
      IF(BREAK.LT.(1.5*C3)) ISTEP=1
      IF(BREAK.LE.(0.5*C3)) ISTEP=0
      IF(BREAK.GE.C3) GO TO 31
      RSLT(2)=-C2*(DEP(1)-XO)-C4*(RSLT(3)-XOP)
      RSLT(3)=DEP(2)
      RETURN
31    RELV=DEP(2)-RSLT(3)
      RSLT(2)=-C2*(DEP(1)-XO)-C1*SGN(RELV)
      RSLT(3)=XOP+C3*SGN(RELV)
      RETURN

* MODEL 4 EQUATIONS - ELASTICALLY COUPLED FRICTION ISOLATOR
*      MODEL E   *

35    BREAK=DABS((DEP(3)-XO)-(DEP(1)-DEP(3))*ZN)
      RSLT(1)=DEP(2)
      IF(BREAK.GE.(1.5*C3)) ISTEP=0
      IF(BREAK.LT.(1.5*C3)) ISTEP=1
      IF(BREAK.LE.(0.5*C3)) ISTEP=0
      IF(BREAK.GE.C3) GO TO 40
      RSLT(2)=-C2*(DEP(3)-XO)/ZN
      RSLT(3)=DEP(2)
      RETURN
40    RELV=DEP(2)-RSLT(3)
      RSLT(2)=-C2*(DEP(1)-DEP(3))-C1*SGN(RELV)
      RSLT(3)=(ZN*DEP(2)+XOP)/(1+ZN)
      RETURN

* MODEL 3 EQUATIONS - ELASTICALLY COUPLED FRICTION ISOLATOR
*      MODEL A   *

50    BREAK=DABS(DEP(3)-XO)
      RSLT(1)=DEP(2)
      IF(BREAK.GE.(1.5*C3)) ISTEP=0
      IF(BREAK.LT.(1.5*C3)) ISTEP=1
      IF(BREAK.LE.(0.5*C3)) ISTEP=0
      IF(BREAK.GE.C3) GO TO 55
```

```
      RSLT(2)=-C2*(DEP(1)-X0)-C2*(DEP(1)-X0)/ZN
      RSLT(3)=DEP(2)
      RETURN
55    RELV=DEP(2)-XOP
      RSLT(2)=-C2*(DEP(1)-X0)-C1*SGN(RELV)
      RSLT(3)=XOP
      RETURN

*  MODEL 5  EQUATIONS  -  SIMPLE FRICTION ISOLATOR  *

60    RELV=DEP(2)-XOP
      IF(DMAX.GT.DAMP) DMOD=DMAX
      IF(DMAX.LE.DAMP) DMOD=DAMP
      VBRK=XIN*3*DMOD/(50*FREQ)
      ARELV=ABS(RELV)
      IF(ARELV.GE.(1.5*VBRK)) ISTEP=0
      IF(LVB.EQ.1) GO TO 62
      IF(ARELV.LT.(1.5*VBRK)) ISTEP=1
      IF(ARELV.LT.VBRK) GO TO 61
62    RSLT(2)=-C2*(DEP(1)-X0)-C1*SGN(RELV)
      RSLT(1)=DEP(2)
      RETURN
61    RSLT(2)=-C2*(DEP(1)-X0)-C1*RELV/VBRK
      RSLT(1)=DEP(2)
      RETURN

*  MODEL 2  EQUATIONS  -  SIMPLE VISCOUS ISOLATOR  *

100   RSLT(2)=-C2*(DEP(1)-X0)-C1*(DEP(2)-XOP)
      RSLT(1)=DEP(2)
      RETURN

*  MODEL -1 EQUATIONS - ELASTICALLY COUPLED VISCOUS ISOLATOR
*     MODEL E     *

110   RSLT(1)=DEP(2)
      RSLT(2)=-C2*(DEP(1)-DEP(3))-C1*(DEP(2)-RSLT(3))
      RSLT(3)=DEP(2)+C3*((DEP(1)-DEP(3))-(DEP(3)-X0)/ZN)
      RETURN

*  MODEL 0 EQUATIONS - ELASTICALLY COUPLED VISCOUS ISOLATOR
*     MODEL A     *

120   RSLT(1)=DEP(2)
      RSLT(2)=-C2*(DEP(1)-X0)-C1*(DEP(2)-RSLT(3))
      RSLT(3)=DEP(2)-C3*(DEP(3)-X0)
      RETURN
      END
```

```
      SUBROUTINE PULSE(STEPMOD,XIN,FREQ,D,INPUT,VIN,DRATIO
     *  ,XO,XOP,INDEP)

      DOUBLE PRECISION INDEP,XO,XOP
      PHI=3.1415925
      ZEXP=2.7182818
      TIME=FREQ*D*INDEP

      IF(INPUT.NE.8) GO TO 100
      TAO=PHI/(FREQ*D)
      IF(INDEP.GE.TAO) GO TO 101
      W1=2.*FREQ*D
      XO=VIN*(INDEP-DSIN(W1*INDEP)/W1)/2.
      XOP=VIN*(1-DCOS(W1*INDEP))/2.
      RETURN

100   IF(INPUT.NE.7) GO TO 105
      TAO=PHI/(FREQ*D)
      IF(INDEP.GE.TAO) GO TO 101
      W2=FREQ*D
      XO=VIN*(1-DCOS(W2*INDEP))/W2
      XOP=VIN*DSIN(W2*INDEP)
      RETURN

105   IF(INPUT.NE.6) GO TO 115
      TAO=PHI/(FREQ*D)
      IF(INDEP.GE.TAO) GO TO 101
      IF(INDEP.GE.(DRATIO*TAO)) GO TO 106
      XO=VIN*(INDEP)**2/(2*DRATIO*TAO)
      XOP=VIN*INDEP/(DRATIO*TAO)
      RETURN
106   XO=VIN*(2*INDEP-DRATIO*TAO-INDEP*INDEP/TAO)/(2-2*
     *    DRATIO)
      XOP=VIN*(1-(INDEP-DRATIO*TAO)/((1-DRATIO)*TAO))
      RETURN
101   XO=XIN
      XOP=0.0
      RETURN

115   IF(INPUT.NE.4) GO TO 145
      W3=FREQ*D
      T1=3.1415926/W3
      IF(INDEP.GE.(69*T1)) GO TO 160
      IF(INDEP.GE.(61*T1)) GO TO 180
      IF(INDEP.GE.(13*T1)) GO TO 178
      IF(INDEP.GE.T1) GO TO 176
      XO=XIN*(1-DCOS(W3*INDEP))/2.
      XOP=XIN*W3*DSIN(W3*INDEP)/2.
      RETURN
176   RTIME=W3*(INDEP-T1)/2.
      XO=XIN*COS(RTIME)
      XOP=-XIN*W3*SIN(RTIME)/2.
```

```
      RETURN
178   RTIME=W3*(INDEP-13*T1)/8.
      ZETA=0.1
      DECAY=ZEXP**(-ZETA*RTIME)
      XO=XIN*DECAY*COS(RTIME)
      XOP=-W3*XIN*DECAY*(SIN(RTIME)+ZETA*COS(RTIME))/8.
      XLAST=XO/2.
      STEPMOD=1
      RETURN
180   RTIME=W3*(INDEP-61*T1)/8.
      XO=XLAST*COS(RTIME)+XLAST
      XOP=-XLAST*W3*SIN(RTIME)/8.
      STEPMOD=1
      RETURN

145   IF(INPUT.NE.3) GO TO 5
      FREQ1=6.2831852
      TA02=0.7
      TA03=4.20
      IF(INDEP.GE.4.7) GO TO 160
      IF(INDEP.GE.4.2) GO TO 155
      IF(INDEP.GE.0.9) GO TO 150
      XDELF=FREQ1*INDEP
      XO=.5*(1.0-COS(XDELF))
      XOP=.5*FREQ1*SIN(XDELF)
      RETURN
150   XDELF=FREQ1*(INDEP-TA02)
      XO=.3*COS(XDELF)/(ZEXP**(XDELF*0.07))
      XOP=-0.3*FREQ1*(SIN(XDELF)+0.07*COS(XDELF))/(ZEXP**
     *  (0.07*XDELF))
      RETURN
155   XDELF=FREQ1*(INDEP-TA03)
      XO=-0.04*(1.0+COS(XDELF))
      XOP=0.04*FREQ1*SIN(XDELF)
      RETURN

5     IF(INPUT.NE.2) GO TO 10
160   XO=0.0
      XOP=0.0
      RETURN

10    IF(INPUT.GE.1) GO TO 20
      XO=XIN*(1.-(1.+TIME)/(ZEXP**TIME))
      VEL=FREQ*XIN*D
      XOP=VEL*TIME/(ZEXP**TIME)
      RETURN

20    XO=XIN*(ZEXP*TIME)**2.0/(4.0*(ZEXP**TIME))
      VEL=FREQ*XIN*D*(ZEXP**2.)/4.
      XOP=VEL*(2.*TIME-(TIME**2.0))/(ZEXP**TIME)
      RETURN
      END
```